Evaluation of Groundwater Vulnerability to Pollution using three different assessment models in the Halabja-Saidsadiq Hydrogeological Basin, North-East/Iraq

A Thesis

Submitted to the Council of the college of

Science at University of Sulaimani in partial fulfillment

of the requirements for the degree of doctor of philosophy in

Geology (Hydrogeology)

By

Twana Omer Abdullah

M.Sc. in Engineering Geology – 2009

University of Portsmouth, England

Supervised by

Dr. Salahalddin Saeed Ali   **Dr. Nadhir Al-Ansari**

Professor   **Professor**

May, 2018   Gulan, 2718

بِسْمِ اللَّـهِ الرَّحْمَـٰنِ الرَّحِيمِ

وَمَا أَنْزَلَ اللَّهُ مِنَ السَّمَاءِ مِنْ مَاءٍ فَأَحْيَا بِهِ الْأَرْضَ بَعْدَ مَوْتِهَا.......

﴿١٦٤-البقرة﴾

Supervisor's Certificate

We certify that this thesis entitled "Evaluation of Groundwater Vulnerability to Pollution Using three different assessment models in the Halabja-Saidsadiq Hydrogeological Basin North-East/Iraq" is accomplished by (Twana Omer Abdullah), was written under our supervisions in the college of Science, at the University of Sulaimani and Department of Civil, Environmental and Natural Resources Engineering at Lulea University of Technology in Sweden, as a partial fulfillment of the requirements for the degree of Doctor of Philosophy in Geology (Hydrogeology).

Signature:

Name: Dr. Salahalddin Saeed Ali

Title: Professor

Date: 25 /01 /2018

Signature:

Name: Dr. Nadhir Al-Ansari

Title: Professor

Date: 25 /01 /2018

In view of the available recommendation, I forward this thesis for debate by the examining committee:

Signature:

Name: Dr. Mushir Mustafa Qadir

Title: Assistant Professor

Address: Head of Department of Geology

Date: 25 /01 /2018

Linguistic Evaluation Certificate

This is to certify that we, **Dr. Shilan Ali Hama Sur, Dr. Saza Ahmad Fakhry, Dr. Azad Hassan Fatah, and Tayeb Abdulrahman** , have proofread this thesis entitled 'Groundwater Vulnerability Mapping and Environment Study of Halabja Saidsadiq Basin, North- East /Iraq' conducted by **Twana Omer Abdulla**. After marking and correcting the mistakes, the thesis was handed again to the researcher to make the corrections in this last copy.

Proofreader:

Dr. Saza Ahmad Fakhry,

Tayeb Abdulrahman

Dr. Shilan Ali Hamasur

Dr. Azad Hassan Fatah,

Date: 4/3/ 2018

Department of English, College of Languages, University of Sulaimani.

Examining Committee Certificate

We certify that we have read this thesis entitled "Evaluation of Groundwater Vulnerability to Pollution Using three different assessment models in the Halabja-Saidsadiq Hydrogeological Basin North-East/Iraq" prepared by (Twana Omer Abdullah), and as an Examining Committee, we examined the student with its content and we agreed that this thesis meets the basic requirements of the degree of Doctor of Philosophy in Geology "Hydrogeology".

Signature:

Name: Dr. Sadiq B. Jawad
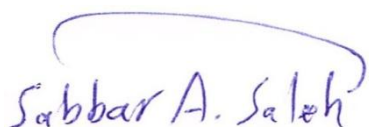
Title: Professor

Date: 10 /05 /2018

Signature:

Name: Dr. Qusai Y. Al-Qubaisi

Title: Professor

Date: 25 /05 /2018

Signature:

Name: Dr. Sabbar A. salih

Title: Professor

Date: 10 /05 /2018

Signature:

Name: Dr. Alaa M. A. Al-Abadi

Title: Professor

Date: 25 /05 /2018

Signature:

Name: Dr. Diary A. Mohammad

Title: Assistant Professor

Date: 10 /05 /2018

Signature:

Name: Dr. Salahalddin S. Ali

Title: Professor

Date: 25 /05 /2018

Signature:

Name: Dr. Nadhir Al-Ansari

Title: Professor

Date: 10 /05 /2018

Approved by the Dean of the College of Science:

Signature:

Name: Dr. Soran Mohammed Mamand

Title: Assistant Professor

Date: /   /2018

Dedication

To my late father and lovely mother

To my respectable wife, Shadan

To my son, Aro

To all my brothers and only sister

To my great supervisors, Prof. Dr. Salahalddin and Prof. Dr. Nadhir

To all my family and my friends

To the people of Halabja City and Saidsadiq District

To the memory of 5000 spotless citizens who were killed in March 16, 1988

Twana

Acknowledgement

I am very thankful to my supervisors Prof. Salahaldddin S. Ali in Sulaimani University-Iraq, Prof. Nadhir Al-Ansari in Lulia University of Technology-Sweden and Prof. Sven Knutsson in Lulia University of Technology-Sweden, for providing me the opportunity to be one of their postgraduate students, and for their continuous guidances in most areas of life; for many crucial discussions as and when required and efforts in managing things so that I can work smoothly.

I am indebted to all my colleagues and the staffs of College of Science-University of Sulaimani, Specifically to Dr.Diary Al-Manmi , Dr.Dara Hamamin, Dr. Sirwan Hama Ahmed, for their continuous assistances. In addition to all staffs at Lulea University of Technology in Sweden for all kinds of support. A special appreciation I give to Dr.Azhar Bety , who introduced me to remote sensing and its linkage with GIS, he willingly shares his precious time helping me with maps specially LU/LC and Lineament maps.

My sincere thanks also go to the staffs of Groundwater Directorate of Sulaimani. Especially, Hawzheen Abdullah , Farhad Hama. And to all other staffs at GWD-Sulaimani, Sarmad Abdwlhamid, Ibrahim Faraj, Alwang Saeed, Bakr , Azwar Hama-Amin and to Babarasul Gafour (Previous directorate of GWD), all those have crucial roles in providing me an important required data for my study.

My great thanks go to Dr.Aras Omar Kareem, whose help was vital for the fulfilment of this work, especially for analyzing several samples at the laboratory of Freiberg University in Germany.

Furthermore I would also like to acknowledge the role of the staffs of Sulaimani Environment Directorate/ Chemical Laboratory Department, for analyzing water samples for hydrochemical analyses.

I would love to extend my great appreciation to Shadan, my wife, and to Aro, my son, for their continuous supports during the period of my study.

Abstract

The augmentation of human population regularly corresponds with change in the land cover, including expansion of urban areas, which imposes increasing the available amount of domestic and drinking water. The study area, *Halabja-Saidsadiq Basin*, is situated in the Northeast of Iraq and is considered to be one of the major groundwater sources of the region. As the surface water sources are not enough in the studied area, it has become necessary to use groundwater at an increasing rate. Usually, a huge amount of groundwater is plentiful in the alluvial deposits or rock outcrops where the urban areas are frequently situated. Such areas face a huge risk of pollution of groundwater due to producing different sources of contaminant from human's activity. Keeping these aspects in view, groundwater vulnerability studies have been carried out in the current studied basin. The objective of this work is to investigate the environmental impacts and recognize the groundwater vulnerability in the area so that the groundwater can be protected from probable contaminations.

In the current study, DRASTIC model has been applied since it is considered to be one of the most proper useful methods available for the assessment of the groundwater vulnerability. This model has been modified and different methods have been applied such as: VLDA and COP for the studied basin. In addition, the applied model was validated by comparing its findings against the groundwater ages and the observed water characteristic qualities within the region in two successive seasons.

Field and official data were collected to review several environmental impacts and were used to map standard DRASTIC vulnerability model for the study basin. Based on this model, the study area was classified into four zones of vulnerability indexes, comprises a very low, low, moderate and high vulnerability index with a coverage area of (34%, 13%, 48% and 5%) respectively.

The first modification is classified according to the rate and weight adjustment based on two methods, nitrate concentration from 39 groundwater samples for modifying the recommended rating value using Wilcoxon rank-sum nonparametric statistical test and sensitivity analysis to modifying recommended weighting value. To calibrate the modified rate, the Pearson's correlation coefficient was applied to estimate the relation between DRASTIC values and nitrate concentrations. For the modified model, the correlation coefficient was 72% that was significantly higher than 43% achieved for the standard model. The modified model classified the area into five vulnerability classes (very low, low, moderate, high and very high) with covered area of (7%, 35%, 19%, 35% and 4%), respectively.

The second modification of DRASTIC model was based on Land Use and Land Cover for the studied area. The Land Use and the Land Cover (LULC) map prepared using ERDAS IMAGINE software from two different scenes of landsat Thematic Mapper (TM). The LULC map indicates that only five classes of LULC can be identified: these are: barren land, agricultural land, vegetation land, urban area and wet land or water body. The modified DRASTIC based on LULC map classified the area into five classes: very low (1.17%), low (36.82%), moderate (17.57%), high (43.42%) and very high (1.02%).

The third modified method of the current study is the modification of DRASTIC model based on Lineament feature of the study basin. A lineament map is extracted from Enhanced Thematic Mapper plus (ETM+) satellite imagery using different techniques in remote sensing and GIS. The lineament density map demonstrates that only six classes of lineament density can be identified ranged from (0-2.4). The modified model classified the area into four categories: very low (28.75%), low (14.31%), moderate (46.91%) and high (10.03%).

The fourth effort to modify standard DRASTIC model is the application of Analytical Hierarchical Process (AHP) to assess the weight value of each parameters. The modified DRASTIC vulnerability index values based on AHP

method ranged between (65.82 – 224.1) with five vulnerability classes comprises (very low to very high).

VLDA and COP models also applied to map vulnerability system in the study basin. The vulnerability outcome based on VLDA model revealed that a total of 4 ranges of vulnerability indexes had been distinguished ranging from low to very high with vulnerability indexes (2.133-9.16). While, based on the COP model, the area is also divided into four vulnerability classes ranging from very low to high with index value ranged from (0.79) to(6.2).

All applied models in the study basin were compared to each other and also validated to clarify the validity of the theoretical sympathetic of current hydrogeological conditions and to show the accuracy of the modeled vulnerability system. Two methods were applied for the validation of the result, in the first approach; nitrate concentration analysis has been selected. The nitrate differences between two following seasons (dry and wet) were analyzed from (39) wells. In the second approach, groundwater vulnerability was assessed based on tritium (^{3}H) value and groundwater age. The results of both validation methods, verify the sensibility of the gradation and distribution of vulnerability levels acquired using the modified DRASTIC model based on (rate and weight modification and using AHP method, effect of LULC) and VLDA model.

Table of Contents

List of Appendices

Appendix (1.1) Results of all pumping test analysis

Appendix (1.2 a) Concentrations of the major ions and minor compound of the groundwater samples in the dry season for the study basin (mg/l)

Appendix (1.2 b) Concentrations of the major ions and minor compounds of the groundwater samples in the wet season for the study basin (mg/l)

Appendix (2.1) Infiltration test sites and results

Appendix (2.2) All SPSS results

Appendix (3.1) Time-drawdown data of the aquifer pumping test (W12)

Appendix (3.2) Groundwater fluctuation from (well and pit) from May 2014 to October 2015

Appendix (3.3) Location of all used wells for depth to water table computation

Appendix (4.1a) Precision (CV%) for water samples chemical analysis (dry season), (mg/l)

Appendix (4.1 b) Precision (CV%) for water samples chemical analysis (wet season), (mg/l)

Appendix (4.2 a) Accuracy (Electroneutrality EN%) of water samples chemical analysis (dry) season

Appendix (4.2 b) Accuracy (Electroneutrality EN%) of water samples chemical analysis (wet) season

Appendix (4.3 a) Physical propertise of groundwater (dry season)

Appendix (4.3 b)Physical propertise of groundwater (wet season)

Appendix (4.4)Heavy metals analysis for the wet season in the studied basin, (mg/l)

List of Figures

List of Plates

List of Tables

List of Published Papers

Paper (1)

Groundwater Vulnerability Mapping Using Lineament Density on Standard DRASTIC Model: Case Study in Halabja Saidsadiq Basin, Kurdistan Region, Iraq

Paper (2)

Groundwater Assessment of Halabja Saidsadiq Basin, Kurdistan Region, NE of Iraq Using Vulnerability Mapping

Paper (3)

Groundwater Vulnerability Using DRASTIC and COP Models: Case Study of Halabja Saidsadiq Basin, Iraq

Paper (4)

Vulnerability of Groundwater to Pollution Using VLDA Model in Halabja Saidsadiq Basin, Iraq

Paper (5)

Assessing the Vulnerability of Groundwater to Pollution Using DRASTIC and VLDA Modelsin Halabja Saidsadiq Basin, NE, Iraq

Paper (6)

Vulnerability of Groundwater to Pollution Using Three Different Models in Halabja Saidsadiq Basin, Iraq

Paper (7)

Groundwater Vulnerability to Pollution Assessment using Two Different Models in Halabja Saidsadiq Basin, Iraq

List of Abbreviations

Abbreviations	Descriptions
AHP	Analytical Hierarchy Process
AIA	Alluvium Intergranular Aquifer
AET	Actual Evapotranspiration
APWL	Accumulated Potential Water Loss
AWC	Available Water Capacity
A-Map	Aquifer Media Map
CFA	Cretaceous Fissured Aquifer
COP	C is the properties of overlying layers, O is the concentration of flow and P is the precipitation
CKFA	Cretaceous Karstic Fissured Aquifer
CN	Curve Number
CV	Coefficient of Variation
CR	Consistency Ratio
CI	Consistency Index
C-Map	Hydraulic Conductivity Map
DEM	Digital Elevation Model
DI	Vulnerability Index Value
D-Map	Depth to water table map
dSW	Change in Soil Water
DO_2	Dissolved Oxygen
EPIK	Epikarst, Protection cover, Infiltration condition and Karst network development
EC	Electrical Conductivity
EU	European Union
EN	Electro-neutrality
ET	Evapotranspiration
ET_o	Reference Evapotranspiration
Eg	Eigen value
ETM+	Enhanced Thematic Mapper Plus
F_p	Infiltration rate
HTO	High-Temperature Oxidation
HR	High Restriction
IC	Ion Chromatography
IQS	Iraqi Drinking Water Standard
IWQI	Irrigation Water Quality Index
IDW	Inverse Distance Weight

I-Map	Impact of Vadose Zone Map
JKA	Jurassic Karstic Aquifer
Kc	Crop Coefficient
LU/LC	Land Use/Land Cover
LWIA	Liquid Water Analyser Isotop
LR	Low Restriction
m.a.s.l	Meter above Sea Level
MR	Moderate Restriction
MPN	Most Probable number
N.D.	Not Detected
NTU	Nephelometric Turbidity Unit
NR	No Restriction
OS	Overlying Soil
OL	Overlying Lithology
PET	Potential Evapotranspiration
Peff	Effective Rainfall
P_{eff}	Effective Rainfall
Pr	Parameter Rate Value
Pw	Parameter Weight Value
PQ	Quantity of Precipitation
PI	Temporal Distribution of Precipitation
Qi	Quality Measurment of the ith parameter
RI	Random Index
R-Map	Net Recharge Map
SW	Soil Water Content
SR	Sever Restriction
S-Map	Soil Media Map
sf	Surface Feature
sv	Slope and Vegetation
SD	Standard Deviation
SMOW	Standard Mean Ocean Water
TAT	Tanjero Aquitard
TKA	Tertiary Karstic Aquifer
TM	Thematic mapper
T-Map	Topography Map
VLDA	V is Lithology of Vadose Zone, L is the Pattern of Land Use, D is Groundwater Depth, and A is the Aquifer Characteristics.
Wi	Weight of the ith Parameter

Chapter One

Introduction

Chapter One

Introduction

1.1 Preface

Groundwater is a valuable water sources of domestic, irrigation and agricultural purpose in several regions around the world. If this important source is polluted, it may reveal to a serious health hazard and environmental problems. Groundwater can be contaminated through a wide variety of human and other activities, which may include land disposal of waste materials and sewage, and the leaching of fertilizers and pesticides. Since late 1970s, occurrences of chemical components such as nitrate, bacteria and pesticides in groundwater have exhibited a significant increase in concentration and have stimulated research on the subsurface fate of contaminants. Prevention of groundwater contamination is the key to efficient and effective environmental management, as the groundwater treatment is expensive and slow. In order to protect groundwater resources, areas prone to contamination by human activity need to be delineated, which can be best accomplished through groundwater vulnerability assessment (National Research Council, 1993).

In the studied basin, groundwater plays an important role in providing water for drinking, industrial and agricultural activities, particularly, some parts within the area which that is characterized by the lack of a water project. In addition, a considerable economic development, enhances security in the studied basin and after many years of destruction in the area with many war circumstances and the administrative structure of Halabja which has changed from District to Governorate in March 2014. The City of Halabja will mark the beginning of greater economic development. A striking point is the increase of the number of people heading to this basin and its surrounding region, this means that water consumption is on the rise. According to the data obtained from the Directorate of Groundwater in Sulaimani City, the area holds several thousand deep wells.

Thus, the study of the groundwater resources and its potential pollution in the area has become necessary. Moreover, it is worth noting that no other previous studies have been conducted on this vital area in terms of contamination. This leads to making this study of particular importance. In addition, all of the municipal wastewater from the cities of Halabja and Saidsadiq and all other sub-district sites within this basin may infiltrate into the groundwater every year. These reasons play an important role to select this site as a case study to reveal the applicability of the proposed vulnerability and environmental assessments.

1.2 Study Area

Halabja Saidsadiq Basin, located in the north-east of Iraq, (Figure 1.1). This basin was divided into two sub-basins by Ali (2007) including Halabja-Khurmal and Said Sadiq sub-basins. The whole coverage area of both sub-basins is about 1278 Km^2. Geographically, it is located between UTM coordinates 3,880,000 and just below 3,940,000 to the north and 560,000 and just above 610,000 to the east. The studied basin is characterized by distinct continental interior climate with hot summers and cold winters of the Mediterranean type with the average annual precipitation ranging from 500-700 mm. About 57% of whole studied area is characterized by arable area due to its suitability for agricultural lands and usability of fertilizers and pesticides are common practices, so, it affects the groundwater quality (Huang et al., 2012).

1.3 Division of Basin

The studied basin is divided hydrologically into two sub-basins as follows:

1.3.1 Halabja- Khurmal Sub-basin

This sub-basin as named after Ali (2007) and is located at the east of the Sharazoor-Piramagroon basin , this name be referred to the two largest cities; Halabja and Khurmal (Figure 1.1). This sub-basin is occupying nearly 542 km^2

with equal sides of rectangular in shape. It contains many large springs such as Zalm, Chawg, and Biara. All the surface runoff and the groundwater discharge of this sub-basin drained to the Darbandikhan reservoir by Zalim and Biara streams. The basin boundary at the north, northeast, and southeast coincides with the summits of Avroman, Shinrwe and Balambo mountains, respectively.
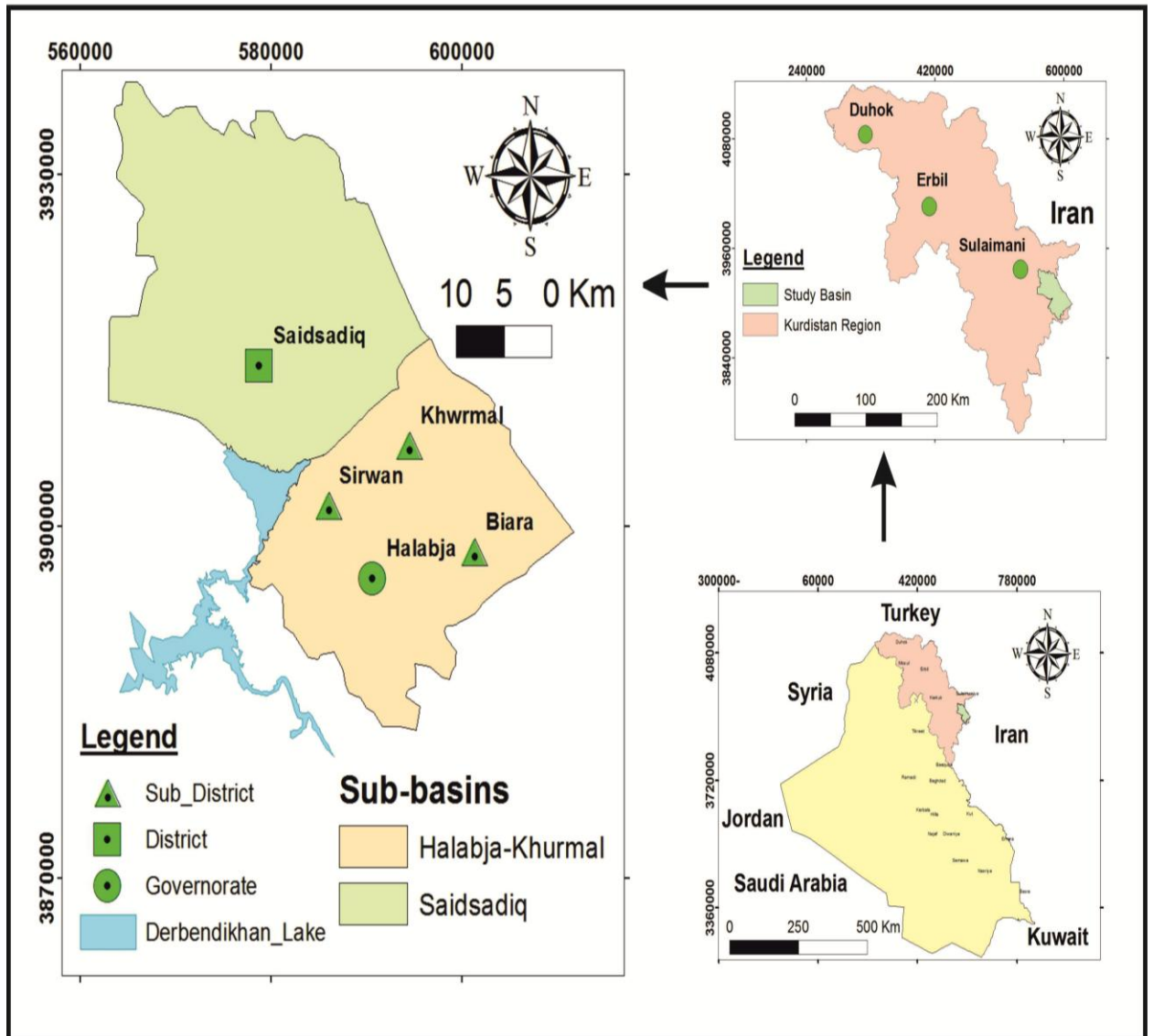
Figure 1.1: Location map of the studied basin

1.3.2 Said Sadiq Sub-basin

This sub-basin is located approximately at the northwest of the Sharazoor-Piramagroon basin, and named in reference to its largest town of Said Sadiq (Figure 1.1). The most of the large karstic springs such as Reshen, Saraw, and Mowan are located in this sub-basin. It has semi-circular shape with surface area of more than 736 km^2. All the groundwater discharges and the surface runoff of this sub-basin discharged into the Darbandikhan reservoir by the Chaqan and Surajo streams. The basin boundary at the western part is 2 km at the west of Khurmal town. While the boundary to the north, northeast is specified by the runoff divide line from the top of Kura Kazhaw and Suren mountains, respectively.

1.4 Scope of the Work

Presently, there is no environmental and vulnerability assessment in Halabja Saidsadiq Basin and the area which will mark the beginning of greater economic development and advancement. This leads to increase the contaminant materials from human waste and constructing several factories. In addition, groundwater aquifers in the study area are considered to be the main source of water supply to various urban requirements. This means that groundwater can be easily contaminated.

In the present study, different available methods were revised for assessing groundwater vulnerability namely; DRASTIC, COP and VLDA has been investigated, along with the modifying DRASTIC model to build a suitable model for the studied basin. It is also planned to validate the vulnerability by comparing the results with the observed groundwater quality and groundwater age using a radioactive isotope of hydrogen (Tritium) of the study basin.

1.5 Approach

The approach comprises the following steps adopted in this study:

- Reviewing different approaches and methods of aquifer vulnerability assessment.

- Characterizing the geological and hydro-geological setting necessary for applying the vulnerability analysis.

- Analyzing the climatic characterizes of the studied area using the most recently methods.

- Evaluating the hydrochemical properties of the aquifers and validity for drinking, irrigation and industrial usage depending on the most recently models.

- Investigating the soil, groundwater quality and LULC in the studied area.

- Using remote sensing technique to analyses land use and land cover and lineament features in the studied basin from the most recent available satellite images.

- Preparing the aquifer vulnerability maps employing some of the available approaches including (original DRASTIC, VLDA and COP) models.

- Modifying DRASTIC models to prepare the most accurate aquifer vulnerability map for the study area.

- Comparing between constructed groundwater vulnerability maps.

- Validating the result using the existing groundwater age and groundwater quality scenarios, to map the best vulnerability situation to reveal the probable contamination hazard.

1.6 Methodology

1.6.1 Field Work

To collect necessary data from the studied area, the following field works were organized and implemented:

1. A reconnaissance survey was put into practice in May 2014 to take a general overview about the geology successions, hydrogeology, number

and distribution of wells and springs for collecting groundwater samples , plate (1.1A).

2. Depth to groundwater level was measured from approximately 1400 wells (appendix 3.3) by using the electrical groundwater depth detector device , plate (1.1B).

3. Seasonal water table monitoring in 14 water wells and piezometers, as in plate (1.1B), the information on the well sites explained in Appendix (1).

4. Pumping well-achieved tests conducted in the field on 89 water wells in 2014 for obtaining aquifer hydraulic properties, plate (1.1C); information about all used well sites are explained in Appendix (1.1).

5. Collecting information about lithological description of an aquifer, water bearing layers, properties of unsaturated zones directly from drilling records, Plate (1.1D).

6. Using Double Ring Infiltrometer method to apply infiltration tests for 27 sites to cover all studied area, (see Plate 1.2A). Once an area of about 50 x 50 cm was selected, the debris removed from the top layer, and then the infiltrometer was installed to a depth of 10cm. The accumulated volume of infiltration at each 1.025 liter was recorded using a timer watch. This process is continuous until the infiltration reached a more or less constant value. Finally the SPSS software program is used in analyzing and estimating infiltration capacity rate using Horton's equation (1945):

$$F_p = F_c + (F_0 - F_c)\, e^{-kt} \;……..(1.1)$$

Where**:**

F_p: is the infiltration capacity.

F_c: *is* the minimum or ultimate infiltration capacity.

F_0: is the initial or maximum infiltration rate at the beginning of the test.

K: is the rate of decrease in the infiltration capacity.

t: is the total duration test time.

7. Field measurement instrument (TPS/90FL-T Field Lab. Analyzer) was fully calibrated before the starting sampling of groundwater. It is used for measuring temperature, electrical conductivity, pH, and turbidity in situ during the field work in 2014, (Plate 1.2-B).

8. Meteorological data were collected from Halabja Meteorological Station, as in Plate (1.3A) for using it in calculating water balance for the studied area.

9. Groundwater samples from thirty water wells and nine springs (appendix 1.2a) were collected, between two following seasons (dry and wet) to detect the seasonal variations, Plates (1.3B and 1.3C). The samples were collected and analyzed on the end of September 2014 for the dry season and end of May 2015 for the wet season, and these are chemically tested for major cations , anions , minor compounds, and heavy metals, (Appendixes 1.2 a and 1.2 b). Figure (1.2) shows sites of all the collected samples. All water samples were filtered through cellulose acetate syringe filters Ø:25 mm with pore size 0.20 μm for cation and anion analyses during or upon return from the field.

10. Twenty samples from groundwater wells penetrate the alluvium intergranular aquifer, fissured and fissured karstic aquifer and Qulqula aquitard and one rain water sample (Table 1.1) were collected for analyzing unstable isotopes explicitly (Tritium) to predicting the groundwater age. These samples were collected and based on the laboratory instruction of Joanneum Research Resources - Institute for Water, Energy and Sustainability in Austria, Plate (1.3D), and Figure (1.3).

Plate 1.1: Field Works

(A) Geological survey, stratigraphic and lithologic description

(B) Water level measurement using groundwater level detector device at Jalela well

(C) Pumping well test for obtaining aquifer hydraulic properties

(D) Drilling sample description to recognize lithology of aquifer and unsaturated zone

Plate 1.2: Field Works

(A) Infiltration test using double ring infiltro-meter method

(B) Measuring physical parameters in situ
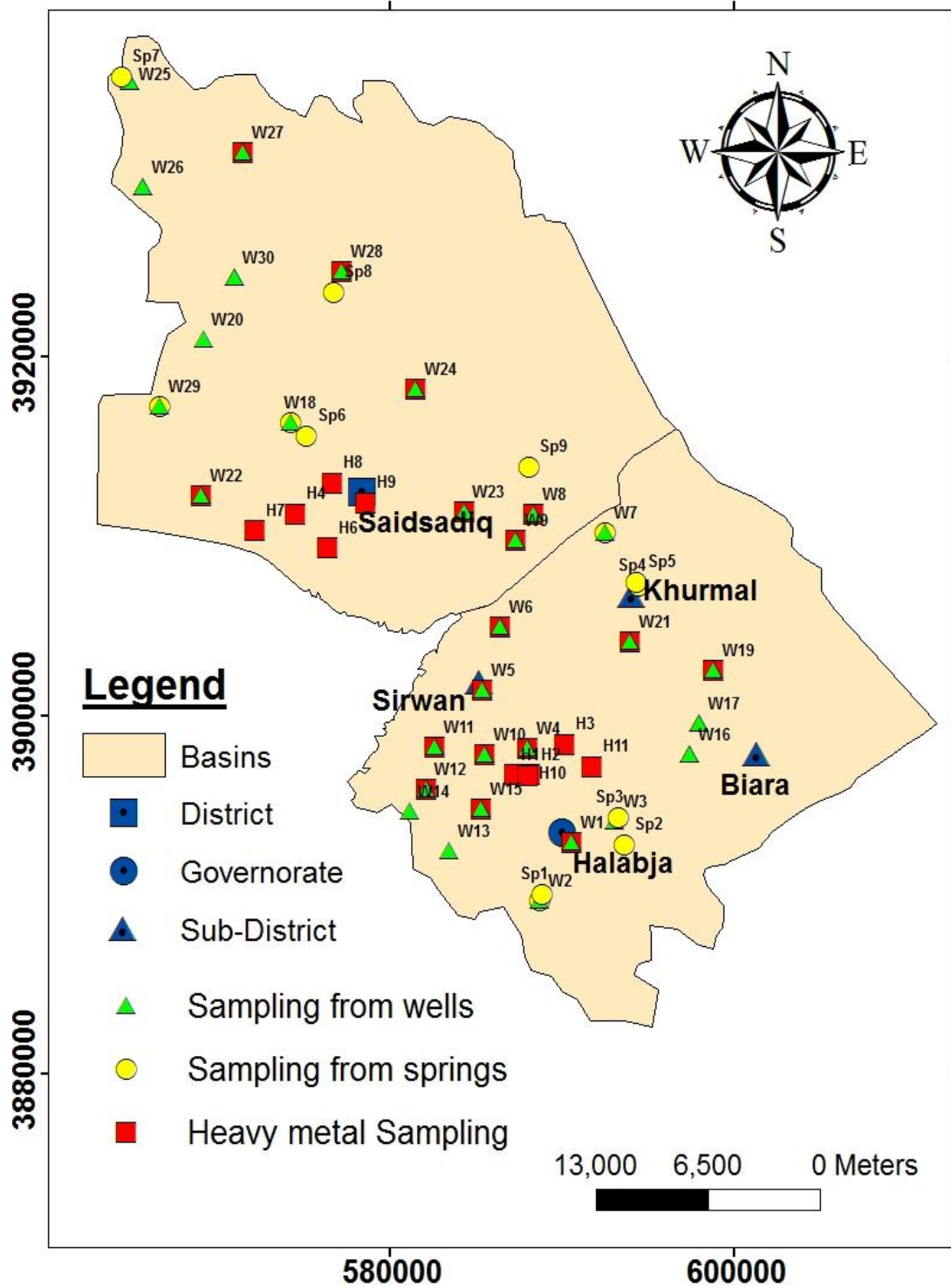
Figure 1.2: Locations of selected wells and springs samples used for chemical analyze

Table 1.1 Well water samples site for tritium unstable isotope analysis ^{3}H

N	Code	Well Name	^{3}H (TU)	Average ^{3}H (TU)	X	Y
1	ITB	Banishar Mosques Well	4.7	4.28	592512	3910225
2	ITB2	Basak Well	3.8		564939	3935331
3	ITJ	Jalela Village Well	4		593112	3984078
4	ITS1	Saraw Swbhan Agha	4.5		575191	3915553
5	ITM	Mzgawta	4		579321	3920460
6	ITSb	SheraBara	4.3		567247	3920654
7	ITT2	Tawanawal	4.6		591079	3883866
8	ITD	Darbarulla	4.3		572149	3928423
9	ITTh	Halabaj Taymwr Hassan	3.3	3.03	590571	3892884
10	ITS	Sirwan	2.3		585425	3901433
11	ITSs	Shekhan Shanadactry Road Project	3.1		579675	3914378
12	ITSm	Soila Mesh	3		574585	3909784
13	ITGs	Gulajoy Saroo	3.2		564663	3914321
14	ITMh	Mstakani Haji Ahmad	3		583698	3909515
15	ITT	Taza De	3		591412	3906543
16	ITB3	Bezhawa	3.3		582369	3895184
17	ITX	Kharpane Well	2.4	2.28	597428	3897782
18	ITBk	Balkhay Khwaroo	2.3		604668	3895755
19	ITS2	Sargat	2.1		600875	3905932
20	ITBb	Bani Bnok	2.3		589689	3920900
21	ITR	Rain Water Sample	4.8	4.8	----	

1.6.2 Laboratory Analysis

Laboratory work included chemical, biological and unstable isotopic analysis of groundwater samples and rain water sample during the field work. In Total,

78 samples for the two seasons were collected and analyzed, from which 39 samples for dry season and 39 samples for the wet season were hydrochemically analysed in the Laboratory department of Environmental Directorate of Sulaimani, (Table 1.2). For checking results, several wells and spring water samples were tested in the laboratory of Health and Environmental Protection Office in Sulaimani. Water samples were stored in the refrigerator until they were analyzed to prevent deterioration and changed of their quality as a result of changing temperature of the sample. The technique used for analysis was the standard methods of water analysis as specified by the APHA (2005).

Table 1.2 Hydro-chemical parameters and methods of analysis at laboratory in Directorate of Environmental of Sulaimani

Parameters	Methods
T.D.S	Gravimetric
HCO^{3-}, Cl^-, TH as $CaCO_3$, Ca^{2+}, Mg^{2+}	Titration
$SO4^{2-}$, NO^{3-}, PO_4^{3-}	Colorimetric
Zn^{2+}, Pb^{2+}, Cu^{2+}, Cr^{2+}, Cd^{2+}, Ni^{2+}, Fe^{total}	Atomic absorption

To determine groundwater age in each aquifer, 20 groundwater samples (Figure 1.3) from 20 wells were collected and analysed for tritium (^3H) at the laboratory of Joanneum Research Resources - Institute for Water, Energy and Sustainability in Austria. Tritium (T) or ^3H is a radioactive isotope of hydrogen (having two neutrons and one proton) with a half-life of 12.4 years. Tritium concentrations are measured by tritium units (TU) where 1 TU is defined as the presence of one tritium in 10^{18} atoms of hydrogen (H), (Blavoux et al., 2013). Tritium is typically measured by a liquid scintillation counter. Tritium can be measured by mass spectrometry, but dissolved gases such as H_2O, CO_2, O_2, and

N$_2$ must be removed first, generally by exposure to heated titanium, (Kumar and Somashekar, 2011)
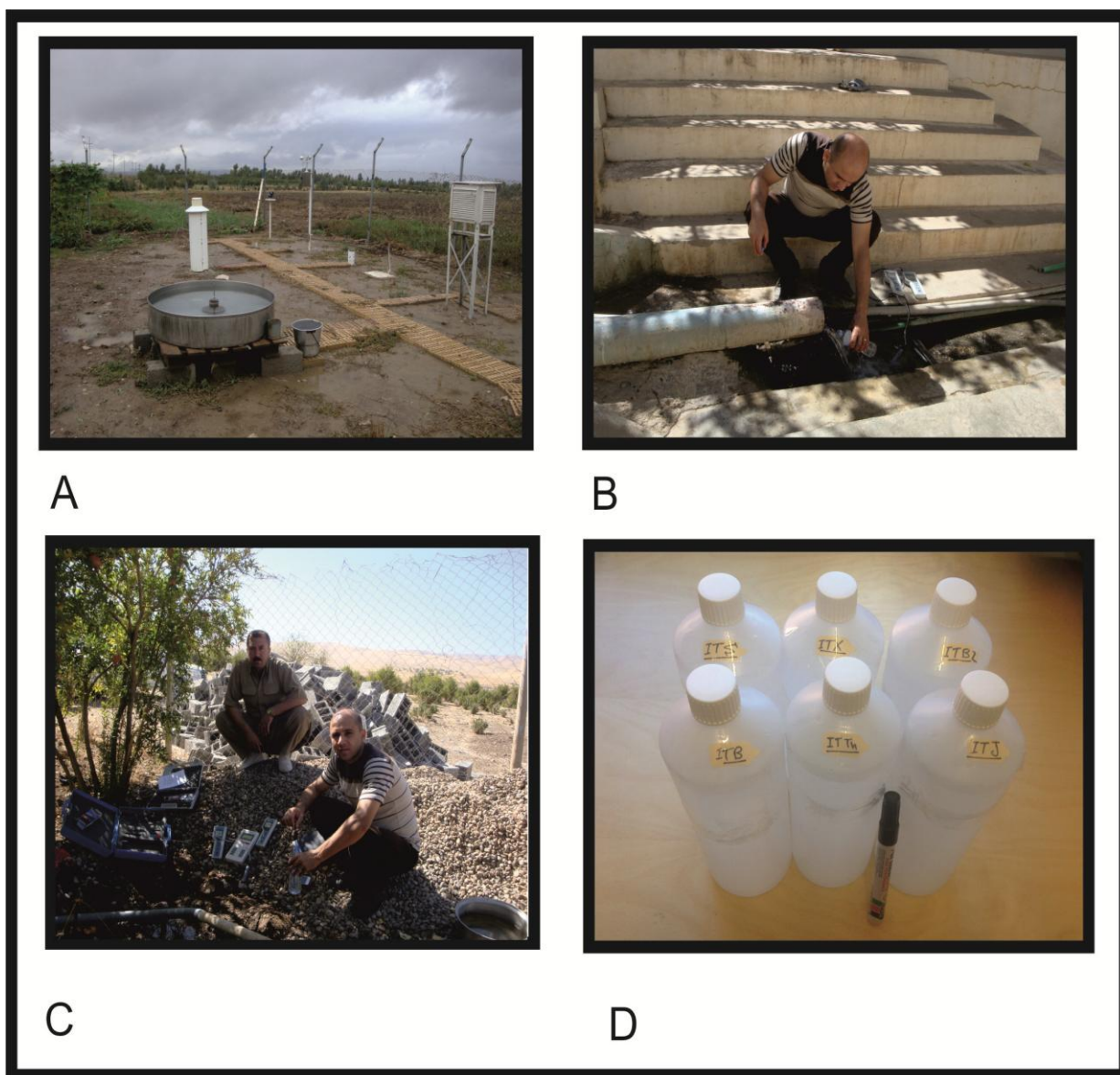
Plate 1.3: Field Works

(A) Rain water collection at Halabja Agro-Meteorological Station.

(B) Water sample collection for chemical analysis from springs.

(C) Water sample collection for chemical analysis from water wells.

(D) Water samples ready for unstable isotopes (Tritium) analysis.
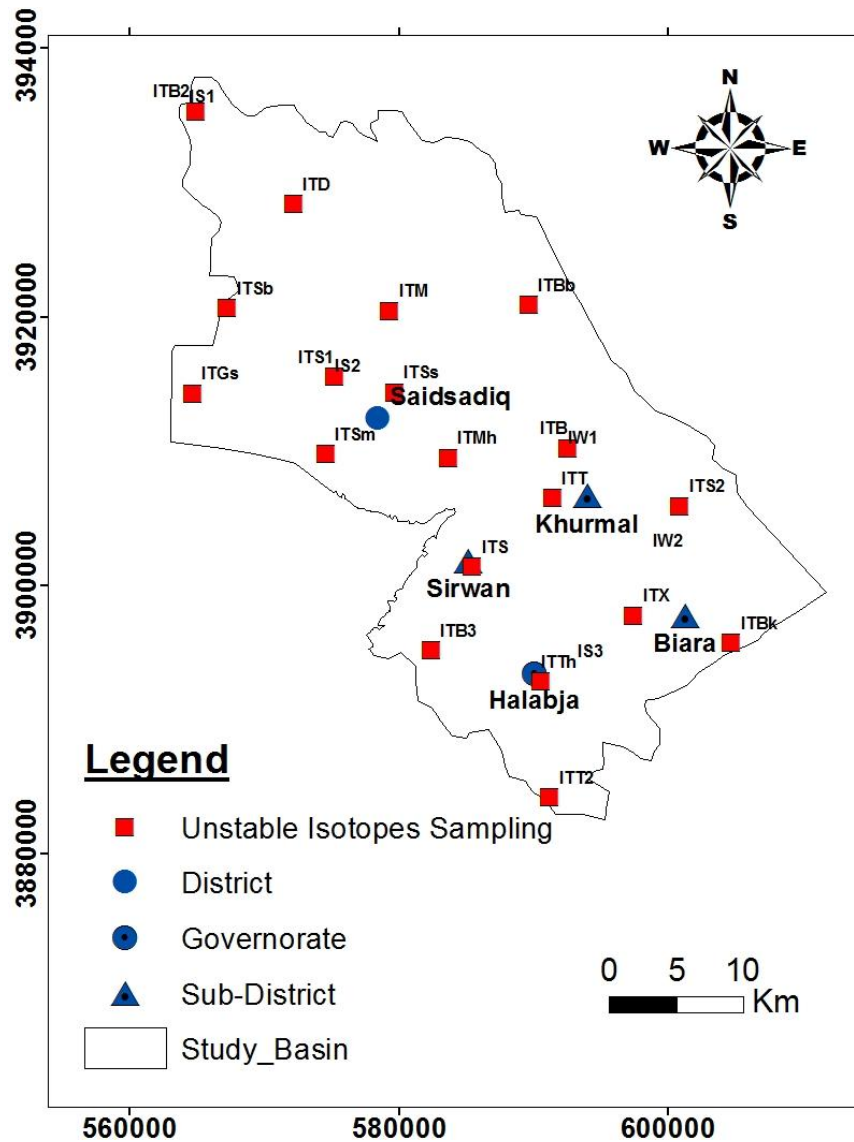
Figure 1.3: Location of selected water well samples used for unstable isotopic analysis.

1.6.3 Office Works

The office works were comprised representation of all the field works, collected data and analyzing laboratory data. The required software and programs which were used for this study for analyses and mapping are:

- CROPWAT version 8.0 (FAO-2009) is used for making crop water requirements and estimating evapotranspiration and effective rainfall using FAO Penman-Monteith method.

- ArcGIS 10.3, for constructing all basic maps and required maps for preparing vulnerability mapping, groundwater quality analysis and lineament density map.

- SPSS statistics program for estimating infiltration capacity using Horton's equation.

- AQTESOLV version 4.0 (2006) for pumping test analysis.

- RockPlot3D15 (2015) software for hydrochemical data presentation, such as Piper , Durov and Pie charts diagrams.

- Adobe Photoshop CS6 Portable and Corel DRAW X7, for creating and editing some figures, plates and cross-sections.

- Ms-word 2007 and Ms-Excell 2007 were used for typing, data tabulation, solving equations, constructing charts and diagrams.

- ERDAS IMAGINE software is used to prepare the digital image classification.This classification is used to map landuse and landcover for the studied basin.

- PCI Geomatica software for analysis and mapping a lineament distribution over the studied basin.

1.7 Geological Setting

The Geological setting is described in the following sections:

1.7.1 Tectonics and Stratigraphic Description

The studied basin is located within Western Zagros Fold-Thrust Belt. Structurally, it is located within the high folded zone, Imbricated, and thrust zones (Buday and Jassim, 1987; Jassim and Goff, 2006). The age of the geological formation ranges from Jurassic to recent, as explained in Figures (1.4 & 1.5).

Early Jurassic includes Sarki formation (thin beded fine grained cherty and dolomitic limestone) and Sehkanian formation (comprises dark saccharide dolomites and dolomitic limestone with some solution breccias), (Bellen et al,

1959). Lower and middle Jurassic rocks included Barsarin (limestone and dolomitic limestone), Naokelekan (bituminous limestone) and Sargalu formations, the last one consists of well-bedded and well-crystallized, black bituminous limestone and dolomitic limestone and occasionally contains shells of posidoni, (Ali, 2007).

The Qulqula Group consists of two formations, the Qulqula Radiolarian and the Qulqula conglomerate. It occupies the lower part of the southwestern limb of the Avroman and Suren anticlines. As Cited in (Ali, 2007) and proved by Baziany (2006) and Baziany and Karim (2007), the Qulqula conglomerate formation does not exist and this has been proved again during the field work of this study from the log of drilled wells. In addition, Bolton (1958) and Buday (1980) mentioned that the later formation is equivalent to the Quaternary sediments which exist in the foothills of Suren Mountains.

The Upper Cretaceous Kometan (Turonian) and Lower Cretaceous Balambo (Valanginian-Cenomanian) Formations are widespread and are exposed in both sub-basins. Both are lithologically very similar and composed of well bedded, white or grey pelagic limestone. The only difference is that the limestone of the latter formation is occasionally marly and containing interbeded marl. Shiranish Formation (Campanian) is composed of a succession of bluish white marl and marly limestone. Lithologically, Tanjero Formation is composed mainly of an alternation of thin beds of sandstone or siltstone with interbeds of shale, marl or rarely marly limestone (cited in Ali, 2007).

Quaternary (Alluvial) deposits are the most important unit in the area in terms of hydrogeological characteristic and water supply. These sediments are deposited as debris flows on the gently sloping plains or as channel deposits or as channel margin deposits and over bank deposits (Ali, 2007). As recorded from drilled well logs, this unit consists of angular and poorly sorted clasts of boulder, gravel and sand with more or fewer amounts of clay as separate deposits and some amount of limestone and chert fragments. The thickness of

these deposits was recorded previously up to 200 m thick (Ali, 2007), while for the first time, this study has been recorded for about 300 m or more in thickness.
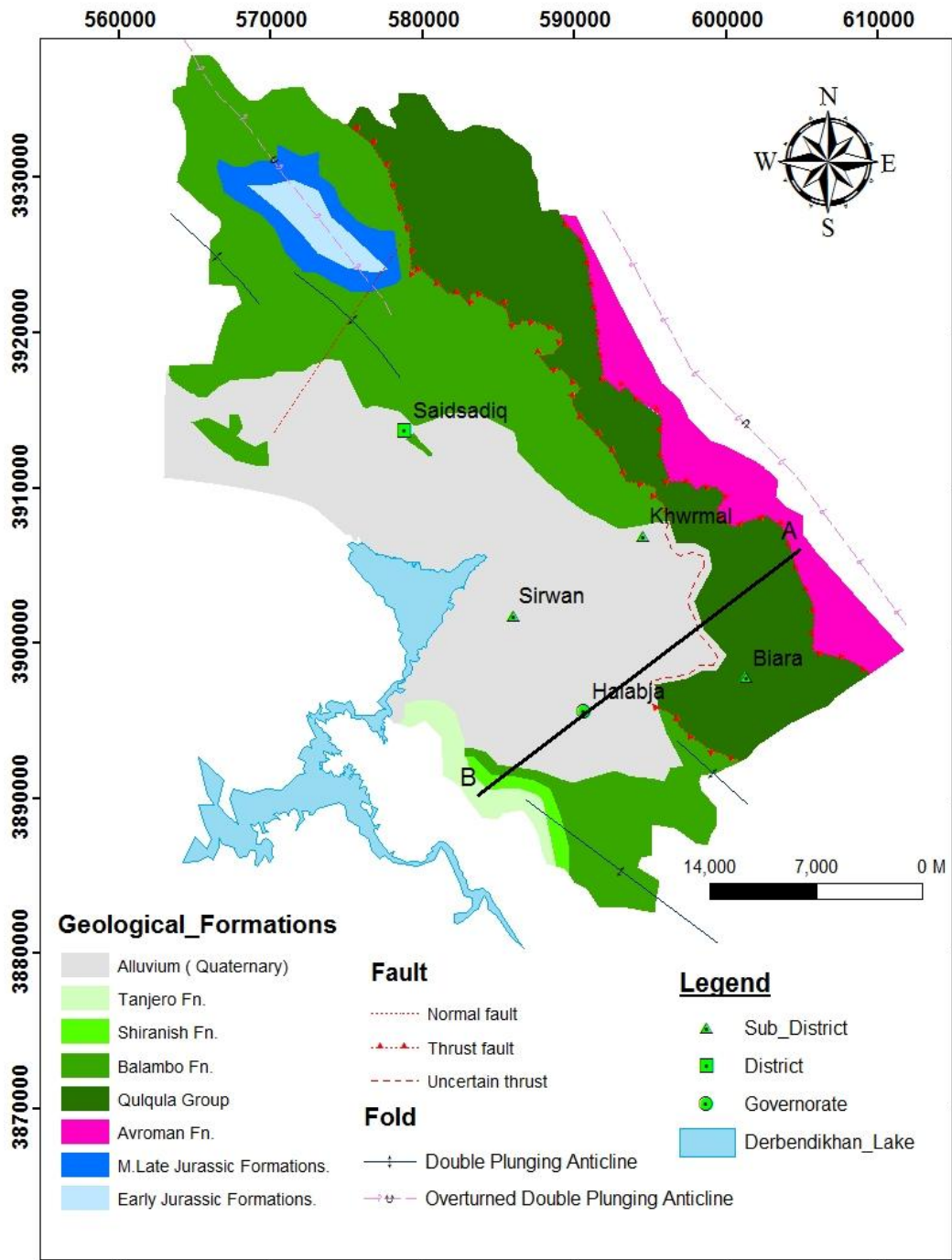
Figure 1.4: Geological map of the studied basin, modified from (Ali, 2007)
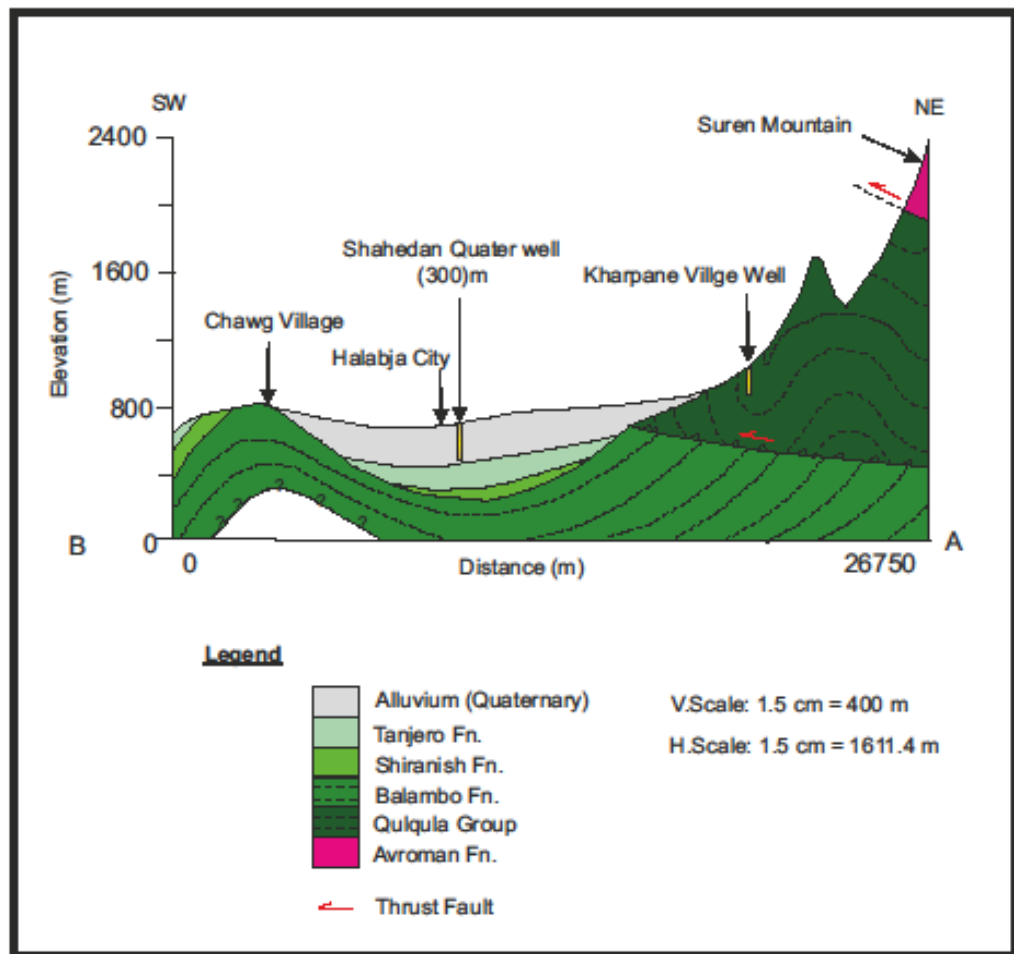
Figure 1.5: Cross Section through A-B Line

1.7.2 Lineament Features

The lineament feature is defined as linear features in a landscape identified on satellite images and aerial photographs, most likely have a geological origin, (Karim et al., 2009). Generally, lineaments are underlined by structural zone, fractured zone, a series of fault or fold-aligned hill zone of localized weathering and zones of increased permeability and porosity.

Regional lineament features in Kurdistan Region was previously studied by several researchers (Buday and Jassim, 1987; Stevanovic and Markovic, 2004, Jassim and Goff, 2006; Ali 2007 and Karim et. al, 2009). On the Basis of these studies, Kurdistan Region as it is part of Western Zagros mountain series shows well developed large lineaments which could be seen in the field and by aerial photography and satellite images. These lineaments generally reflect the effect and direction of the thrusting front of Iranian plate and the the general direction

of north east-south west which is normal to the direction of the imposed stress by the Iranian plate front. Details about this regional lineament features can be found from the above mentioned study. This study focused on the density of lineament features over the studied basin, to detect the impact of these features on the hydrogeological conditions, groundwater recharge and the vulnerability to contamination assessments. Therefore, in the studied area, the specific map of lineament distribution from satellite images was constructed for the first time.

Lineament distribution for the studied basin has been prepared by using image of landsat 8 Thematic Mapper (TM$^+$). Images consist of nine spectral bands with cell size (30x30 m). The Operational Land Imager (OLI) spectral band in gray scale was used. Nearly, scene size is 170 km north-south by 183 km east-west and the date back to (11-02-2013). Figure (1.6) shows the TM landsat image for the study basin with extracted lineament distribution.

A lineament distribution over the site extracted using PCI Geomatica technique. The lineament extraction algorithm of PCI Geomatica software consists of edge detection, thresholding and curve extraction steps (PCI Geomatica, 2001). Figure (1.7) illustrates the final lineament distribution over the studied basin extracted from previously mentioned satellite image. In the interpretation of lineament data, it is of interest to sort out surface features that are accidental and not related to structures in the underlying bedrock or somehow correlated with geological structures such as faults.

Consistent with previous lineament studies in the Region, it was possible to map a considerably greater number of lineaments from shaded relief data than other data sources due to the resolution and refinement of detail at mappable scales. Conversely, unique lineament expression was found within the area with short length and different direction which are not connected to each other.

1.8 Literature Review

The vulnerability mapping approaches have been greatly studied. In the early 1980s, the uses of parameter weighting schemes and the utilization of GIS technology have been carried out (Corwin et al., 1997; Fuest et al., 1998). An excellent example of this is the DRASTIC approach of Aller et al., (1985). This entire analysis has been recently shown to be feasible through the use of the GIS technology (Fabbri and Napolitano, 1995).

Though DRASTIC has been successfully validated for the occurrence of a specific pollutant such as pesticides and nitrates in the groundwater system (Navulur and Engel, 1998). Yet, it has been considered to be a poor predictor of general groundwater vulnerable regions (Maas et al., 1995; Barbash and Resek 1996; Garrett et al., 1989; Koterba et al. 1993; USEPA 1993). Groundwater vulnerabilities had been studied in the world by several researchers such as the following:

- Secunda et al., (1998) have used composite models along with DRASTIC for the assessment of groundwater vulnerability in Israel. The methodology employed extensive agriculture land use data and empirical means to characterize aquifer vulnerability.

- Al-Adamat et al., (2003) have produced groundwater vulnerability and risk maps for Azraq basin of Jordan using GIS, remote sensing and DRASTIC.

- Lowe et al., (2003) applied a similar overlay index approach on the existing data for western United States of America to produce pesticide sensitivity and vulnerability maps using GIS methods.

- Babiker et al., (2005) have also used a GIS integrated DRASTIC model to evaluate the vulnerability of Kakamigahara aquifer in Central Japan.
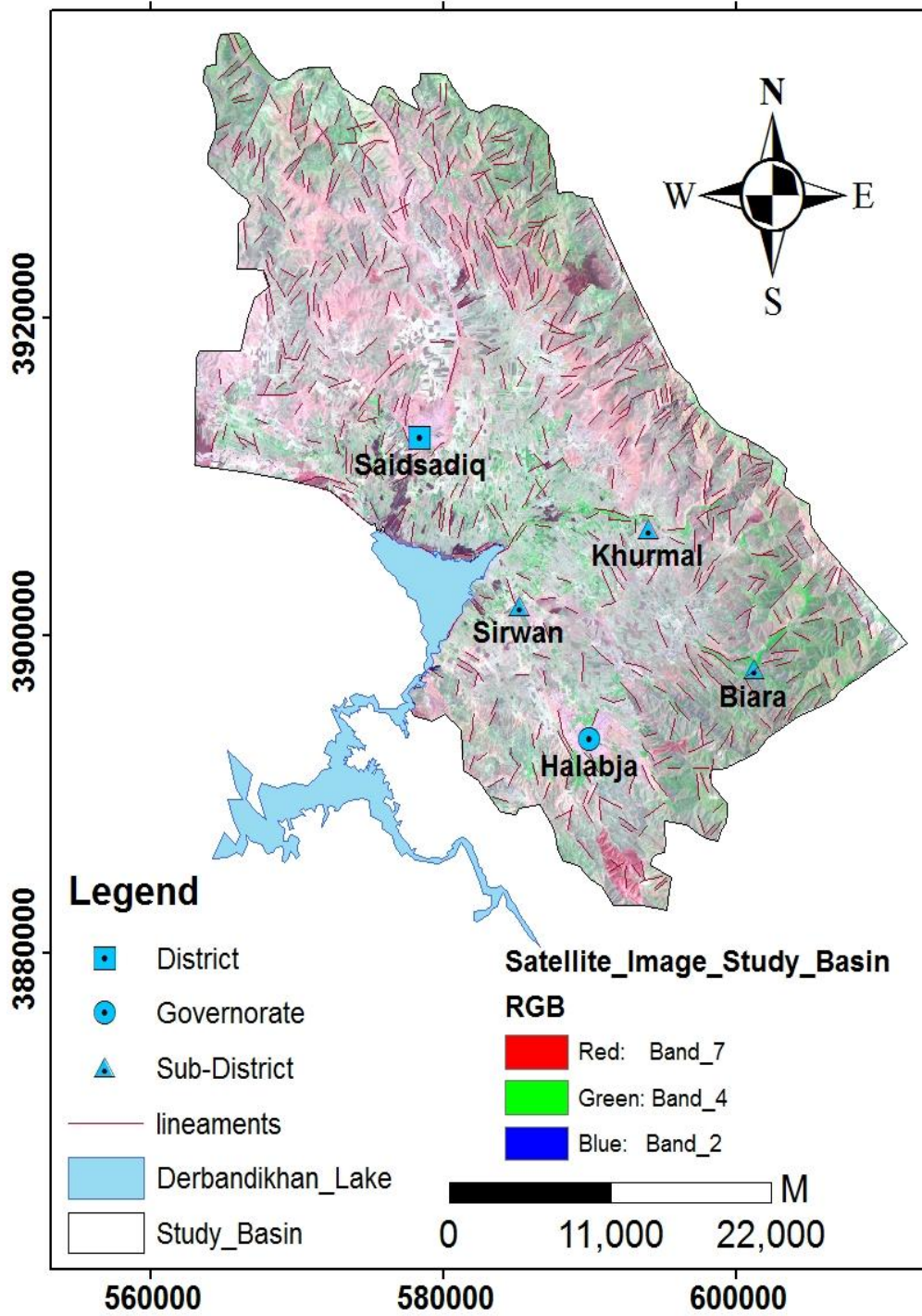
Figure 1.6: TM landsat 7 image (2013) of the studied basin with extracted lineament features.
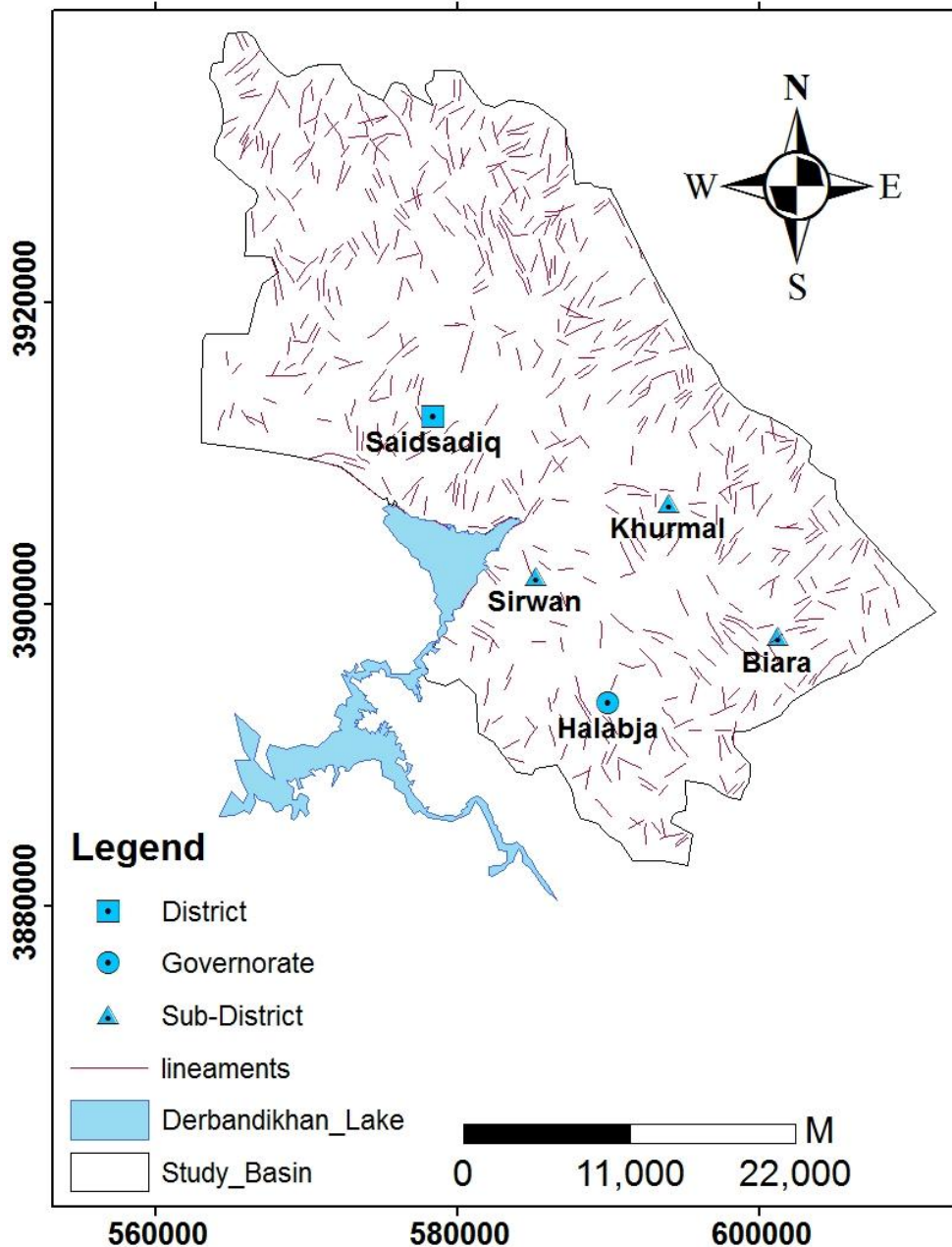
Figure 1.7: Extracted lineament map of the studied basin.

- Worral and Kolpin (2004) have examined the validity of the UK vulnerability system and found it to be in complete statistical disagreement with the actual groundwater contamination observations.

- Hussain (2004) has studied groundwater vulnerability assessment of the Ganga-Yamuna interfluves area in India using GIS. It was visualize the methods currently available for assessment of the groundwater vulnerability and to develop an appropriate method suitable for the

alluvial aquifers of the Ganga-Yamuna interfluves' area. Attempts have been made to develop a multipurpose database in GIS environment, and to validate the developed method by comparing its findings against the observed water quality characteristics of the region.

- Dixon (2005) has also developed similar ground water vulnerability maps through the use of three newly developed indices based on the detailed land use and land cover, pesticide and soil structure information and the selected parameters from the DRASTIC model. GIS, GPS, remote sensing and fuzzy rule-based methods were used for generating groundwater sensitivity maps.

- Worrall and Tim (2005) have evaluated the vulnerability of groundwater to pesticide contamination based on a Bayesian method for the major aquifer units of southern England.

- Groundwater vulnerability and risk mapping assessment based upon a source–pathway– receptor approach are presented by Nobre et al., (2007) for an urban coastal aquifer in northeastern Brazil.

- Ducci (2010) has studied aquifer vulnerability assessment methods: The non-independence of parameters problem in southern Italy.

- Neha Gupta (2014) studied groundwater vulnerability assessment using DRASTIC method in Jabalpur district of Madhya Pradesh in India.

- A number of other alternative indicies methods based on a range of parameters such as landuse (Crowe and Booty, 1995); travel time (Maxe and Johansson, 1998); chronic toxicity (Britt et al., 1992) and attenuation and retardation factors have been developed (Rao et al., 1985). For example, Shukla et al., (2000) have applied an attenuation factor based method of Rao et al., (1985) to show that there was a general agreement between the vulnerability prediction and observed groundwater contamination. Zektser et al., (2004) used a Point Count System (PCS) to study the impact of pollution on the Snake River aquifer system in eastern

Idaho, United States. Stewart et al., (2004) have applied a Type Transfer Function (TTF) approach to generate a regional-scale non point-source ground water vulnerability assessment for the San Joaquin Valley, California. The development and application based decision support framework of a GIS that integrates field scale models for assessment of nonpoint-source pollution of groundwater in canal irrigation project areas was presented by Chowdary et al., (2005).

In relation to making of vulnerability mapping for Kurdistan Region, for the first time in the Region, groundwater vulnerability mapping was studied by (Hamamin, 2011). He has studied hydrogeological assessment and groundwater vulnerability map of Basara Basin in Sulaimani Governorate using DRASTIC Model. Therefore, the current study is considered to be the second attempt in Kurdistan region and the first attempt on the study basin in terms of groundwater vulnerability mapping. Conversely, this study attempt to modify DRASTIC model based on the current groundwater quality and then to apply a different recommended model for comparing and validating the result of vulnerability zonation achieved from different models.

Some other provincial studies are directly or indirectly related to hydrogeological and hydrological conditions which have been done around the studied area. These studies can be summarized as follow:

- Parsons (1957) has investigated the groundwater resources in Sulaimani Liwa area. The investigation included collection, evaluation and correlation of geological and hydrogeological information pertaining to groundwater in the area (Parsons, 1957).

- The Hydrological condition of Sharazoor plain was studied by Polservice (1980).

- Hydrology, climate, and morphometric measurements of some watersheds in Sulaimani region have been studied by Barzinji (2003).

- Rauf (2004) has studied the most feasible economically and technically proposed system to satisfy the present and the future water supply demand of Halabjay Shaheed, Sirwan and Said Sadiq.

- Stevanovic and Markovic. (2003 and 2004) have studied the regional geology and hydrogeology of the governorates of Sulaimani, Erbil, and Dohuk, through the FAO United Nation program.

- Ali (2005) has studied effect of slide masses on groundwater occurrence in some areas of Sharazoor plain-NE of Iraq.

- Ali and Al-Manmi (2005) have studied geological and hydrochemical study of Zalim Spring, Shahrazoor, Sulamania, Iraq.

- Karim and Ali (2005) have examined the Origin of Dislocated Limestone Blocks on the Slope Side of Baranan (Zirgoez) Homocline: it is an attempt to outlook the development of western part of Sharazoor plain.

- Parsons (2006) has offered a report of public water supplies, the demand and growth parameters have also predicated on the expansion of the distribution systems in the urban areas to serve the full population.

- Stratigraphy and lithology of the Avroman Limestone Formation (Triassic) were studied in Iraq and Iran by Karim (2006).

- Ali (2007) has studied the investigation of the Sharazoor-Piramagroon basin in details in terms of Hydrogeological and morphometrical point of view. So the aquifers properties recharge estimation, chemical and bacteriological tests, sustainability of the groundwater resources, as well as the main risks and problems which have currently have an impact on the basin are also exposed.

- The water balance method was used by Al-Tamimi (2007) for conjunctive use of surface and subsurface water in Diyala basin. He had divided the basin into three sub basins, top Diyala, middle Diyala and south Diyala. The top Diyala sub-basin has represented by Darbandikhan basin.

- Baziany and Karim (2007) have re-studied possible the Qulqula conglomerate Formation in Halabja - Avroman area for the second time. They have proposed a new concept for the origin of accumulated conglomerate, those studies are considered the Qulqula conglomerate Formation as a part of Qulqula group, which overlies Qulqula radiolarian formation.

- Muhammed (2008) has studied drinking water quality assessment of Halabja area.

- Al- Jaf (2008) has presented a research entitle *Error Measurement in Digital Elevation Models in Pinjaween-Halabja Area*, that made a comparative between the Digital Elevation Models (DEM) taken from the Shuttle Radar Topography Mission (SRTM) and the data taken by Global Positional System device (GPS) of Garmin type.

- Sharbazheri (2008) has studied the Cretaceous-Tertiary (K/T) boundary section, which crop out within the High Folded Zone, Imbricated Zone and extended in northwest- southeast direction as a narrow trends near and parallel to the Iraqi / Iranian borders.

- Saprof (2008) has arranged the implementation plan for a Sirwan river project in Halabja. The feasibility study analyzes the economic and technical aspects, as well as financial viability of the project.

- Al-Mashhadani, et al., (2009) have studied dominant Landcover/ Landuse type in Sharazur Plain by using remote sensing techniques. The results indicated that there are 12 classes of Landuse / Landcover.

- Karim, et al., (2009) have studied historical development of the lineaments of the Western Zagros Fold-Thrust Belt in the Halabja City. They have also studied sedimentlogy and geochemistry of the limestone successions of the lower member of the Qulqula Formation.

- Raza (2009) has studied the lower member of Qulqula Formation in the Thrust Zone, (Kurdistan Region) near the Iraqi-Iranian borders.

- Al-Jaf and Al-Azawy (2010) have studied the integration of remote sensing images and GIS techniques to locate the mineral showings in Halabja area. Using satellite data received from ETM sensor that borne on Landsat 7 satellites depended on band rationing mean bands, band ratio color composite and threshold techniques.

- The environment, history, and archaeology of the shahrizor survey project have investigated by AL-Taweel, et al., in (2011).

- Land use / land cover changes of the Halabja city in the north part of Iraq over 1986 to 1990 by utilizing multi-temporal remote sensing landsat images (TM) were studied by Al-Doski, et al.,(2013 a & b) .

- Zakaria et al., (2013) have estimated the annual harvested runoff at Sulaymaniyah Governorate, Kurdistan Region of Iraq.

- Rauf (2014) has studied Groundwater Potential Mapping and Recharge Estimation of Halabja Area, North East of Iraq.

- Al-Ansari has studied Climatic change and long term future trends of rainfall at north-eastren Part of Iraq (2014). In this research, long term rainfall trends up to the year 2099 were pridicted in Sulaimani city northeast Iraq to give an idea about future prospects.

- Hamamin (2016) has studied Groundwater Vulnerability Map of Sulaymaniyah Subbasin using SINTACS model, Sulaymaniyah Governorate, Iraqi Kurdistan Region.

- Hamamin et al., (2018) also have studied hazard and risk intensity maps for water-bearing units: a case study in the Sulaimani sub-basin / North East of Iraq. They have applied the intrinsic vulnerability, hazard and risk intensity mapping to assess the risk harmfulness in the Sulaimani sub-basin by combining hydrogeological parameters using the DRASTIC system and the hazard components by taking the product of the weighted hazard value (H_I), the ranking factor (Q_n) and the reduction factor (R_f).

Chapter Two

Hydroclimatic

and

Water Balance Analysis

Chapter Two

Hydroclimatic and Water Balance Analysis

2.1 Climate

According to Koppen's classification, the climate of Kurdistan Region has been identified as arid and semi-arid climate. It is hot and dry in summer and cold and wet in winter, with short spring and autumn seasons compared to summer and winter. In winter, Kurdistan Region falls under the influence of Mediterranean cyclones that moves east to a northeast over the Region. The Arabian Sea cyclones move northward passing over the gulf carrying great amounts of moisture causing large amounts of precipitation over Kurdistan region. Occasionally, European winter cyclones move eastward to the southeast part of Turkey and over the mountainous Region of Kurdistan, bringing substantial amounts of rain and snow. In summer, the Region falls under the influence of sub-tropical high pressure belts and Mediterranean anticyclones. The sub-tropical high pressure centers that move from west to north and northeast passing over the Arabian Peninsula carrying sand and dust to the Region (Al-Ansari et al.,2014) and (Saeed and Abas, 2008).

Due to the unavailability of gauging and recently operated meteorological stations in Saidsadiq area, the climatic data of meteorological department station in Halabja city during the periods of 2002-2014 was utilized to analyse the climatic condition for the entire study area. The available climatic variables for this station are daily relative humidity in percent (%), wind speed (m/s), wind direction and speed, minimum, maximum, and mean temperature (°C), open free surface evaporation (mm), rainfall (mm), and sunshine duration (hrs). The maximum average monthly temperature was around 45 $^{\circ}$C in July and August while the lowest average degree was around -2 $^{\circ}$C recorded in January and February. This extreme characteristic is one of the main conditions of continental climate.

2.2 Climate Elements

The following climatic elements were used to analyze the climatic conditions with the study basin:

2.2.1 Precipitation

Precipitation was considered to be one of the most important parameters in analyzing water balance and aquifer recharge, as well as in assessing aquifer vulnerability. The study area is a part of the region affected by the Mediterranean climatological system, so precipitation occurs entirely during winter and spring seasons. The majority of the annual precipitation occurs from October to May. The four remaining months are commonly dry. The monthly maximum average precipitation is 135.74 mm in February. The average annual precipitation was 691.2 mm during the period of 2002–2014. Figures (2.1 and 2.2) show the monthly average and annual precipitation during the periods of 2002–2014, respectively.

	Oct.	Nov.	Dec.	Jan.	Feb.	Mar.	Apr.	May	Jun.	Jul.	Aug.	Sep.
Average	36.88	74.36	114.5	101.1	135.7	88.84	103.8	34.33	0.85	0.00	0.04	0.63
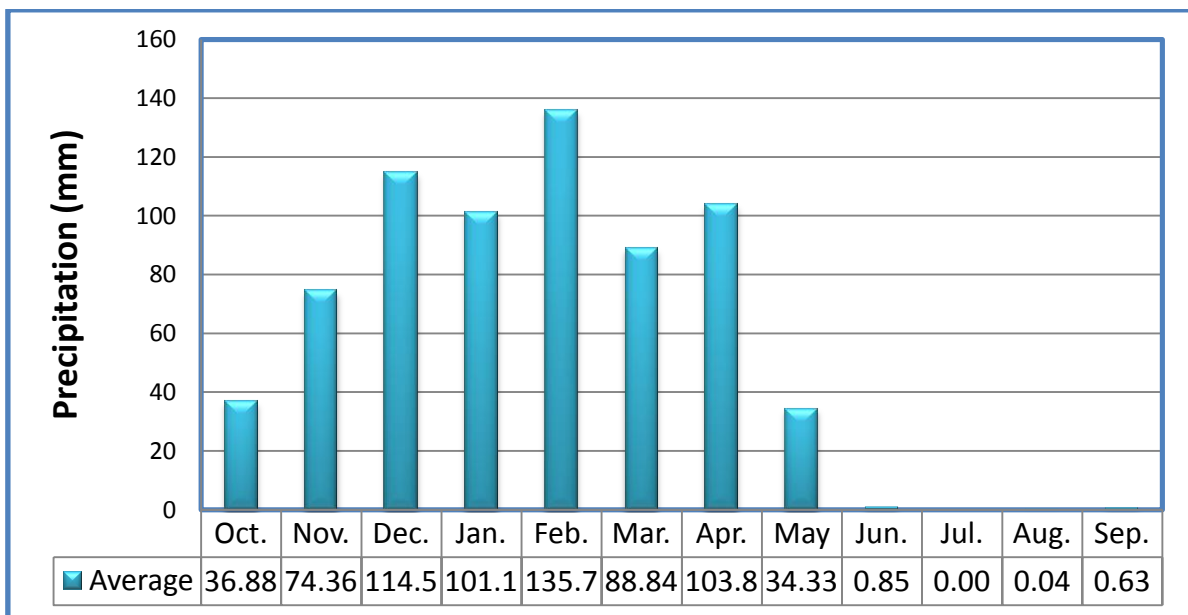
Figure 2.1: Average monthly precipitation of Halabja Station for the period (2002- 2014)

| Average | 895.7 | 705.4 | 823.6 | 872.7 | 684.4 | 396.1 | 473.9 | 857.2 | 626.9 | 585.3 | 886.8 | 486.4 |
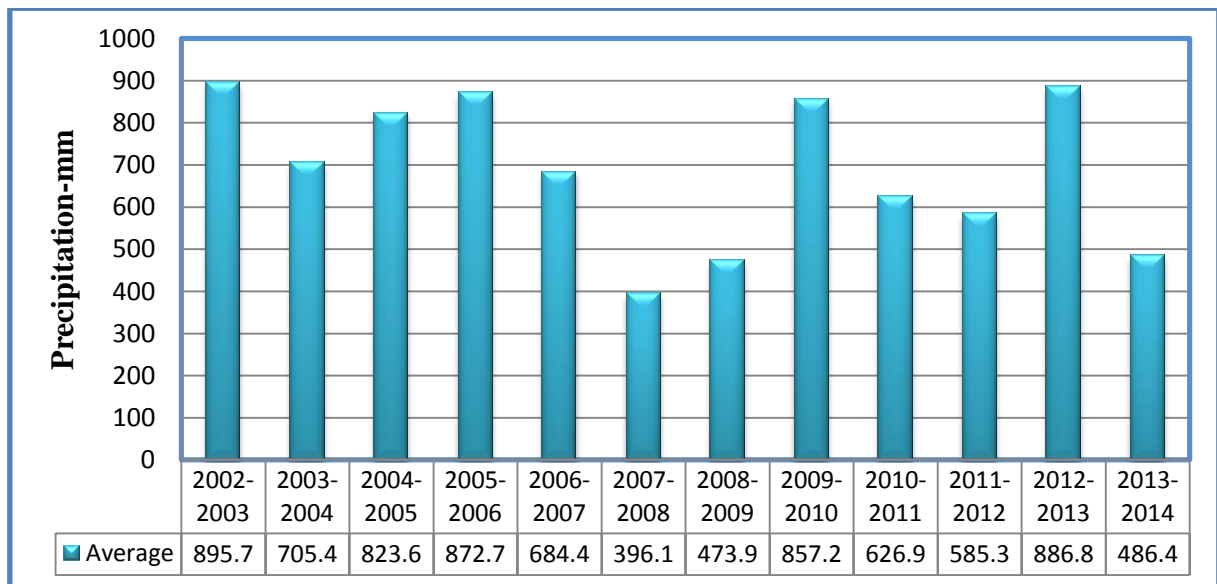
Figure 2.2: Annual precipitation of Halabja Station for the period (2002-2014)

2.2.2 Temperature

The monthly average air temperature value for the period of (2002–2014) at Halabja Meteorological Station was 21 ℃, and the monthly maximum average temperature was 35.27 ℃ in July, while the minimum was 8.18 ℃ in January. Figure (2. 3) shows the monthly annual average air temperature for the periods of 2002–2014.

2.2.3 Wind Speed

The prevailing wind direction in the Halabja station is mainly northwesterly winds. During summer, the northwestern wind blowing over the study basin. The monthly average of wind speed for the period 2002-2014 is shown in the Figure (2.4). The speed of these winds is often strong during the day and slightly decreases at night. The annual average of wind speed is 1.4 m/s. The monthly average, minimum and maximum values of wind speed in the study basin were 1.2 m/s, in November and 1.6 m/s in March and August respectively. Mountain winds are highly variable since the terrain and the upslope/ down slope winds vary the wind direction and speed diurnally.

Average	Oct.	Nov.	Dec.	Jan.	Feb.	Mar.	Apr.	May	Jun.	Jul.	Aug.	Sep.
	23.82	14.35	9.03	8.18	8.80	13.45	18.33	23.70	32.14	35.27	35.08	30.00
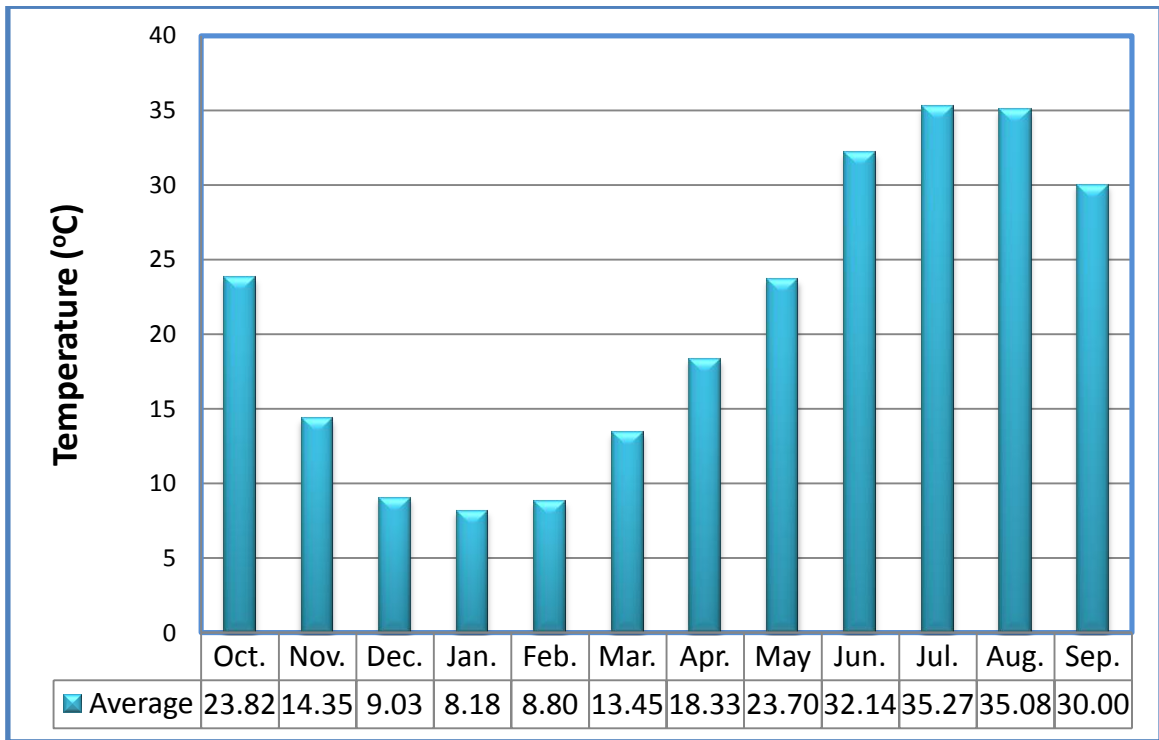
Figure 2.3: Average monthly temperature of Halabja Station for the periods (2002- 2014)

Average	Oct.	Nov.	Dec.	Jan.	Feb.	Mar.	Apr.	May	Jun.	Jul.	Aug.	Sep.
	1.4	1.2	1.3	1.2	1.3	1.6	1.4	1.5	1.4	1.5	1.6	1.5
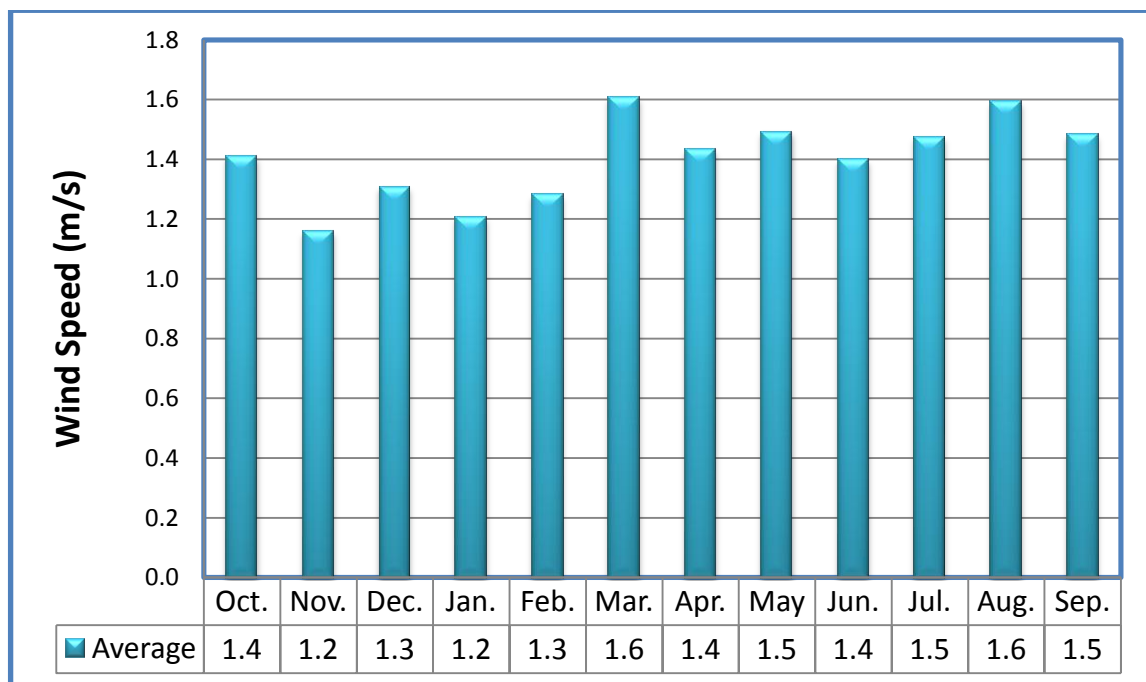
Figure 2.4: Monthly average wind speed of Halabja Station for the periods (2002- 2014)

2.2.4 Sunshine Duration

Sunshine is a climatological indicator, measuring duration of sunshine in a given period. It depends upon the position of the sun and is hence a function of latitude and day throughout the year. The longest sunshine duration occurs during the summer months, which is almost cloudless; it is expressed as hours of sunshine. The monthly average maximum sunshine duration occurs in August with an absolute value of 11 hours / day, and the monthly average minimum duration occurs in December to February with an absolute value of 5.4 hours/days. Figure (2.5) shows an average annual sunshine for the period of 2002-2014.

2.2.5 Relative Humidity

Relative humidity is the ratio of the water vapor density to the saturation water vapor density. Relative humidity is one of the most important factors that directly affects evapotranspiration and usually is expressed as percentage. The average of annual relative humidity is 43%. Minimum monthly average relative humidity occurs in June 23% and 60% was the monthly maximum average relative humidity in February. The monthly averages of relative humidity for the Halabja station for the periods 2002-2014 are shown in Figure (2.6). The relative humidity was maximum in winter months and minimum in summer months. An inverse relationship between air temperature and relative humidity exists, as temperature increases the relative humidity decrease and vice versa, see Figure (2.7).

2.2.6 Evaporation from Class (A) Pan

Pan evaporation is a measurement that combines or integrates the effects of several climatic elements: temperature, humidity, rainfall , drought dispersion and wind speed, (Chattopadhyay and Hulme,1997). The annual sum value of evaporation from class (A) pan was 2325 mm. The maximum monthly average evaporation was 402.4 mm in July, while the minimum was 47.9 mm in January;

Figure (2.8) shows an annual average evaporation from class (A) pan for the periods 2002–2014 at Halabja Meteorological Station.

■ Average	Oct.	Nov.	Dec.	Jan.	Feb.	Mar.	Apr.	May	Jun.	Jul.	Aug.	Sep.
	7.9	6.6	5.4	5.4	5.4	6.1	6.9	8.4	10.9	10.8	11.0	10.1
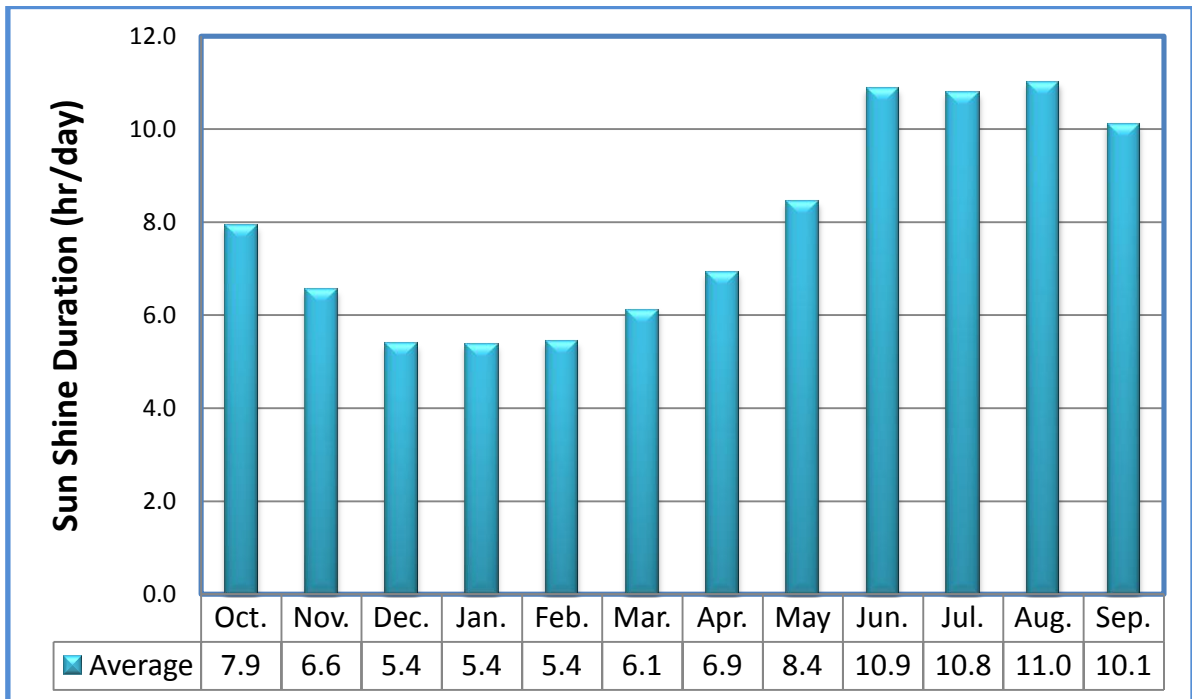
Figure 2.5: Average of monthly sunshine duration of Halabja Station for the periods (2002-2014)

■ Average	Oct.	Nov.	Dec.	Jan.	Feb.	Mar.	Apr.	May	Jun.	Jul.	Aug.	Sep.
	35	52	57	59	60	51	49	39	23	29	30	36
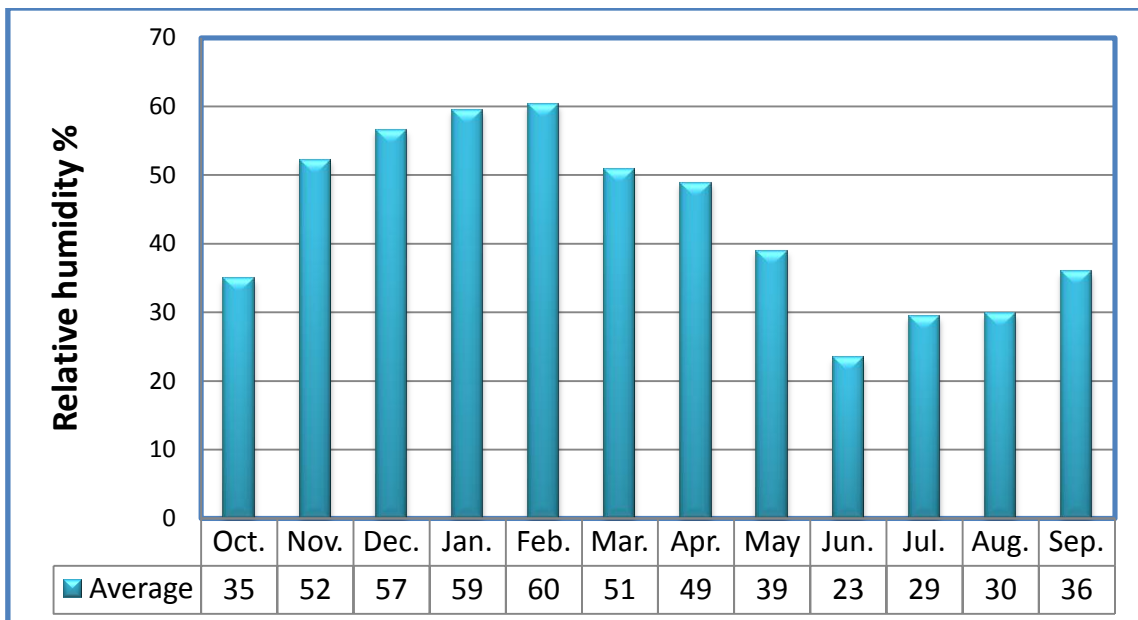
Figure 2.6: Monthly average of relative humidity of Halabja Station for the periods (2002-2014)
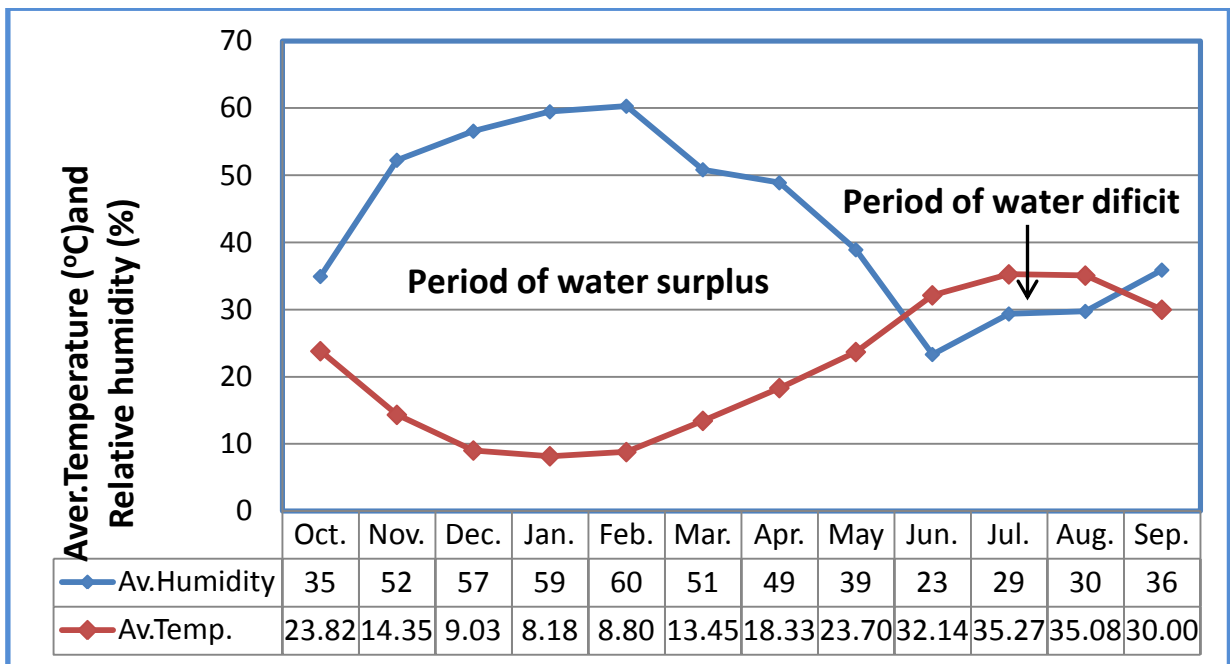
Figure 2.7: Relationship between temperature and relative humidity of Halabja Station

	Oct.	Nov.	Dec.	Jan.	Feb.	Mar.	Apr.	May	Jun.	Jul.	Aug.	Sep.
Av.Humidity	35	52	57	59	60	51	49	39	23	29	30	36
Av.Temp.	23.82	14.35	9.03	8.18	8.80	13.45	18.33	23.70	32.14	35.27	35.08	30.00
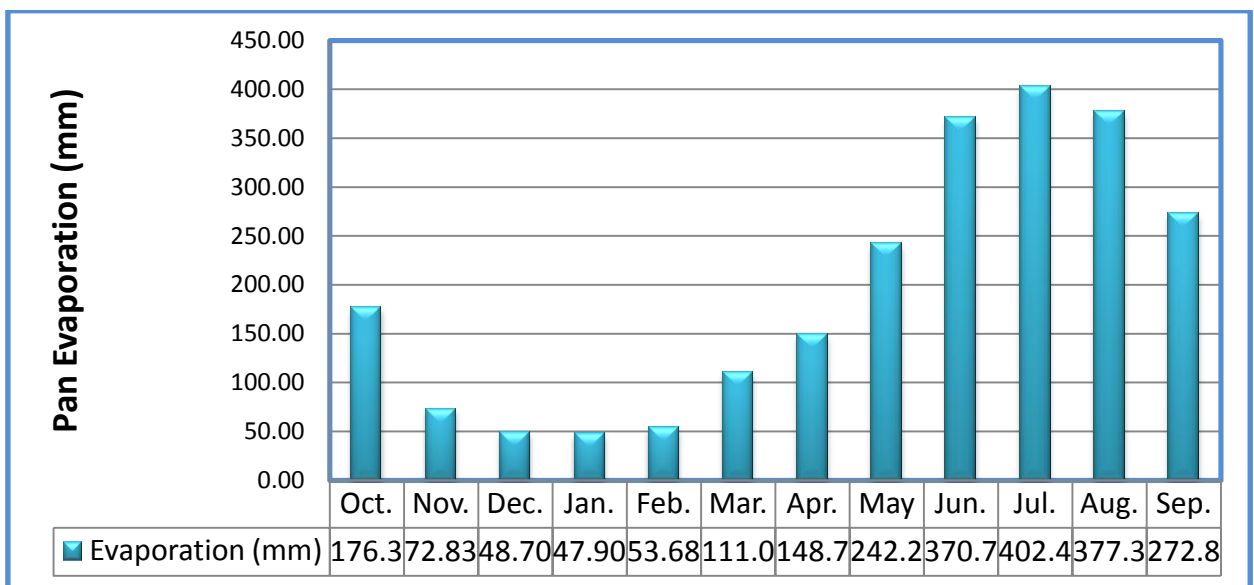
Figure 2.8: Monthly average of pan evaporation of Halabja Station for the periods (2002-2014)

	Oct.	Nov.	Dec.	Jan.	Feb.	Mar.	Apr.	May	Jun.	Jul.	Aug.	Sep.
Evaporation (mm)	176.3	72.83	48.70	47.90	53.68	111.0	148.7	242.2	370.7	402.4	377.3	272.8

2.3 Climatic Classification

To establish the climate type and the aridity index of the studied basin, the recommended classification by AL–Kubaisi (2004) was applied as explained in Table (2.1). Based on this classification, the following modes were used:

34

- Mode (1), this option is to identify the possible climatic zonation as (Humid, Moist) and (Arid, Sub–arid) by using the following equation:

$$\text{AI-1} = (1*P) / (11.525 * t) .... (2.1)$$

- Mode (2), this option is to evaluate the sub-zones from the results of type 2 mode as in table (2.1) , it is calculated based on the following equation:

$$\text{AI-2} = 2\sqrt{P}/t .... (2.2)$$

Where: AI= Aridity Index

P = Annual rainfall (mm)

t = Average temperature (C$^{\circ}$)

Aridity index was calculated by applying equations 2.1 and 2.2, which are equal to 2.86 and 2.5 respectively. According to this classification, the climate of the studied basin classified as humid to moist and moist for both modes 1 and 2, respectively.

2.4 Evapotranspiration

Evapotranspiration is the combination of two separate processes whereby water is lost on the one hand from the soil surface by evaporation from the crop by transpiration which is referred to as evapotranspiration (ET) on the other hand. Actual evapotranspiration (AET) is playing a significant role in the global water balance. This variable is defined as the quantity of water that is transferred as water vapour to the atmosphere from an evaporating surface (Wiesner, 1970) under real conditions (e.g. water availability, vegetation type, physiological mechanisms and climate).

Potential evapotranspiration (PET) is defined as the maximum amount of water capable of losing water as vapour, either by evaporation or transpiration in a given time by actively growing vegetation completely shading the ground, of the uniform height, and with adequate water through the soil profile

(Chattopadhyay & Hulme, 1997). The influence of surface types in PET is removed by using the concept of reference evapotranspiration (ET_o).

Table 2.1: Type1 and type2 mode options climate classification (after Al–Kubaisi, 2004)

Type 1	Evaluation	Type 2	Evaluation
AI. 1 > 1.0	Humid to moist	AI. 2 > = 4.0	Humid
		AI. 2 < 4.0 AI. 2 >= 2.5	Humid to moist
		AI.2 < 2.5 AI.2 > = 1.85	Moist
		AI.2 < 1.85 AI.2 >= 1.5	Moist to Sub-arid
AI. 1 < 1.0	Sub–arid to arid	AI.2 < 1.5 AI.2>= 1.0	Sub- arid
		AI.2 < 1.0	Arid

The ET_o represents the atmospheric evaporative demand of a reference surface (generally, a grass crop having specific characteristics), and it is assumed that the water supply from the land is unlimited (Allen et al., 1998). Evapotranspiration of any crop could be estimated by multiplying the reference crop evapotranspiration with the crop coefficient of the crop of interest. The FAO Penman-Monteith method is considered to be the most convenient method for determining evapotranspiration. It uses more parameters than other methods such as solar radiation, air temperature, air humidity and wind speed data. According to Allen et al., (2006), the equation is expressed as:

$$ETo = \frac{0.408\Delta(Rn-G)+Y\frac{900}{(T+273)}U2(es-ea)}{\Delta+Y(1+0.34U2)} \quad \ldots\ldots\ldots\ldots\ldots (2.3)$$

Where:

ET_o: Reference evapotranspiration [mm day^{-1}]

R_n: Net radiation at the crop surface [MJ m^{-2} day^{-1}]

G: Soil heat flux density [MJ m^{-2} day^{-1}]

T: Mean daily air temperature at 2 m height [$^{\circ}$C]

U_2 :Wind speed at 2 m height [m s^{-1}]

e_s :Saturation vapour pressure [kPa]

e_a :Actual vapour pressure [kPa]

e_s-e_a :Saturation vapour pressure deficit [kPa]

Δ: Slope vapour pressure curve [kPa $^{\circ}$C $^{-1}$]

γ: Psychrometric constant [kPa $^{\circ}$C $^{-1}$]

The mean monthly values of the required parameters for calculating reference evapotranspiration (ET$_0$) and effective rainfall were measured during the periods 2002 – 2014 using CROPWAT version 8 software programs. Results are tabulated in Table (2.2) and presented in Figure (2.9).

The results of the FAO Penman-Monteith method confirmed that a very high evapotranspiration rate was recorded during the summer (205, 226.8 and 223.2) mm on June, July and August, respectively. While the rates decrease to reach the lowest amount in December and January 29 mm where the monthly average temperature was around 8 $^{\circ}$C. Thus, with the starting of the dry season from June to the beginning of the wet season October, the loss by evapotranspiration will be higher than the total amount of precipitation that falls into the basin. Accordingly, temperature has a great effect on the evaporation rate in the area.

Table 2.2: Monthly mean values of effective rainfall and reference evapotranspiration for the studied area calculated by CROPWAT 8.0

	Oct.	Nov.	Dec.	Jan.	Feb.	Mar.	Apr.	May	June	July	Aug.	Sept.	Total
P$_{eff}$ (mm)	0	0	110.4	82.0	104.6	44.5	0.0	0.0	0.0	0	0	0	341.49
ET$_o$ (mm)	124.3	56.0	29.0	29.0	38.0	51.0	105.0	160.0	205.0	226.8	223.2	174.4	1421.59
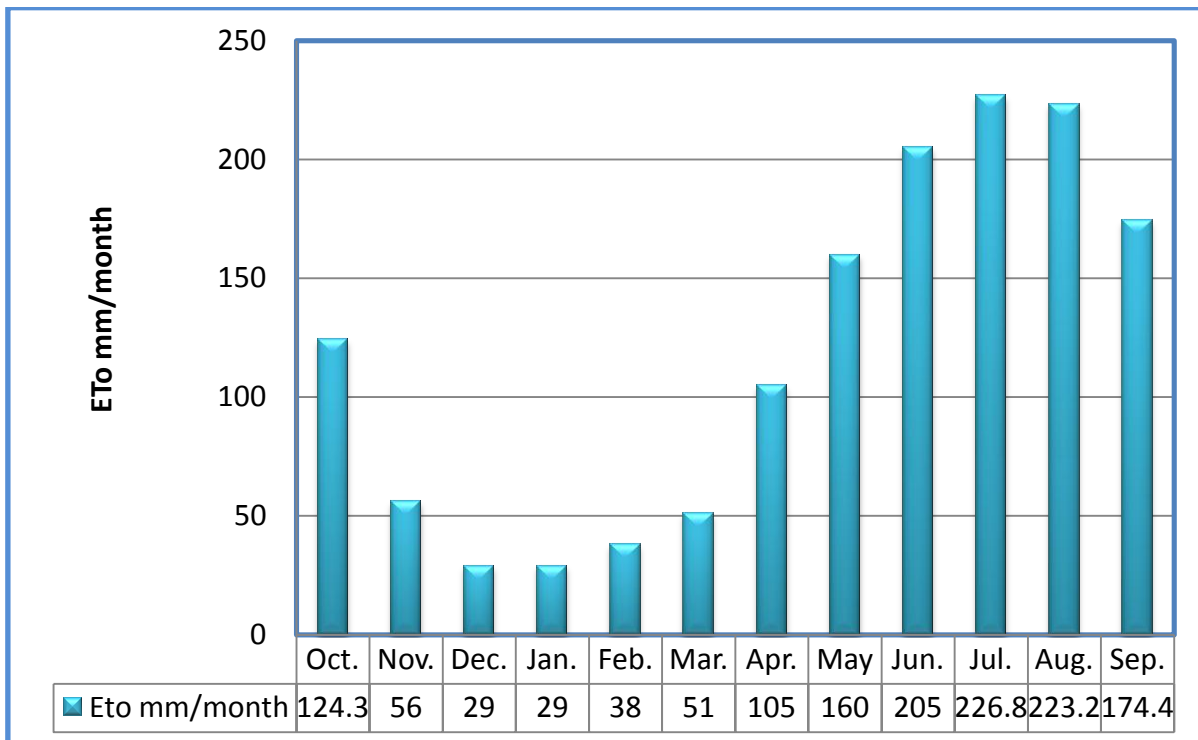
Figure 2.9: Monthly average reference evapotranspiration of Halabja Station for the periods (2002-2014)

2.5 Land Use and Land Cover

Land use and land cover (LULC) are an essential environmental parameters for understanding the causes and trends of human and natural processes (Meyer, et. al., 1992). Basically LULC consist of two terms; Land use (LU) and land cover (LC). LC covers the surface of the earth such as water, snow, forest, grassland, and bare soil; while land use describes how the land cover is modified in to use for example agricultural land, built up land and urban areas (Cihlar, et. al., 2001). Two different scenes of landsat Thematic Mapper 8 (TM) are used to prepare LULC map since the study basin is located in between them. Images consist of seven spectral bands for both of them with cell size 30x30 m for Bands 1 to 5 and 7. While spatial resolution for Band 6 (thermal infrared) is 120 meters, however this band is re-sampled to 30-meter pixels. Nearly, scene size is 170 km north-south by 183 km east-west and the date back to 03/May /2013). Figure (2.10) shows the TM Landsat image for the studied basin.

The most important step in LULC preparation is the classification processes because it shows the degree of accuracy. There are several proposed methods for LULC classification in the world but the USGS system that is developed by Anderson et al. (1976) was selected to apply in this study. The USGS system of classification consists of four levels, from, I to IV; the difference between them depends on the resolution of remote sensing data used for classification, (Bety, 2013). ERDAS IMAGINE software was used to prepare a digital image classification of the study basin. Supervised classification for level I of USGS is done with a band combination RGB / 742 for image covered basin. The study area is extracted from the results of classified map according to the boundaries of the catchment of the studied basin using ArcGIS software. The analyses of this study are supported by field works, many points were taken with GPS as a reference point and several photos were taken in order to check the accuracy and validity of the final map of classification.

The LULC map of the study basin is exposed in Figure (2.11). This produced map is based on USGS method of classification (Bety, 2013), using remote sensing and GIS techniques from satellite landsat images (ETM+, 2013). The map demonstrates that only five classes can be recognized as explained in Table 2.3 with percent and the area of land covering of each. In which two classes represent more than 95% of all studied area, while the other three classes covered less than 5%.

The map illustrates that barren land covered most of the studied basin land with an area of 766.36 km^2 or 59.97% of the total studied area. In addition, agriculture land mostly covers an area of 449.77 km^2 or 35.19% and occupies the central and northwestern parts of the studied basin. The remaining classes of vegetation, urban area and water and wet land covering areas of 39.75, 16.79 and 5.33 Km^2 or 3.11%, 1.31% and 0.42% of the whole studied area, respectively. To check the accuracy of the final LULC map, several points within the field were taken with GPS in each class and matched on the map. In addition, several photos of each point were taken too; all results verify the

accuracy of this classification and the result of the field survey coincides with the theoretical classification using remote sensing. Plates (2.1 and 2.2), illustrate urban area and agriculture land as an example for checking accuracy with coordinate value of 579195, 3912525 and 589644, 3909281, respectively and both points placed on LULC map, (Figure 2.11).
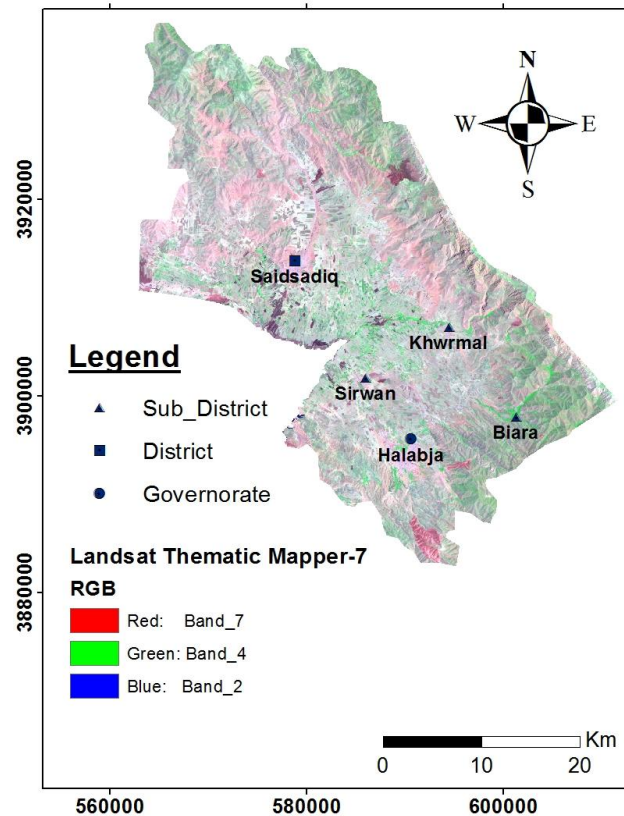
Figure 2.10: TM landsat-7 map (2013) of the studied basin

Table 2.3: LULC classes type in the studied basin

Level I Classes	Area (Km^2)	Area(%)
Urban	16.79	1.31
Agriculture	449.77	35.19
Barren Land	766.36	59.97
Vegetation	39.75	3.11
Water and wet land	5.33	0.42

2.6 Soil Classification

Normally, the soil of the study area is the product of weathering, erosion and sedimentation during the Quaternary period. The soils of the plains and the outer parts of the depression are generally permeable and well to moderately well drained (Berding, 2003); while soils in mountain regions are variable due to the differences in exposure, rate of runoff, topography and soil depth.

Plate 2.1: Urban area at saidsadiq district   **Plate (2.2) Agriculture land close to Banishar village**

In the studied basin, sand, silt and clay contents vary within rather narrow limits and the vast majority of soils have silty clay loam over silty clay. The silt content is typically higher than the clay content with 50-65% silt, 30-45% clay and 5-10% sand. The recent alluvial deposit (lower terraces) close to the rivers is the texture more variable and includes sandy and loamy soils. The aeolian/fluviatile cover is thin or has been eroded and the underlying gravel (and cobble) beds are exposed. The gravel and cobble content of the soils may then change over short distances from nil to more than 40%. Gravelly/cobbly soils are estimated to occupy less than 10% of the plains, (Berding, 2003).
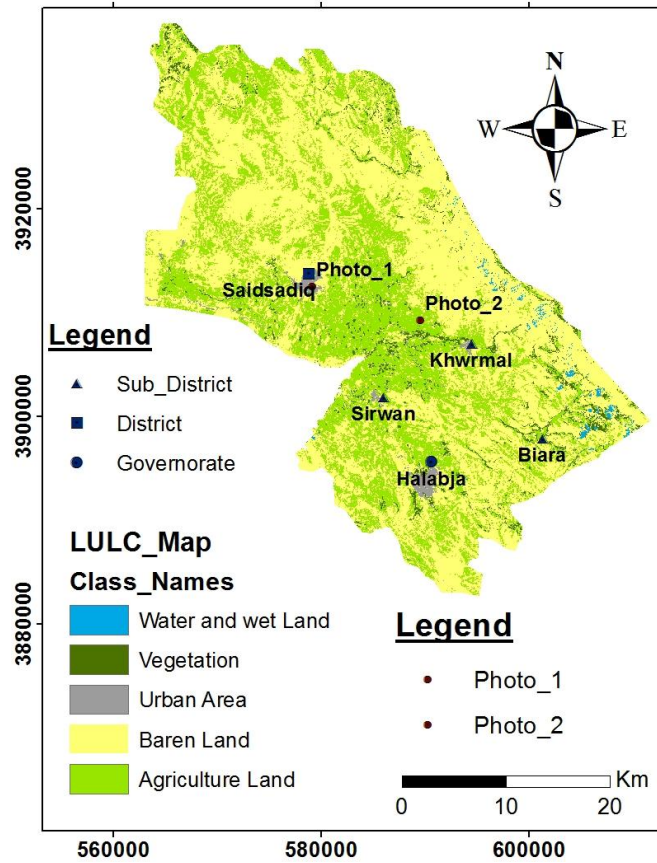
Figure 2.11: LULC map for the studied basin

Generally, the soils of the study basin are rich in lime (20 to 40 % CaCO3 are commonly found values) and very often have a pH between 7.5 and 8.2, (Ali, 2007). The high lime content and the associated mild alkalinity of the soils reflect the geological pattern and overwhelming presence of limestone rocks in the various sedimentary formations which form the parent materials. According to (Barzinji, 2003), the dominant soils of the plains are Chromoxererts and Calcixerolls, while Rendolls is dominant on the northern facing slopes of the mountains. On the other hand, Xerorthents is the dominant group on the southern facing slopes.

The soil infiltration capacity of the studied basin was carried out for 27 selected sites, (viz section 1.7.1), which overlying different geological units and covering most of the studied area, figure (2.12), a part from mountain area in which soil is very thin or absent. Details about the infiltration test sites and iteration by SPSS program is given in Appendixes (2.1 & 2.2) respectively.

Based upon the soil classification by Nikolov (1983), the results of (27) locations of the test sites, illustrated three zone soil class in terms of intensity of infiltration rate including (slow-moderate, moderate and moderate to rapid) classes. 21 sites are classified as moderate infiltration rates which are located in the alluvial deposits and several sites have been underlying by Balambo Formation. One location (3) was slow to moderate type, underlined by alluvial deposits and the soil totally consists of clay materials. Results of the reaming sites 1, 4, 11, 15 and 22 have showed moderate to rapid infiltration classes have occurred because the upper layer was comprised mainly of impermeable clayey layers (Table 2.4).

Three different soil classes were found in the area based on the soil map proposed by (FAO, 2001 and Berding, 2003), including Lime rich ,gravely to gravely silty-clay to clay, loamy to clayey soil and drained loamy to clayey soil (Figure 2.13).

2. 7 Water Balance

The existing imbalance of water availability and water demand cause water scarcity to be one of the most pressing environmental issues around the world today, therefore, without an accurate study of water balance; it is difficult to manage water resources for any country. A water balance includes accounting all amounts of volume of water that enters and leaves the system in a specific period. When working on the water balance, it is predictable to confirm that existance of water within a country is a highly dynamic and variable process both spatially and temporarily.

The water balance prediction of an area cannot be taken as a final result, because there are several factors that play an important role in controlling water balance such as the human influence, change with the water demands and climatic variations. The water balance process must be monitored, controlled, and updated continuously. Major role of each water balance is a long term sustainable management of water resources for a given area *(*Rauf, 2004). For

the studied basin, the water balance shows that the input and output are equal, where any change for one of these elements will lead to a change in the storage.

Input (P) – output (ET+R_O) = change in storage (ΔS) ………… (2.4)

Where (P) is precipitation and considers the only input, (R_o) is surface run-off and (ET) is evapotranspiration , and is considered as the maximum water loss.
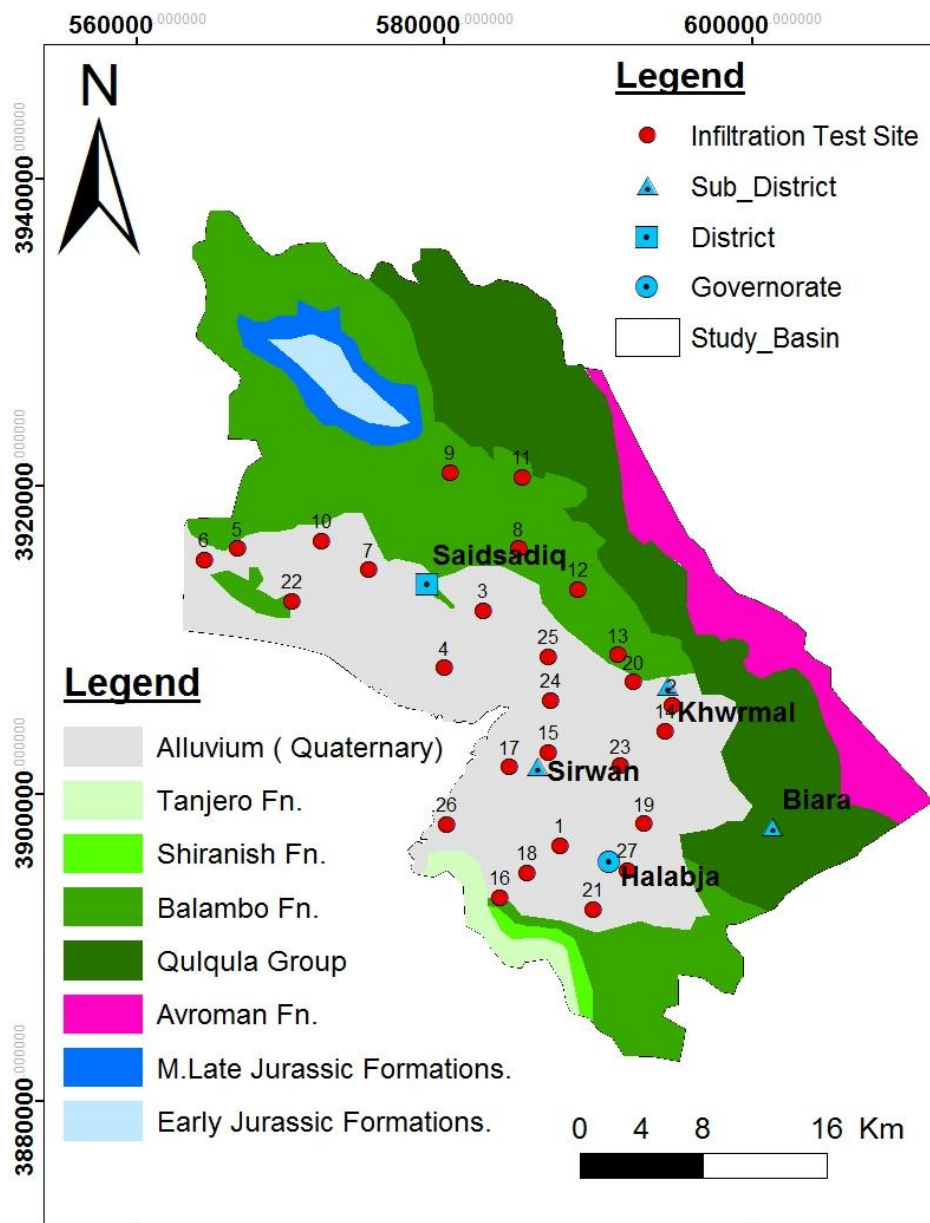
Figure 2.12: Location sites for infiltration test in the studied basin

Table 2.4: Results of infiltration test using double ring infiltrometer

Location	F_p(mm/hr)	Type	Underneath Geological Formation
Site-1	115.8	Moderate_Rapid	Quaternary deposits
Site-2	57.7	Moderate	Quaternary deposits
Site-3	9.0	Slow_Moderate	Quaternary deposits
Site-4	89.3	Moderate_Rapid	Quaternary deposits
Site-5	58.4	Moderate	Quaternary deposits
Site-6	42.4	Moderate	Quaternary deposits
Site-7	59.8	Moderate	Quaternary deposits
Site-8	48.3	Moderate	Balambo Fn.
Site-9	55.5	Moderate	Balambo Fn.
Site-10	46.3	Moderate	Quaternary deposits
Site-11	63.2	Moderate_Rapid	Balambo Fn.
Site-12	37.0	Moderate	Balambo Fn.
Site-13	42.7	Moderate	Balambo Fn.
Site-14	53.1	Moderate	Quaternary deposits
Site-15	63.3	Moderate_Rapid	Quaternary deposits
Site-16	47.0	Moderate	Quaternary deposits
Site-17	46.8	Moderate	Quaternary deposits
Site-18	51.0	Moderate	Quaternary deposits
Site-19	47.7	Moderate	Quaternary deposits
Site-20	46.1	Moderate	Quaternary deposits
Site-21	57.0	Moderate	Quaternary deposits
Site-22	60.9	Moderate_Rapid	Quaternary deposits
Site-23	49.1	Moderate	Quaternary deposits
Site-24	41.8	Moderate	Quaternary deposits
Site-25	52.1	Moderate	Quaternary deposits
Site-26	49.7	Moderate	Quaternary deposits
Site-27	46.9	Moderate	Quaternary deposits
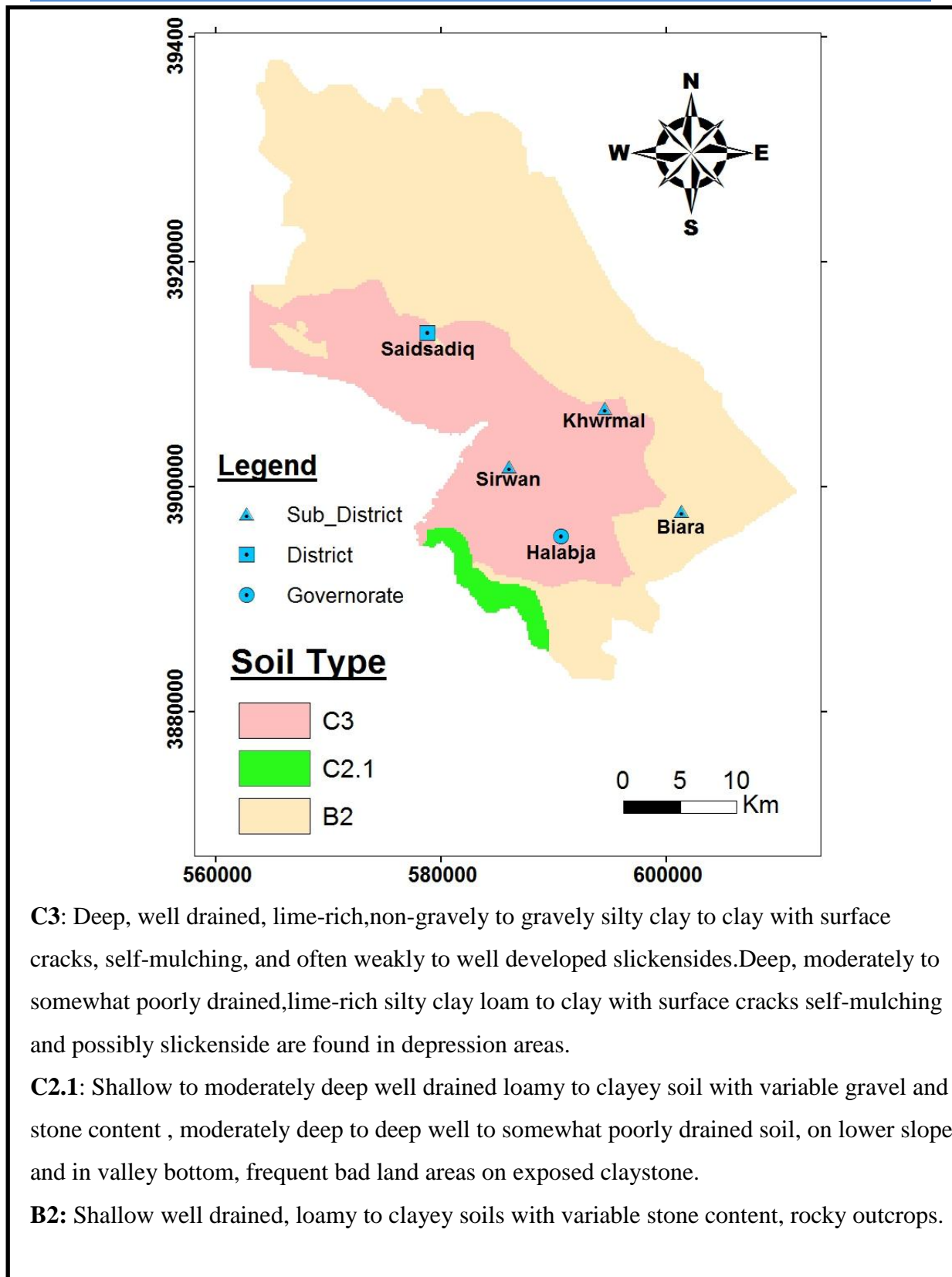
C3: Deep, well drained, lime-rich,non-gravely to gravely silty clay to clay with surface cracks, self-mulching, and often weakly to well developed slickensides.Deep, moderately to somewhat poorly drained,lime-rich silty clay loam to clay with surface cracks self-mulching and possibly slickenside are found in depression areas.

C2.1: Shallow to moderately deep well drained loamy to clayey soil with variable gravel and stone content , moderately deep to deep well to somewhat poorly drained soil, on lower slope and in valley bottom, frequent bad land areas on exposed claystone.

B2: Shallow well drained, loamy to clayey soils with variable stone content, rocky outcrops.

Figure 2.13: Dominant soil type of studied basin (after Berding, 2003)

2. 8 Water Balance Calculation Methods

There are different methods for water balance calculation for any area; the majority of them estimate water balance that is based on the meteorological conditions and climatic elements. In addition to that, details of the land use, vegetal cover, cropping pattern and soil map are necessary for water management and development.

2.8.1 Crop Water Balance Method

In the arid and semi-arid climatic condition, irrigation is essential to recompense for the deficit by evaporation due to insufficient or erratic precipitation. Therefore, estimating the crop water requirement in such an environment is important in assessing water balance method especially where the dry season of the area is regularly dry (Allen, 2006). To run crop water balance model, several different software programs were developed while the most widely used is CROPWAT 8.0 which is developed by FAO for planning and management of irrigation water. CROPWAT 8.0 for Windows is a computer program for the calculation of reference evapotranspiration, crop water requirements and irrigation requirements and more specifically the design and management of irrigation schemes (Behmanesh, 2003). Furthermore, the program permits the development of irrigation schedules for different management conditions and the calculation of scheme water supply for varying crop patterns (Swennenhuis, 2009). All calculation procedures as used by this program are based upon the FAO guidelines (Allen et al 1998). In order to estimate the crop water requirement, the following parameters are required:

2.8.1.1 Climate / Reference Crop Evapotranspiration (ETo)

The Climate/ET_o module has been calculated by using the FAO Penman–Monteith equation, which requires basic information on the meteorological station, such as 'altitude', 'latitude' and 'longitude' together with climatic data, that can be an input on a monthly or daily basis. Regarding the present study, a monthly basic climatic data required for estimating ET_o included: minimum and

maximum air temperature, relative humidity, sunshine duration and wind speed, (Table 2.5).

2.8.1.2 Effective Rainfall Data

The effective rainfall can be defined as that portion of rainfall which contributes to groundwater storage. Rainfall data is another required information on the precipitation values on a monthly decade or daily basis to calculate the effective rainfall. In the present study, the monthly rainfall data was used too, (Table 2.5).

2.8.1.3 Cropping Pattern

The crop module is one of the most required parameter as data input in order to estimate the crop water requirement. For running cropping pattern, the: (Planting data, crop coefficient Kc, rooting depth, critical depletion fraction and planted area) parameter are required. In this study, different land covers are considered to be the major land cover in the study basin and are used in estimating of evapotranspiration including arable area with non-arable area (orchard, forest, natural pasture and residential area). All assumptions were made based on the Land cover types such as rooting depth and growth stage. However, variables like crop coefficient and water capacity in the root zone were assigned by an average value weighted by the area covered with particular land use. While, assumptions are introduced where there are no published values for variables of a certain land cover type in a specific environment similar to the study area. After inputting all the required data, the software (CROPWAT 8.0) was used based on the monthly input data, and the output for different cultivated crops in the studied area is tabulated and summarized in Table (2.5).

2.8.2 The Mehta Simple Water Balance Model

This model is a modification of Thornthwaite-Mather, (1955) model for estimating water balance, which is done by Mehta et. al., (2006).

The soil types divided into different groups that are based on the previous work carried out by Stevanovic et al. (2004) and from soil infiltration test

carried out during this work, as used in the calculation of the available water capacity of the root zone, (see Figure 2.13).

Based on the table proposed by Thornthwaite and Mather (1957) for calculating AWC (Table 2.6), is benefited from the ratios of each zone of the soil cover calculated from the soil map. The AWC of the studied basin was estimated as 112 mm (Table 2.8) regarding the soil texture, crop type and weight of each type of soil. The weight of each zone with the area that each class occupied was calculated, and then this result was putted into the model to calculate the Soil Water Content (SWC), and later in assessing the water balance method.

The water balance is estimated based on the average monthly climatic variables over the period of (2002-2014). The general equation applied to the soil water balance model presented in the table (2.6). Table (2.7) illustrated the results of running model as Excel spreadsheet software which is prepared by (Mehta et. al., 2006). Regarding the average precipitation which is required for this model, average monthly rainfall was used, (Figure 2.1). Reference potential evapotranspiration was calculated by the Penman-Monteith methods .

As indicated in Figure (2.14) and Table (2.9), the predicted runoff model has occurred by the beginning of November and continued into the middle of April where the rate of both actual and potential evapotranspiration exceeding the amount of precipitation. This effect continues during the dry season. Accordingly, the total amount of annual water surplus was estimated as 341.5 mm, which comprises 46% from the annual precipitation fall over the catchment area.

When $P > PET$ then $AET = PET$

When $P < PET$ then $AET = dSW + P$

Where;

P is precipitation ,**PET** is a potential evapotranspiration **AET** is an actual evapotranspiration and **dSW** is the change i n soil water content.

Table 2.5*: Results of main cultivated crops in the studied area using CROPWAT 8.0

Crop Type \ Parameters	Barley	Wheat	Chickpea & lentil	Winter vegetation	Summer vegetation	Fallow
Total rainfall (mm)	635	635	225	690	115.2	320.6
ET_c (mm/dec)	374.2	430.1	397.2	1385.1	450.9	274
Effective rainfall (mm/dec)	276	321	130.2	405.2	78.2	180.4
Total rain loss (mm/dec)	359	314	94.8	284.8	37	140.2
Actual water use by crop in (mm)	367.5	425.2	390.6	1382.3	448.2	271.2
Actual Irrigation required(mm/dec)	111.2	105.6	263.5	1021.2	366.5	95.2
Moist deficit at harvest (mm)	105.2	105	40.5	131.2	39.6	95.2
Efficiency rain (%)	43.5	50.6	57.9	58.7	67.9	56.3

2.9 Soil Conservation Service Method (SCS-CN)

The SCS-CN method is applied to estimate the annual volume of surface runoff in the study basin. In the SCS model, runoff is calculated monthly as a function of a soil's infiltration capacity, the land cover, and the antecedent soil moisture. The variable requirements of this method are rainfall amount and curve number. The curve number is based on the area's hydrologic soil group, land use,

treatment and hydrologic condition (USDA, 2004).The empirical rainfall-runoff relation is, (Mehta et al.,2006):

Table 2.6: Equations of the soil water balance model (Mehta et al.,2006)

Situation in the watershed	SW	APWL	Excess
Soil in drying Δp<0	=AWC exp(APWLt /AWC)	= APWL $_{t-1}$ +Δ p	= 0
Soil in wetting Δp>0, but SW $_{t-1}$ + Δp $\leq$ AWC	= SW $_{t-1}$ + p	=AWC ln (SWt /AWC)	= 0
Soil is wetting above capacity _Δp>0, but SW $_{t-1}$ + Δp > AWC	= AWC	= 0	= SW$_{t-1}$ + p−AWC

$$Q = \frac{(P-0.2S)^2}{(P+0.8S)} \dots\dots\dots\dots\dots\dots(2.5)$$

Where:

Q = runoff in (mm), P = Total precipitation in (mm) (average monthly record is used), S = retention including the initial abstraction which is calculated from the following equation, (Mehta et al.,2006):

$$S = \frac{25400}{CN} - 254 \quad \dots\dots\dots\dots\dots\dots\dots(2.6)$$

Where CN = curve number.

Table 2.7: Suggested available water capacity for combinations of soil texture and vegetation (Thornthwaite and Mather, 1957)

Vegetation	Soil texture	AWC (% volume)	Rooting depth (m)	AWC (mm)
Shallow rooted crops (spinach, peas, beans beets, carrots, etc)	Fine sand	10	0.5	50
	Fine sandy loam	15	0.5	75
	Silt loam	20	0.62	125
	Clay loam	25	0.4	100
	Clay	30	0.25	75
Moderately deep rooted crops (corn, cereals, cotton, tobacco)	Fine sand	10	0.75	75
	Fine sandy loam	15	1	150
	Silt loam	20	1	200
	Clay loam	25	0.8	200
	Clay	30	0.5	150
Deep rooted crops (alfalfa, pasture, grass, shrubs).	Fine sand	10	1	100
	Fine sandy loam	15	1	150
	Silt loam	20	1.25	250
	Clay loam	25	1	250
	Clay	30	0.67	200
Orchard	Fine sand	10	1.5	150
	Fine sandy loam	15	1.67	250
	Silt loam	20	1.5	300
	Clay loam	25	1	250
	Clay	30	0.67	200
Mature forest	Fine sand	10	2.5	250
	Fine sandy loam	15	2	300
	Silt loam	20	2	400
	Clay loam	25	1.6	400
	Clay	30	1.17	350

Table 2.8: Ratio and exposed area for the land use and vegetal cover zones

Arable Area	Wheat	Barley	Chickpea	Lentil	Winter Vegetation	Summer Vegetation	Fallow	Sum
Hectar	66.58	4.501	0.52	0.01	1.28	9.17	35.15	**117.21**
Km^2	416	28.13	3.24	0.08	8.00	57.32	219.70	**732.58**
% of arable area	56.80	3.84	0.44	0.01	1.09	7.82	29.99	**100**
% of basin	27.31	1.85	0.21	0.01	0.52	3.76	14.42	**48.08**

	Arable area	Non arable Area	Orchard	Forest	Natural Pasture	Residential	Sum
Hectar	117.2	18.43	1.17	13.91	36.95	6.26	**193.92**
Km^2	733	115	73	87	231	39	**1278**
% of basin	57	9	6	6.80	18.07	3	**100**
AWC	75	50	250	300	150	75	**150**
AWC by area (Km^2)	43	4.5	14	20	27	2.30	**112**

Table 2.9: Long term of the studied basin catchment soil water balance

Months	Oct	Nov	Dec	Jan	Feb	Mar	Apr	May	Jun	Jul	Aug	Sep	Total
P	36.8	74.4	129.6	101.2	135.7	88.84	88.81	34.3	0.9	0.0	0.0	0.6	691.2
ET_O	124.3	56.0	29.0	29.0	38.0	51.0	105.0	160.0	205.0	226.8	223.2	174.4	1421.6
K_C	0.7	0.7	0.7	0.7	0.8	0.9	0.9	0.8	0.7	0.6	0.6	0.6	0.7
PET_{crop}	82.1	37.0	19.1	19.1	31.2	44.4	96.6	126.4	145.5	129.2	127.2	99.4	957.2
P-PET	-45.2	37.4	110.4	82.0	104.6	44.5	-7.8	-92.1	-144.7	-129.2	-127.2	-98.8	
APWL	-644.9	-121.8	0.0	0.0	0.0	0.0	-7.8	-99.9	-244.5	-373.8	-500.9	-599.7	
SW	0.4	37.8	112.0	112.0	112.0	112.0	104.5	45.9	12.6	4.0	1.3	0.5	
dSW	-0.2	37.4	0.0	0.0	0.0	0.0	-7.5	-58.6	-33.3	-8.6	-2.7	-0.7	
AET	37.0	37.0	19.1	19.1	31.2	44.4	96.3	92.9	34.2	8.6	2.7	1.4	423.9
Deficit	45.0	0.0	0.0	0.0	0.0	0.0	0.3	33.5	111.4	120.6	124.5	98.0	533.3
Surplus	0.0	0.0	110.4	82.0	104.6	44.5	0.0	0.0	0.0	0.0	0.0	0.0	341.5
Units	**All units in mm**												

	Oct.	Nov.	Dec.	Jan.	Feb.	Mar.	Apr.	May	Jun.	Jul.	Aug.	Sep.
P	36.8	74.4	129.6	101.2	135.7	88.8	88.8	34.3	0.9	0.0	0.0	0.6
PET	82.1	37.0	19.1	19.1	31.2	44.4	96.6	126.4	145.5	129.2	127.2	99.4
AET	37.0	37.0	19.1	19.1	31.2	44.4	96.3	92.9	34.2	8.6	2.7	1.4
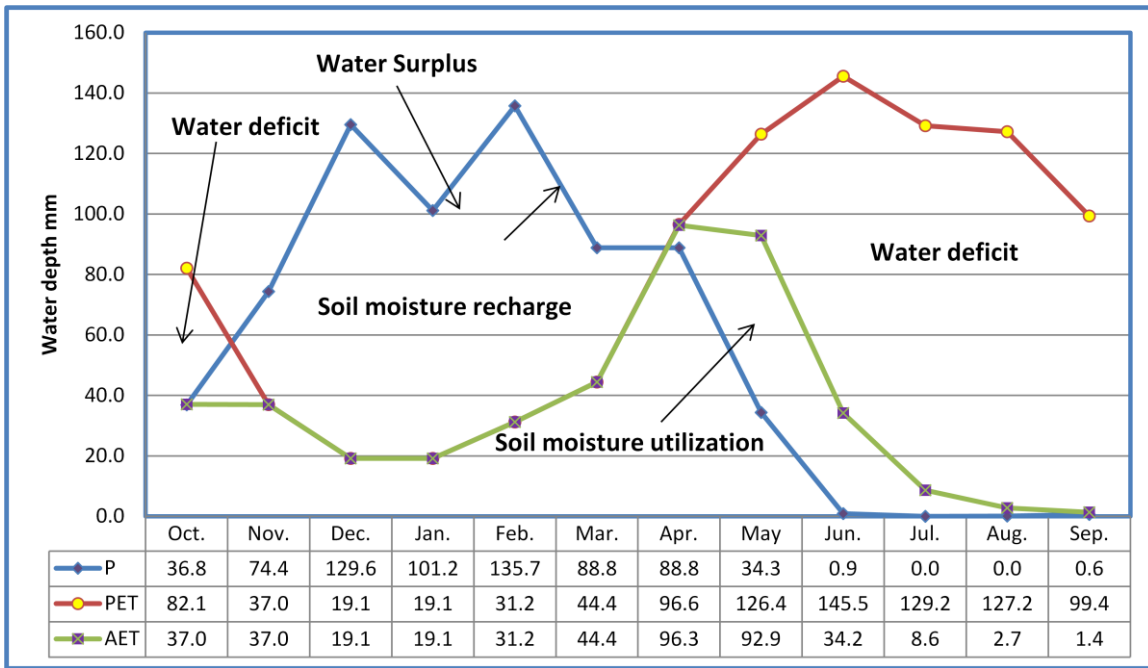
Figure 2.14 Studied basin catchment long term monthly soil water balance

The runoff curve number CN is an empirical parameter used in hydrology for predicting direct runoff or infiltration from rainfall excess. The curve number method was developed by the USDA –United State Department of Agriculture. Previously, the studied basin was divided into several curve numbers by Ali (2007). To confirm the credibility of these curve numbers and using it in the construction of runoff percentage map, the characteristics of each curve number are compared to the specific characteristics of the studied basin in terms of topographical, geological and soil maps. In addition to the results of infiltration test, and also using graphical solution of the runoff equation after Hawkin (2004). Finally, curve numbers for each zone are assumed, and the basin is classified into different zones of the runoff curve number (see Figure 2.15 and 2.16) .

Figure (2.17) illustrates results of the monthly surface runoff percentage from total monthy precipitation over the studied basin ; as can be noted, the study basin watershed is divided into 5 subzones. The predicted lowest percentage of runoff is with locations dominated by Avroman Formation 4% and followed by

Balambo Formation 14% because those areas are characterized by joint and fracture network systems which provide good paths for percolating the precipitation. Zone of Alluvial deposits and Qulqula formatin have a moderate surface runoff 32% and 41% of the whole monthly runoff respectively,while the urban area has high runoff potentials 48%. Thus after computing the effect of each hydrologic zone with its own area, the expected monthly amount is calculated over the whole catchment, as shown in Table (2.10). Accordingly, the total rate of 169 mm or 24.5% from all fallen precipitation 691.16 mm over the whole catchment is predicted as an average runoff ratio based on the mean average monthly precipitation of the last 12 years.

Curves on this sheet are for the case $I_a = 0.2S$, so that

$$Q = \frac{(P - 0.2S)^2}{P + 0.8S}$$
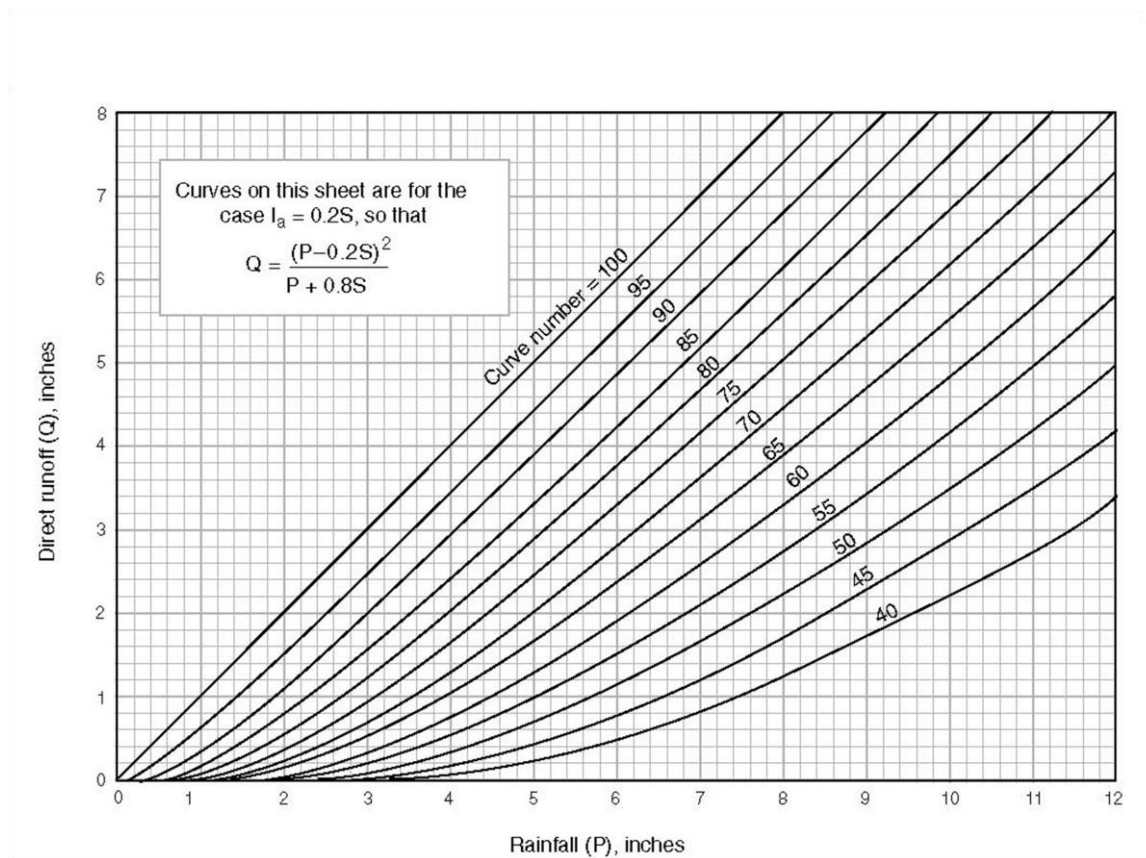
Figure 2.15: Graphical solution of the runoff equation (after Hawkin, 2004)
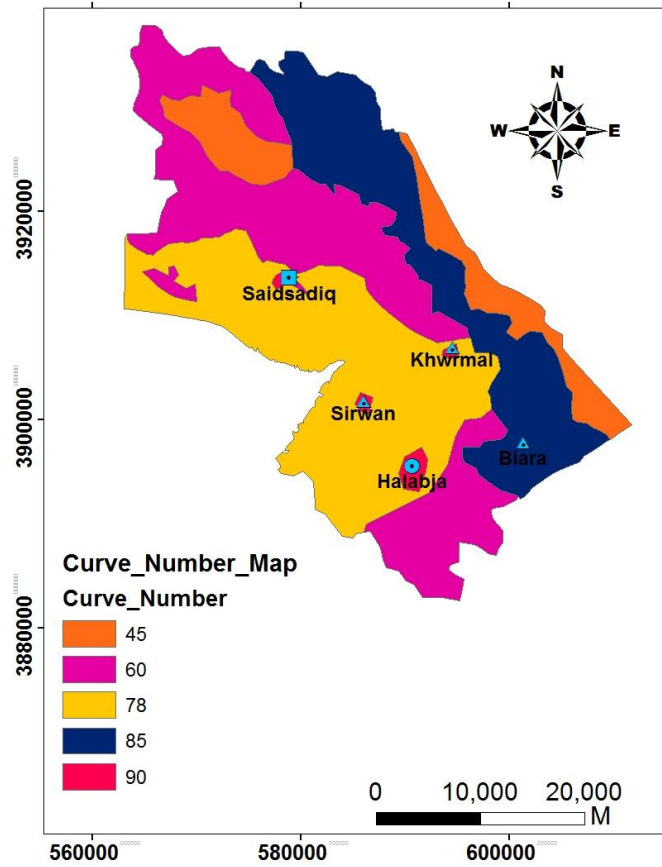
Figure 2.16: Runoff curve number map of the studied basin
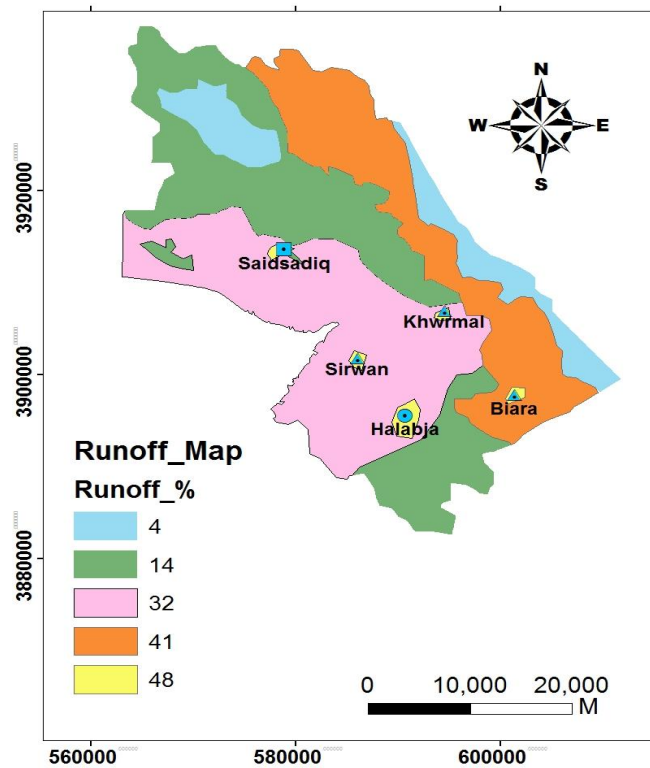
Figure 2.17: Runoff percentage of the studied basin using SCS and soil water balance methods

Table 2.10: Monthly runoff for each geological formation zone, based on SCS-CN method

Month	Oct.	Nov.	Dec.	Jan.	Feb.	March	April	May	June	Total			
P	36.8	74.4	114.6	101.2	135.7	88.8	103.8	34.3	0.9	691.16			
Surplus	0	0	110.4	82.0	104.6	44.5	0	0	0	341.5			
CN	Runoff in (mm)									Area (Km^2)	Volume (* 10^6 m^3)	Runoff (mm)	Runoff (%)
90	0	0	86.5	73.7	106.9	62.1	0	0	0	16.5	5.4	329.3	47.6
85	0	0	74.1	62.0	93.7	51.2	0	0	0	286.6	80.5	281.0	40.7
78	0	0	58.5	47.6	76.4	38.0	0	0	0	341.0	75.1	220.4	31.9
60	0	0	26.0	19.1	38.3	13.5	0	0	0	471.8	45.7	96.9	14.0
45	0		7.6	4.4	14.1	2.1	0	0	0	162.3	4.6	28.2	4.1
T. runoff x10^6 m^3	0.00	0.00	56.13	44.95	74.99	35.34	0.00	0.00	0.00	**211.4**			
T. runoff in mm	0.00	0.00	44.83	37.10	59.37	27.65	0.00	0.00	0.00	**169.0**			
Total										1278.2	211.4		

Chapter Three

Hydrogeology

Chapter Three

Hydrogeology

3.1 Hydrogeology

Geological conditions and tectonic processes usually control the hydrogeology of the study basin that affects groundwater occurrence, water level and movement. In addition, permeability and porosity are the main principal factors in determining the potential of the area to be considered as a water-bearing aquifer. Accordingly, based on the classification done by Ali (2007), different types of aquifers are nominated in the study basin. All aquifer types and thickness are explained in (Table 3.1). It is clear from the data recorded from field work and from groundwater level archives by Ground Water Directorate that the mountain series which surround the basin in the northeast and southeast are characterized by high water table level, while the center and the southeastern parts have a lower water table level. The groundwater movement is usually from north and northeastern to the southwest and from south and southeast towards southwest. All The aquifers represented by their geological formations were described in the geological part (viz section 1.8).

Additionally, the study basin comprises several rivers and streams such as Sirwan river, Zalm stream, Chaqan stream, Biara, Reshen stream and Zmkan stream. All these rivers and streams are considered as a main recharge source of Derbandikhan Lake , located in the southeast of the basin. There are several springs inside the basin (Figure 3.1). These springs are classified into three classes (Ali, 2007), less than 10 l/sec such as Anab , Basak, Bawakochak and 30 other springs, 10-100 l/sec such as Sheramar, Qwmash , Khwrmal, Garaw and Kani Saraw springs and more than 100 l/sec such as Ganjan, Reshen, Sarawy Swbhan Agha springs.

Table 3.1: Aquifers system in the studied basin

Aquifer Type	Geologica Formation	Thickness (m)	References, Regarding Aquifer Thickness
Intergranular Aquifer (AIA)	Quaternary Deposits	>300	Author
Fissured Aquifer (CFA)	Qulqula Group	>500	Jassim and Goff,2006
Fissured-Karstic Aquifer (CKFA)	Balambo Kometan	250	Ali,2007
Karstic-Aquifer (TKA) and (JKA)	Avroman Jurassic	200 80 - 200	Jassim and Goff,2006
Non-Aquifer (Aquitard, TAT) /Aquiclude	Tanjero Shiranish	2000 225	Jassim and Goff,2006

3.2 Hydrogeological System

3.2.1 Aquifers

An aquifer is an underground layer of water-bearing permeable rock, rock fractures or unconsolidated materials (gravel, sand or silt) from which groundwater can be extracted(Ali,2007). The aquifers of the basin consist of sedimentary rocks or sediments of either chemically deposited rocks (marine origin) or clastic rocks and sediments (continental origin). The chemical rocks include limestone, dolomitic limestone and cherts, while the clastic rocks include conglomerates, sandstone, and siltstones in addition to unconsolidated sediments or recent deposits. The Aquifers in the study basin were classified previously by Ali (2007) according to some hydrogeologic and stratigraphic properties. The dominant aquifer types and their properties are shown briefly in

the following sections. For more details about these aquifers refer to the intensive study conducted by Ali (2007).
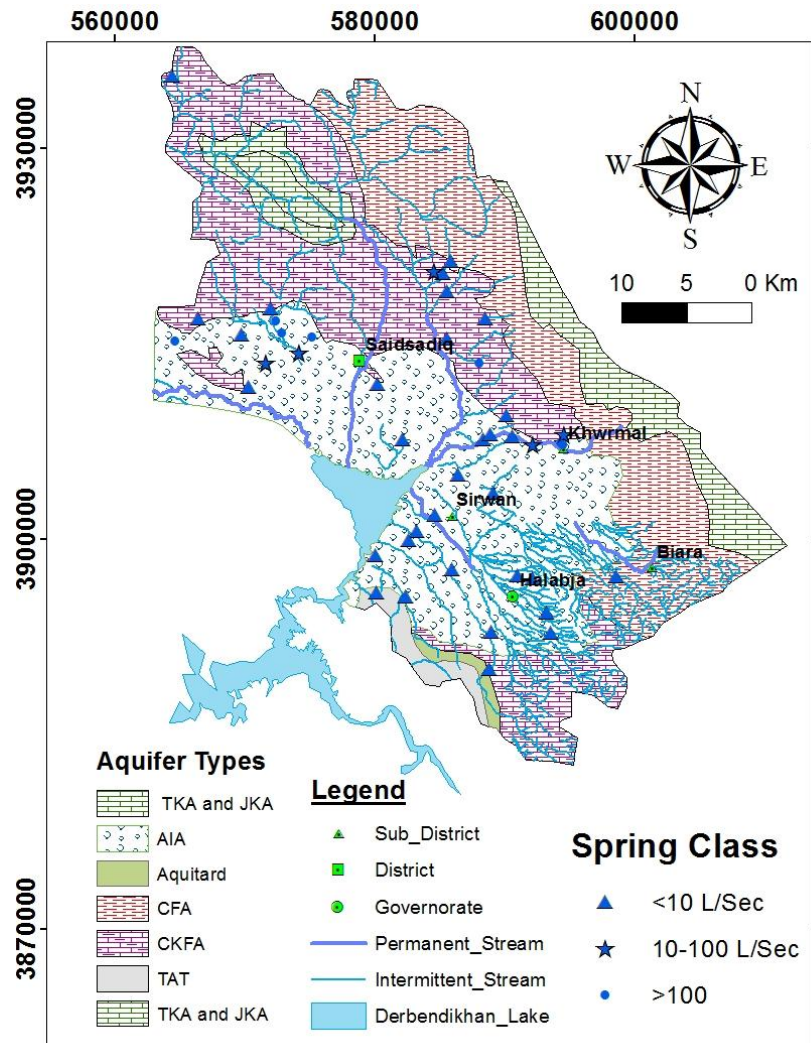
Figure 3.1: Hydrogeological map of the studied basin modified from (Ali, 2007).

3.2.1.1 Intergranular Aquifer (AIA)

In unconsolidated sediments (silts, sands, gravels and boulders) groundwater is stored in the pore spaces between loose grains of sediment. Due to the variation of the size of the particle mixtures from place to place, the hydraulic characteristics are variable too. The coarser sediments have higher values of transmissivity and the wells drilled through them have higher values of specific capacity.

The most important accumulations of alluvium deposits are located in the study basin, mainly in the center and southwestern parts of the study area, with surface area of about 320 km^2 and a variable thickness of 10m to more than 300m (Figures1.4 and 1.5). More than 1000 wells are drilled in this alluvium aquifer. It is recharged by rainfall and sinking streams and comprises the most promising area for the drilling of highly productive wells. There are two horizons of alluvial deposits in the area. The upper horizon is composed mainly of silt, clay and less gravelly deposits with a thickness which may reach 1 to 3 meters. The lower horizon, called the bed load, is composed of sand and gravel; sometimes this part is replaced by talluvium (slope wash) near the foot of the mountain. In most cases these two horizons alternate, forming a thick layer of more than 300 meters. Each of the great number of large or shovel dug wells drilled in the plain around Said Sadiq and south of Halabja town can irrigate more than one hectare (Plate.3.1). Most deep wells were also drilled through these deposits, which sometimes represent the only deposits that are penetrated by the deep wells.

Plate 3.1: Large diameter well (6mx8mx8m) near to Grdanaze village (South of Saidsadiq District)

3.2.1.2 Fissured Aquifers (CFA)

Cretacoues Fissured Aquifer (CFA) is composed mostly of different lithological layers such as limestone, shale, chert, dolomite, and marly limestone. Generally, it is fractured to a lesser extent than that of Karstic-Fissured aquifer types and its fractures are narrower. These aquifers are of less importance and their transmissivity is much less than the karstic and karstic-fissured aquifers and of limited extent exposures. This type of aquifers is represented by the Qulqula (marly limestone + chert) formation. The most important hydrogeological properties of the Qulqula Radiolarian Formation are the existence of local aquifers. The formation is mostly in the low lands. It often acts as a barrier to the groundwater movement in the karstic aquifers and results in rising up the groundwater and flowing out as large karstic springs as in the case of Jomarase, Reshen and Zalim springs. The minimum discharge of these springs is about 1 m^3/s, (Ali, 2007), (Figures 1.4 and 1.5).

3.2.1.3 Karstic- Fissured Aquifers (CKFA)

This type of aquifer is developed in different type of rocks such as the limestone, dolomitic limestone, marly limestone and dolomite. The fracturing sets are high in terms of density along these rocks, which prevent karstification processes from developing the hydrogeologic unit into a pure karstic aquifer, as the accumulated water flows through a great number of fractures and fissures (Ali, 2007). The karstic-fissured aquifers are characterized by high permeability and transmissivity values but to a lesser extent than those in karstic aquifer. The Karstic-fissured aquifer unit or formation in the study basin are represented by Balambo and Kometan Formations, (Figures 1.4 and 1.5).

3.2.1.4 Karstic Aquifers (TKA) and (JKA)

Depending on the degree of the karstification, those type of aquifers are characterized by high permeability and transmissivity values, as groundwater

flows through channels and cavities of different diameters (Hamamin and Ali , 2012). Furthermore, based on several karstic aquifer tests achieved from the field work of this study, the drawdown values in the wells that are drilled in that aquifers are relatively small. The karstic aquifer units or formations in the study basin are (Avroman Triassic Limestone Formation, TKA) and (Jurassic Karstic Aquifer, JKA), (Figures 1.4 and 1.5).

3.2.2 Aquiclude

Aquiclude refers to any geological formation that absorbs and holds water but does not transmit it at a sufficient rate to supply springs and wells. In the study area aquiclude is represented by Shiranish Formation (Figures 1.4 and 1.5), which acts as a barrier for separating the upper and lower aquifers. This aquiclude bed varies considerably in its thickness and compaction due to the degree of deformation and effects of weathering.

3.2.3 Aquitard

Aquitard refers to any geological formation whose permeability is so low that it cannot transmit any sufficient amount of water. In the study area, aquitard is represented by Tanjero Formation (TAT), which contains medium beds of limestone and sandstone (Ali, 2007). Due to jointing and fracturing, sufficient effective porosity to reserve and transmit groundwater is lost and acts as aquitards. As a result, many wells drilled in the Tanjero Formation inside and around the study area with good groundwater utilized for different purposes.

3.3 Aquifer Hydraulic Characteristics

To obtain the hydraulic parameters of water bearing beds, pumping test analysis is used. In addition, drilling well log is used for estimating saturated thickness for the aquifers within the studied basin. The achieved parameters comprise the transmissivity (T) and storage coefficient (S) with the aid of the

computer software programs, AQTESOLVE 4.0 which is applied on the tested wells; it is capable of computing these parameters even for the single well and partially penetrating cases.

For the present study, well tests are carried out on 89 water wells, which are partially penetrating different geological formations, (Figure 3.2). The pumping test methods are "Theis, Cooper - Jacob, Hantush-Jacob, Walton and Neuman's methods". Each method is applicable under certain hydrogeological conditions. In total of 89 well pumping tests, 84 wells tests performed by using single well test method, while the other five sites were selected for performing pumping tests by using the principal of observation well in different aquifer types (W8,W12,W16,W21 and W68). The duration of the well tested ranges from 25 – 630 minutes based on stability of water drawdown and the water recovery situation of the well, the wells were let to be recovered after switching off the pump, and recovery measurements were immediately done. All methods were applied; the steady and non-steady states flow condition for both constant and recovery test analyses.

The computation of transmissivity from the resultant curve was carried out only in the initial drawdown measurements when the unsteady state conditions were accessible, consequently, the transmissivity values obtained by the methods applying drawdown test measurements are lower when compared to those applying recovery test measurements. Therefore, the transmissivity values obtained by the recovery test are of high accuracy as compared to those obtained by the constant pumping tests because in recovery test water proceeds naturally to the well without the involvement of pumping.

One of the selected well (W14) is located inside the Halabja City with depth of 140m penetrating Alluvial deposits (AIA), in which one previously drilled wells were penetrating the same aquifer (AIA), and it has a depth of around 100m and the distance of 40m. One of the wells was used as a monitoring well

and from the other well the process of pumping was started. Both constant and recovery tests were applied (Figure 3.3), and the results are tabulated in Appendix (3.1). The duration of the pumping test lasted for 290 minutes; the recorded drawdown was 23 m with pumping discharge of 3 L/s.
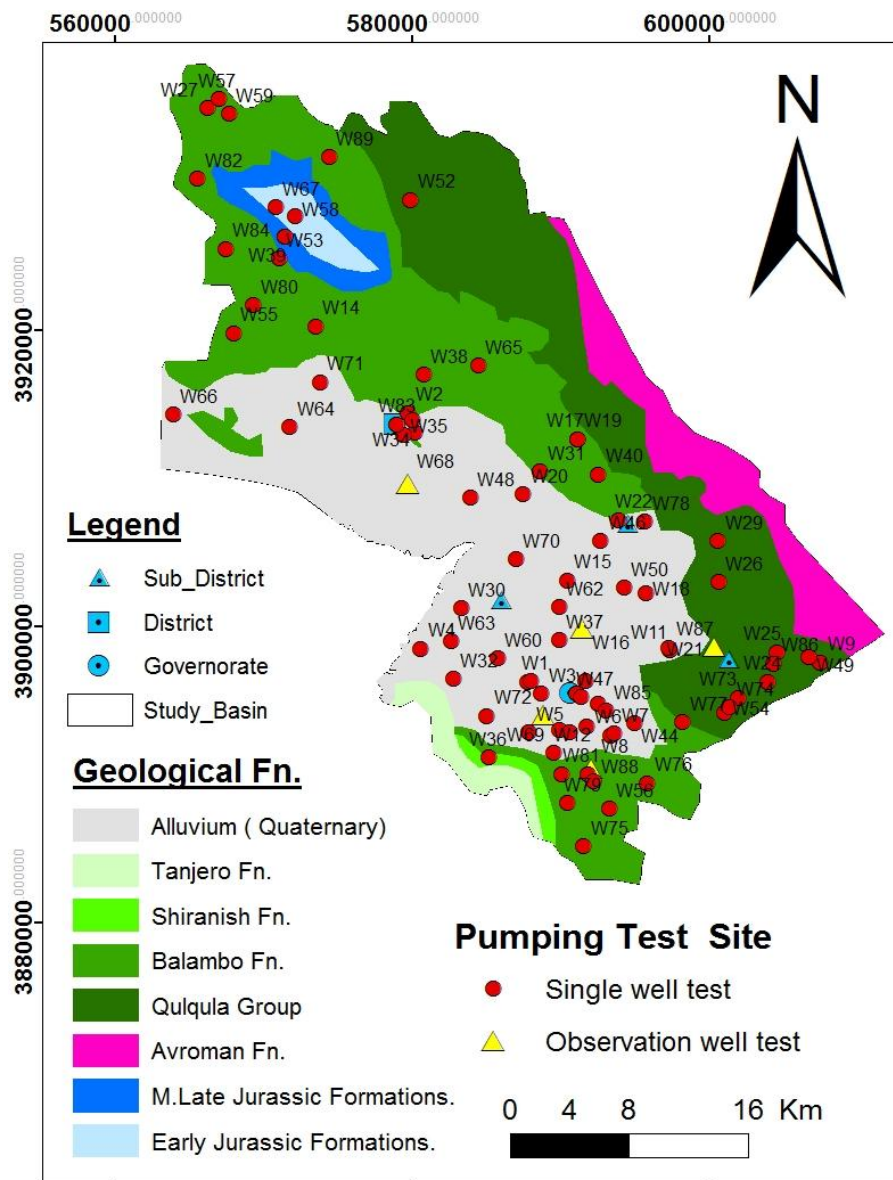
Figure 3.2: Selected wells for pumping test analysis
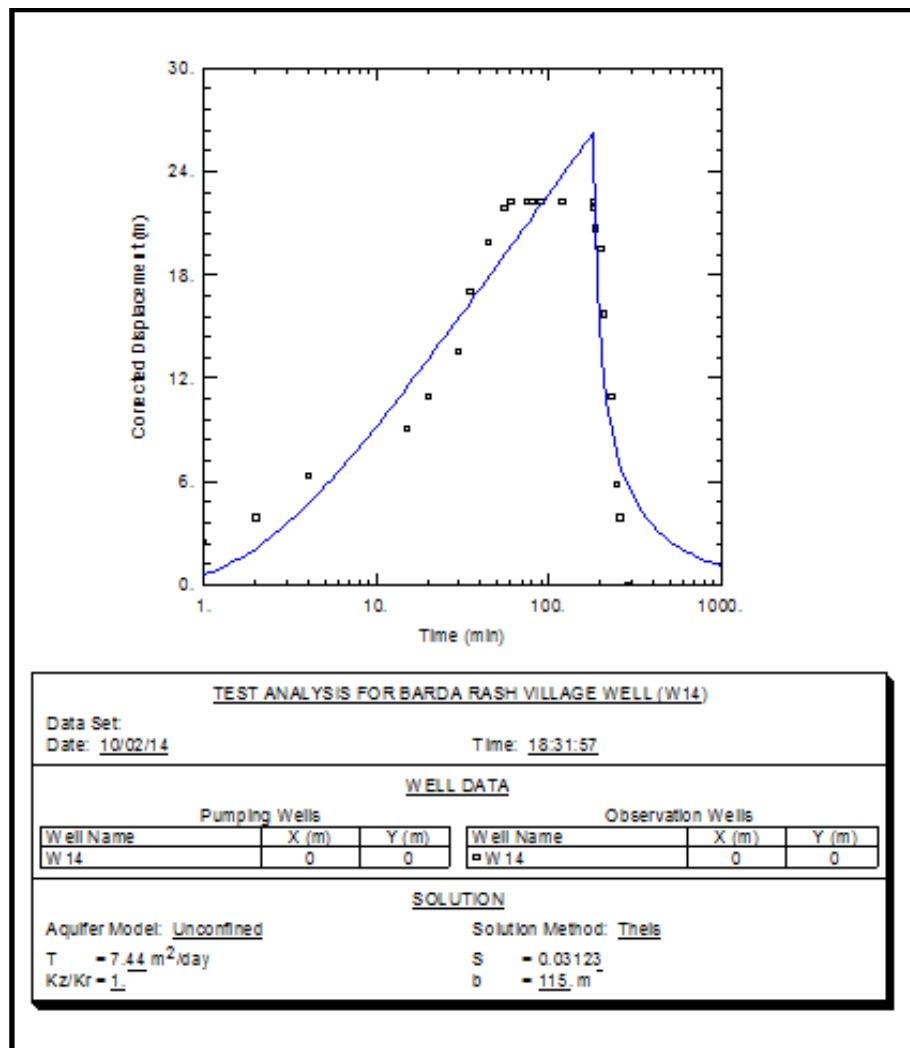
Figure 3.3: Pumping test analysis for observation well (W14) – AIA (penetrating Alluvial Deposits)

In addition, two more sites are selected for drilling two monitoring wells, for the purpose of evaluating AIA and to estimate the aquifer hydraulic parameters. The first drilling piezometer well was in a plain area located close to Khurmal Subdistrict (W50). The distance between them is 40 m and both are penetrating Alluvial deposits. Duration of the pumping test lasted for (105) minutes; the recorded drawdown was 13 m with pumping discharge of (5.7) L/s, (Figure 3.4).

The other piezometer was drilled near to Saidsadiq District for a depth of 73 m, (W68). After completion of the drilling process, screen pipes were inserted in permeable units to receive water from all horizons during the pumping test. The

distance between both wells is 48m, and pumping test continued for 75 minutes. The recorded drawdown was 3 m with pumping discharge of 9 l/s, (Figure 3.5).
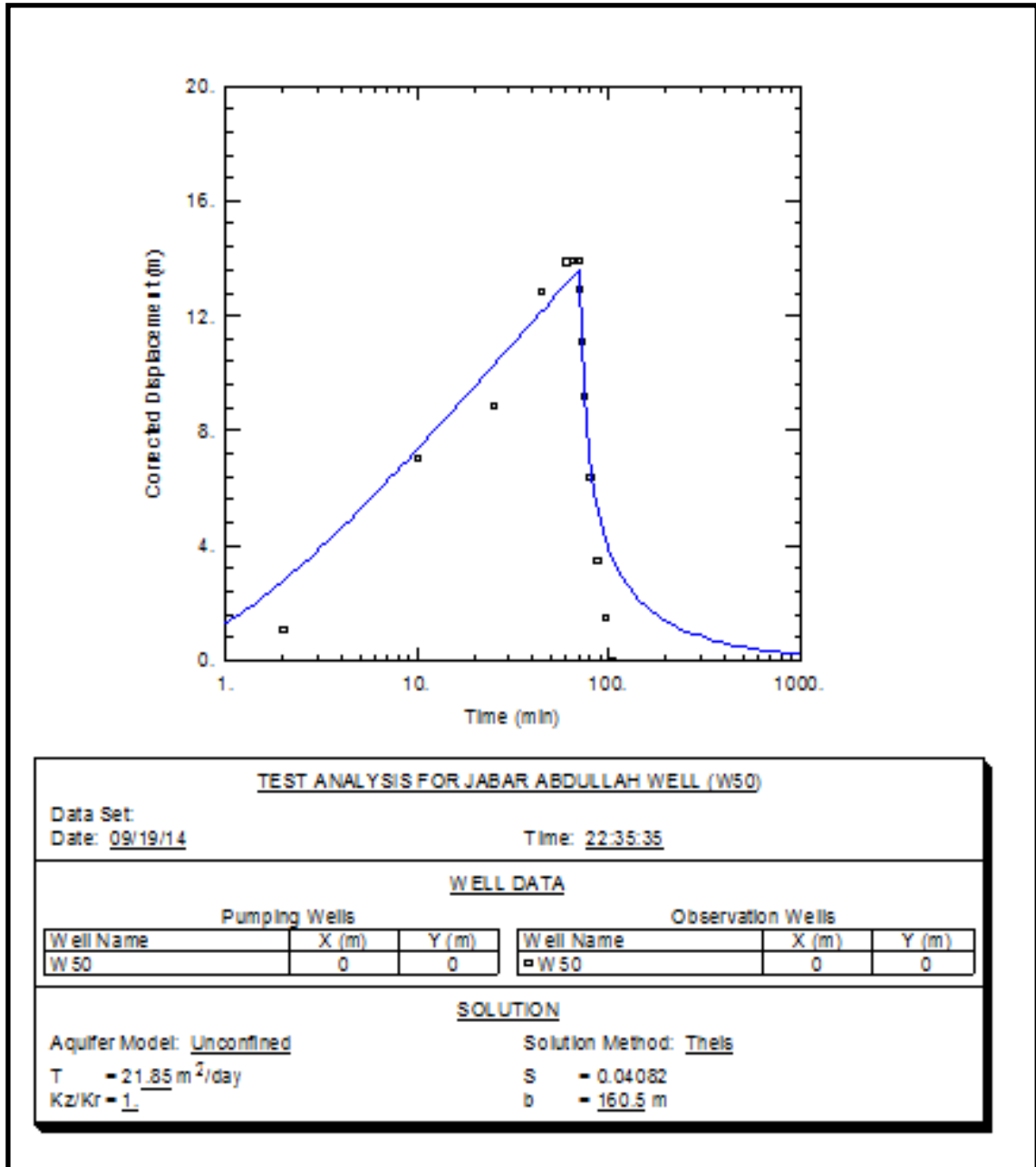
Figure 3.4: Pumping test analysis for observation well (W50) – AIA

(Penetrating Alluvial Deposits)
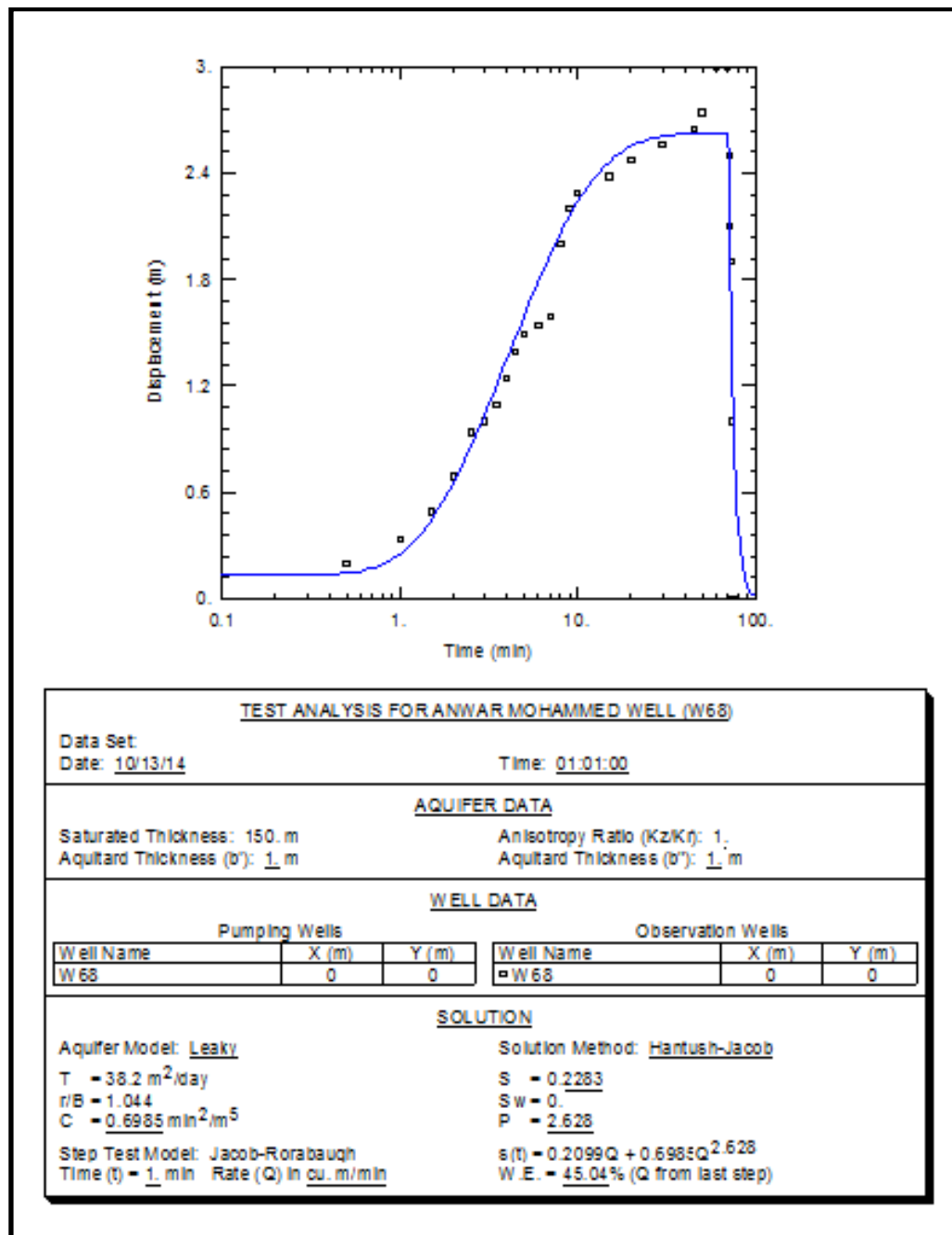
Figure 3.5: Pumping test analysis for observation well (W68) – AIA (Penetrating Alluvial Deposits)

For the purpose of evaluating CFA and to estimate the hydraulic charatrestics for Qulqula Radiolarian Formations, one site is selected for drilling monitoring well (W24). This well is close to one of the private deep wells; the distance between them is 55 m, and both are penetrating Qulqula Radiolarian Formations. Duration of the pumping test lasted for 110 minutes; the recorded drawdown was 21.58 m with pumping discharge of 1.33 L/s (Figure 3.6).

Additionally, to evaluate CKFA and to estimate the hydrogeologic parameters for Balambo Formation, one site is selected for drilling monitoring well (W7) near to Halabja Governorate. The distance between this well and one previously drilled deep well is 50 m, and both are penetrating Balambo Formations. The duration of the pumping test lasted 130 minutes; the recorded drawdown was 13 m with pumping discharge of 12.65 L/s, (Figure 3.7).
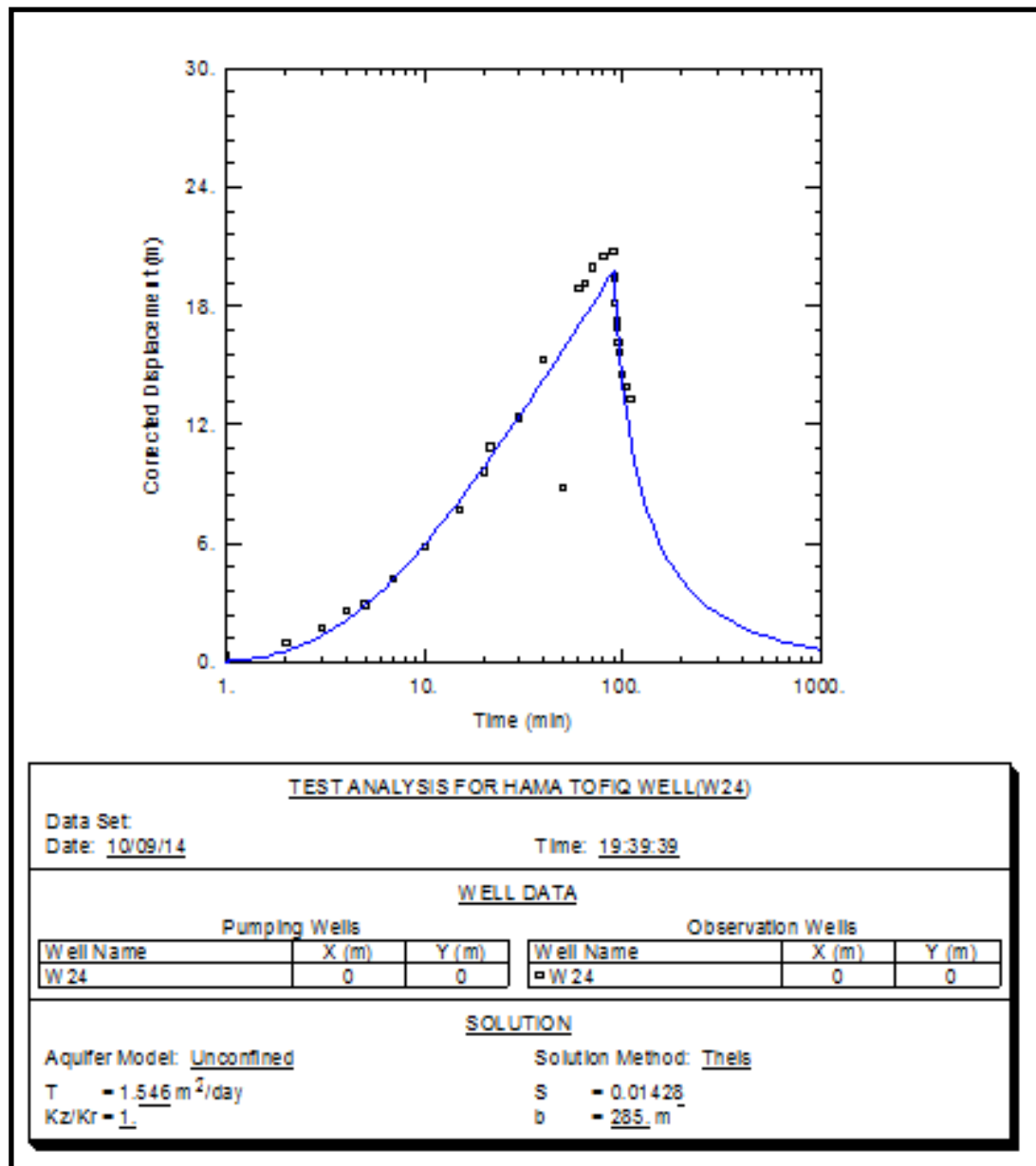
Figure 3.6: Pumping test analysis for observation well (W24) – CFA (Penetrating Qulqula Radiolarian Formation)

Generally, The results of nearly 35 single pumping tests for the wells penetrating inter-granular aquifers (AIA), and even the observation well tests which were applied during this study have shown the transmissivity to be in a range between 0.22 to 810.9 m2/day, while the hydraulic conductivity was 0.002 to 12.8 m/day and the storage coefficient was 0.001 to 2.171. The well discharge is at the range of 0.36 to 16 L/s, (Appendix 1.1). Simultaneously, the variation in aquifer parameters, especially for the intergranular aquifers may refer to lateral and vertical variation in the lithology of the water bearing beds. The physical characteristics of the hydro-stratigraphic beds, such as grain size, compaction and cement material might be varied from one sit to another. Technical problem such as unsuccessful well design causes hydraulic
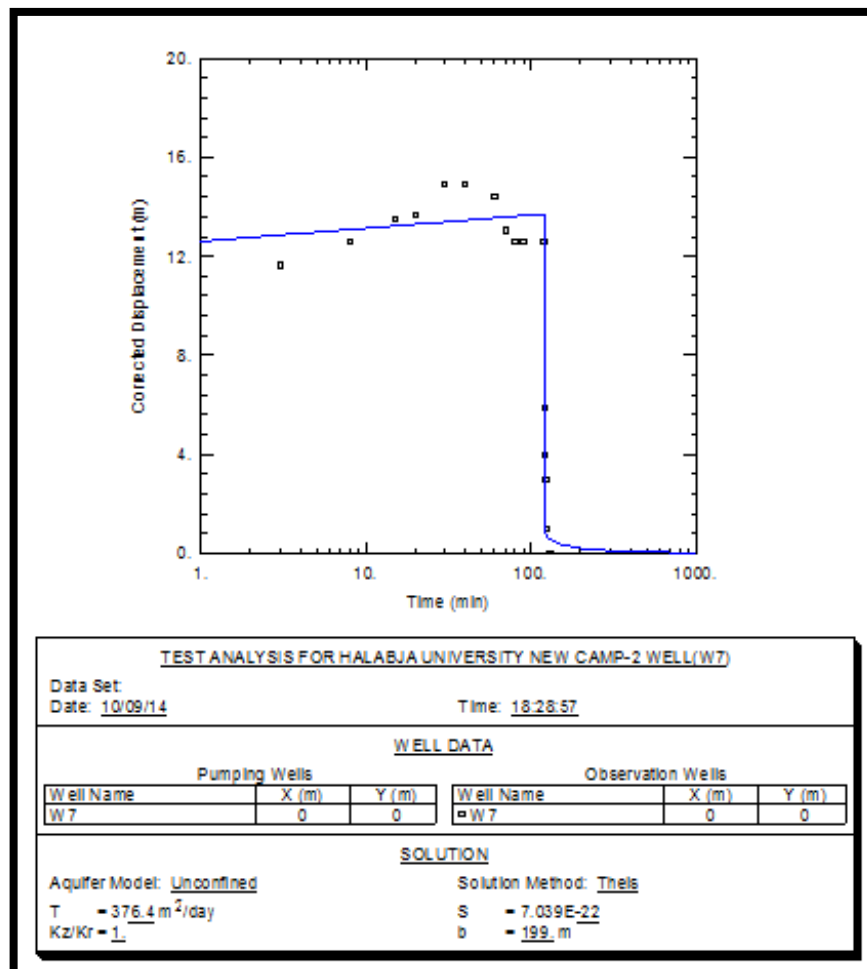
Figure 3.7: Pumping test analysis for observation well (W7) – CKFA (Penetrating Balambo Formation)

loss and resistance for screen zones, particularly for the drilled old wells. The results of some hydrogeologic parameters of different types of aquifers in the study basin achieved from several single well tests and observation well tests are tabulated in the Table (3.2). The results of all pumping tests are attached and tabulated as Appendix (1.1). Many factors appeared to have affected this variation in aquifer characteristics in the study basin, such as lithological properties of the aquifers, variation in the well depth and well design and the type of pumping equipments and the capacity of the pump.

Table 3.2: Results of the well pumping test analysis in different aquifers

Aquifer	N.of tested wells	Transmisivity (m2/day)	Hydraulic Conductivity (m/day)	Storage Coefficent	Discharge (l/s)
TAT	4	0.1-3.4	0.00062-0.5	0.001-0.011	0.45-2.9
CFA	22	0.73-2254	0.007-26.4	0.001-2.715	0.5-16.8
CKF A	23	7.4-1747.5	0.05-35.6	0.001-0.663	1.0-18.0
TKA & JKA	4	6.05-156.5	0.03-1.2	0.002-0.026	2-5.4
AIA	36	0.22-810.9	0.002-12.8	0.001-2.17	0.36-16

3.4 Groundwater Recharge of the Basin

Groundwater recharge is one of the most difficult parameters to be measured in the assessment of groundwater aquifers. Estimation of the net groundwater recharge is necessary for both groundwater modeling and water resources management. A number of methods exist for estimating the recharge rate of a given area. None of these methods are standard, and each method has its own strengths and weaknesses. Generally, the main sources of the recharge of the

aquifers in the study basin are from the precipitation during the precipitation season. The main streams which are flowing inside the area are generated from rainfall and issuing springs that drained water from all kinds of the aquifers inside the catchment area. This clearly felt from the layer of the drainage pattern and spreading of springs from the hydrogeological map in the Figure (3.1).

For the estimation of the annual volume of recharge in the study basin, the simple water balance and SCS-N methods were applied. Part of this method was explained previously (viz section 2.9) in which a total amount of runoff (using SCS-N method) was calculated and the rate of evapotranspiration using FAO Penman-Monteith method was estimated (viz section 2.8.2); the remainder represents the amount of the net recharge percolated downward to reach the groundwater storage.

Net recharge has been calculated taking into reflection the variable geology of the area and the different response of each consideration hydrostratigraphic layer for contributing and infiltrating water from rainfall. Therefore the net recharge in each geological zone was calculated based on the water surplus minus the total runoff (including soil moisture) for each month separately as shown in Table (3.3). Accordingly, the net recharge map was created and shown in Figure (3.8).

From the expected figure of annual net recharge to the groundwater (Figure 3.8), the watershed is divided into 5 subzones in the study basin. The expected highest rate of the net recharge is about 45% for the area underlain by TKA which is represented by (Avroman Formation) and JKA represented by (Chia Gara, Barsarine and Naoklekan) formations, while the minimum is located in an Urban area 5% from the total annual precipitation.

The rate of recharge within the TKA and JKA is approximately 313 mm/year, if the total annual rainfall is taken as 691 mm (Table 3.3). These rocks are all located in the Thrust and Imbricate Zones; therefore, they are intensively

deformed. These deformations during prolonged underground weathering transformed to karstified aquifer, which has the advantage of precipitation infiltration. The rate of recharge within CKFA is about 245 mm/year.
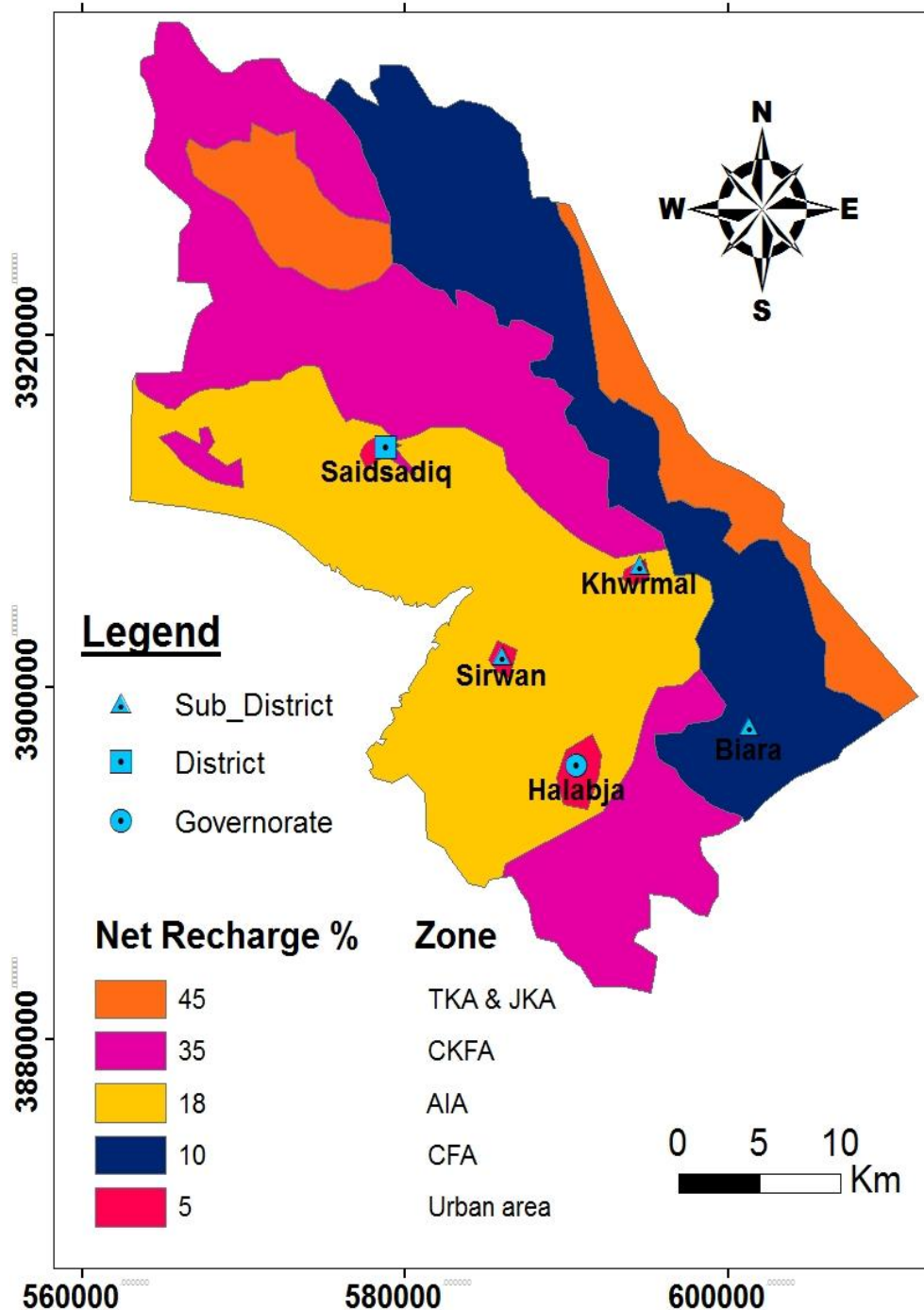
Figure 3.8: Annual net recharge to the groundwater in (%) from rainfall of the studied basin

Table 3.3: Estimated amount of net recharge based on SCS and soil water balance methods

Months	Oct	Nov	Dec	Jan	Feb	Mar	Apr	May	Jun	Jul	Aug	Sep	Total			
P	36.84	74.36	114.57	101.15	135.74	88.84	103.81	34.33	0.85	0	0.04	0.63	**691.16**			
Surplus	0	0	110.43	82.01	104.58	44.47	0	0	0	0	0	0	**341.49**			
Runoff	0	0	44.83	37.10	59.37	27.65	0	0	0	0	0	0	**169.0**			
CN	Net Recharge in (mm)												Area (Km^2)	Volume (10^6 m^3)	NR (mm)	NR %
90	0	0	23.92	8.29	0	0	0	0	0	0	0	0	16.47	0.53	32.21	5
85	0	0	36.29	19.98	10.92	0	0	0	0	0	0	0	286.59	19.26	67.2	10
78	0	0	51.97	34.44	28.22	6.48	0	0	0	0	0	0	396.0	47.96	121.1	18
60	0	0	84.38	62.88	66.3	31.0	0	0	0	0	0	0	416.82	101.9	244.5	35
45	0	0	102.8	77.6	90.5	42.4	0	0	0	0	0	0	162.3	50.85	313.3	45
Total													1278.2	220.5		
T.NR x10^6 m^3	0	0	83.2	58.31	56.63	22.4	0	0	0	0	0	0	**220.54**			
T.NR (mm)	0	0	65.1	45.62	44.30	17.5	0	0	0	0	0	0	**172.54**			

The reason for such relatively high net recharge rate within these zones compared to the other zones may refer to the nature of the joint and fracture network which provide excellent paths for percolating the precipitation. The rate of recharge of AIA is about 121 mm/year. This may be attributed to the sediments of the fans accumulated in the plain area especially inside the Halabja-Khurmal sub basin. This sediments consist mainly of silt, sand and clay in addition to the coarse fragments of poorly sorted and sub-angular flat clasts of limestone, derived from surrounding mountains. In addition, rate recharge of CFA is about 67 mm/year. The chert packages in Qulqula radiolarian formation, in most cases, are underlain by shale or marl which makes suitable stratigraphic conditions for numerous perched aquifers, the infiltration of rainfall or snow melting recharges the limited depth of these rocks and flow through the underground for a short distance until discharging as small springs, depressions or contact springs. In contrast, most of the urban areas have the lowest amount of recharge 32 mm/year or 2% from the fallen annual precipitation, because it is mostly covered by building and paved roads which transformed all the fallen precipitation into surface runoff.

3.5 Aquifer Discharge

The mechanism of the aquifer discharge is expected basically to be through the following ways:

1. Drainage through springs and subsurface drainage
3. Artificial discharge by pumping wells

Spring's discharge consists the main groundwater outflow, particularly in the area of karstic and karstic-fissured aquifers of JKA, CKFA and TKA. There are several factors that influence the emergence of springs at specific locations, (Stevanovic and Iurkiewicz, 2004 and Ali, 2007) including:

a) The location of water bearing layers and impermeable rocks

b) The presence and distribution of tectonic elements

c) Climatic conditions and resources of the aquifer system actually dictate the amount of water discharged through outlet points.

Subsurface water discharge designates that there is a transfer of the most or part of water from an aquifer to another type of aquifer or directly into the river beds of surface streams. This is a typical feature in karstic aquifer with deeper karstification. The possibilities for subsurface outflow depend on geometry and permeability of rock. The occurrence of groundwater discharge can be identified on the basis of simultaneous river gauging, thermometric and electric conductivity measurement of stream water and also by using certain geophysical methods (Al-Manmi, 2008). Many disperse or concentrated springs with high varying discharge have been recorded in the study basin (Figure 3.1). The registered springs in the study basin were studied extensively in terms of the spring flow regime by Ali (2007), categorized these springs according to their discharge values and geologic settings into:

1. Large karstic and karstic-fissured springs which include those springs with minimum discharge varying between 500 to >2000 l/s, TKA, JKA and CKFA comprise their main aquifers. Saraw group, Reshen and Zalm springs are categorized under this group.

2. Medium discharge karstic-fissured springs, with a discharge magnitude varying between 100 to <2000 l/s, such as Kani Panka, Greza, Shiramar, Said Sadiq, Sargat and Bawa Kochak.

3. Low discharge springs, which cluster all the springs with very low discharge rate during recession periods; they reach less than 0.1 l/s, and maximum discharge sometimes exceed 500 l/s. A relatively large number

of springs in this category occur in the studied area with different geological settings. They can be classified as the following:

a) Those discharging from CFA, covering a large number of springs appearing either under structural control or contact springs by topography. Examples of these springs are Biara, Khurmal, Kani Spika.

b) Those issuing from AIA; these types of springs are spread over the area of the basin around Said Sadiq and Khurmal.

c) Several springs which emerge from Balambo formation, such as those appearing near Zalim spring and Reshen springs.

Artificial drainage by pumping the wells caused withdraws of the huge volume of water from the groundwater aquifers in the study basin. Due to the lack of information that determines the number of the wells which are working and those which are not working, the estimation of the total volume of discharged water seems to be very difficult. Within the last few years, the studied basin became compactly residential and highly industrial, but the problem arises when there are few water distribution projects. As a result, people started drilling wells in range of few meters to several tenths of meters, without any control by the local government. Therefore, more than 2000 wells were drilled legally inside the studied basin, in addition to many thousand wells without permission from the related governmental offices. Consequently, the overutilization and pollution risk in this basin is predictable because most of these wells are neither correctly drilled nor protected.

3.6 Groundwater Level Fluctuation

The seasonal and annual fluctuations of the groundwater level reflect the recharge and discharge processes (Hassan, 1998). Monthly measurements of static water level in 14 deep wells in the study basin distributed in different

aquifer systems (se Figure 3.9) and Appendix (3.2), were observed from period of May 2014 to October 2015. Seven of them penetrate AIA (W3,W4,W6,W8,W9,W11 and W14), five wells penetrating CKFA of the Balambo Formation including W1,W2,W10,W12 and W13, one well penetrate CFA of Qulqula group including W7 and one well penetrating TAT represented by Tanjero Formation (W5). The groundwater level observation data are presented in figures (3.10, 3.11, 3.12 and 3.13) for all the wells in the study basin. As it is illustrated in the graphs, considerable fluctuations of the groundwater level took place during the observation period. The highest water levels were measured at December 2014, while the lowest water level was observed in May 2015.

For AIA, the range of decline of the SWL recorded in seven wells was 4.2-5 m, , figures (3.10 and 3.11). Groundwater fluctuation in AIA was studied by Ali (2007) from 2004 to 2006 in the study basin, and he also used the previously monitoring of the groundwater level fluctuation through deep drilled wells by the FAO Groundwater monitoring network program in Iraqi Kurdistan from 2000 to 2003. He recorded the range of decline of the SWL which was about 2.85 to 5 m , five deep wells in this sub-basin penetrate CKFA, figure (3.12). The recorded decline was 6-8 m, while Ali in (2007) recorded a decline of SWL of about 5.87-11.75 m. For the piezometers installed in the private well in Kharpane village (Ahmad Hssen Well), penetrating (CFA), figure (3.13), a decline of about 3 m is recorded between the maximum recharge periods to the lower recession period. The range of the decline line for the piezometers installed in TAT in Ghwlami Saroo well was 4 m, Figure (3.13).

Obviously from the groundwater level fluctuation hydrograph over the studied period, we conclude that there is an excellent response of the SWL to precipitation magnitude and its distribution. In addition, the ground water level

fluctuations are also caused by an intense recharge into the upstream part of the alluvium aquifer. Presumably, groundwater recharge into the aquifer comes predominantly from percolation of water along the connecting streams such as Chaqan and Surajo Zamaki, Hasanawa and Darashesh valley beds (Ali,2007).
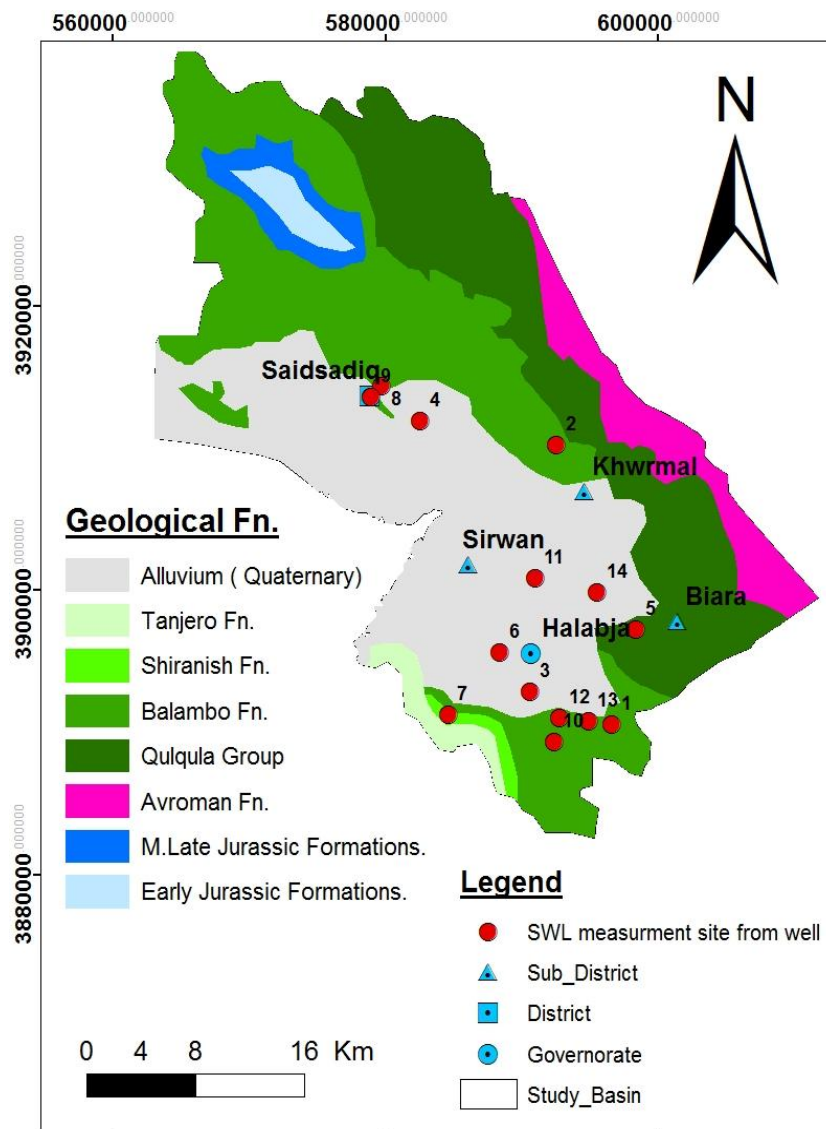
Figure 3.9: Well Site for groundwater level fluctuation monitoring
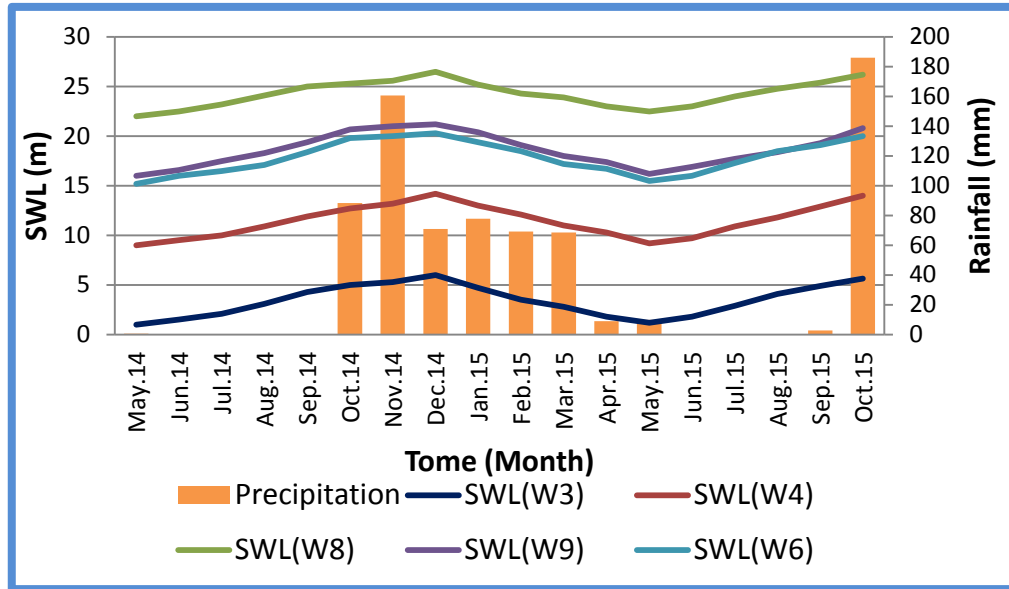
Figure 3.10: Groundwater level fluctuations in 5 wells of AIA in the studied basin
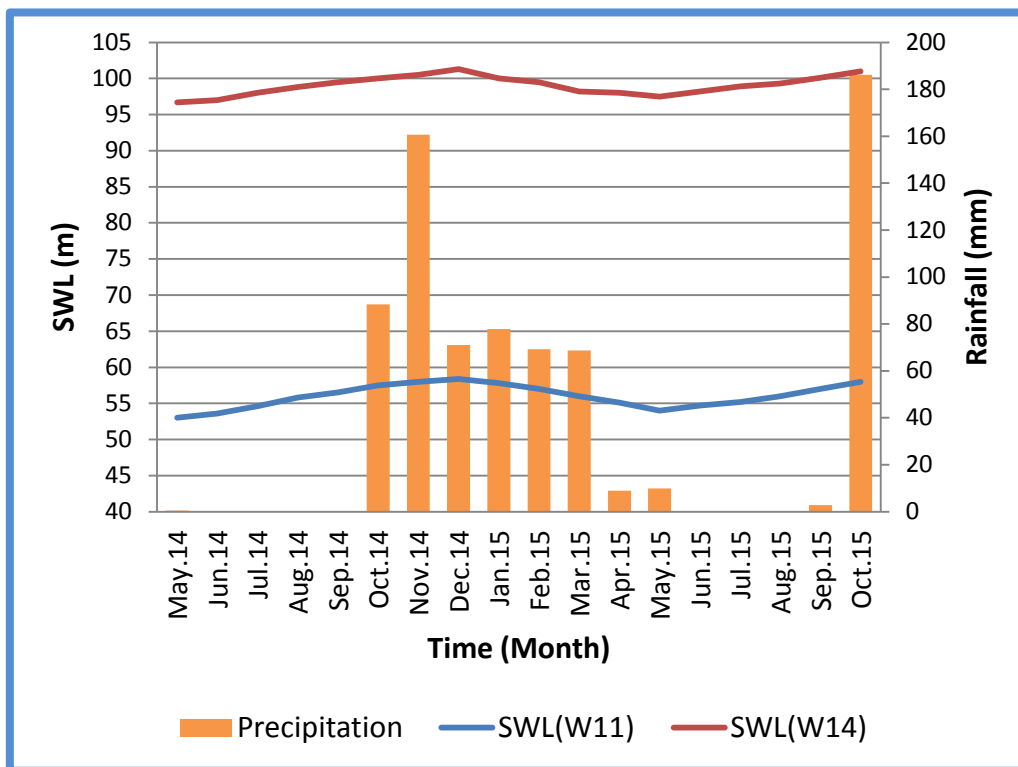
Figure 3.11: Groundwater level fluctuations in 2 wells of AIA in the studied basin
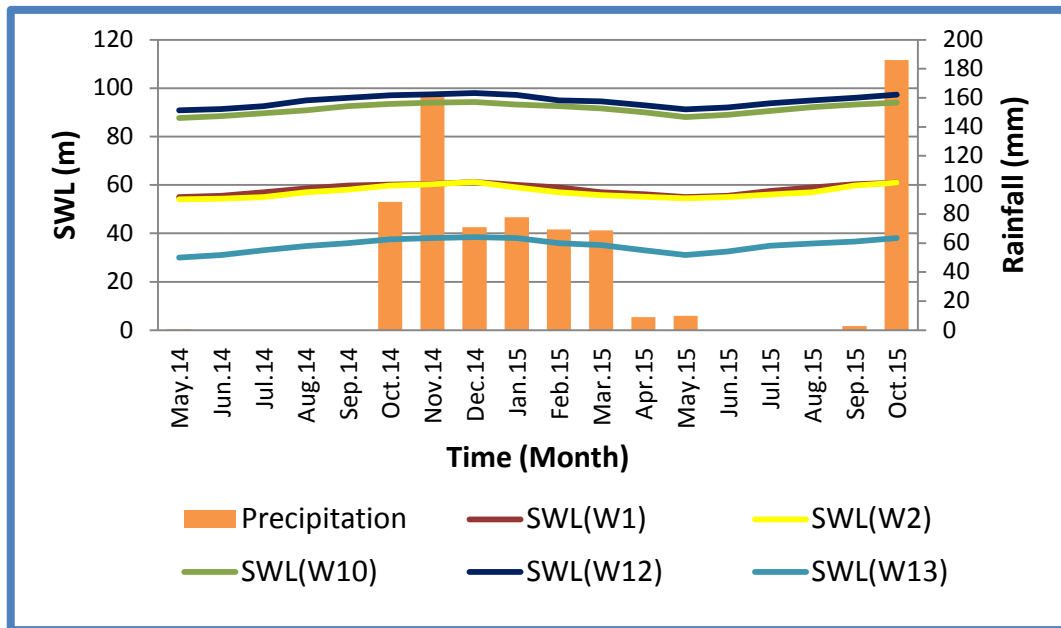
Figure 3.12: Groundwater level fluctuations in 5 wells of CKFA in the studied basin
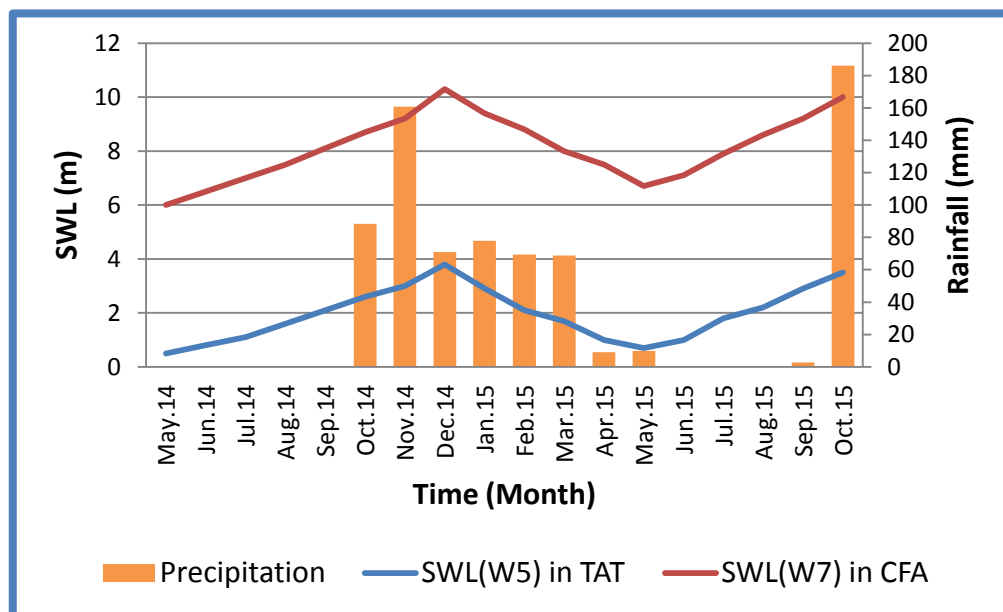
Figure 3.13: Groundwater level fluctuation of TAT and CFA in the studied basin

3.7 Groundwater Flow Direction (Flow Net)

Groundwater movement which depends upon the hydraulic gradient and hydraulic conductivity may be quantitatively described by graphical analysis of

flow nets. Generally, the 1100 m.a.s.l water table along the axis of Shinirwe Mountain descends westwards to an elevation of about 480 m.a.s.l at the shore Darbandikhan Lake. As stated by Moore (2002), movement of water flows usually from a higher head to a lower head and the water table above sea level have the same shape as the topography of the earth's surface; therefore, the water level in areas of lower elevation is closer to the surface than of higher elevation. The flow net map is constructed by using ArcGIS and by using the information of nearly about 1400 wells in different aquifers. This was determined by using archived data from Sulaimani Groundwater Directory and after checking and updating most of these data from field during the period of field work in 2014 and 2015.

Generally, the used data included coordinates, elevations, and static water levels. Static water table above sea level was determined by subtracting the elevations of the land surface from the depth of static water levels, Appendix (3.3).According to the Figure (3.14), which shows flow direction of groundwater based on the surface topography (Figure 3.15) and groundwater levels of the studied basin, the groundwater movement is usually from north and northeast to the southwest and from south and southeast towards southwest. Generally, groundwater movement is away from the mountains surrounding the studied basin to the nearly flat area, which topographically is a flat area and consists of sediments of recent deposit and is closed to the Darbandikhan Lake.
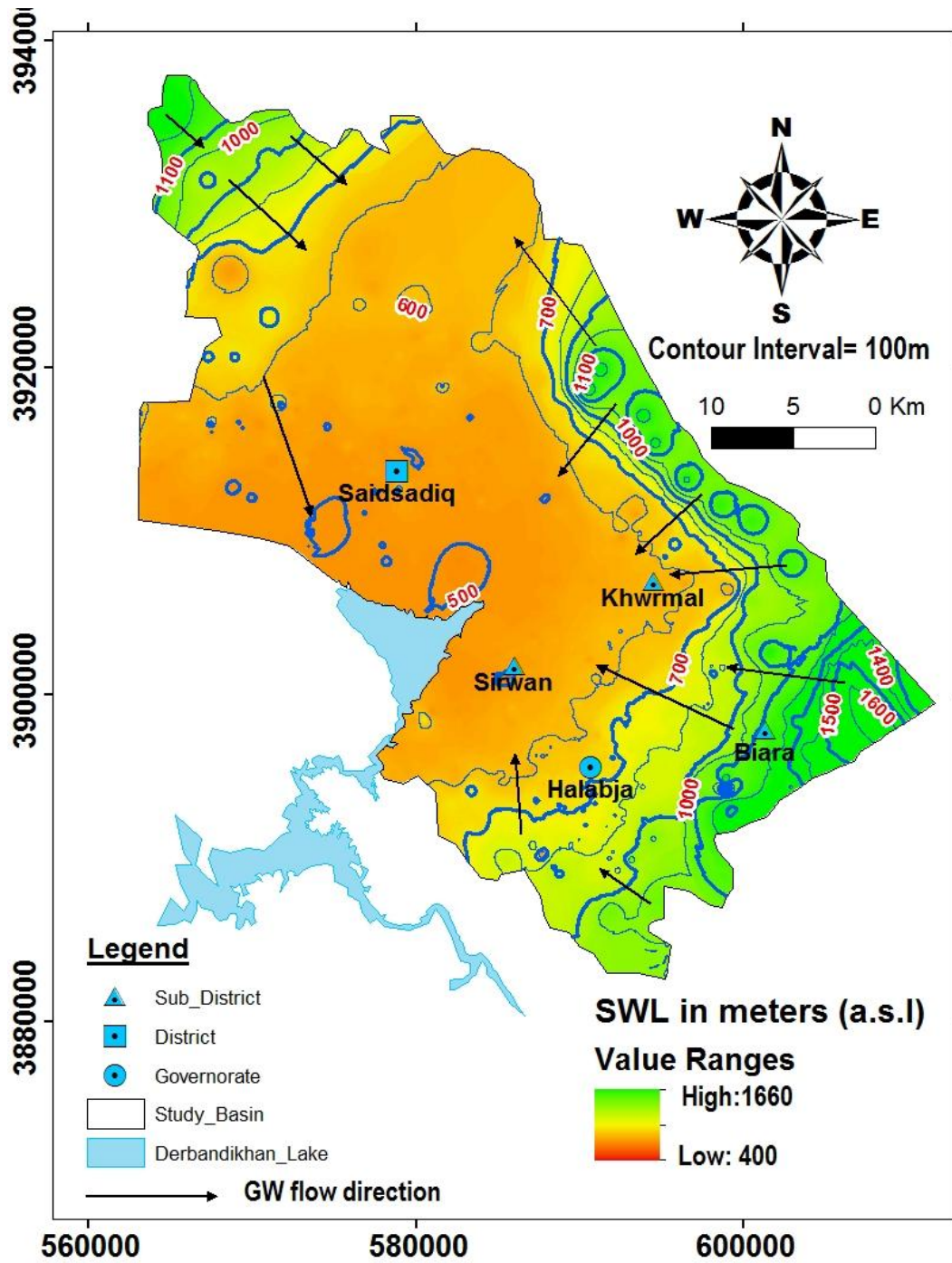
Figure 3.14: Flow net map for the studied basin
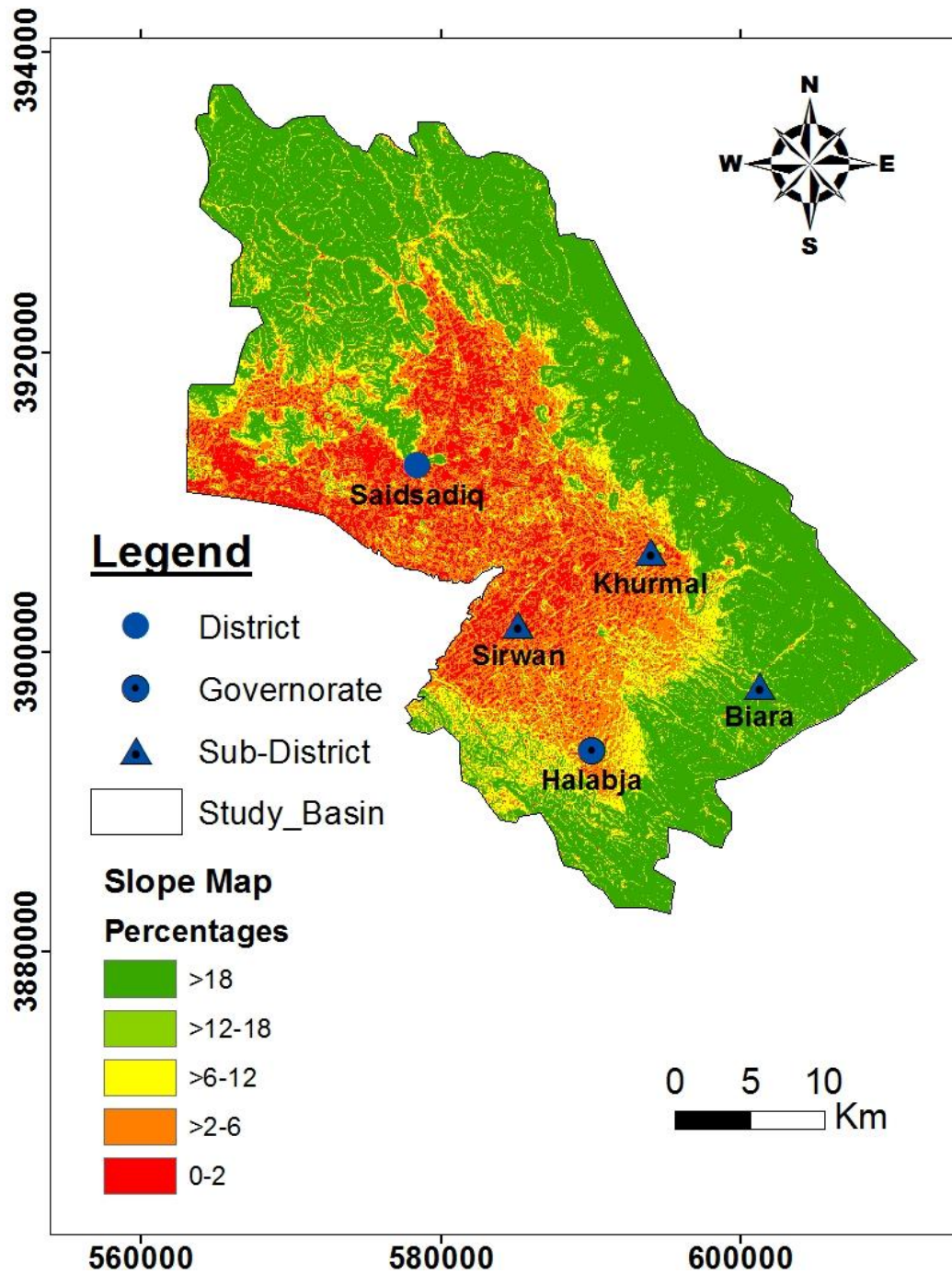
Figure 3.15: Topographic (Slope) map for the studied basin

Chapter Four

Environmenta Impacts Hydrochemistry and GW Quality

Chapter Four

Environmental Impacts, Hydrochemistry and GW Quality

4.1 Preface

The insufficiency of freshwater resources has become an important concern worldwide. Groundwater is of particular importance for public drinking water supply, especially for the residents of arid and semi-arid regions (Mtoni et al, 2013). However, rapid urbanization and increasing populations have accelerated the consumption of groundwater resources and caused serious environmental problems in the last few decades (Yakirevich et al, 2013), and various studies have shown sever groundwater pollution.

In order to evaluate the quality of groundwater in the studied area 78 groundwater samples were collected and analyzed during the dry season September 2014 and wet season May 2015 from both surface and groundwater, for major, minor and heavy metals to evaluate the seasonal variation in groundwater quality. Temperature, electrical conductivity, pH, and turbidity in situ were measured instantaneously using multi-parameter portable device model (TPS/90FL-T Field Lab Analyzer). Sample collection from the drilled wells was often conducted after continuous pumping of 5 -10 minutes. For the chemical analysis, a 250 ml plastic bottle was filled at each locality (Plate 1.3B).

4.2 Environmental Impacts

A sufficient awareness stand for current status of physical environment and understanding of the process involved is required for the health and safety assurance of the people who depend on urban resources particularly water resources. As declared by Montgomery (1997), human activities are modifying chemicals and element concentrations especially trace elements which enter environment and cause pollution and disease and influence

health. In the studied basin, rapid industrial and agricultural growth has taken place recently. This is likely to become manifold in near future particularly in areas like Halabja City and SaidSadiq District.

The dispose of the municipals' wastewater to the environment in the studied basin is through much sewage effluent boxes around the city (Plate 4.1). This sewage is a complex mixture of water consisting of wastes of human, domestic and industrial origin. Associated environmental hazards with use of sewage are contamination of groundwater and accumulation of heavy metals such as cadmium (Cd) and toxic organics in surface soils and water bodies (Roy, 2000). Sewage farm workers are also liable to become infected with cholera if irrigation is practiced with raw wastewater derived from an urban area in which a cholera epidemic is in progress (Shuval et al., 1985). However, morbidity and serological studies on wastewater irrigation workers or wastewater treatment plant workers occupationally exposed to wastewater directly and to wastewater aerosols have not been able to demonstrate excess prevalence of viral diseases.

With the rapid increase in population and growth of industrialization in the area, pollution of surface and groundwater by municipal and industrial wastes has increased tremendously The method of waste disposal in the studied basin is land filling (Plate 4.2). This process of waste disposal focuses on burying the waste in the land. In the absence of well-designed sanitary landfills, municipal and industrial solid waste is invariably dumped on land, creating general nuisance and degradation of soil and water in quality.

In addition, with the advent of industrial revolution and rapid growth of population in the studied basin have been came the demand for a better source of energy such as petrol filling station. Petrol stations are classified as objects of a potentially high environmental impact. Several petrol stations, fuel bases and fuel tanks are operated in the studied basin, (Plate 4.3). The establishment of such industries has led to environmental pollution.

A: Sewage effluent boxes at south east -Halabja City

B: Sewage effluent boxes at north west-Halabja City

C: Sewage effluent boxes at NW of SaidSadiq District

Plate 4.1: Sewage effluent boxes at the studied basin

A: Unsystematic waste disposing at Halabja City

B: Unsystematic covering waste after disposing with soil at Halabja City

Plate 4.2: Municipal waste disposal method at the studied basin

With the expanding population during last few decades, agricultural production has also increased to meet their needs. The potential for irrigation has been increasingly tapped to raise both agricultural productivity and the living standards of the rural and urban population. Irrigated agriculture occupies a major place in the studied basin. Extensive use of fertilizers and pesticides has

been observed in the studied basin, increasing the risk of contamination of groundwater by nutrients and toxic pesticide residues.

Plate 4.3: Contaminated land from petrol products inside of the Halabja City

4.3 Uncertainty Measurement of Chemical Analysis

Every measurement is subject to an element of uncertainty, which may be condensed by improving the method or re-analyzing but can never be entirely eliminated. This uncertainty consists of two contributions: systematic error (accuracy) and random error (precision) (Gill, 1997; Appelo and Postma, 1999 and Rao, 2006).

4.3.1 Precision (Random Error) of Chemical Analysis

Random error of chemical analysis is the precision of a measurement, which is readily determined by comparing data to carefully replicated experiments under the same conditions. The term "precision" is used in describing the agreement with a set of results among themselves (Al–Manmi, 2002). Precision is usually expressed in terms of the standard deviation obtained from replicating measurements. The smaller the standard deviation, the more precise the analysis. As explained by Stoodly (1980), precision or "Coefficient of Variation" which

represents standard deviation from a group data comparing with mean %. So to calculate precision percentages, the following equation has been used:

$$CV(Precision)\% = \frac{2\,SD}{\bar{X}} \; X \; 100 \; ………...……..(4.1)$$

The accepted limit or certain limit (95 % confidence) according to Maxwell, (1968) is between 5 to 25 %.

The accuracy of analysis was calculated according to the equation (4.1). Four samples were taken for this purpose for cations and anions for each dry and wet season, and two samples for heavy metals only for the wet season. Each sample was divided into three equal portions, and then analyzed separately under the same conditions. The results were found to descend within the accepted limit, which means they can be reliable for hydrochemical interpretations. The results from two samples are explained in the Table (4.1), the other two samples are attached as Appendixes (4.1a and 4.1 b).

4.3.2 Accuracy (Systematic Error) of Chemical Analysis

The accuracy (systematic error) of the chemical analysis for major ions can be estimated at the Electroneutrality condition. This is done by taking the relationship between the total cations (Ca^{2+}, Mg^{2+}, Na^+, and K^+) and the total anions ($SO4^{-2}$, $HCO3^-$ and Cl^-) for each set of complete analyses of water sample (Mathhess 1982; Domenico and Schwartz 1990) using the following equation:

$$EN\% = \frac{\sum cation - \sum cation}{\sum cation + \sum cation-} \; X100 \; …………….. \; (4.2)$$

Where EN% (Electroneutrality) is the percent/reaction error and Σ is the total cations and anions expressed in milliequivalents per liter. The accepted limit or certain limit is between 0–5%, while 5–10% should be carefully

Table 4.1: Precision of hydrochemical analysis of water samples

Sample	Parameters	Dry season			Wet season		
		Mean	S.D	C.V (95%)	Mean	S.D	C.V (95%)
W1	Ca^{2+}	41.37	0.57	2.75	38.73	1.10	5.69
Sp1		43.1	0.10	0.46	40.73	0.64	3.16
W1	Mg^{2+}	23.93	0.38	3.16	21.33	0.25	2.37
Sp1		49.37	0.32	1.3	47.17	0.29	1.22
W1	Cl^{-}	19.70	0.66	6.66	19.73	0.46	4.68
Sp1		32.4	0.46	2.83	24	0.10	0.83
W1	NO_3^{-}	0.83	0.02	3.70	41.67	1.15	5.54
Sp1		1.33	0.03	3.98	11.10	0.17	3.12
W1	HCO_3^{-}	191.07	4.77	4.99	191.37	4.15	4.33
Sp1		206.37	1.18	1.15	209.33	0.58	0.55
W1	Na^{+}	1.97	0.03	2.69	1.9	0.10	10.53
Sp1		5.03	0.06	2.29	3.93	0.12	5.87
W1	K^{+}	0.5	0.01	0.46	0.24	0.01	4.88
Sp1		0.52	0.03	11.17	0.12	0.01	9.36
W1	SO_4^{2-}	9.5	0.46	9.65	8.73	0.25	5.76
Sp1		5.97	0.06	1.94	4.8	0.2	8.33
H2	Cd^{+}				0.004	0	0
H4					0.004	0.0001	0
H2	Pb^{+}				0.0363	0.0006	3.18
H4					0.1051	0.0001	0
H2	Zn^{+}		Not Analyzed		0.0294	0.0004	2.7211
H4					0.0342	0.0008	4.4323
H2	Cu^{+}				0.0001	0	0
H4					0.0113	0.0001	2.0498
H2	Ni^{+}				n.d	n.d	n.d
H4					n.d	n.d	n.d

dealt with or should be probable certain and > 10 % (uncertain) which is not useful for geochemical interpretation and must be eliminated from the subsequent analyses. By applying the above methods to the water samples, the results for both seasons were found within the acceptable limit, Table (4.2) for ten wells samples (entire samples attached as Appendixes 4.2a and 4.2b) and Table (4.3) for all spring water samples.

Table 4.2: Accuracy of the hydrochemical analysis of water well samples

No.	Dry season		Wet season	
	En%	Type	En%	Type
W1	3.3	Certain	1.1	Certain
W2	4.8	Certain	3.9	Certain
W3	6.7	P. Certain	8.7	P. Certain
W4	7.4	P. Certain	9.3	P. Certain
W5	3.6	Certain	7.1	P. Certain
W6	4.7	Certain	1.9	Certain
W7	7.9	P. Certain	9.9	P. Certain
W8	4.2	Certain	5.4	P. Certain
W9	4	Certain	6.3	P. Certain
W10	8.7	P. Certain	4.4	Certain

4.4 General Evaluation of the Water Analysis

The results of range and median values of chemical analysis of water samples for two seasons are tabulated and represented in Table (4.4). In addition, the results of chemical and physical analysis for both wet and dry seasons are tabulated in Appendixes (1.2a, 1.2b, 4.1a 4.1b, 4.2a 4.2b, 4.3a   and 4.3b). As mentioned by Hasan et al (2007) and cited in Almanmi (2008), the median value taken since it is more consistent for samples that have outlier values.

Table 4.3: Accuracy of the hydrochemical analysis of spring water samples

	Dry season		Wet season	
No.	**En%**	**Type**	**En%**	**Type**
Sp1	8.6	P. Certain	0.8	Certain
Sp2	1.7	Certain	0.9	Certain
Sp3	4.6	Certain	5.6	P. Certain
Sp4	7.1	P. Certain	7	P. Certain
Sp5	1.9	Certain	9	P. Certain
Sp6	9	P. Certain	1.9	Certain
Sp7	8.2	P. Certain	7.5	P. Certain
Sp8	6.1	P. Certain	2.6	Certain
Sp9	1.7	Certain	6.9	P. Certain

4.5 Physico-Chemical Properties of the Groundwater

The crucial ambition of the physical, chemical and bacteriological analysis of groundwater samples is to establish the origin of water and the degree of pollution (Detay, 1997). The physical properties of groundwater are interpreted in the following sections.

4.5.1 Color, Odor, and Taste

Natural fresh water does not have any color, odor and taste. Color and odor are the most important parameters to be carried out, that the reason for the existence of color and odor is the presence of organic materials such as algae and humic compounds or by increasing concentration of dissolved (Fe and Mn) ions, (Pierce et. al., 1998).The water samples in the studied basin are characterized by colorlessness, odorlessness, and tastelessness. Taste of water may be a result of

increasing carbonate hardness, total dissolved solids (TDS), decreasing dissolved oxygen (D.O2), and extreme bacterial activity.

4.5.2 Temperature (T°C)

Temperature is one of the conventional properties of groundwater; it influences the density and viscosity properties of water (Todd, 1980). As stated by WHO, (2006), temperature impact the suitability of a number of other inorganic elements and chemical contaminants that may affect the taste. All geochemical reactions depend on temperature, so it is essential to measure the temperature to evaluate the type of balance quotient (Saether and Caritat, 1997). Temperature of the water samples was determined in situ during the water sampling.

Several factors effects water temperature variation including, season, elevation, geographic location, and climatic conditions and it is influenced by stream flow, streamside vegetation, groundwater inputs, and water effluent from industrial activities. There is no abnormal value in temperature, and the temperature values of water samples for both dry and wet seasons are presented in Table (4.5). Wells median temperature is 21.1 and 19.5 °C and have the range of 17.6-22.6 and 16.5-23 °C for dry and wet seasons respectively Springs median temperature is 18.3 °C and have the range of 16.8-22°C for the dry season, while for the wet season, the median value is 18.2 °C and the range value is 14.1-23.5 °C. The temperature values of water samples were shown in the Appendices (4.3a and 4.3 b).

4.5.3 Hydrogen Ion Concentration (pH)

Hydrogen Ion Concentration (pH) is defined as the negative log of the hydrogen ion activity. The pH values of the groundwater are explained in the Table (4.6).

Table 4.4: Range and median values of hydrochemical parameters for water samples (well and spring)

Parameters	Dry Season				Wet Season			
	Wells		Springs		Wells		Springs	
	Range	Median	Range	Median	Range	Median	Range	Median
Ca^{2+} (mg/l)	38.5-145.5	78.6	43.2-90.8	68.8	34.3-140.2	74.35	41.2-85.2	67
Mg^{2+} (mg/l)	4.32-43.2	28.3	30.2-79.9	36.7	3-40.2	23.1	28.1-76.4	35
Cl^- (mg/l)	18.4-49.4	34.85	17.3-49.4	32.9	15-45.4	29.55	24.1-45.1	27.5
NO_3^- (mg/l)	0-51.6	10.05	0.16-10.4	1.34	16.8-58	39.5	6.1-18.6	13.7
HCO_3^- (mg/l)	180.5-312.5	236.55	195.7-302.5	231.7	182.1-314.2	244.15	198.5-310.2	240
Na^+ (mg/l)	2-43	8	4-19	5	1.8-39.5	6.95	3-17	4
K^+ (mg/l)	0.5-4.8	1.6	0.02-6	1.7	0.24-4	1.35	0.02-4	1
SO_4^{2-} (mg/l)	7.14-116	27	5.9-108.8	13.7	5.2-110.2	21.6	4-95.1	10.2
Cd^+ (mg/l)	Not Analyzed				0.004-0.0825	0.0041	n.d	n.d
Pb^+ (mg/l)					0.037-0.2369	0.1517	0.00009-0.0007	0.0004
Zn^+ (mg/l)					0.00292-0.0397	0.0298	n.d	n.d
Cu^+ (mg/l)					0.0001-0.0707	0.0126	0.0006-0.0008	0.0007
Ni^+ (mg/l)					0.2231-0.3264	0.27475	n.d	n.d
pH	7.26-8.2	7.66	7.4-8.13	7.58	7.4-8.08	7.7	6.48-7.74	7.53
T.D.S (mg/l)	130-600	220	170-630	250	120-550	195	150-12100	230
T (^{o}C)	17.6-22.6	21.1	16.8-22	18.3	16.5-23	19.5	14.1-23.5	18.2
EC (µS/cm)	296-1430	480	379-717	470	264-1152	393.5	360-2400	430
Turbidity	2-5	4	2-8	3	2-5	3	2-10	3
T.H (mg/l)	202-402	314.9	268.1-454.6	351	186.3-378.5	302.7	256.1-429	328.4

From this table, the pH values in the wet season for the spring and well samples are slightly greater than the values in the dry seasons. This situation might be related to the aquifer recharge from precipitation during the wet season, and leads to excess HCO_3, due to the reaction between H_2O and CO_2.

Table 4.5: Range of temperature values of groundwater samples for wet and dry seasons

Dry Season				Wet Season			
Wells		Springs		Wells		Springs	
Range	Med.	Range	Med.	Range	Med.	Range	Med.
17.6-22.6	21.1	16.8-22	18.3	16.5-23	19.5	14.1-23.5	18.2
Unit (^{o}C)							

Table 4.6: Range of pH values of groundwater samples for wet and dry seasons

Dry Season				Wet Season			
Wells		Springs		Wells		Springs	
Range	Med.	Range	Med.	Range	Med.	Range	Med.
7.26-8.2	7.6	7.4-8.13	7.53	7.4-8.08	7.7	6.48-7.74	7.58

4.5.4 Electrical Conductivity (EC)

Electrical conductivity is defined as the ability of water to conduct an electric current at a standard temperature of 25°C and is measured in microsiemens per centimeter (μS/cm), and it depends on the total amount of soluble salts (Todd, 2005). Electrical conductivity is indirect measurement of salinity and its temperature dependent (Hem, 1991 and APHA,1998). The electrical conductivity of water samples was measured by multi-parameter (TPS/90FL-T Field Lab. Analyzer) in the field. The results of EC value of water samples is revealed in Figure (4.1) and Table (4.7). The values of the

wet season are slightly lower than dry season due to the process of dilution by precipitation.

Concerning conductivity and mineralization, Detay, (1997) recommended a table of relation between water conductivity and mineralization, table (4.8). According to this classification, most of the water samples in the dry season represent moderately mineralized water except for W9, W16, W26, W27, W28 and W29 well samples and Sp5, Sp6 and Sp7 spring water samples which are classified as highly mineralized water. Samples W25 and W30 are classified as excessively mineralized water, while in the wet season, samples W9, W15, W16, W26, W27, W28, W29, and Sp6 are classified as highly mineralized water, and samples W25 and W30 are classified as excessively mineralized water. While the entire samples are classified as moderately mineralized water.

Table 4.7: Range of EC values of groundwater samples for wet and dry seasons

Dry Season				Wet Season			
Wells		Springs		Wells		Springs	
Range	Med.	Range	Med.	Range	Med.	Range	Med.
296-1430	480	379-717	470	264-1151	393.5	26-568	430
Unit (µS/cm)							

4.5.5 Total Dissolved Salt (TDS)

Total Dissolved Solids (TDS) signifies the total amount of residual solids while a water sample evaporates to dryness (Drever, 1997). Total dissolved solids comprise inorganic salts (mostly calcium, magnesium, sodium, potassium, bicarbonates, sulfates and chlorides) and a small amount of organic matter that is dissolved in water.

Table 4.8: Relation between water conductivity and mineralization

(Detay, 1997)

EC (µS/cm)	Mineralization
<100	Very weakly mineralized water (granite terrain)
100-200	Weakly mineralized water
200-400	Slightly mineralized water (limestone terrain)
400-600	Moderately mineralized water
600-1000	Highly mineralized water
>1000	Excessively mineralized water

The TDS values of water samples are shown in Table (4.9). Results of TDS values illustrate that spring and well water are situated within a range of palatable water according to (WHO, 2006 and EU, 2004). In addition, both spring and well water are classified as fresh water according to Altoviski (1962) and Drever (1997), Table (4.10), apart from Garaw spring in Khurmal subdistrict which is classified as (brackish to salty water). This situation referring to the enrichment of the groundwater by the sulfate seems to be the result for such concentration.

Table 4.9: Range of TDS values of groundwater samples for wet and

dry seasons

Dry Season				Wet Season			
Wells		Springs		Wells		Springs	
Range	Med.	Range	Med.	Range	Med.	Range	Med.
130-600	220	170-630	250	120-550	195	150-1140	250
Unit (mg/l)							
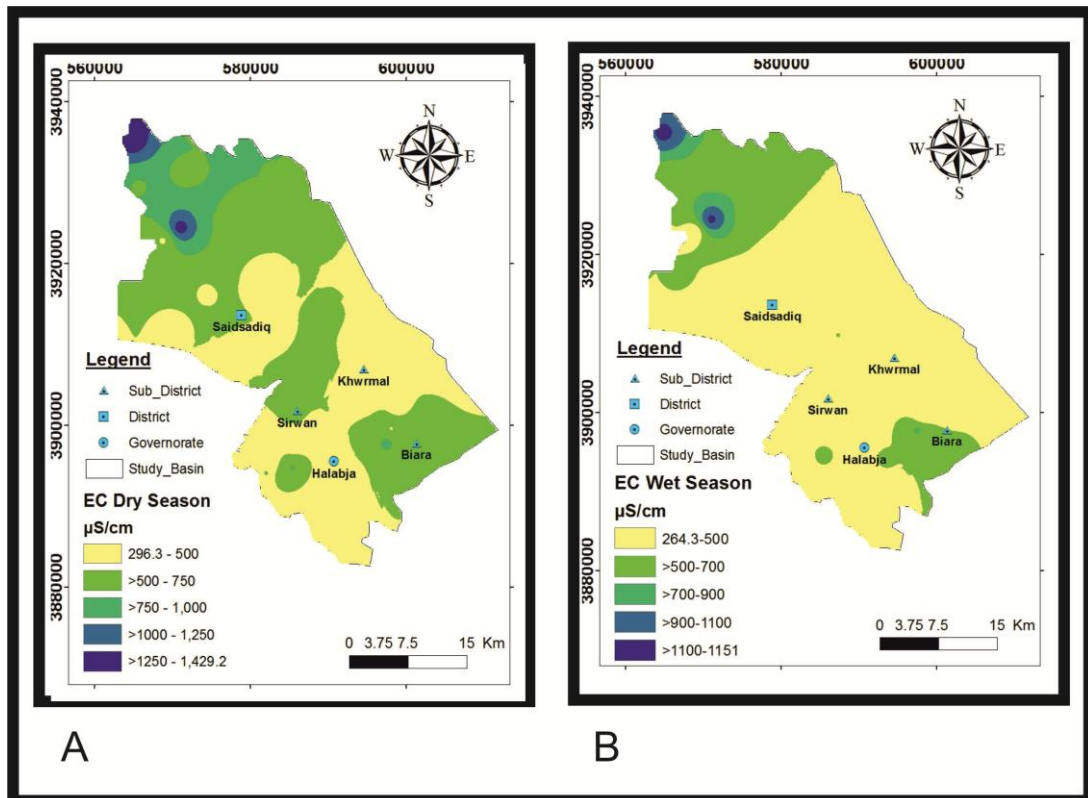
Figure 4.1: EC zones for the studied basin during:

A. Dry season   B. Wet season

Table 4.10: Classifications of water according to (TDS) content in

(mg/l), (Drever, 1997)

Water Class	Drever (1997)	Gorrel (1958)	Altoviski (1962)
Fresh Water	<1000	0-1000	0-1000
Slightly brackish water	-----	-----	1000-3000
Brackish Water	1000-20,000	1000-10,000	3000-10,000
Salty water	-----	10,000-100,000	10,000-100,000
Saline Water	20,000-35,000	-----	-----
Brine Water	>35,000	>100,000	>100,000

The TDS values in the studied basin vary from 130 to 598 mg/l and 120 to 574 mg/l for the dry and wet seasons, respectively (Figure 4.2). High TDS zone is recorded in the southeastern and central parts of the studied basin within the Halabja sub basin. Customarily, the variation in TDS concentration at the southeastern and central parts of the studied basin may attribute to the lithology characteristic and slow to moderate intensity rate of infiltration which provides enough time for the evaporation process which led the TDS to be accumulated especially in the summer season.

4.5.6 Turbidity

Turbidity is the amount of suspended particulate matter in water which is caused by clay, silt, fine organic and inorganic matter and microorganisms (Dybas, 2003). It can be used as a pollution indicator (Al-Manharawi and Hafiz, 1997). The appearance of water with a turbidity of less than 5 NTU is generally acceptable for consumers. The distribution of TU in the studied basin is shown in the Table (4.11). Turbidity of water samples has median value of 3 NTU and range of 2-5 and 2-8 NTU for both wells and springs in the dry season respectively, while for the wet season the turbidity values are slightly higher than in the dry season. This situation corresponds to the recharge process from precipitation.

Table 4.11: Range of turbidity values of groundwater samples for wet and dry seasons

Dry Season				Wet Season			
Wells		Springs		Wells		Springs	
Range	Median	Range	Median	Range	Median	Range	Median
2-5	3	2-8	3	2-5	4	2-10	3
Unit (NTU)							
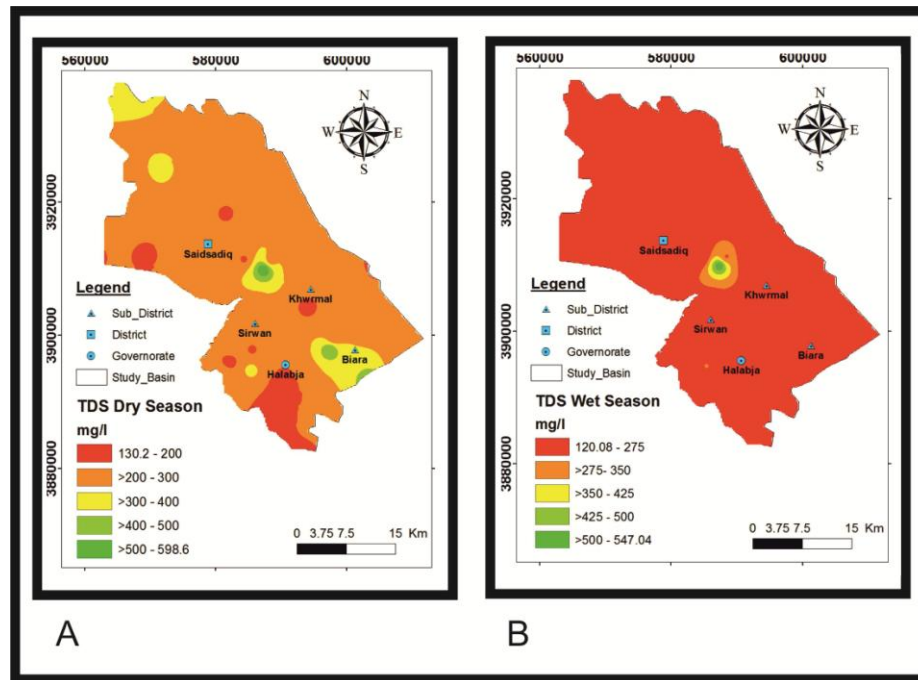
Figure 4.2: TDS zones for the studied basin during:

A. Dry season   B. Wet season

4.6 Chemical Properties of the Groundwater

Chemical characteristics of natural waters depend on several factors such as the lithology of the geological strata in which groundwater is flowing, time of residence of water in the aquifer, and environmental conditions. Ranges and median values of chemical analysis for the groundwater samples in the studied basin are tabulated in the Table (4.4).

4.6.1 Cations

4.6.1.1 Calcium (Ca^{2+})

Calcium is one of the most abundant cations in the studied basin; this may refer to the impact of lithology. The main source of Ca^{2+} is the chemical weathering of rocks and minerals containing calcite, dolomite, and clay minerals (Hem, 1991), in which both carbonate rocks are represented by limestone and quaternary deposits which are composed mostly of eroded fragments of the surrounding limestone, and both occupying more than 80%

of the studied basin. The ranges and median values for calcium concentration for both wells and springs water in the wet and dry seasons are tabulated in the Table (4.4) , and laboratory analysis results are illustrated in the Appendixes (1.2a and 1.2b). Generally, the concentration of Ca^{2+} ion has been observed to be relatively high in the groundwater (Figures 4.3 A and B), especially in the dry season. This may be a result of a number of interrelated geochemical processes like the dissolution and precipitation of calcite and dolomite minerals, which are present in the studied basin from several geological formations.
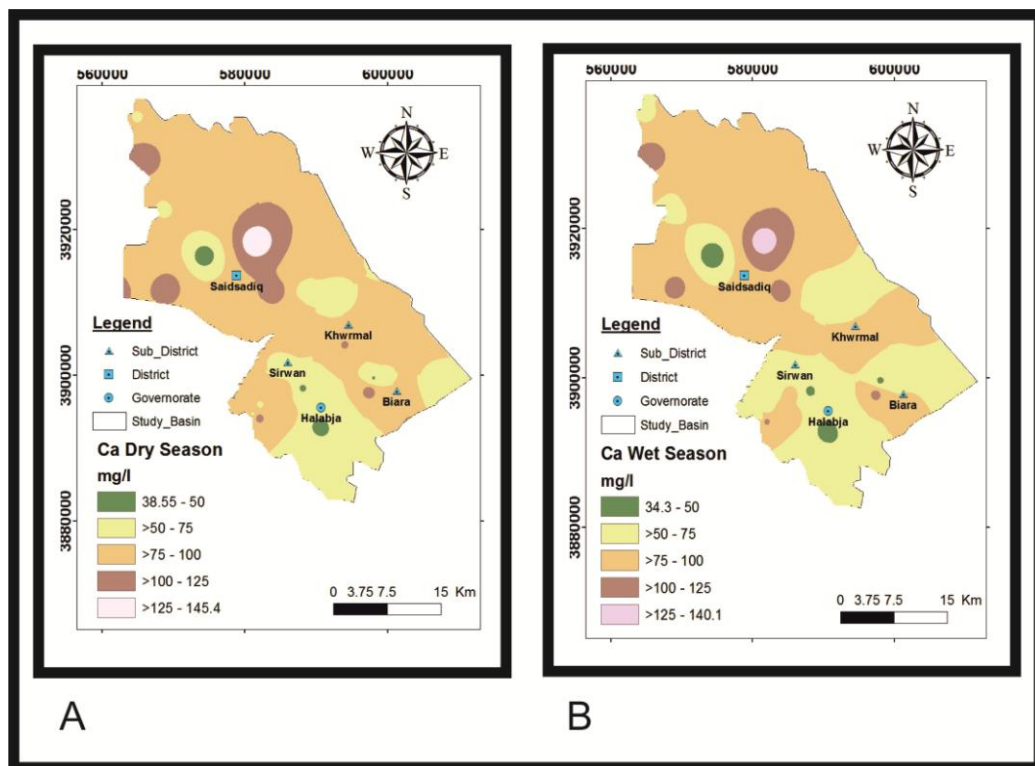
Figure 4.3: Ca^{2+} zones for the studied basin during:

A. Dry season   **B. Wet season**

4.6.1.2 Magnesium (Mg^{2+})

Magnesium is abundant in the carbonate rocks, where it may occur as dolomite and clay minerals (Collins, 1975). In addition, the fertilizers and municipal wastewaters are other sources of Mg^{2+}. Magnesium in fresh water is typically present at concentrations ranging from <10 to 50 mg/l, (Hem,

1991). Magnesium ions are smaller than sodium or calcium ions in natural water because of the solubility of dolomite, which is slower than calcite and limestone (Al-Manmi, 2002). Appendixes (1.2a and 1.2b) show the results of magnesium in well and spring water samples. Median and ranges values are tabulated in the Table (4.4).

Figures (4.4) illustrate the Mg^{2+} concentrations distribution within the studied basin. Mg^{2+} concentrations in different aquifer types vary considerably along the flow direction. Most of the groundwater samples issuing from alluvial deposits have Mg^{2+} concentration higher than issuing from most of formation within the studied basin. This might be attributed to the high residence time of groundwater flow as compared to that of relatively fissured or karstified aquifers. As a result more chance is supposed to be available for ionic exchange to take place.
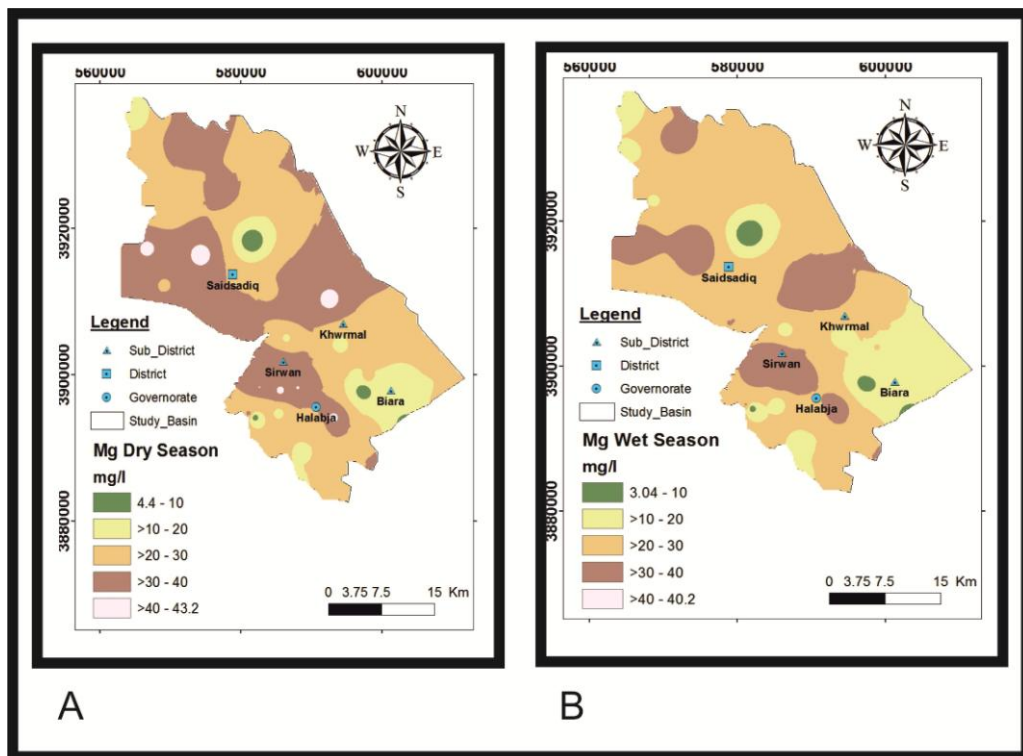
Figure 4.4: Mg^{2+} zones for the studied basin during:

A. Dry season   B. Wet season

4.6.1.3 Sodium (Na$^+$)

The main source of sodium is clay minerals and industrial waste. Rain water is a further source of enrichment of groundwater with sodium that has basically originated from evaporation of sea water (Langmuir, 1997). Human activities can have a significant influence on the concentration of sodium in groundwater. The distribution of Na$^+$ ions is shown in the Figure (4.5) and Appendices (1.2a and 1.2b). Median and ranges values are tabulated in the Table (4.4). In general, sodium values give the impression to be very low in the studied basin; this may be related to presence of geological formations with low concentration of sodium ion.
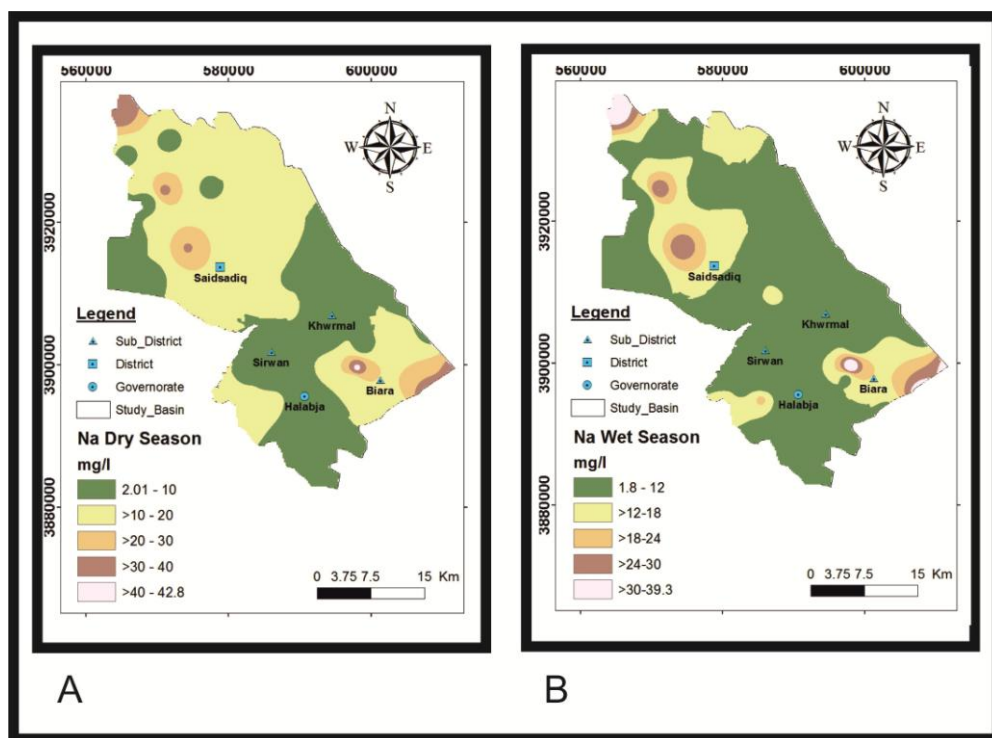
Figure 4.5: Na$^+$ zones for the studied basin during:

A. Dry season   B. Wet season

4.6.1.4 Potassium (K$^+$)

Common sources of potassium in groundwater are feldspars and mica of igneous and metamorphic rocks. The potassium content in natural waters is usually less than that of sodium, magnesium and calcium (Faust and Aly,

1981). The concentration of K^+ ranges between less than 1mg/l in most locations occupied by CFA and TKA to attain a maximum value of 4.8 mg/l in JKA and AIA, Figure (4.6) and Table (4.4).
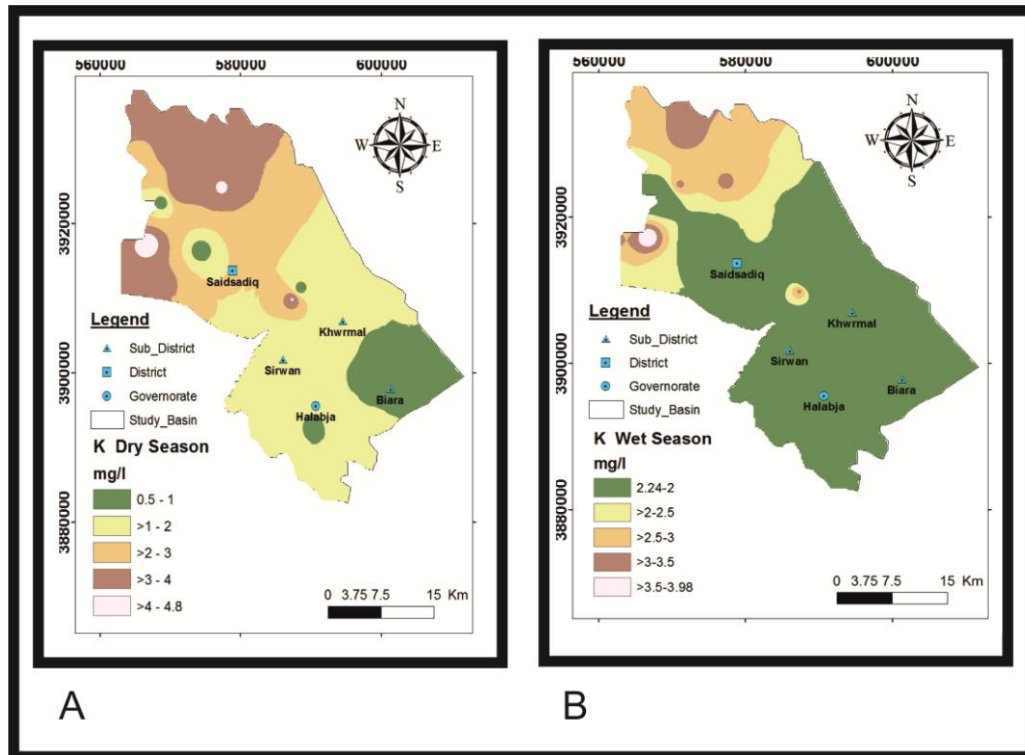
Figure 4.6: K^+ zones for the studied basin during:

A. Dry season   B. Wet season

4.6.2 Anions

4.6.2.1 Bicarbonates (HCO_3^-)

Bicarbonates are the sources of water alkalinity, which is the capacity of water to accept H+ ion and a measure of acid neutralizing capacity (Kiely, 1997). The distribution of HCO_3^- in the studied basin is shown in the Figure (4.7) and Appendixes (1.1a and 1.1 b). Median values are 196.3 and 207.2 mg/l. The ranges value are 155.3-284.8 and 164.3-244.6 mg/l for wet and dry seasons respectively for water samples collected from wells, Table (4.4).

The higher concentration of this ion in the studied area is found within the Saidsadiq sub basin which ranges between >250 to 280 mg/l, High concentration of HCO_3^- in the groundwater may be explained by natural

processes such as the dissolution of carbonate mineral and dissolution of atmospheric and soil CO_2 gas contributed by natural and anthropogenic sources in the groundwater (Todd, 1980) .Therefore, the majority of the groundwater samples issuing from AIA and JKA aquifer is relatively higher in HCO_3^- content than those flowing from TKA aquifer. This might be attributed to the difference in residence time of groundwater flow in the two aquifers. Due to the karstic nature of Avroman aquifer the flow rate is relatively higher than that of AIA and JKA aquifers which consequently increases HCO_3^- content in the later aquifers.
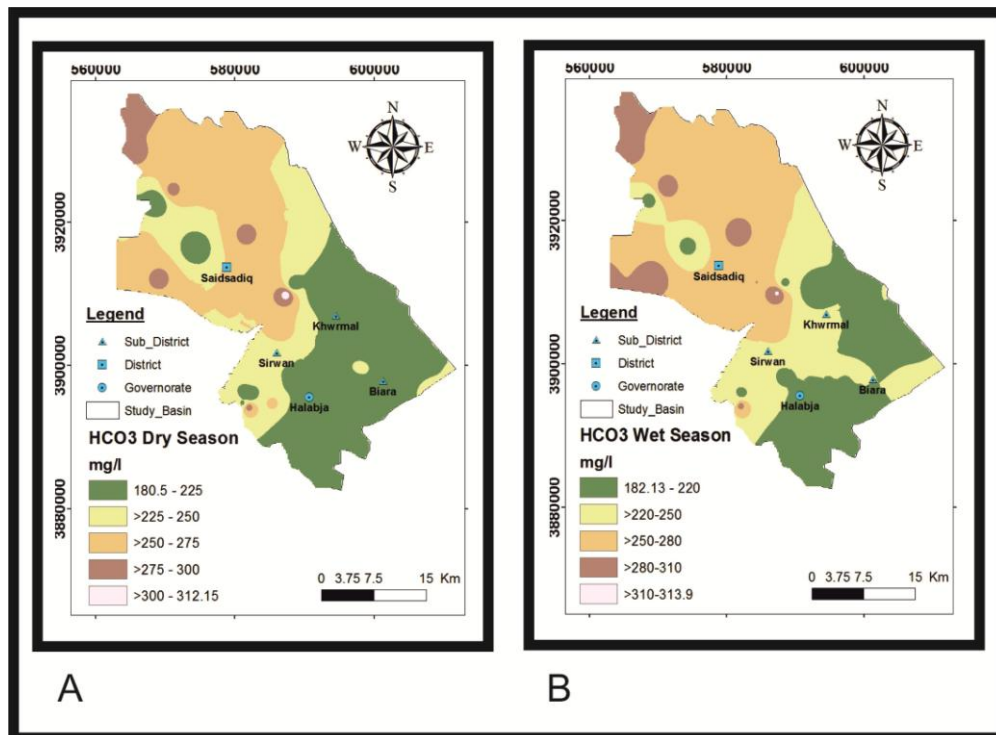
Figure 4.7: HCO_3^- zones for the studied basin during:

A. Dry season   B. Wet season

4.6.2.2 Sulfates (SO_4^{2-})

Sulfates occur naturally in many minerals and are used commercially, and principally in the chemical industry. They are discharged into water industrial wastes and through atmospheric deposition. Besides the natural sources from

dissolution of evaporated rocks, sulfate may be derived from chemical fertilizers, detergents, pesticides and tannin (WHO, 2006). The sulfate concentration of water samples in the studied basin is demonstrated in the Figure (4.8) and Appendixes (1.1a and 1.1b). Median and ranges values are tabulated in Table (4.4).

Sulfate concentration in spring water of the studied area is ranges between 5.9 and 108.8 mg/l and 4-95.1 for the dry and wet season respectively; the highest value was for the Khurmal Sulphide Spring and then the Qawella spring, which is a very low discharging one issuing from JKA in the Galal valley. The lowest concentration was for water samples from the Chawg spring and the Basak spring issuing from CKFA. For the deep wells, sulfate concentration was within the range of 7.14 to 116 mg/l for the dry and wet season respectively; the highest concentration was in two wells. The wells drilled in CKFA, JKA and CFA show a relatively high concentration of SO_4^{2-}.
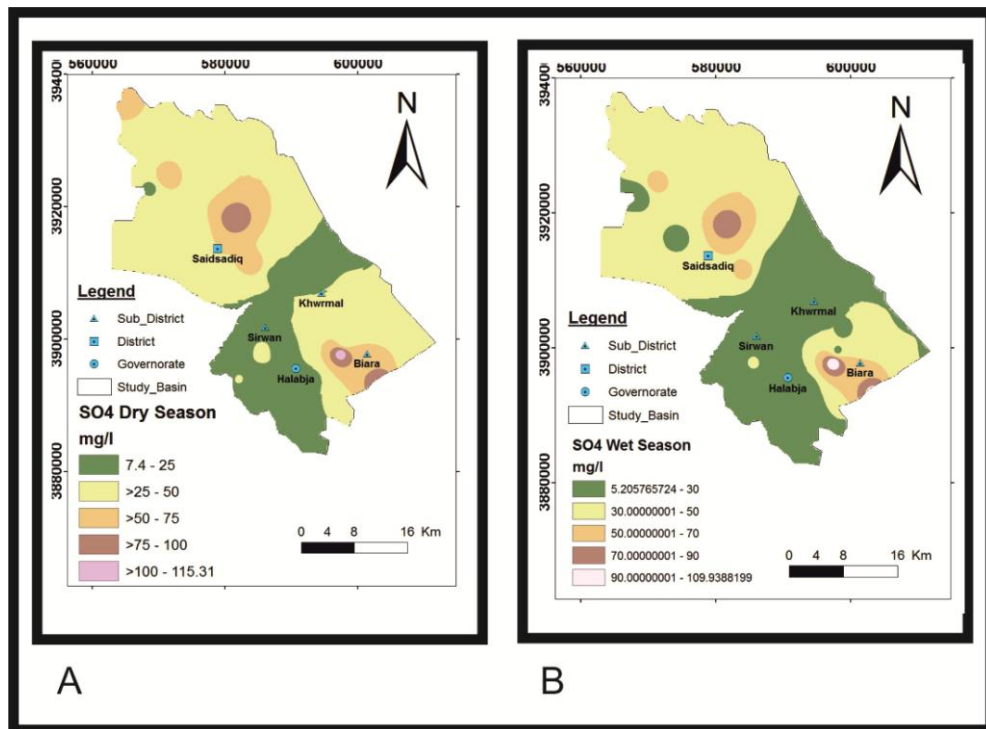
Figure 4.8: SO_4^{2-} zones for the studied basin during:

A. Dry season   **B. Wet season**

4.6.2.3 Chloride (Cl $^-$)

Chloride ions are usually present in natural waters. High concentrations of chloride give a salty taste to water, (WHO, 2008). Chloride concentration ranges from 7.8 ppm in surface water to 20 ppm in the ground water, and 3.2 ppm in rain waters (Langmuir, 1997). The ranges and median values of chloride concentration of water samples are shown in the Table (4.4) and Figure (4.9).

Chloride concentration in the groundwater samples of the studied basin ranged between 18.4- 49.4 and 17.3-49.4 mg/l for the wells and spring's sample in the dry season. While for the wet season, the ranges were 15-45.4 mg/l for wells and 24.1-45.1 mg/l for spring samples.   The highest concentration was for the Gwlakhana well (CKFA), which most likely reached this concentration from sewage water. The lowest concentration was for the wells penetrating CKFA in the Basak village. The Khurmal sulfuric spring shows the highest value of chloride concentration 49.4 mg/l in the dry season. This high value more likely attained through deep geo-hydrochemical processes which, have been taking place in the related Jurassic aquifer.

As a whole, the richness of the lower groundwater in both sulphate and chloride in approximately all the aquifer types within the studied area, led to sustaining better groundwater quality in the area. In most of the CKFA and the AIA sites, when groundwater recharge by precipitation, it influence the process of new water intrusions that contain less Cl$^-$ and Na$^+$ which reforms the chemistry of the groundwater and consequently dilute the concentration of these anions.

4.6.2.4 Nitrate (NO$_3^-$)

Nitrate is classified as a minor compound and is found naturally in the environment and is an important plant nutrient. It is commonly present in

surface and ground water since it is the final product of the aerobic decomposition of organic nitrogenous matter (Bartram and Balance, 1996).
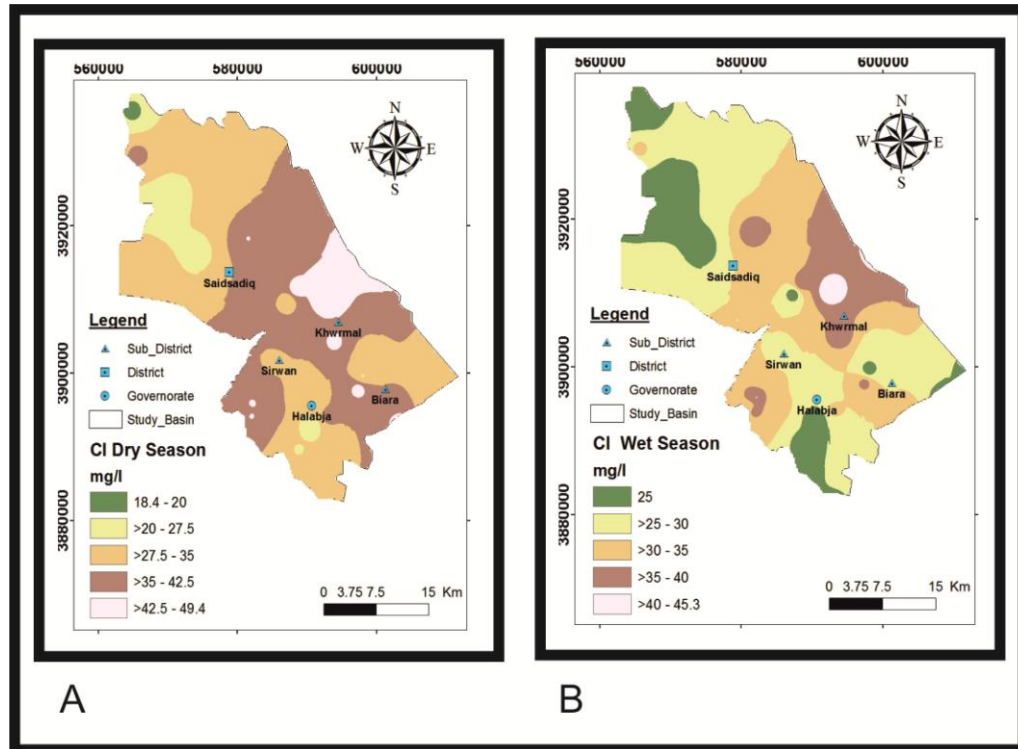
Figure 4.9: Cl⁻ zones for the studied basin during:

A. Dry season   B. Wet season

Nitrate can reach both surface water and groundwater as a consequence of agricultural activity, including excess application of inorganic nitrogenous fertilizers and manures, wastewater disposal and from oxidation of nitrogenous waste products in human and animal excreta, including septic tanks (WHO, 2011).The ranges and median values tabulated in the Table (4.4) and Figure (4.10) illustrate the distribution of nitrate concentration in both dry and wet seasons.

The nitrate detected in all water samples of the springs and well water ranged between 0 and 51.6 mg/l ,with median value of 10.05 mg/l in the well samples and 1.34 mg/l in spring samples, for the dry season. While the range value for the wet season was 16.8-58 mg/l and 6.1-18.6 mg/l for well and spring samples respectively, (Table 4.4). Almost all the spring samples

showed nitrate concentration within the allowable limit based on the (WHO, 2008) and (IQS, 1996), While, some wells recorded higher levels of nitrate than the allowable limit (appendixes 1.1a and 1.1b). In addition, considerable variation in nitrate was noted from dry to wet seasons, Figure (4.10). This condition can be contributed to several main factors such as, rising up the water table in the wet season and vice versa for the dry season; the impact of land use activity in wet season specifically using chemical contaminants (nitrate) for agricultural purposes; and finally, rainfall which plays an important role in transporting nitrate based on specific conditions of aquifer characteristics.
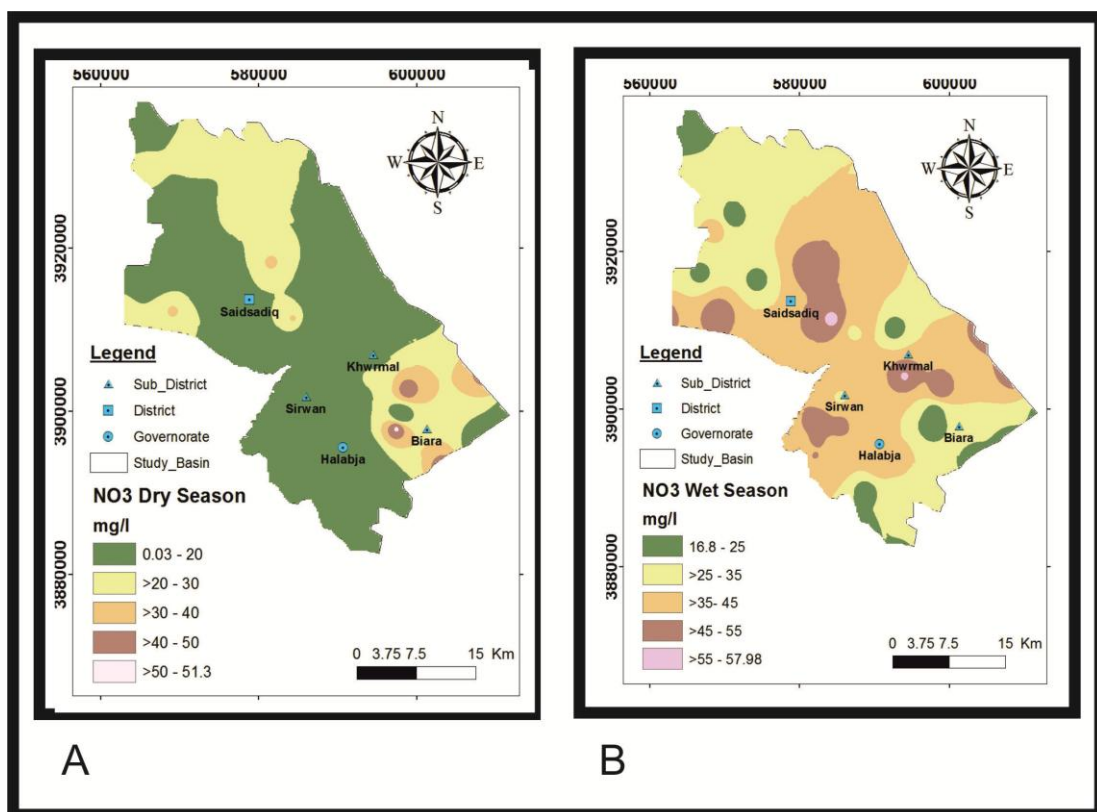
Figure 4.10: NO$_3^-$ zones for the studied basin during:

A. Dry season   B. Wet season

4.6.3 Heavy Metals

Extreme anomalous concentration of heavy metals in water leads to contamination (Tesconi, 2000). To analyze heavy metals, 10 samples for

111

analyzing (Cd, Cu, Zn, Pb, and Ni) were taken and analyzed in the Laboratory of the Director of Environment of Sulaimani. Highly urbanized and sites close to the areas of sewage effluent boxes around and inside Halabja and Saidsadiq cities have been selected for analyzing heavy metals. The range and median values of these analyses are shown in the Tables (4.4) and concentration of these metals presented in Appendixes (4.4). Brief descriptions of some of the above heavy metals are presented in the following section:

Cd - The concentration of cadmium in the analyzed water samples of the studied area ranged between 0.004 - 0.0825 mg/l, with an average of 0.0041mg/l for deep wells and not detected in the spring samples. The level of cadmium in samples (H_1, H4 and H_8) shows a significantly higher concentration than the permissible level of 0.003 mg/l according to WHO (2006) and IQS (1996); particularly in samples from wells penetrating AIA in areas surrounding the unboxed sewerage system in Halabja and Saidsadiq sybbasins. Pollution of groundwater in the area may result from a leakage of sewage waste water. This is accredited to the fact that shallower aquifers are more vulnerable to the impact of surface water or sewages wastewater infiltration predominantly, because most of these wells are not protected and covered properly.

Pb- The concentration of Pb in the well water sample is in the range of 0.037 to 0.2369 mg/l with median value of 0.1517 mg/l. For spring samples it ranged between 0.00009-0.0007 with median value of 0.0004 mg/l. Most of the wells penetrating AIA are slightly polluted with Pb as its concentration in these samples exceeds the recommended value for drinking, 0.01mg/l according to WHO, (2011), EU, (2004) and IQs (1996), (Appendix 4.4).

Zn- Zinc concentration in groundwater samples from the well was in the range of 0.00292 to 0.0397 mg/l with median value of 0.0298 mg/l, while this element was not detected in the spring samples. The water samples were

below the recommended value in groundwater of 0.05 ppm according to WHO (2006).

Cu- The concentration of Cu for the water sample of the studied area was in the range of 0.0001 to 0.0707 mg/l for well samples and 0.0006-0.0008 mg/l for spring samples. This means all water samples fall under the permissible limit with regard to copper concentration according to WHO (2006).

Ni- The concentration of Ni in the well water samples ranges between 0.2231 and 0.3264 mg/l. In general; the majority of the water samples are not contaminated with Ni, except for those exceeding the permissible level of 0.02 ppm recommended by WHO (2006), EU (2004) and IQS (1996). Two Shallow wells from the area close to the end of the sewages system of Halabja and Said Sadiq Sub-basins, show a higher concentration of this element, this kind of pollution of groundwater with Ni might be resulted from a leakage in the sewages system.

4.6.4 Total Hardness (TH)

Hardness is a property of water which causes difficulty of lather with soap. Hardness is caused by calcium and magnesium and depends on the interaction of other factors, such as pH and alkalinity. Total hardness for the analyzed samples was calculated based on equation (4.3) proposed by (Faure, 1998), and the distribution of TH is shown in the Table (4.4). Median values are 314.9 and 351 mg/l; the ranges of values are 202-402 and 268.1-454.6 mg/l for wells and springs, respectively in the dry season. For the wet season, the total hardness is slightly lower than in the dry season; median values are 302.7 and 328.4 mg/l, the ranges of values are 186.3-378.5 and 256.1-429 mg/l for wells and springs, respectively.

Total Hardness = 2.497 (Ca^{2+} mg/l)+ 4.115 (Mg^{2+} mg/l) ………….. (4.3)

Analyzed samples were classified with regard to hardness using Boyd (2000) classification, Table (4.12). From this classification, it is concluded that the samples of wells and springs are belong to very hard to hard water categories.

Table 4.12: Different classifications of water hardness

Boyd (2000)	
T.H **(mg /l CaCo3)**	**Type**
T. H ≤ 50	Soft
50< T.H ≤ 150	Moderately hard
150<T.H ≤ 300	Hard
T. H > 300	Very hard

4.7 Bacteriology

Total coliform bacteria comprise a wide assortment of aerobics and facultative anaerobic capable of growing in the presence of relatively high concentrations of bile salts fermentation of lactose and produce of acid or aldehyde within 24 hours at 35-37°C (Ali, 2007) . The presence of E coli indicates contamination of water with fecal waste and is considered the most suitable index of fecal contamination and pollution, (WHO, 2006), that may contain other harmful or disease causing organisms. Total coliform bacteria (excluding Escherichia coli) occur in both sewage and natural waters. Some of these bacteria are exerted in the faces of human and animals, but many coliform are heterotrophic and able to multiply in water and soil environments.

According to the recommended guideline by WHO (2006), 100 ml of water must be free from total coliform and E coli, while based on the guideline by Abawi and Hasan, (1990), the most probable number (MPN) of total coliform

should not be more than 5/100 ml for each sample and 0/100 ml per couple of successive samples. (MPN) E coli must be less than 1/100 ml and the total count of bacteria must not exceeding 1/ 50 ml. Several samples were taken for bacteriological tests from different sites around Halabja and Saidsadiq main sewerage systems and from several wells in different aquifers. Tables (4.13 and 4.14) demonstrate the results of bacteriological test of both wells and spring water samples of the studied basin.

Table 4.13: Bacteriological test results of the spring water samples of the studied basin

Site	Dry Season		Wet Season	
	MPN 100 ml E Coli	MPN 100 ml Coliform	MPN 100 E Coli	MPN 100 ml Coliform
Chawg Spring	-ve	2.3	-ve	3
Ababaele Spring	-ve	3.4	-ve	4
Jalela Spring	-ve	2.1	-ve	3.2
Ganjan Spring	-ve	4.3	-ve	5
Garaw Spring	-ve	3.5	-ve	5
Sarawy Swbhan Agha Spring	-ve	2.2	-ve	3.2
Basak Spring	-ve	3	-ve	4
Chawgay Mwan	-ve	2	-ve	3
Reshen	-ve	1.8	-ve	2.5

Table 4.14: Bacteriological test results of the well water samples of the studied basin

Site	Dry Season		Wet Season	
	E Coli	MPN 100 ml Coliform	E Coli	MPN 100 ml Coliform
Shallow wells Halabja/1	+ve	>16	+ve	>16
Shallow wells Halabja/2	+ve	>16	+ve	>16
Shallow wells Saidsadiq/1	+ve	>16	+ve	>16
Shallow well Saidsadiq-2	+ve	>16	+ve	>16
Shallow well Saidsadiq-3	+ve	>16	+ve	>16
Jalela Spring	-ve	2.2	-ve	3
Zalm Well	+ve	>16	+ve	>16
Qadafari well	+ve	>16	+ve	>16
Taemor_Hassan	-ve	1.8	-ve	2.2
Chawg_Well	-ve	2	-ve	3
Kharpane_Village	-ve	1.7	-ve	2.2
Basak well	-ve	2.3	-ve	2.8
Qawela well	-ve	2.1	-ve	3
Pari Hero	-ve	1.1	-ve	2
Qawela	-ve	2.3	-ve	3

From the above table, it is obvious that most of the water samples in the studied basin are polluted with bacteria at variable rates. Shallow wells

demonstrate higher percentages of pollution which is actually ascribed to the unacceptable way of drilling and well completion in terms of protective concrete zones against wastewaters. In addition, Ali (2007) conducted an extended studied about bacteriological analysis in different spring waters and aquifers in the studied basin; he also detected that most of the water samples are polluted with bacteria at variable rates.

4.8 Classification of Groundwater

The chemistry of water is very dynamic, largely controlled and modified by its medium of contact namely rocks and soil. Water type and hydrochemical facies evaluations are extremely useful in providing a preliminary idea about the complex hydrochemical processes in the subsurface. Determination of hydrochemical facies is extensively used in the chemical assessment of groundwater and surface water for several decades. Several researchers recommended a variety of classification modes for water classification, including Piper's chart by Hill, (1940), Durov diagram by Durove, (1948). and Chadha's diagram by Chadha, (1999). The groundwater samples of the studied area are classified according to the Piper and Durov classifications.

4.8.1 Piper Diagram

Piper's diagram was made in such a way that the milliequivalents percentages of the major cations and anions are plotted in a separate triangle. These plotted points in the triangular fields are projected further into the central diamond field, which provides the overall character to the water.

The plot of chemical analysis on a Piper diagram(Figures 4.11 and 4.12) for the dry and wet seasons, respectively, shows that the majority of the groundwater samples belong to the field (a and b) of alkaline water with existing bicarbonate with sulfate and chloride. Similarily, Ali (2007) classified groundwater in the same studied basin using Piper's diagram as normal earth alkaline water with prevailing bicarbonate with sulfate and

chloride. The results of both studied confirm the precision and reality of this classification. The impact of the carbonate rocks on the composition of the groundwater type within this group is clear. Thus, high content of the alkaline earth metals could be attributed to the groundwater recharge from the carbonate rock represented by Avroman , Balambo and Jurassic formations that surround the studied catchment.
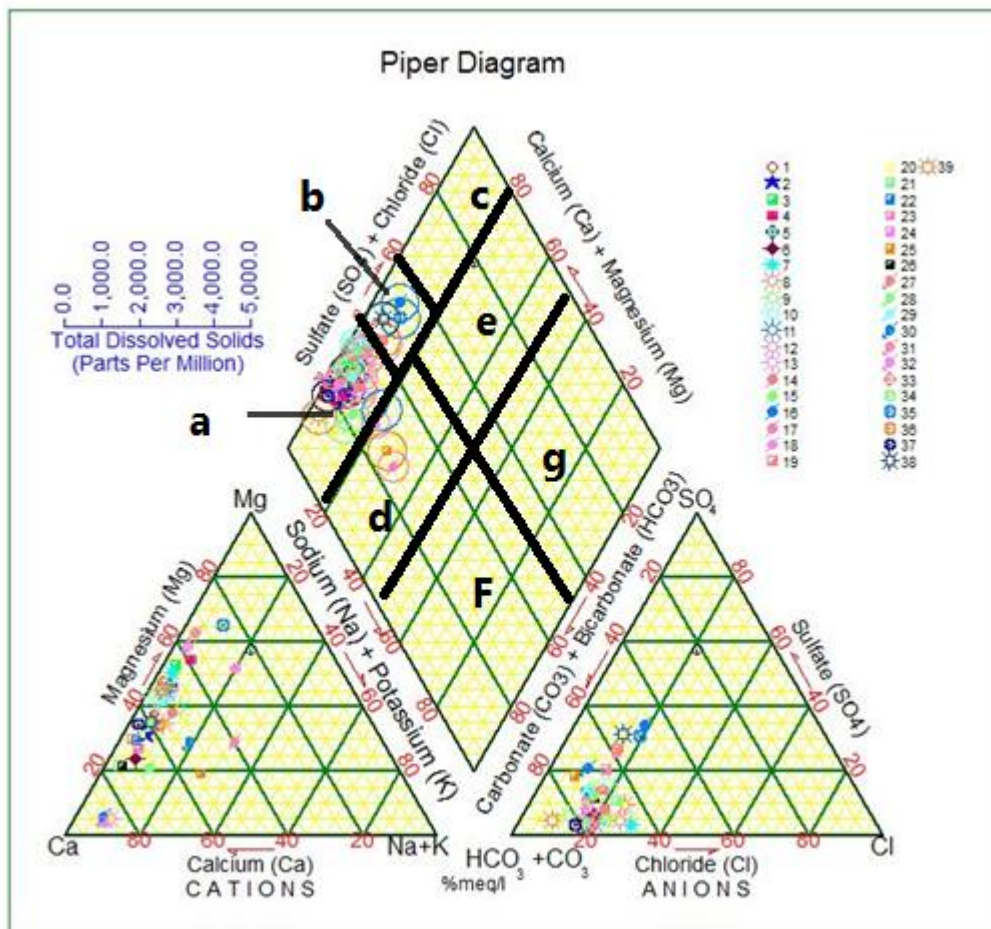
Figure 4.11: Piper diagram shows the hydrochemical composition of the groundwater samples (in %meq/l) from the studied basin in the dry season

4.8.2 Durov Diagram

From Figures (4.13 and 4.14), it is clear that almost all water samples quality fall into the field representing earth alkaline waters with prevailing

weak acid anions. This type of water represents temporary hardness and this region is revealed to be Ca-Mg-HCO$_3$ water type.
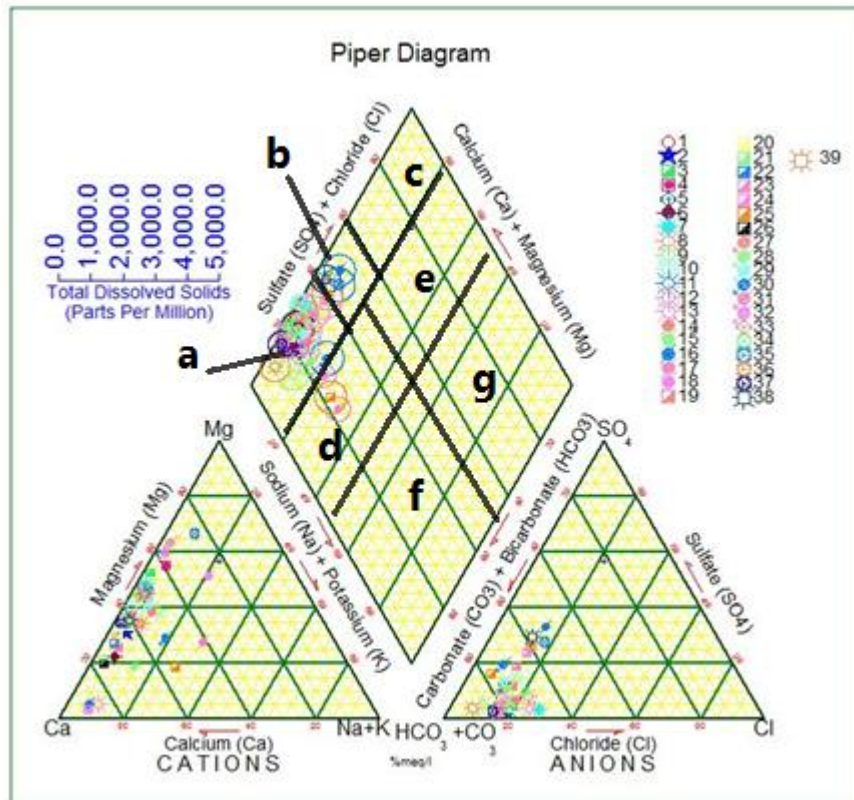
Figure 4.12: Piper diagram shows the hydrochemical composition of the groundwater samples (in %meq/l) from the studied basin in the wet season

4.9 Groundwater Quality Index

Groundwater is the main source of water that meets the agricultural, industrial and household requirements. Population growth, socioeconomic development, technological and climate changes had increased the demand for potable water manifolds in the past few years (Alcamo et al., 2007). One of the internationally accepted human rights is the access to safe drinking water which is the basic need for human health and development (WHO, 2001).
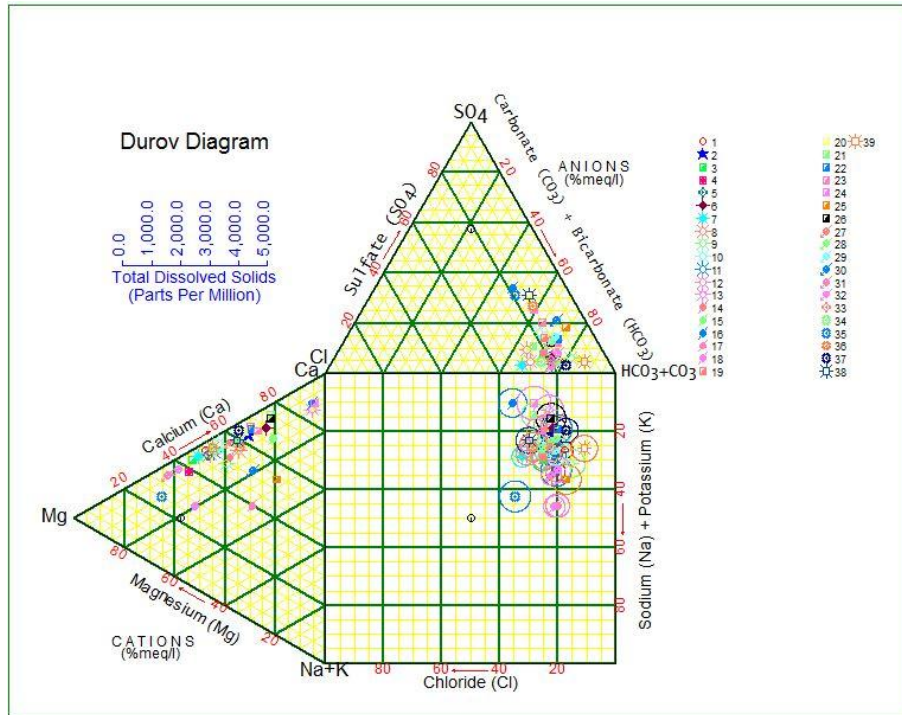
Figure 4.13: Durov diagram shows the hydrochemical composition of the groundwater samples (in %meq/l) from the studied basin in the dry season
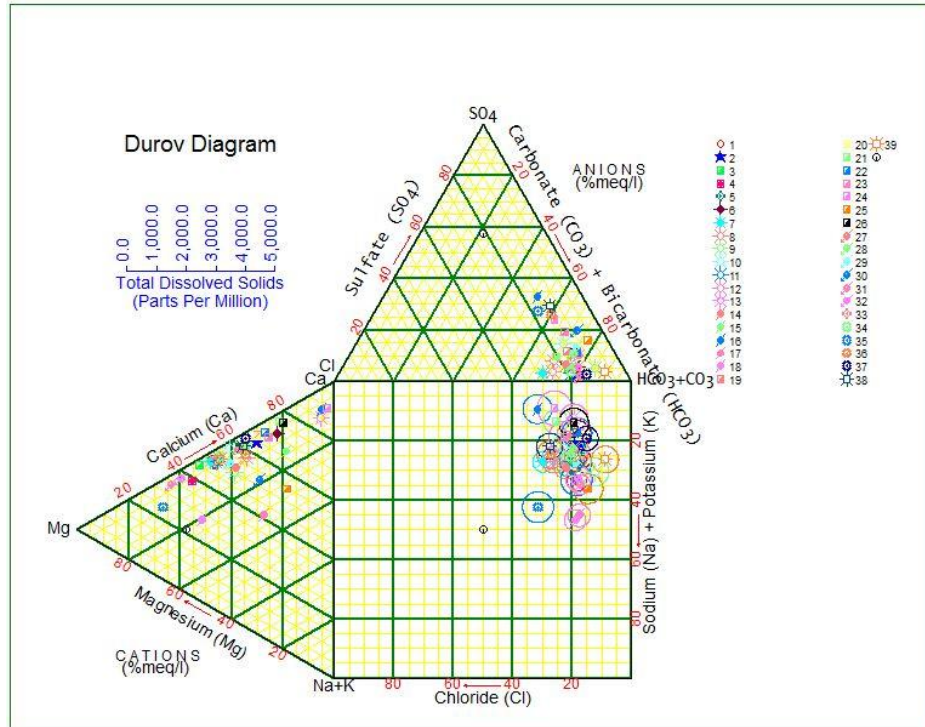
Figure 4.14: Durov diagram shows the hydrochemical composition of the groundwater samples (in %meq/l) from the studied basin in the wet season

120

4.9.1 Domestic Groundwater Quality Index

Assessment of groundwater quality is necessary to determine its suitability for different uses. Goyal et al., (2010) classified the suitability of groundwater for domestic uses on the basis of hydrogen ion concentration (pH), total dissolved solids (TDS) and total hardness (TH). In addition, in the past few years the Geographic Information System (GIS) has become an efficient and effective tool in solving problems where data varies in spatial extent. Therefore, it is widely used for evaluation and assessment of water quality and developing solutions for water resources related problems (Chaudhary et al., 1996).The present study has been carried out to assess the seasonal variations on the groundwater quality in the dry and the wet periods and to compare its suitability for domestic uses confirming to the latest quality standards.

The chemical analysis results obtained were compared to the drinking water standards of WHO, 2008 and IQS 1996, to arrive at conclusions. Hydrogen ion concentration was measured in terms of pH values. Although pH usually has no direct impact on health of consumers, it is one of the most important operational water quality parameters. In the studied basin pH values was found to vary between 7.26 to 8.2 and 7.4 to 8.1 in the dry and the wet seasons respectively, for the period of September 2014 to May 2015. As per WHO (2008) standards, the suitable range of pH for domestic use is 6.5 to 9.2, and per Iraqi standard in 1996 the suitable range is 6.5 to 8.5, this reveals that groundwater in the studied basin had hydrogen ion concentration in the desirable range.

TDS refers to any minerals, salts, metals, cations and anions dissolved in water (viz section 4.5.5). It is reported that TDS levels less than 600 mg/l is considered to be good and concentration greater than 1000 mg/l decreases the palatability of the drinking water (WHO 2008). Values of TDS in the studied

area varied between 130 to 600 and 120 to 550 with an average value of 254 mg/l and 200 mg/l in the dry and wet seasons respectively. The spatial distribution map of TDS (figure 4.15) shows that most of the studied areas have desirable concentration of TDS in groundwater both in the dry and the wet seasons. Increased average value of TDS in the dry season indicates that the augmented groundwater expulsion and the evaporation process lead to the extreme deposition of desirable salts.
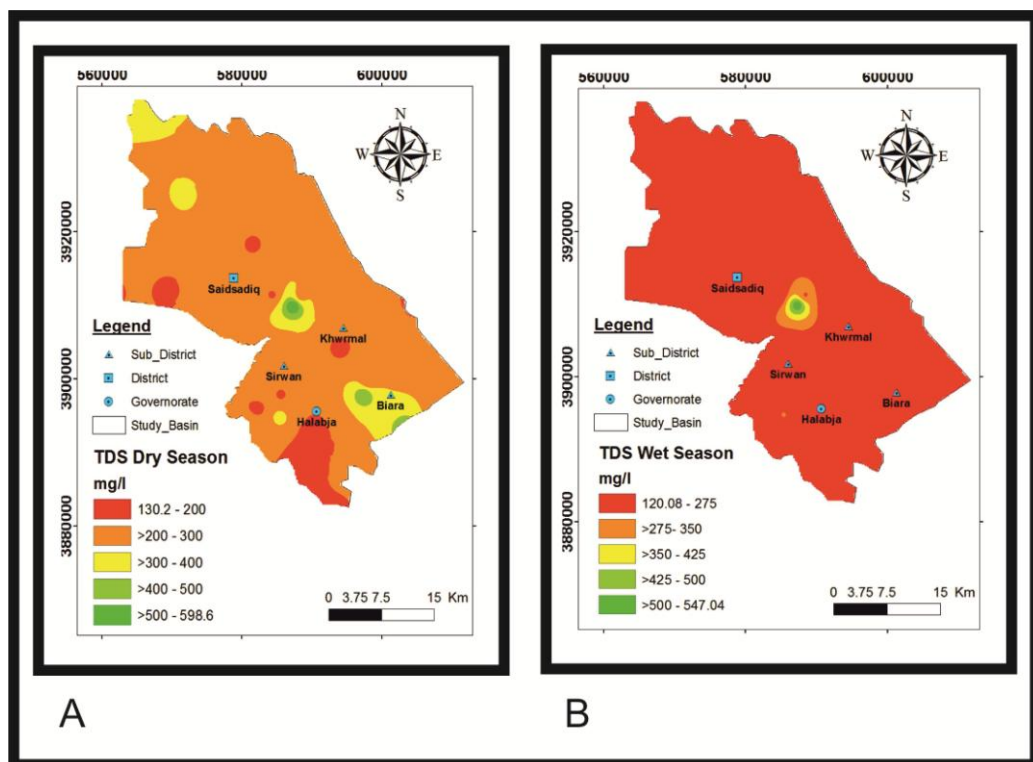
Figure 4.15: Suitability of groundwater for domestic purpose based on spatial distribution of TDS: A. Dry season B. Wet season

Hardness is a very important property of water from its drinking application point of view (Goyal et al., 2010). The spatial and temporal variation of groundwater hardness is mapped in the Figure (4.16). Analysis reveals that water in the studied area is hard to very hard in general base on the classification of Boyd (2000), because the average hardness is 318 mg/ l and 299 mg/l for the dry and the wet seasons, respectively. The acceptable limit for TH as per IQS (1996), norms is 500 mg/l. Consequently, the results of analysis reveal that the whole studied basin has an accepted limit of total

hardness in groundwater for drinking purpose both in the dry and the wet seasons.
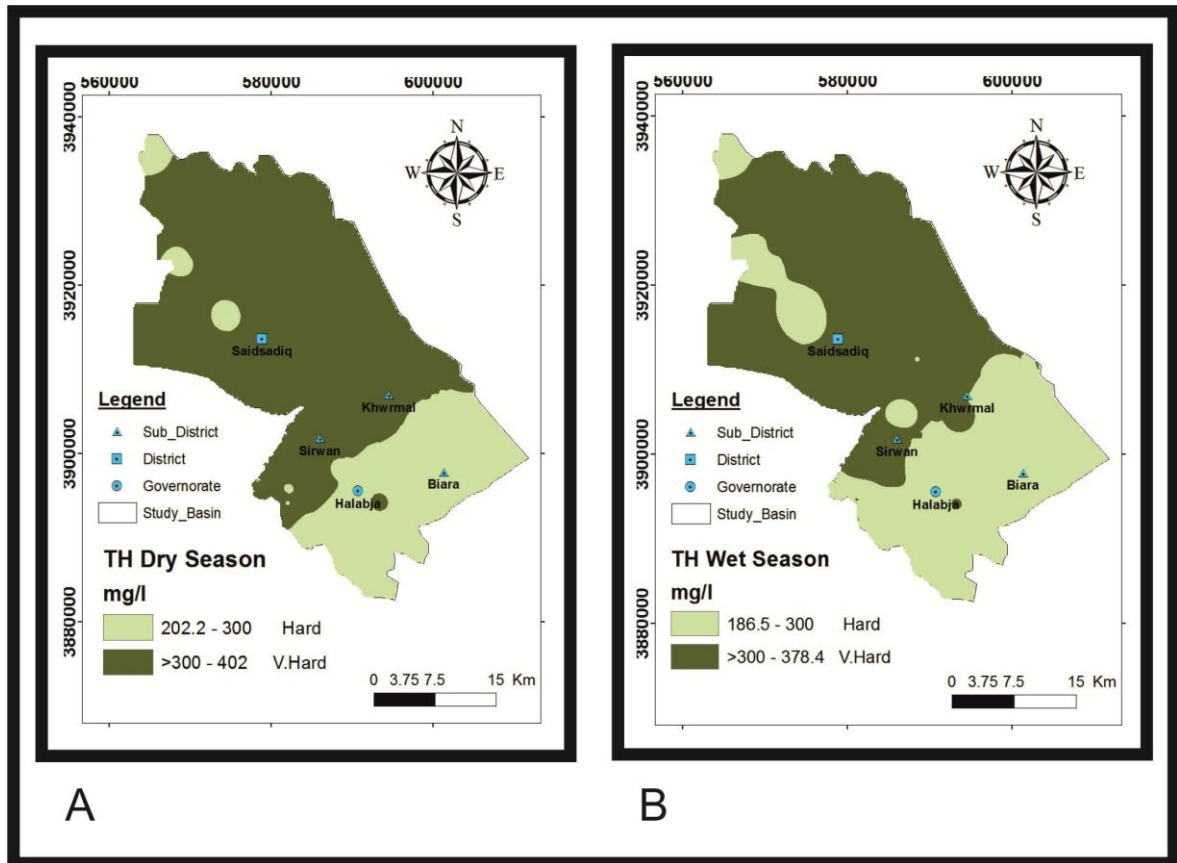
Figure 4.16 Suitability of groundwater for domestic purpose based on spatial distribution of TH: A. Dry season B. Wet season

4.9.2 Irrigation Water (Groundwater) Quality Index

The water quality evaluation model is applied to this study in two steps .In the first step, water quality indexes WQI model is used. A designation of quality measurement values (Qi) and aggregation weights (Wi) were recognized. Values of (Qi) were estimated based on each parameter value shown in (Table 4.15) which is recommended by Ayers and Westcot (1999). Water quality parameters were symbolized by a non-dimensional number;the higher the value, the better the water quality. Values of Q_i were computed using the following equation, based on the laboratorial result of water quality analysis and the tolerance limits, shown in Table (4.16).

$$Q_i = q_{imax} - [\frac{(Xij - Xinf)x^2}{Xamp} qiamp] \ldots\ldots\ldots\ldots(4.4)$$

Where qi_{max} is the maximum value of q_i for the class, X_{ij} is the observed value for the parameter, X_{inf} is the corresponding value to the lower limit of the class to which the parameter belongs; qiamp is the class amplitude; X_{amp} is the class amplitude to which the parameter belongs. In order to evaluate X_{amp} of the last class of each parameter, the upper limits were considered to be the highest value determined in the physical-chemical and chemical analysis of the water samples. The weight of each parameter used in the IWQI is explained on Table (4.16) which is recommended by (Meireles et al., 2010). The aggregation weights (W_i) were normalized such that their sum equals one.

By summation of both Q_i and W_i , the Irrigation Water Quality Index (IWQI) was calculated as(Hussain et al ,2014):

$$IWQI = \sum_{i=1}^{n} Qi * Wi \ldots\ldots\ldots\ldots(4.5)$$

Table 4.15: Parameter limiting values for quality measurement (q_i) calculation (Meireles et al., 2010)

Qi	EC (μS/cm)	SAR (mmol/L)$^{1/2}$	Na$^+$	Cl$^-$	HCO$_3^-$
				(mmol/L)	
85 – 100	200≤EC<750	2 ≤SAR< 3	2 ≤ Na < 3	1 ≤ Cl < 4	1≤ HCO$_3$<1.5
60 – 85	750≤EC<1500	3 ≤SAR< 6	3 ≤ Na < 6	4 ≤ Cl < 7	1.5≤ HCO$_3$<4.5
35 – 60	1500≤EC<3000	6≤SAR<12	6 ≤ Na < 9	7 ≤ Cl < 10	4.5≤ HCO$_3$<8.5
0 – 35	EC<200 or EC≥3000	SAR<2 or SAR≥12	Na < 2 or Na ≥ 9	Cl< 1 or Cl≥ 10	HCO$_3$<1 or HCO$_3$≥ 8.5

Table 4.16: Weights for the IWQI parameters (Meireles et al., 2010)

Parameters	W_i
Electrical Conductivity (EC)	0.211
Sodium (Na^+)	0.204
Chloride (Cl^-)	0.194
Bicarbonate (HCO_3^-)	0.202
Sodium Adsorption Ratio (SAR)	0.189
Total	**1.00**

IWQI is a dimensional parameter ranging from 0 to 100; Qi is the quality of the ith parameter, a number from 0 to 100, function of its concentration or measurement, w_i is the normalized weight of the ith parameter, function of importance in explaining the global variability in water quality.

Classes division according to the proposed water quality index was based on existent water quality indexes, and classes were defined considering the risk of salinity problems, soil water infiltration reduction, in addition to toxicity to plants as observed in the classification presented by (Bernardo, 1995) and (Holanda and Amorim, 1997). Restriction of water to use classes was characterized and explained on Table (4.17).

In order to develop the applied IWQI, several parameters were used including EC, Cl, Na, HCO3 and SAR. The weight (Wi) of each parameter was used based on (Table 4.16). The quality measurement (Qi) was calculated based on equation (4.4).The result of both quality measurement and applied weight is presented in the Table (4.18) and Figures (4.17 and 4.18).

The Irrigation Water Quality Index (IWQI) maps were produced according to the equation (4.5). The spatial analysis tool of GIS environment was used for overlapping of the thematic maps for the parameters used in this model (EC, Na^+, Cl^-, HCO_3- and SAR).

Table 4.17: IWQI characteristics (Meireles et al, 2010)

IWQI	Water Use Restriction	Recommendation	
		Soil	**Plant**
85 ≤100	No restriction (NR)	May be used for the majority of soils with low probability of causing salinity and sodicity problems, being recommended leaching within irrigation practices, except for in soils with extremely low permeability	No toxicity risk for most plants
70 ≤ 85	Low restriction (LR	Recommended for use in irrigated soils with light texture or moderate permeability, being recommended salt leaching. Soil sodicity in heavy texture soils may occur, being recommended to avoid its use in soils with high clay levels 2:1.	Avoid salt sensitive plants
55 ≤ 70	Moderate restriction (MR)	May be used in soils with moderate to high permeability values, being suggested moderate leaching of salts.	Plants with moderate tolerance to salts may be grown.
40 ≤ 55	High restriction (HR)	May be used in soils with high permeability without compact layers.High frequency irrigation schedule should be adopted for water with EC above 2.000 dS m-1 and SAR above 7.0.	Should be used for irrigation of plants with moderate to high tolerance to salts with special salinity control practices, except water with low Na, Cl and HCO3 values
0 ≤ 40	Severe restriction (SR)	Should be avoided its use for irrigation under normal conditions. In special cases, may be used occasionally. Water with low salt levels and high SAR require gypsum application. In high saline content water soils must have high permeability, and excess water should be applied to avoid salt accumulation.	Only plants with high salt tolerance, except for waters with extremely low values of Na, Cl and HCO3.

Table 4.18: Weight and quality range for IWQI parameters

Parameters	Dry season		Wet season	
	Wi	Qi-Range	Wi	Qi-Range
EC	0.211	62.3-97.4	0.211	45-98.3
SAR	0.189	0.1-35	0.189	0.22-35
HCO_3^-	0.202	56.1-72.8	0.202	55.9-72.6
Na^+	0.204	0-35.0	0.204	0.06-35
Cl^-	0.194	16.8-100	0.194	13.4-99.8

Figure (4.19) illustrates spatial distribution of IWQI in the studied basin. According to these figures, the area is divided into three different ranges of groundwater quality of both seasons, which are 33.1-40, >40-55 and >55-66.9 in the dry season and 33.42-40, >40-55 and >55-66.9 in the wet season. Consequently, the spatial distribution of IWQI was reclassified based on ranges of water characteristics given by (Meireles et al, 2010). The suitability classes are elucidated in the Figure (4.20). Three classes have been recognized at the studied basin within both seasons due to the effect of saline constituent on groundwater. The high restriction (HR) classes occupies an area of 52.4% of the whole studied area in the dry season and 83.3% in the wet seasons, while Sever Restriction (SR) and Moderate Restriction (MR) occupy an area of 1.4% and 46.2% and 0.7% and 16% for the dry and the wet seasons respectively.

The result illustrates considerable variations materialized between (SR, HR and MR) from dry to the wet seasons, HR increased dramatically in wet season and MR and SR decreased significantly as well in the wet season. This is due to decreasing the IWQI value of the wet season as a result of dilution of water or aquifer recharge from precipitation and decreasing the water discharge from wells.
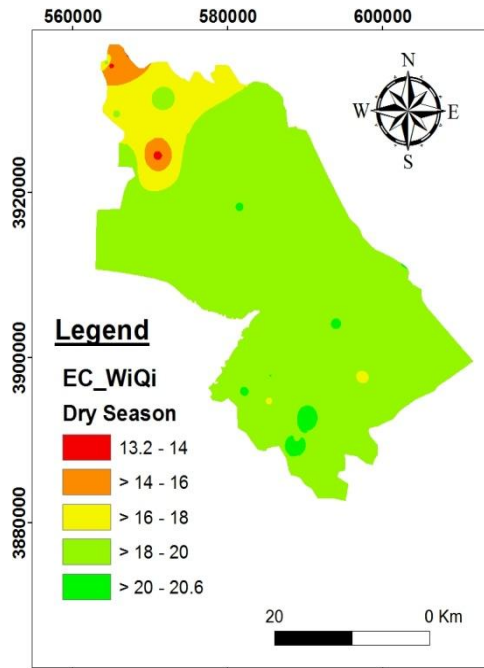
A1: EC-WiQi-dry season
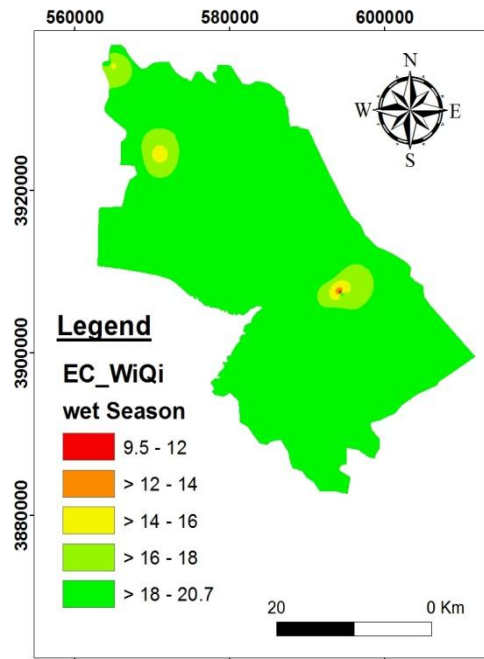
A2: EC-WiQi-wet season
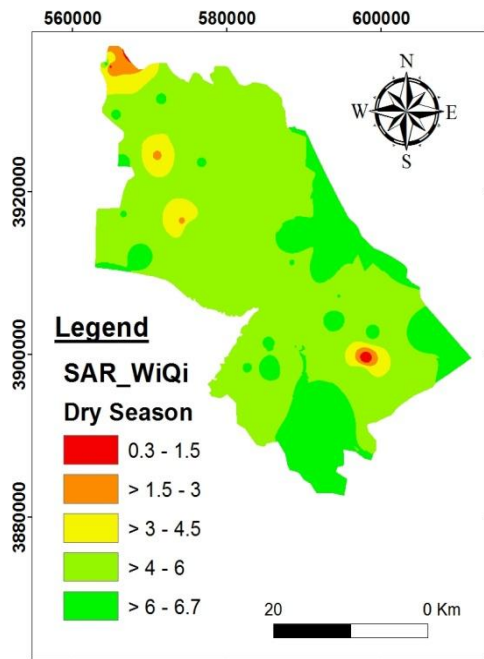
B1: SAR-WiQi-dry season
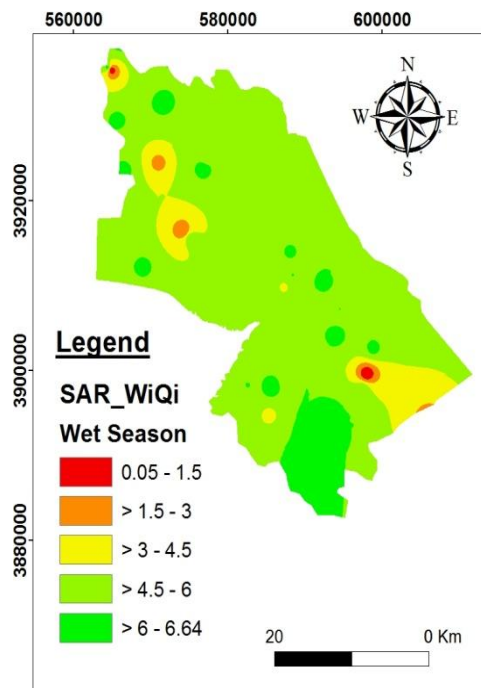
B2: SAR-WiQi-wet season

Figure 4.17: Spatial distribution for the concentration of (EC and SAR) in dry and wet seasons
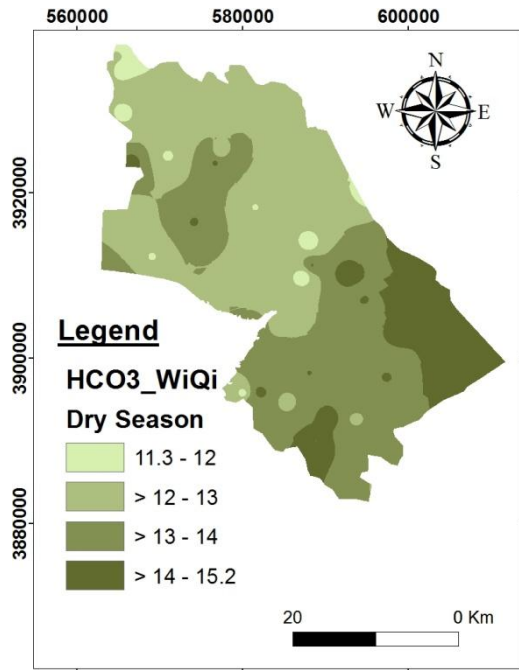
A1: HCO₃⁻WiQi-dry season
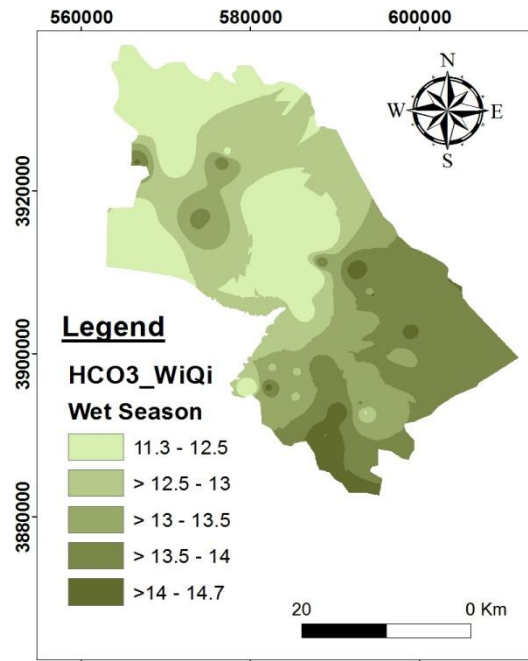
A2: HCO₃⁻WiQi-wet season
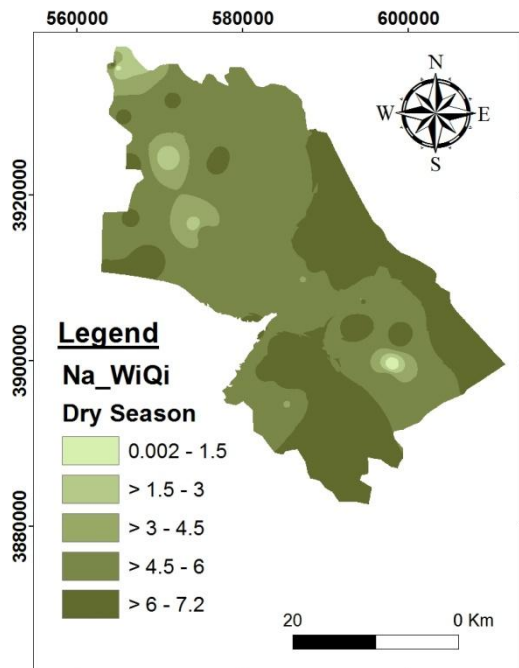
B1: Na⁺WiQi-dry season
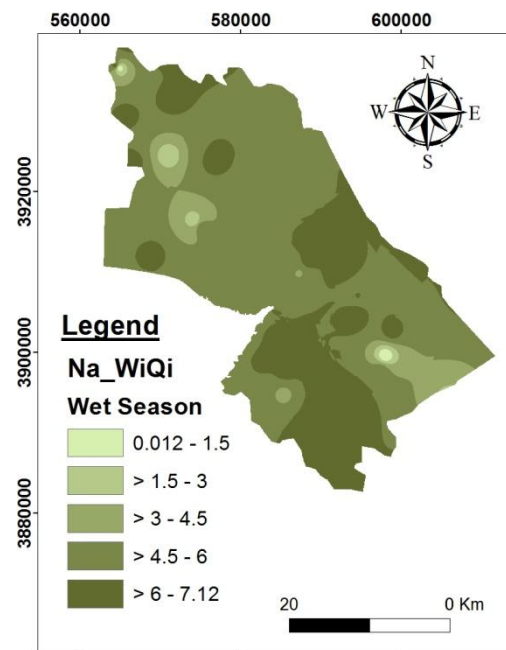
B2: Na⁺WiQi-wet season
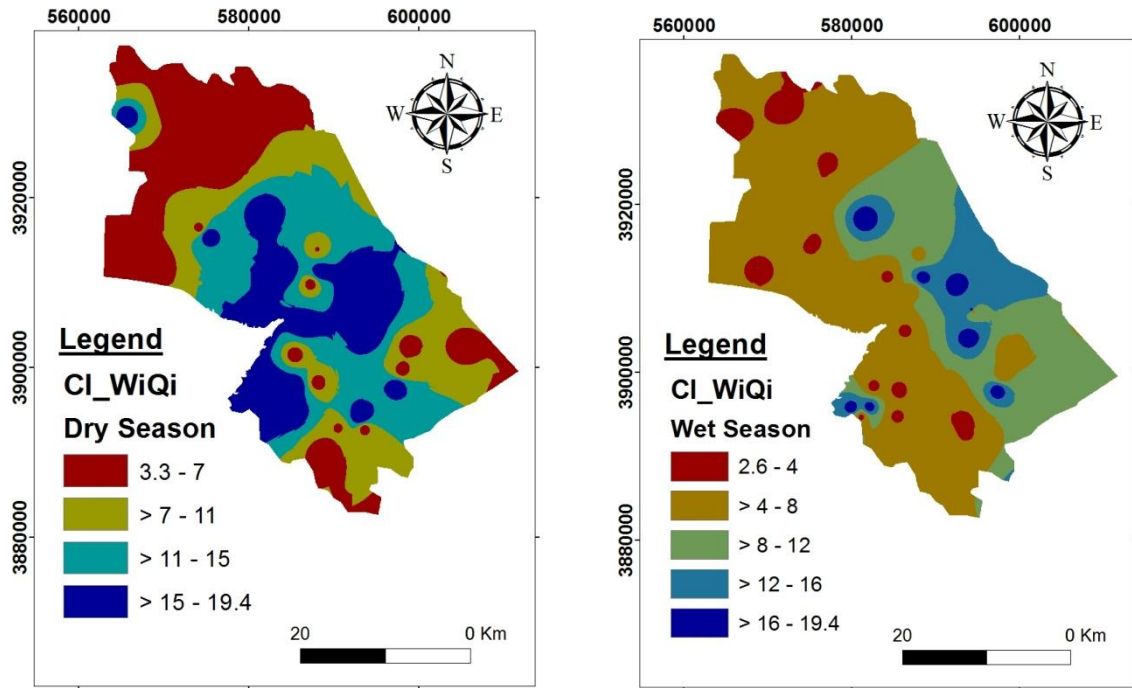
C1: Cl⁻ WiQi-dry season   **C2: Cl⁻ WiQi-wet season**

Figure 4.18: Spatial distribution for the concentration of (HCO⁻3, Na⁺ and Cl⁻) in the dry and wet seasons
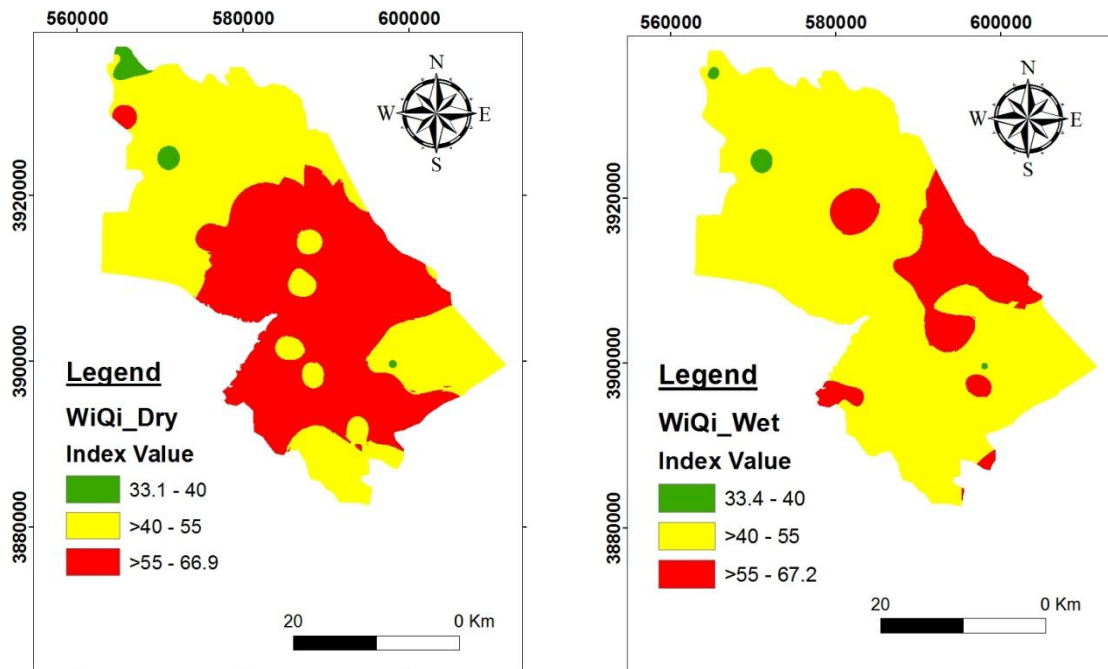
A: Dry season   **B: Wet season**

Figure 4.19: Spatial distribution of IWQI map in the studied basin in the dry and wet seasons

A:Dry season   **B: Wet season**
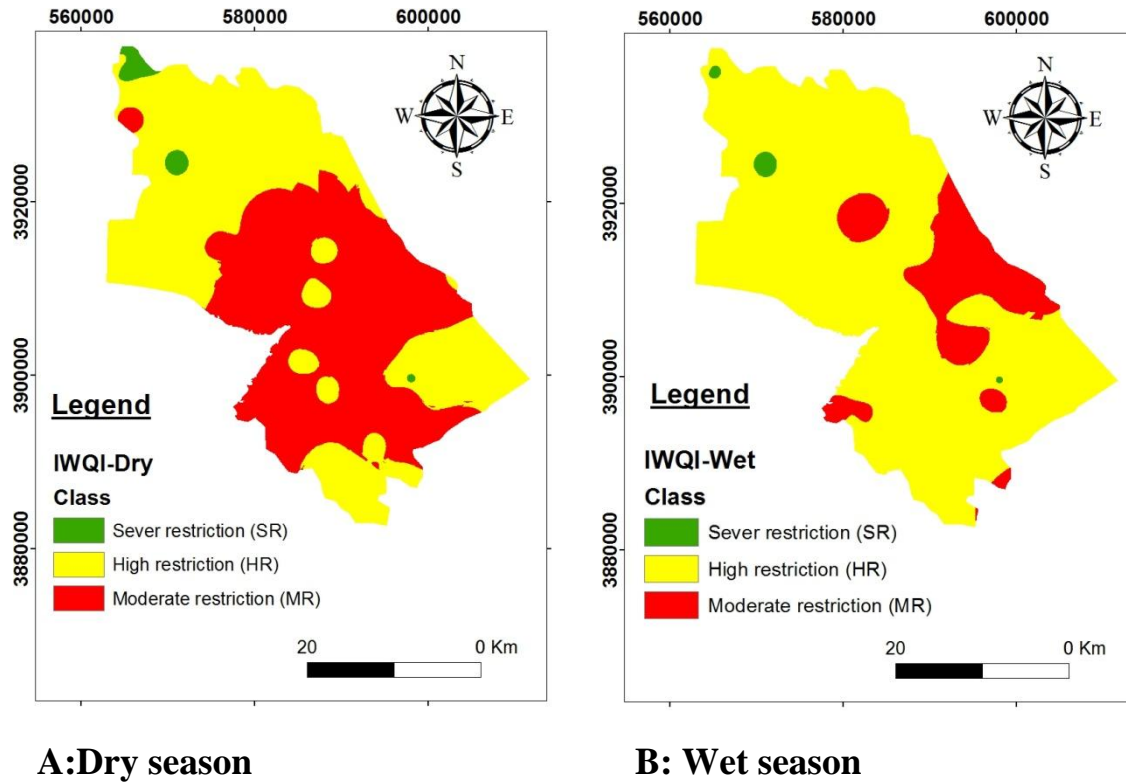
Figure 4.20: Reclassified IWQI map in the studied basin in the dry and wet seasons

4.9.3 Industrial Groundwater Quality Index

The quality of water obligatory in different industrial processes varies substantially. Salinity and hardness are important in terms of industrial water. Based on the water quality guide proposed by Hem (1991), majority of groundwater samples of the studied basin are suitable for some industries, excluding textile, chemical pulp and paper (Table 4.19), because Ca^{2+} and Mg^{2+} concentrations exceed maximum allowable values.

Table 4.19: Water quality standards for industrial uses (after Hem, 1991)

Parameters	Textile	Chemical pulp and paper		Wood chemicals	Synthetic rubber	Petroleum products	Canned, dried Frozen fruits and vegetables	Soft-drinks bottling	Leather tanning	Hydraulic cement manufacture
		Unbleached	Bleached							
Ca^{2+}	---	20	20	100	80	75	---	100	---	---
Mg^{2+}	0	12	12	50	36	36	30	---	---	---
Cl^-	0	200	200	500	---	300	250	500	250	250
HCO_3	0	---	---	250	---	---	---	---	---	---
SO_4^{2-}	0	---	---	100	---	---	250	500	250	250
NO_3	0	---	---	5	---	---	10	---	---	---
Cu	0.01	---	---	---	---	---	---	500	---	---
Zn	---	---	---	---	---	---	---	---	---	---
TH	25	100	100	900	350	350	250	---	Soft	---
TDS	100	---	---	1000	---	1000	500	---	---	600
pH	2.5-10.5	6-10	6-10	6.5- 8	6.5- 8.3	6-9	6.5 – 8.5	---	6-8	6.5– 8.5
$T(^oF)$	---	---	95	---	---	---	---	---	---	---
Suitable samples	Unsuitable	Unsuitable	Unsuitable	%77 suitable	%53 suitable	%47 suitable	%47 suitable	%77 suitable	Suitable	Suitable

Chapter Five

GW Vulnerability Assessment

Chapter Five

GW Vulnerability Assessment

5.1 Groundwater Vulnerability

As water travels through the ground, usual processes are in charge of attenuation of convergence of numerous contaminants including harmful microorganisms. How much attenuation happens is reliant on the sort and type of soil and aquifer attributes, the kind of contaminant and the associated activity. In general, the term groundwater vulnerability is used to represent the intrinsic characteristics of the aquifer which determine whether it is likely to be affected by an imposed contaminant load (National Research Council, 1993). There are two classes of vulnerability, intrinsic vulnerability, which depends exclusively on the properties of the groundwater system, and specific vulnerability, where these intrinsic properties are referenced to a particular contaminant or human activity.

Vulnerability assessment is based on the expected travel time for water to move from the ground surface to the water table. The greater the travel time, the greater is the opportunity for contaminant concentration. Aquifer vulnerability can also be measured by employing appropriate mathematical framework further subdivided into broad classes like very high, high, low and very low, depending upon the governing criteria.

5.1.1 Groundwater Vulnerability in the Studied Basin

Water plays an important role in every society. Not only it is vital for life, it also sustains the environment, contributes towards the development of economic, health, social, recreational and cultural activities. As surface water quantity and quality continue to diminish over the years as a result of rapid population growth, urbanization and pollution, in developing areas such as Halabja Saidsadiq Basin, groundwater becomes the source of potable water

supply. In addition, significant unsystematic economic progresses of the studied basin were noted, such as, construction of many oil refineries, petrol stations with unsafe design in terms of oil leakage. In addition to unsystematic municipal waste disposal and sewage system that have many environmental impacts (viz. section 4.2).

Moreover, it is worth noting that no previous studies have been conducted on this vital area of study in terms of contamination assessment, which makes this study of particular importance. This emphasizes the growing vulnerability and susceptibility of groundwater potential pollution challenges. In view of the above mentioned reasons, it was felt that there is a need for ascertaining groundwater vulnerability in the study basin, involving additional dynamic factors like impact of land use and land cover changes, and effects of surface features such as lineaments along with its validation using realistic groundwater quality data.

5.2 DRASTIC Vulnerability Model

To achieve the intrinsic groundwater vulnerability, the scope of groundwater pollution was analyzed by developing the seven map layers and generating the DRASTIC model which is recommended by The United States Committee of Environmental Protection Agency (Aller et al., 1987).Each parameter has a specific rate and weight value in order to evaluate the intrinsic vulnerability index as explained in Table (5.1). Geological and hydrogeological characteristic as mentioned by (Aller et al. ,1987) are the fundamental criteria which was used to assign the label unit of the map. In addition, Aller et al (1987) defines the seven parameters by the short abriviation of "DRASTIC" which is used to map groundwater Vulnerability. Rating from 1 to 10 and weighting from 1 to 5 was recommended to assign each parameter. The standard DRASTIC index (DI(w-r)) is calculated based on the linear combination of all factors as demonstrated by the following equation:

$$DI = D_w D_r + R_w R_r + A_w A_r + S_w S_r + T_w T_r + I_w I_r + C_w C_r \ldots\ldots\ldots(5.1)$$

Where: DI is the DRASTIC Index, (D, R, A,S,T,I and C) are the seven parameters, w is the weight of the parameter and r is the rate of the parameter. D is the depth of groundwater. R is the net recharge. A is the aquifer media. S is the soil media. T refers to the topography that describes the slope of the surface area. I is the impact of vadose zone. C is the hydraulic conductivity. All the recommended rate and weight are tabulated in table (5.1).

The data used and their sources for groundwater vulnerability mapping are presented in the Table (5.2). Feature classes were used to create the shape files with (Arc Map 10.3) software, including the geological, hydrogeological, soil map and hydrochemical data for the study area.

Depth to the water table (D-Map) describes the distance of the unsaturated zone that pollutant needs to travel through to reach the water table. Areas with a shallow water table are more vulnerable to contamination than areas with a deeper water table if the overlying materials are the same. Generally, deep water table does not allow contaminated infiltrating waters enough contact time with aquifer material for their associated attenuation process to be effective in removing contamination. Therefore, the depth to groundwater is assigned a maximum weight (5) in determining the vulnerability using DRASTIC method (Table 5.1). The depth to groundwater level within the study basin for the wet season is applied to construct (D-Map) because the wet season is considerd to be more critical with respect to the groundwater vulnerability (as the water table is shallowest), the water table map for this period was considered.

Table 5.1: Standard DRASTIC weight and rate after (Aller et al., 1987)

Depth to water Range (m)	Rating	Net Recharge Range (mm/year)	Rating	Aquifer Media Range	Rating	Soil Media Range	Rating	Topography (Slope) Range %	Rating	Impact of vadose Zone Range	Rating	Hydraulic Conductivity Range (m/day)	Rating
0-4.5	10	<50	1	Massive shale	2	Thin or Absent ,Gravel	10	0-2	10	Confining layer	1	<4	1
1.5-4.5	9	50-100	3	Metamorphic/ Igneous	3	Sand	9	2-6	9	Silty/clay	3	4-12	2
4.5-7.5	8	100-175	6	Weathered metamorphic/ Igneous	4	Peat	8	6-12	5	Shale	3	12-30	4
7.5-10	7	175-250	8	Glacial Till	5	Shrinking and/ or aggregated clay	7	12-18	3	Limerstone	6	30-40	6
10-12.5	6	>250	9	Bedded sandstone, limestone, shale	6	Sandy loam	6	>18	1	Sandston, Beded Lim.	6	40-80	8
12.5-15	5			Massive sandstone ,massive limestone	6	Loam	5			sandstone, shale, sand and gravel	6	>80	10
15-19	4			Sand and gravel	8	Silty loam	4			Metamorphic/ Igneous	4		
19-23	3			Basalt	9	Clay loam	3			Sand and gravel	8		
23-30	2			Karst limestone	10	Muck	2			Basalt	9		
>30	1					Non shrinking / non-aggregated clay	1			Karst limestone	10		
weight: 5		**weight: 4**		**weight: 3**		**weight: 2**		**weight: 1**		**weight: 5**		**weight: 3**	

Table 5.2: Source of data for DRASTIC model

Data type	Format	Sources
Depth to water Table	Point	Archieves of Groundwater Directorate in Sulaimani with data of present study.
Net Recharge	Point	Halabja Meteorological Station and Water Balance Method.
Aquifer Media	Map	Archieves of Groundwater Directorate in Sulaimani and Geological Map.
Soil Media	Table and Map	Soil Map by Berding (2003).
Topographic Map	Map	DEM with 30 m pixel size.
Impact of vadose zone	Map	Archieves of Groundwater Directorate in Sulaimani.
Hydraulic Conductivity	Point and Map	Archieves of Groundwater Directorate in Sulaimani with data from field (pumping test).

The depth of the water levels was measured in approximately 1400 water wells within the field using electrical sounder in addition to historical data which was obtained from Groundwater Directorate of Sulaimani. The Inverse Distance Weighted (IDW) were used to interpolate the data to construct the depth to water table layer as a raster format and then reclassified based on the ranges and rating recommended by Aller et al., (1987). In the study basin the depth to groundwater varies from zero to more than 100 m. The depth to groundwater was classified according to DRASTIC rating (Table 5.1) and the

final map to the study area, as generated, is shown in the Figure (5.1D). This map shows ten rating classes 1 to 10. The shallowest water table has been observed in the southern, western and central parts of the study area, while the deeper water table, having a rating of 1, is present in the mountain area surrounding the studied basin, having a Karstic and fissured karstic aquifers.

Net Reccharge (R-Map) defines the amount of water that penetrates into ground and move through the unsaturated zone to reach the water table. The net recharge was estimated from the meteorological data for the period starting from 2001 to 2014 based on the following equation which was recommended by Mehta et al., (2006):

$$NR = P - ET - R_o \ldots\ldots\ldots\ldots\ldots \text{ (5.2)}$$

where, NR: is the net recharge in mm/year, **P**: is the annual precipitation in mm; ET is the calculated evapotranspiration in mm/year, R_o is the total runoff in mm. **P** was calculated from the average total yearly precipitation which is about 691.16 mm/year for the mentioned period. While ET was calculated based on Crop Water Balance method by FAO Penman Monteith method using (CROPWat8.0) software, (Allen et al , 2006). R_0 was calculated based on Soil Conservation Service method (SCS) to estimate the total runoff for the basin. The basin was divided into several curve number (CN) that was recommended by Ali, (2007) and then the following equation was used:

$$Q=(P-0.2S)^2/(P+0.8S) \quad \text{for P>0.2S} \ldots\ldots\text{(5.3)}$$
$$S=(25400/CN)-254 \qquad \ldots\ldots\ldots\ldots\ldots\text{(5.4)}$$

where: Q = accumulated runoff excess in (mm). P = accumulated average monthly rainfall (mm). So the annual runoff of this basin is about 169 mm and the annual net recharge for whole basin is equal to 172.54 mm. Finally, the net recharge map of the basin constructed was based upon the net recharge percent distribution over the basin .

The map for net recharge (Figure 5.1R) shows five rating classes 1,3, 6,8 and 9. The highest score 9 and 8 corresponds to some parts of the northwestern and northeastren part of the study basin, which demonstrate a zone of karstic and fissured-Karstic aquifers. High net recharge has also been observed in the northern part within the study area. The central part around the Derbandikhan Lake has been observed to display a recharge rating of 6, while the rating value 3 has been observed within the area of the fissured aquifer.The lowest score of 1 has been observed in few parts scattered over the entire studied area, including the urban areas.

Aquifer media (A-Map) refers to the consolidated or unconsolidated medium which serves as an aquifer, such as sand and gravel or limestone (Aller et al. 1987). This parameter was assigned a weight "3" in the DRASTIC method (Table 5.1).The hydrogeological description of the study area (viz. section 3.1) indicates four types of aquifers including (fissured karstic and karstic) aquifers with the rating value 9, intergranular aquifer with the rating value 6, fissured aquifer and zone of aquitard having a rating value of 5 and 3, respectively (Aller et al., 1987), (Table 5.1 and Figure 5.1A).

The soil (S-Map) has a significant impact on the amount of recharge which can infiltrate into the groundwater and hence, influences the ability of contaminants to move vertically into the vadose zone. Moreover, where the soil zone is fairly thick, the attenuation processes of filtration, biodegradation, sorption and volatilization may be quite significant. This parameter was assigned a weight "2" in the DRASTIC method (Table 5.1). The soil map was prepared earlier (viz. section 2.6, Figure 2.13). The reclassification of the soil map was done according to the DRASTIC rating (Table 5.1) and a new layer generated for this parameter. The Soil map (Figure 5.1S) shows three segments of soil media in the study basin with rating classes 4 , 7and 10. The high score 10 corresponds to a thin or absent soil layer (present in mountain area). Shrinking and/or aggregated clay soil type rated as 7 and is present in

the central part of the study basin which is underlined by alluvial deposits. Lower score 4 represents the other parts of the study area, where the soil is silty loam.

Topography (T-Map) refers to slope variability of the land surface. Topography helps to control the likelihood of pollutant running off or remaining at the surface in one area long enough to infiltrate. In the DRASTIC framework, the topography parameter was assigned a weight 1. This map was constructed from the digital elevation model (DEM) with pixel size of 30*30m and the slope was then calculated from it in Arc GIS 10.3. The topography of the area was classified into five classes ranging as 0-2%, 2-6%, 6-12%, 12-18% and more than 18% (Figure3.15).The reclassification of the slope was done according to the DRASTIC ratings (Table 5.1 and figure 5.1T) with rating value of 1,3,5,9 and 10. Flat areas were assigned high rates because they slow down the runoff and allow more time for the contaminants to percolate down to reach the groundwater, whereas steep areas increase the runoff washing out the contaminants, hence, are assigned low rates (Babiker et al, 2005).

The impact of the vadose zone (I-Map) is defined as the zone above the water table and is unsaturated (Aller et al., 1987). The type of vadose zone media determines the attenuation characteristics to the material below the typical soil horizon and above the water table. This parameter was assigned a weight 5 in the standard DRASTIC method. Based on the geological description of the study area (viz section 1.8) and from the drilled well logs, three segments of the vadose zone were recognized with organized rating values of 4, 5 and 8 ,(Figure 5.1I).

Hydraulic conductivity (C-Map) describes the ability of the aquifer material to transmit water through it, and contaminant migration is controlled by the permeability of the media (Hamamin, 2011). The hydraulic conductivity map was constructed by employing the pumping test results of

89 wells and pumping test data from archives of GW Directorate (section 3.3 and table 3.2) . The pumping test data were analyzed using (AQTESOL 4.0) software to determine the transmissivity of the aquifer and then equation (5.5) was used to calculate the hydraulic conductivity:

$$C=T/b \ldots\ldots\ldots\ldots(5.5)$$

where: **C** is the hydraulic conductivity in (m/day), **T** is the transmissivity in (m^2/day) and **b** is the aquifer saturated thickness in (m). The area with high hydraulic conductivity revealed higher chance of distributing pollutants. Two classes of conductivity rating were achieved 1 and 4, Figure (5.1C).

   After generating all the seven required reclassified and rated raster, and then multiplied by their respective weighting factor ,the DRASTIC index map was generated. The final index map was divided into several groups as proposed by Aller et al., (1987), (Table 5.3). Small value means low vulnerability potential while the large value represents areas that have high vulnerability potential. Figure (5.2) shows the standard vulnerability map of the studied basin with four zones of vulnerability index. These are: very low, low, moderate and high vulnerability index. The map obviously illustrates the dominance of moderate and very low vulnerability zones which covers an area of 614 Km^2 and 435 Km^2 or 48% and 34% of the whole studied area, respectively. The moderate vulnerability zone occupies two different areas in terms of geological and hydrogeological conditions. The first zone is the area of mountains surrounding the studied basin which comprises the fissured and karstic aquifer, while the second zone comprises the Quaternary deposits surrounding the area of Derbandikhan reservoir in the southwest of the basin. This might be related to the high water table level and high percentage of coarse grain material such as gravel, sand and rock fragment. Furthermore, the zone with low vulnerability comes in the third sequence and occupies 166 km^2 or 13% of the overall surface area within the basin. The zone with high vulnerability index covers only 64 km^2 or 5% of the total area and is located

at the center of the basin. This area is characterized by high water table level
and the presence of several springs with fractured limestone.

D

R

A

S

T

I

C
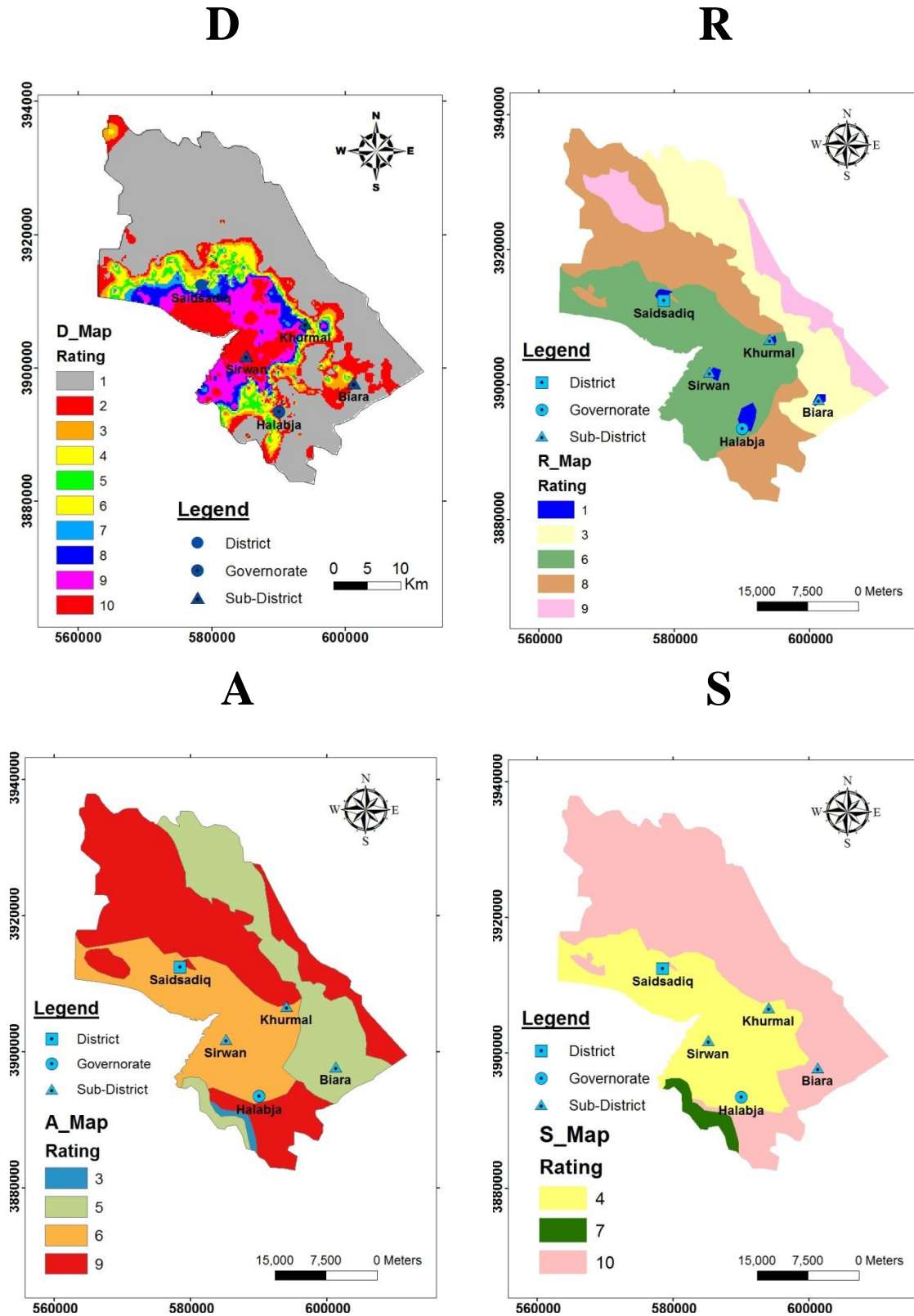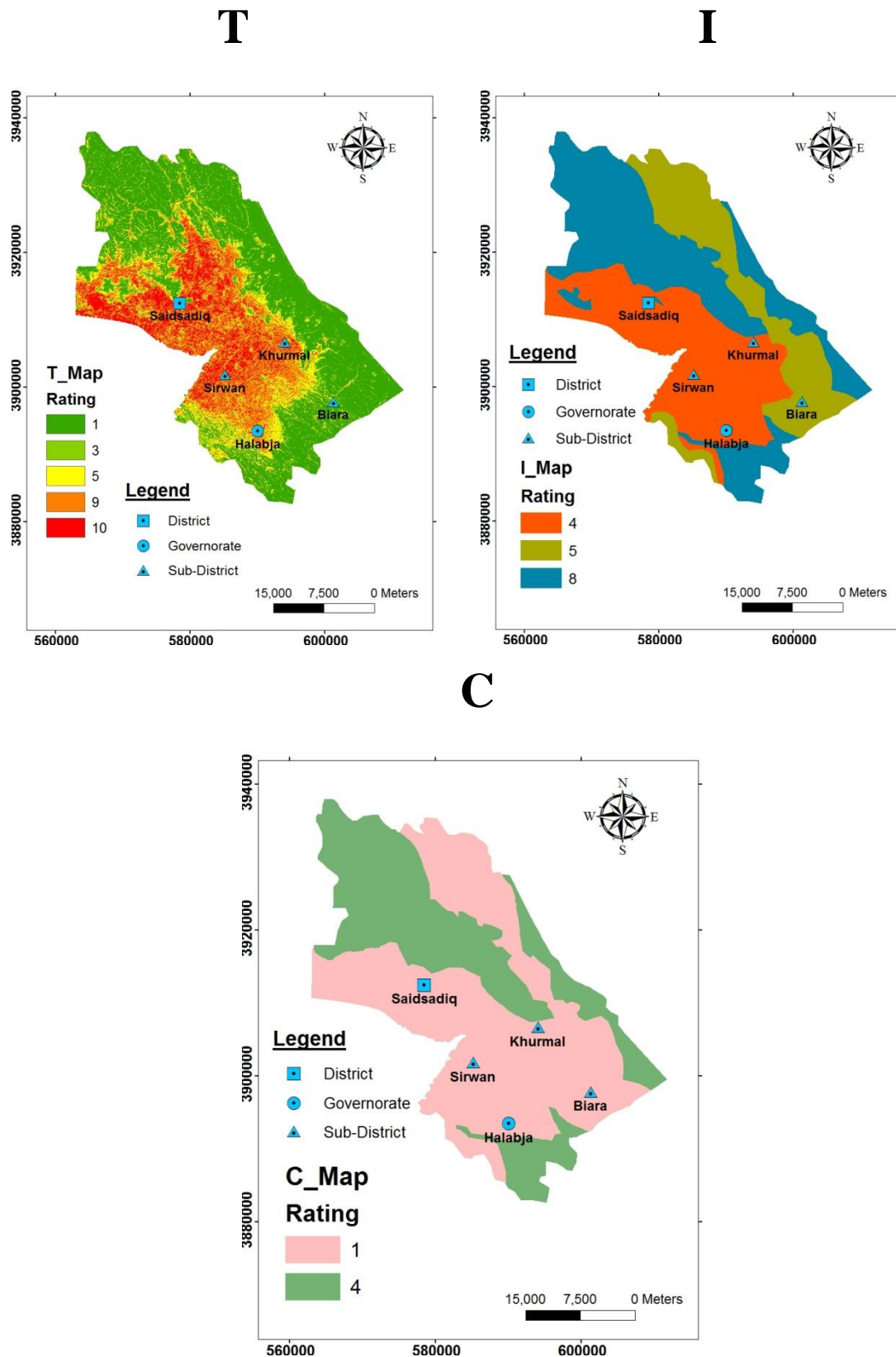
Figure 5.1: Rate Map of all parameters of standard DRASTIC model

**Table 5.3: Ranges of vulnerability degree using DRASTIC method
based on Aller et al., (1987)**

Index of Vulnerability	Vulnerability Degree
<100	Very low
>100 – 125	Low
>125 – 150	Medium
>150 – 200	High
>200	Very High

5.2.1 Validity of DRASTIC Model and Affecting Factors on it

Inherent in each hydrogeological setting are the physical characteristic which affect the groundwater pollution potential. Many different biological, physical and chemical mechanisms may actively affect the attenuation of a contaminant and, thus, the pollution potential of that system. Because it is neither practical nor feasible to obtain quantitative evaluation of intrinsic mechanism from a regional perspective, DRASTIC model has been used to map groundwater vulnerability to pollution in many areas in the world. Since this method is used in different places without any changes, it cannot consider all the effects of pollution type and characteristics. Therefore, the method needs to be calibrated and corrected for a specific aquifer and pollution. DRASTIC model has been designed for a regional scale and might be affected by some local factors of a specific aquifer system; these factors have not been mentioned in this model, as explained below:

- Weights used to calculate the vulnerability index might change (Babiker et al., 2005) based on the different geological and hydrogeological condition of the specified area.

- The rate value to each parameter in DRASTIC model might change from one place to another based on the relationships between each

parameter and the popular chemical component such as nitrate concentration on the groundwater.

- Land uses in developing cities can be complicated by the presence of human and agricultural activities. The agricultural activity increases its size and land coverage in the surroundings of the urban centers. The urbanization processes exceed the capacity of the territorial planning set by the local government. The easiest parameter to evaluate the human impact over the area is land-use which represents directly the human activities and its impact on the natural resources exploitation around the urban area. For this reason, it is important to conclude that land-use is affecting the vulnerability system, and this parameter has not been included in the DRASTIC model.

- The land covers of the earth surface that naturally occurs, such as barren land, forest, grassland, vegetation, snow and water bodies. Different land covers might have different vulnerability behavior. The ability of contaminant to transport from earth surface through the unsaturated zone in agricultural area differs from antiquated land. Therefore, land cover is considered to be one of the most important parameter that affects the vulnerability system.

- Some natural surface features which has a geological origin like lineament feature, fault, joint and fractures; also play an important role to control the vulnerability system depending on its density percentage. These features increase the permeability of the layer underground which helps the contaminant to transport easily through the unsaturated zone.

5.3 Rates and Weights Modification of DRASTIC Model

5.3.1 Rate Modification Using Nitrate Concentration

As mentioned previously, due to the fact that the study area is characterized by an active agricultural exertion, nitrate concentration is used to modify the standard DRASTIC method for the studied basin. Sampling and analysis for nitrate concentration were carried out for 39 well samples on May 2014. Figure (5.3) illustrates the location of the sampled wells.
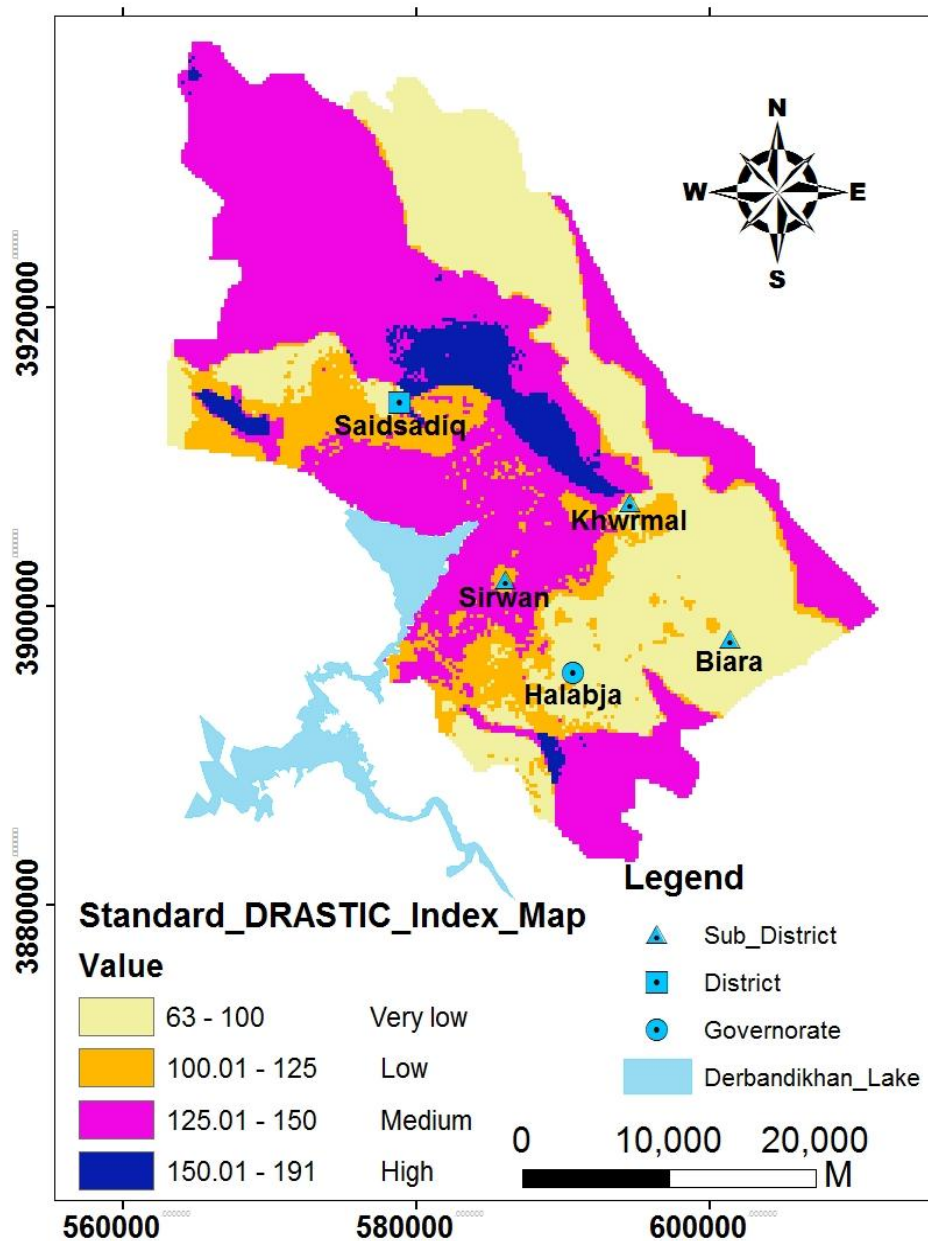
Figure 5.2: Standard DRASTIC index map for the studied basin
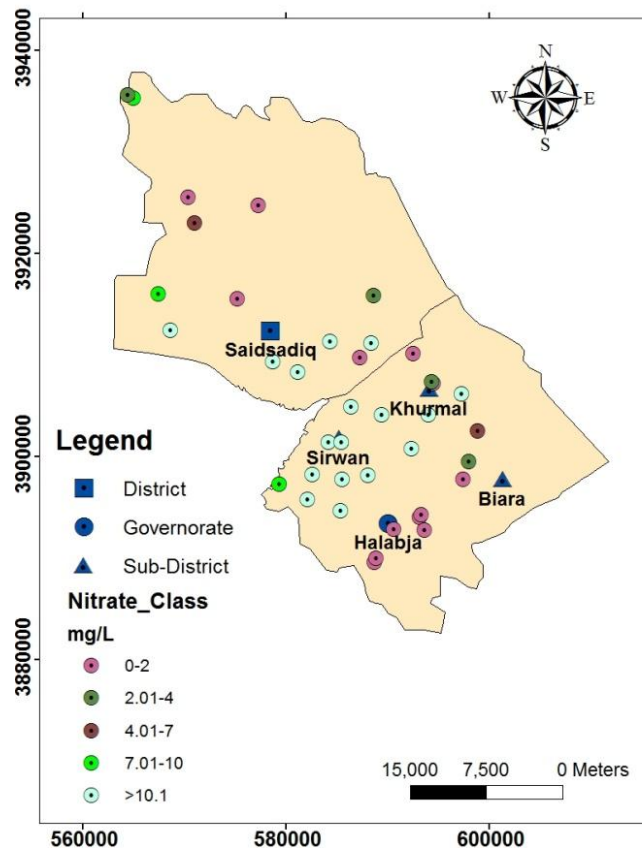
Figure 5.3: Nitrate sampling sites and class of concentration at studied basin

Normally, nitrate moves toward the groundwater from the surface, so it was used as the primary control parameter for contamination. The genuine condition of the area can be established for the vulnerability index by using nitrate as an indicator. As proposed by Panagopoulos et.al., (2006), the rates and weights can be optimized based on the following conditions; the agricultural activities should be the only source of nitrate concentration at the surface, and the reaching nitrate to the groundwater should be due to recharges from the surface over a long period.

In this method, the rates of five maps of DRASTIC methods were modified according to the mean nitrate concentration including (DRSIC), depth to water table, net recharge, soil media, impact on vadose zone and hydraulic conductivity respectively. While both aquifer media and topography remains the same, because they have the same effect on groundwater vulnerability in

both standard and modified situation. The Wilcoxon rank-sum nonparametric statistical test was used to compute the modified rate of each parameter in the DRASTIC method.Based on this model, the highest and the lowest rates were allocated to the highest and lowest mean nitrate concentration respectively and the residual rates were modified linearly (Wilcoxon, 1945). The new DRASTIC map was designed using the new modified rating system (Figure 5.4).

S   **I**

C
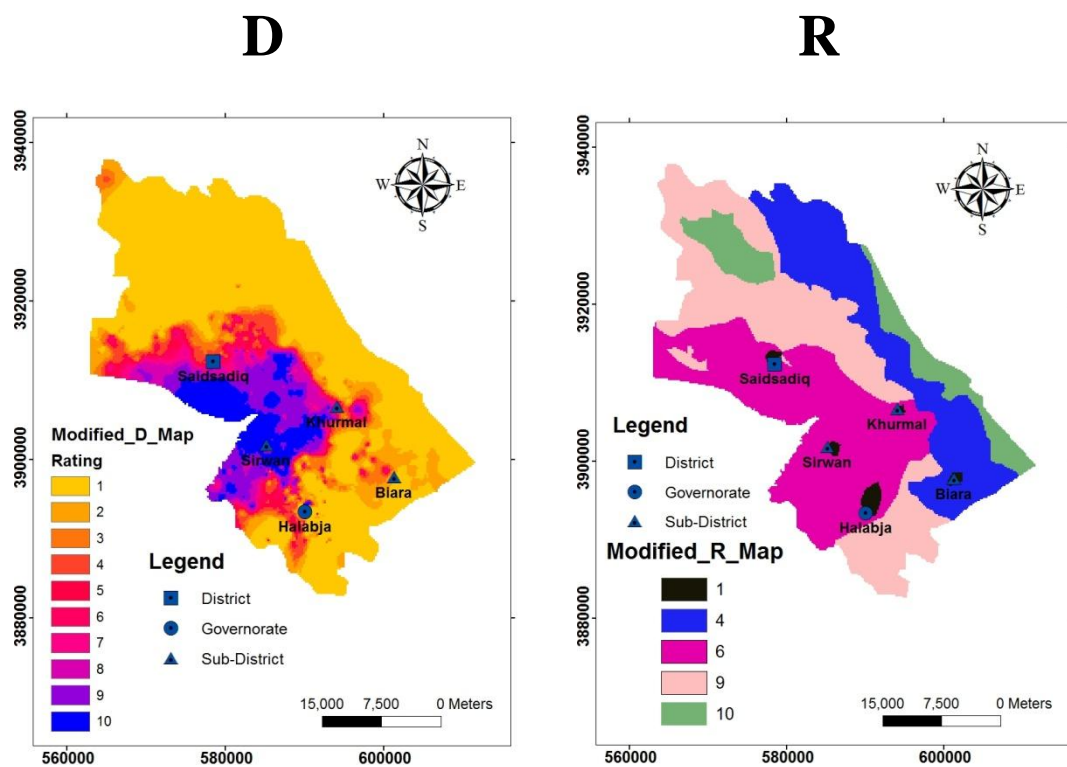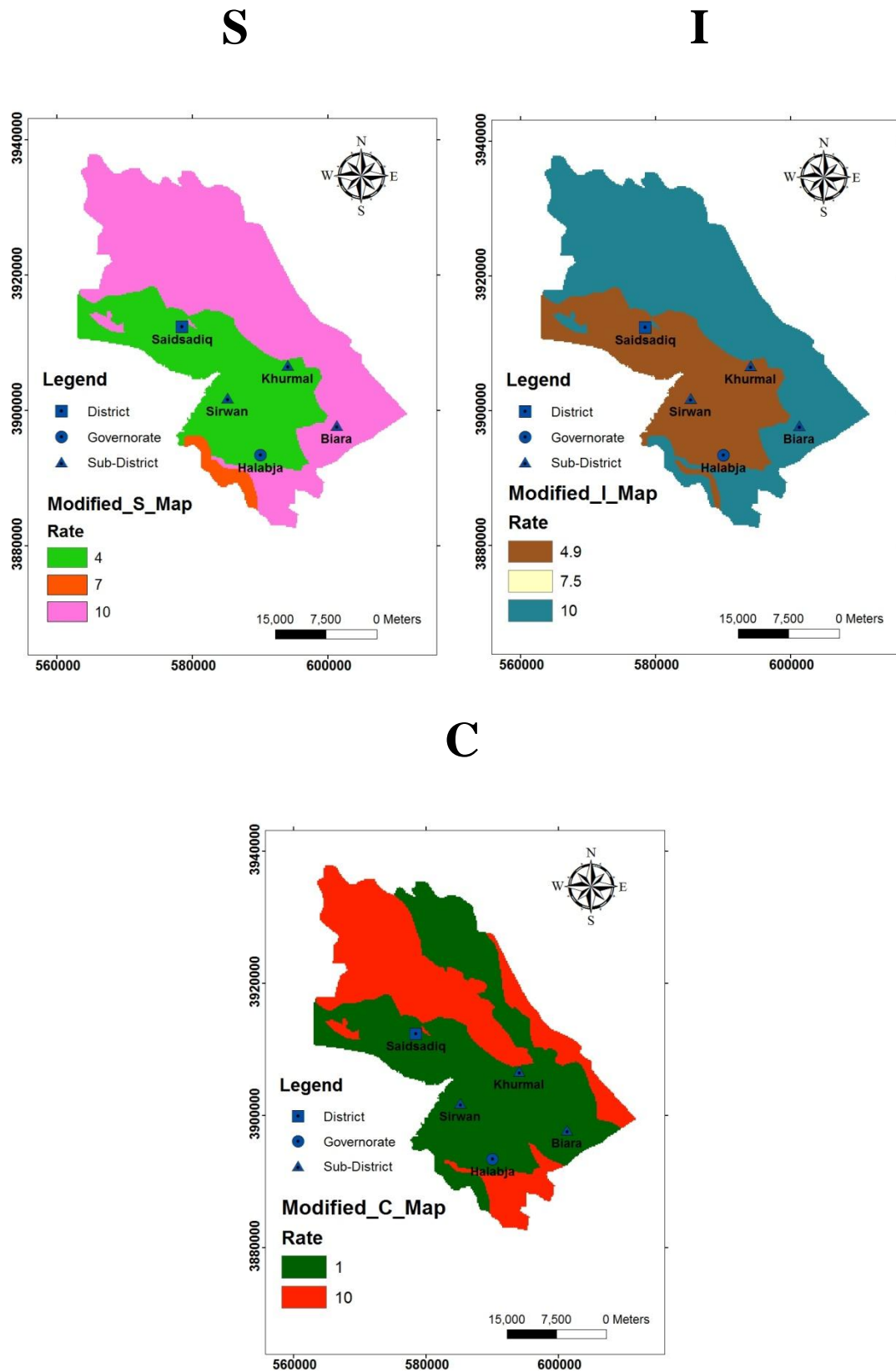
Figure 5.4: Rate modified map of DRSIC parameters in DRASTIC model

Pearson's Correlation Coefficient was applied to standard DRASTIC model (McCallister, 2015) to calculate the relation between standard DRASTIC indexes value and nitrate concentration. This correlation factor refers to linear correlation between two variables (vulnerability index value and nitrate concentration in this study). The outcome was 0.43 that is fairly low (Table 5.7). This means that the intrinsic vulnerability indeces require to be modified to reach a realistic evaluation of the contamination potential for the studied basin. Therefore, nitrate concentration on 39 sampled points was used on the five maps of standard DRASTIC method separately. The nitrate concentration values and DRASTIC rate at each map were extracted and then the mean of nitrate values was calculated at each range of rate. Based on the Wilcoxon rank-sum nonparametric statistical test, the modified rate of DRASTIC parameters was defined. Table (5.4) shows the modified rate of DRSIC layers based on the nitrate concentration.

Figure (5.5) demonstrates the new modified DRASTIC map depending on the new rating. It shows that 15% and 29% of the area fall in the moderate and very low vulnerability zone respectively. These percentages were 48% and 34% respectively before the modification. The calculated area was 15% for low and 38 % for high vulnerability class while before the modification it was 13% and 5% respectively. In addition, very high vulnerability zone was recognized with an area of 3% of the study basin. To show the spatial distribution of the index before and after the modification, the two maps were compared. The result showed that 15% had similar classes, while 85% showed differences in one class or more indicating the effectiveness of the proposed method. The result of Pearson's Correlation Coefficient confirms this effectiveness, because for the rate modified DRASTIC map is 0.69, (Table 5.7) is significantly higher than the standard one which is 0.43.

Table 5.4: Standard and modified rates depending on nitrate concentrations

Parameters	Range	Standard rating	Mean nitrate concentratin (mg/L)	Modified Rating
Depth to water table	0-1.5	10	31	10.0
	1.5-4.5	9	27.6	9.0
	4.5-7.5	8	11.2	8.0
	7.5-10	7	10	7.0
	10-12.5	6	No Data	6.0
	12.5-15	5	No Data	5.0
	15-19	4	7.5	4.0
	19-23	3	5.83	3.0
	23-30	2	No Data	2.0
	>30	1	1.45	1.0
Net Recharge	< 50	1	No Data	1.0
	50-100	3	1.6	4.0
	100-175	6	1.8	6.0
	175-250	8	18.5	9.0
	>250	9	No Data	10.0
Soil Media	Clay loam with rock fragment	4	1.6	4.0
	Silty loam, Sandy loam	7	No Data	7.0
	Thin or absent	10	17.7	10.0
Impact of vadose zone	Sand and gravel with clay	4	1.3	4.9
	Limestone with bedded clay stone	5	2	7.5
	Limestone	8	18.5	10.0
Hydraulic Conductivity	0-4	1	1.6	1.0
	12-30	4	16.55	10.0
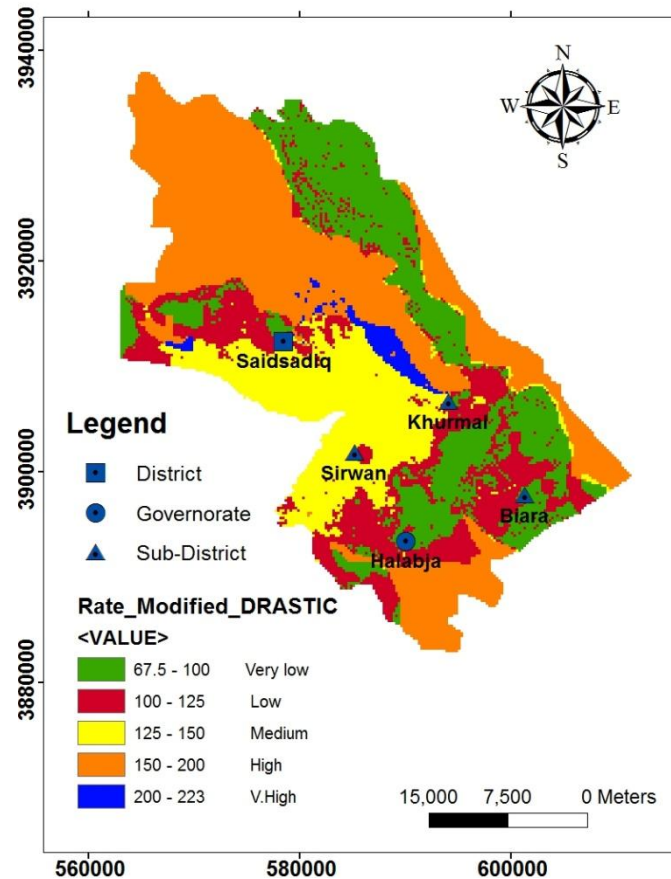
Figure 5.5: Rate modified DRASTIC map using nitrate concentration

5.3.2 Weight Modification Using Sensitivity Analysis

As illustrated by Babiker et al., (2005) the weights used to calculate the vulnerability index might change based on the different geological and hydrogeological condition of the study area. Sensitivity analysis evaluates the effective weights of each parameter and compares it with their original weights. The effective weight is referring to the function of the value of a single parameter as well as the weight assigned to it by the DRASTIC model (Babiker et al., 2005). The impact of each parameter on the index computation was assessed by achieving the sensitivity analysis. Equation (5.6) was used to calculate the effective weight of each polygon (Javadi et al., 2011).

$$W = \left(\frac{P_r P_w}{V}\right) * 100 \ldots\ldots\ldots\ldots\ldots (5.6)$$

Where: W is the effective weight of each parameter, P_r and P_w are the rating value and weight of each parameter, and V is the overall vulnerability index.

New effective weighting factors were obtained using the standard DRASTIC map and then sensitivity analysis method. Obviously, it can be noticed that there are some significant differences in the theoretical values proposed by Aller et al., (1987) as all parameters changed from their weighting value (Table 5.5), because the new weighting values were calculated based upon the vulnerability index achieved from the specific properties in the ground within the study area, while the recommended theoretical values were assumed everywhere in the world. Hydraulic conductivity designates a maximum deviation between the original and new effective weights with 53% decrease; while soil media shows the highest increasing percent which is 31%. The net recharges also decreased from its weight value of only 6%. Moreover, several parameters show an increase in the effective weight value including, depth of water, aquifer media, topography and impact of the vadose zone with increasing percentage of 3%, 12%, 3% and 12%, respectively. Figure (5.6) shows the weight modified DRASTIC map using the computed effective weights. The results are slightly different compared to the standard DARASTIC vulnerability map with four classes of vulnerability. These classes are: very low, low, moderate and high with 32%, 16%, 38% and 14% of the total area respectively. Because the computed weight modified vulnerability index was based on the specific ground conditions of studied basins, so these differences are made and the modified one is considered more reliable, and the Pearson's Correlation Coefficient value confirms this reliability of weight modified model with the value of 0.57 which is slightly higher than standard one   (0.43) .

The modified rate and weight are applied to the DRASTIC model to the intrinsic vulnerability situation in the area. Figure (5.7) illustrates the modified rate-weight applied to DRASTIC model. The outcome map has great dissimilarity with the standard DRASTIC map and is fairly similar to the rate modified using nitrate concentration, with some differences on the rate of the low and very low vulnerability zone (Table 5.6).

Table 5.5: Modified weight for standard DRASTIC based on sensitivity analysis

Parameters	Standard weight	Standard weight (%)	Effective weight (%)			Mean modified weight
			Minimum	Mean	Maximum	
D	5	21.7	10.0	22.4	25.6	5.2
R	4	17.4	8.0	16.3	18.5	3.8
A	3	13.0	18.0	14.7	13.8	3.4
S	2	8.7	16.0	11.4	10.3	2.6
T	1	4.3	2.0	4.5	5.1	1.0
I	5	21.7	40.0	24.5	20.5	5.6
C	3	13.0	6.0	6.1	6.2	1.4

Table 5.6: Result of DRASTIC index ratio for standard and modified maps

Vulnerability class	Standard %	Modified rate %	Modified weight %	Combined modification
Very low	34	29	32	7
Low	13	15	16	35
Medium	48	15	38	19
High	5	38	14	35
Very high	---	3	---	4
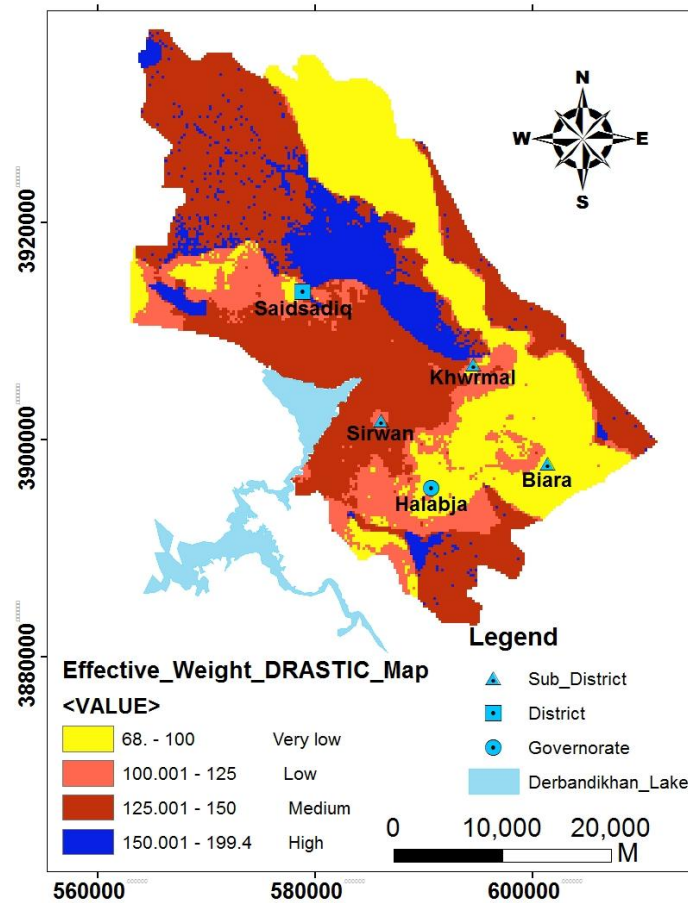
Figure 5.6: **Effective weight (weight modified) DRASTIC map based on sensitivity analysis**

Pearson's correlation factor was calculated statistically between the Modified DRASTIC index value of all rates, rate-weight combination and weight modified methods with mean of nitrate concentration. The result tabulated in Table (5.7) shows an increase in the correlation factor of to 0.72. According to these results, the combination of modified rate and weight method has a higher correlation factor and is recommended as the most appropriate method to be applied for the study basin.
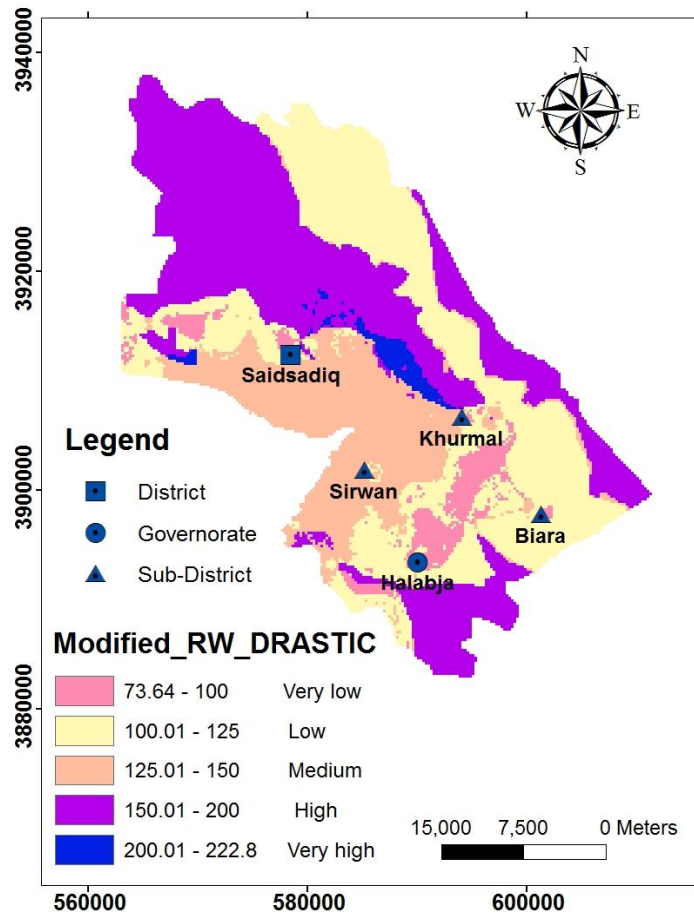
Figure 5.7: Combination of rate-weight modified of DRASTIC vulnerability map

Table 5.7: Pearson's Correlation Factors between the standard and modified vulnerability index and nitrate concentration

Parameters	Number of data	Pearson's Correlation Coefficient
Standard DRASTIC Index	39	0.43
Modified weight DRASTIC Index		0.57
Modified rate DRASTIC Index		0.69
Combined modify rate and weight DRASTIC Index		0.72

156

5.4 Effect of Land Use and Land Cover on DRASTIC Model

The effect of the human and natural processes as a fundamental environmental erratic can be identified from land use/ land cover map (Meyer and Turner, 1992). Land use / land cover is normally marked by a short term of (LULC). Land cover (LC) defines the cover on the earth surface that naturally occurs, such as bare land, forest, grassland, vegetation, snow and water. Land uses (LU) illustrate the modification of land cover due to human processes or man-made modification (Cihlar et al., 2001). Remote sensing technique and field survey can be used to supervise LULC. As mentioned by Mas (1999) and cited in Jwan et.al (2013), remotely sensed satellite images are the most widespread source of data onto mapping LULC, because of its availability and repetitive data acquisition, improved quality of multi-spatial and multi- temporal remote sensing data at different (spatial, spectral, and digital) format; besides it is suitable for computer processing and new analytical techniques.

To modify the likely risk of groundwater vulnerability an additional parameter was inserted into the analysis to show the validity of vulnerability assessment. This study uses LULC map because it strongly affects the quality of groundwater where agriculture, as the main land use type, is the main factor affecting soil nature and hydraulic conductivity (Merchant, 1994).Therefore, LULC map was rated and weighted as an additional parameter and added to the standard DRASTIC model. The LULC rating map was rated based upon the values given in table (5.8). Furthermore, it was converted into a raster grid and multiplied by the weight of the parameters (Lw = 5) to construct the LULC index map. Then, to modify the original DRASTIC indexes map, it was combined with LULC index map based on equation (5.7), (Secunda et al., 1998).The results demonstrate the effect of specific land uses type on the vulnerability system.

$$MD(i) = DI + (LULC\ Index)\ldots\ldots\ldots\ldots\ldots\ldots (5.7)$$

Where: MD(i) is the modified DRASTIC model; DI is the standard DRASTIC index and the LULC index (ratings*weights).

Table 5.8: Rate and weight for LULC classes (Secunda et al., 1998)

Level I Classes	Rate
Vegetation and Barren Land	5
Water and wet area	7
Urban area and agriculture land	8
Weight=5	

The LULC map of the study basin is exposed in the Figure (2.11). This map is produced based on USGS method of classification (Bety, 2013), using remote sensing and GIS techniques from satellite landsat images (ETM+, 2013) (viz section 2.5).The map demonstrates that only five classes can be recognized as explained in Table (2.3).

The map of ratings of LULC (Figure 5.8) illustrates rating of values ranging from 5 to 8, (Table 5.9). Urban areas and agricultural land were assigned a probability rating of 8, because chemical contaminant concentrations, such as nitrogen, from human activities in urban and agriculture areas were higher than in all other land use areas (Secunda et al, 1998). Vegetation and barren land areas were combined and assigned to probability rating of 5, as they contained low nitrogen of nearly similar concentrations. Water body and wet land area were rated 7, (Secunda et al, 1998) as the water act as a good transporter for contaminants.

Table 5.9: Rating value for each LULC classes Type, after (Secunda et al, 1998).

Level I Classes	Rating value	Area%
Vegetation and Barren Land	5	63.1
Water and wet area	7	0.4
Urban area and agriculture land	8	36.5
Weight=5		

Additionally, it can be noted from Figure (5.8), that the rating value of class 5 occupies most of the studied basin with 63.1% of the entire studied area. This class is located in most of the surrounding mountains and areas of high percentage of pasture. Rationally, in terms of land use, these areas have the lowest effect environmentally on vulnerability aspects. Moreover, urban area and agricultural land were rated the probability of 8 and occupied 36.5% of the intact studied area. This refers to human activities within these areas compared to other land use classes. Water body and wet land occupy only 0.4% of the whole area with rating value of 7.

Furthermore, the LULC rating map as a raster grid was multiplied using map algebra in GIS environment by the weight of the parameters (Lw = 5) to construct LULC index map as shown in the Figure (5.9). The index values was classified into three classes 25, 35 and 40 which occupied 63.1% , 0.4% and 36.5% of the total area of the studied basins, respectively.

Figure (5.10) demonstrates the modified DRASTIC index map based on LULC index map with index value ranging of 88-221. The range of index values was divided into five classes including very low to very high vulnerability classes (Table 5.10).
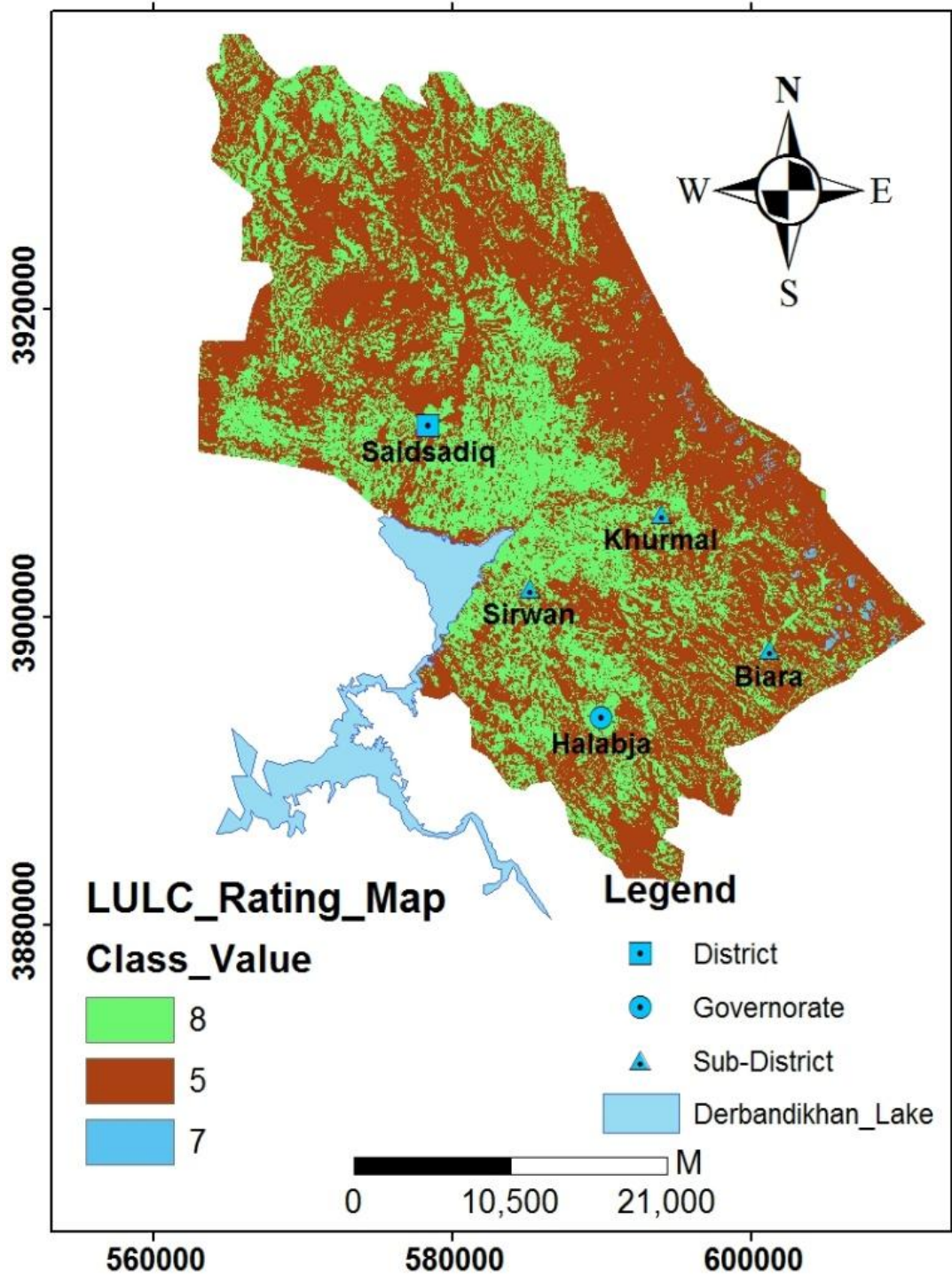
Figure 5.8: LULC rating map for the studied basin
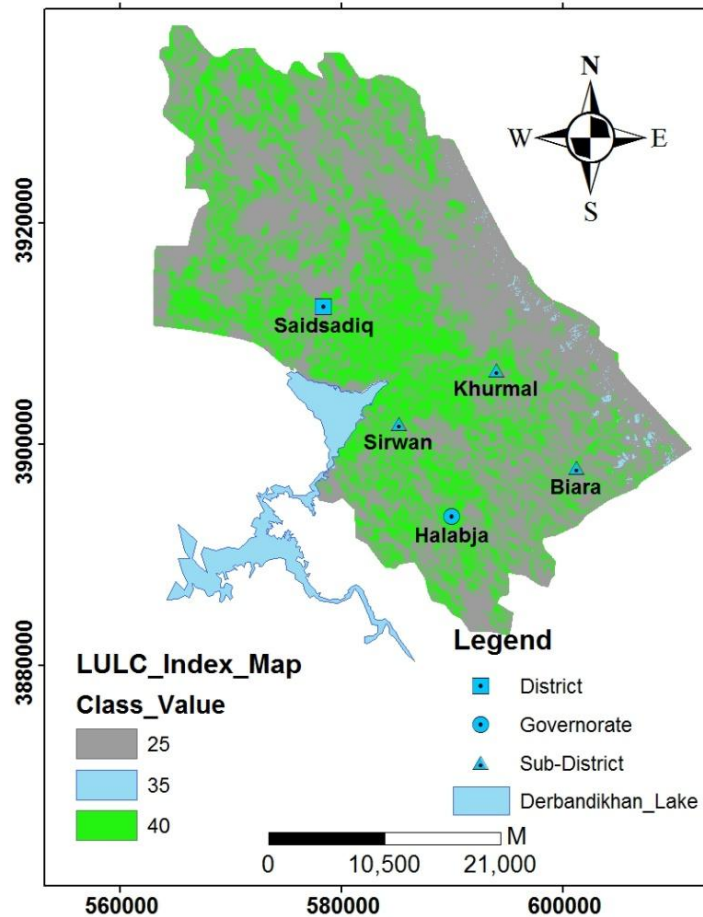
Figure 5.9: **LULC index map for the studied basin**

The modified vulnerability map shows that about 43.42% of the study basin has high vulnerability to contamination with index values ranging from 150 to 200. Low vulnerability is measured as a second effective class of the studied area with 36.82%, while, very low, moderate and very high areas comprise 1.17%, %17.57 and %1.02, respectively.

In terms of land use class, agriculture and barren lands occupied most of the studied basin with total area of 1216.3 Km^2 or 95.17% of the whole studied area. The effect of agriculture activity can be clearly noticed on the modified DRASTIC models compared to standard one, as the agriculture land plays a significant role to convert the moderate vulnerability zone in the central and north western parts to high vulnerability zone. In addition, both barren with agriculture lands are the main factors to rise up very low

161

vulnerability zone to low vulnerability in the north east and south east of the study basin.

Table 5.10: Modified DRASTIC index value of each class at studied basin

Vulnerability class	Drastic Index	Area (Km^2)	Area (%)
Very low	88-100	14.95	1.17
Low	>100-125	470.7	36.82
Moderate	>125-150	224.51	17.57
High	>150-200	554.85	43.42
Very high	>200-221	12.99	1.02

5.5 Effect of Lineament Feature on DRASTIC Model

Lineament features were described previously in section (1.8.2). In the studied basin, most of the aquifers that are surrounding the basin were developed in fractured rock, so groundwater mostly moves through the fracture of these rocks. In addition, there are many linear features that appear in the alluvial deposits as a result of effective against zone of increasing porosity and permeability. So, lineament density measured as a main parameter with DRASTIC model to assess groundwater vulnerability more precisely. The lineament density map as shown in the Figure (5.11) had been rated and weighted. The calculated lineament density was assigned ranges and rating based on Table (5.11).
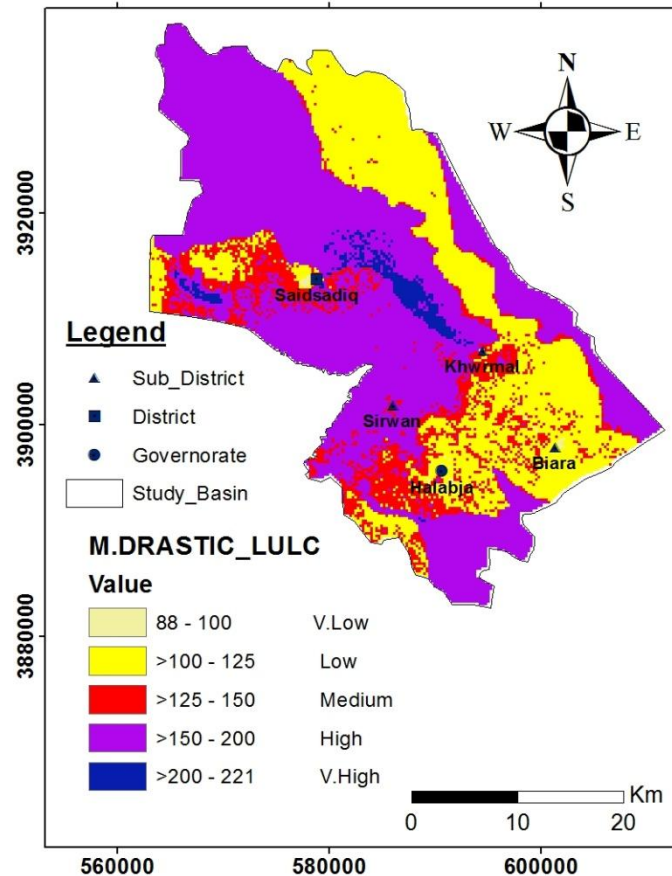
Figure 5.10: Modified DRASTIC map based on LULC for the studied basin

The weight of lineament density was assigned by a value based on its valuable significance and it is measured as 5, (Al-Rawabdeh et al., 2013 and Al-Rawabdeh et al., 2014). Therefore, lineament index map was constructed by multiplying the mentioned weight to the rated lineament map using the map algebra tools of (Arc map 10.3) software.

To modify the possible risk of groundwater vulnerability, an additional parameter has been added to the original DRASTIC model to show the realistic of vulnerability assessment. In this study, Lineament map was used because of its close relationship to occurence and movement of groundwater. In addition, previous study revealed that there is a close relation between lineament and groundwater yield and flow, (Lattman and Parizek, 1964). Therefore, Lineament indexes map as an additional parameter was added to the standard DRASTIC model based on equation (5.8) (Al-Rawabdeh et al.,

2014). The result demonstrates the effect of lineament concentration in the vulnerability system.

$$DL(i) = DI + (\text{Lineament density Index}) \ldots \ldots \ldots (5.8)$$

Where: DL (i) is the modified DRASTIC model based on density of lineament; DI is the standard DRASTIC index and the Lineament density index (ratings*weights).

Table 5.11: Rates and weights for lineament density (Al-Rawabdeh, 2014)

Range of Lineament Density	Rate
0.2-1.1	1
1.2-1.3	2
1.4-1.5	3
1.5-1.8	4
1.9-2.0	5
2.1-2.2	6
2.3-2.4	7
2.5-2.6	8
2.7-2.8	9
2.9-4.0	10
Weight=5	

The lineament density map of the study basin is shown in Figure (5.11). This map is produced by applying GIS techniques from the lineament map extracted from satellite landsat 8 images (ETM+, 2013), (viz section 1.8.2).The map reveals that the studied basin was divided into six classes of lineament density distribution as explained in the Table (5.12) by percent and the area of land covering with each.

Table 5.12: Lineament density classes rating in the studied basin

Class	Range of lineament density distribution	Rating	Area _ Km^2	Area %
Class-I	>2.1-2.4	7	1.5	0.12
Class-II	>1.83-2.1	5	5.4	0.42
Class-III	>1.57-1.83	4	9.2	0.72
Class-V	>1.3-1.57	3	23.9	1.87
Class-VI	>1.05-1.3	2	72.3	5.66
Class-VII	0-1.05	1	1165.7	91.2

From Figure (5.11), it can be noticed that Class-VII which is characterized by low density of lineament distribution covered most of the studied basin lands with an area of 1165.7 km^2 or 91.2% of the total studied area. In addition, the higher lineament density range is Class-I which is occupying only 1.5 Km^2 or 0.12% of the whole studied basin. This is located in the mountain ranges of the northwestern portion of studied basins, coincident with major subsurface structural development along Swren Mountain namely developed thrust fault and overturned double plunging anticline as explained in the geological map (Figure 1.4).

The remaining classes including Class-II, Class-III, Class-V and Class-VI are covering an area of 5.4, 9.2, 23.9, and 72.3 Km^2 or 0.42%, 0.72%, 1.87% and 5.66% of the whole studied area respectively. Furthermore, from the result mentioned above, it can be concluded that the current study basin is considered as relatively low lineament density.
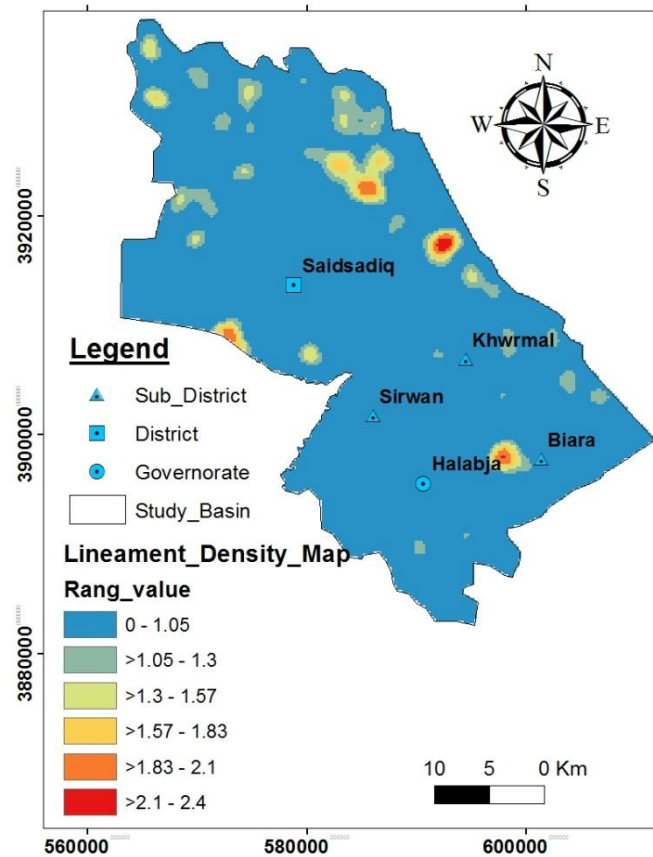
Figure 5.11: Lineament density map for the studied basin

The map of ratings lineament in (Figure 5.12) illustrates rating to value ranging from 1 to 7 (Table 5.12). Class-1 was assigned a probability rating of 7 and occupies only (0.12% of the studied area, because the density range of the lineament considered as high intensity. In contrast, Class-VII assigned a probability rating of 1, as they contain low density range which is only 0 to 1.05. Additionally, density ranges of classes (Class-II, Class-III, Class-V, Class-VI) were rated as 5, 4, 3 and 2, respectively and occupied 0.42, 0.72, 1.87 and 5.66 of the whole studied area, respectively.

The lineament density rating map fraction as a raster grid using map algebra in GIS environment was multiplied by the weight of the parameters (Lw = 5) to construct the lineament index map as shown in Figure (5.13). The index value classified into six classes too, including 5, 10, 15, 20, 25 and 35.
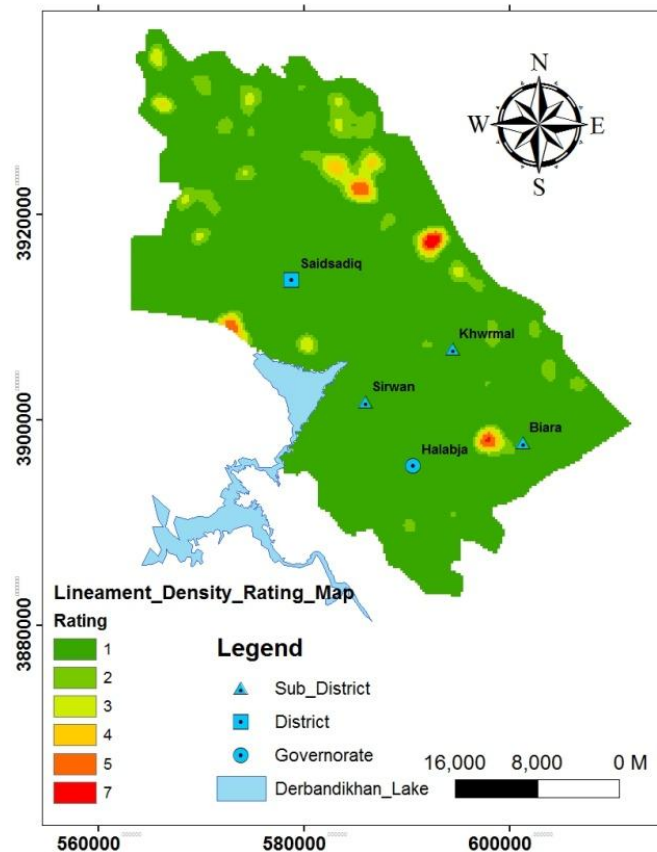
Figure 5.12: **Lineament rating map for the studied basin**

Figure (5.14) demonstrates modified DRASTIC index map based on lineament index map with index value ranging of 68 to 196. The range of index values is divided into four classes including very low to high vulnerability classes (Table 5.13).

The modified vulnerability map delineates that around 47% of the studied area has medium vulnerability to pollution with index values ranging between 125 to 150. While, low vulnerability measured as a second effective class of the examined region with 29% of the whole area. Furthermore, low and high classes covered an area of 14%, and %10 of the total area of the studied basin respectively. By comparison with Standard DRASTIC (Figure 5.2) and its modification in light of lineament density factor,(Figure 5.14) and Table 5.13, there is no significant variation in the index value and the occupied areas as

167

well for classes of low and moderate, while the regions of high and very low classes were slightly different. Generally, this modification can be reasoned by the fact that lineament density has a very little impact on the vulnerability demonstrated for the study basin on the grounds that larger part of the examined region about 91.2% of entire studied basin, which is characterized by low lineament density distribution.
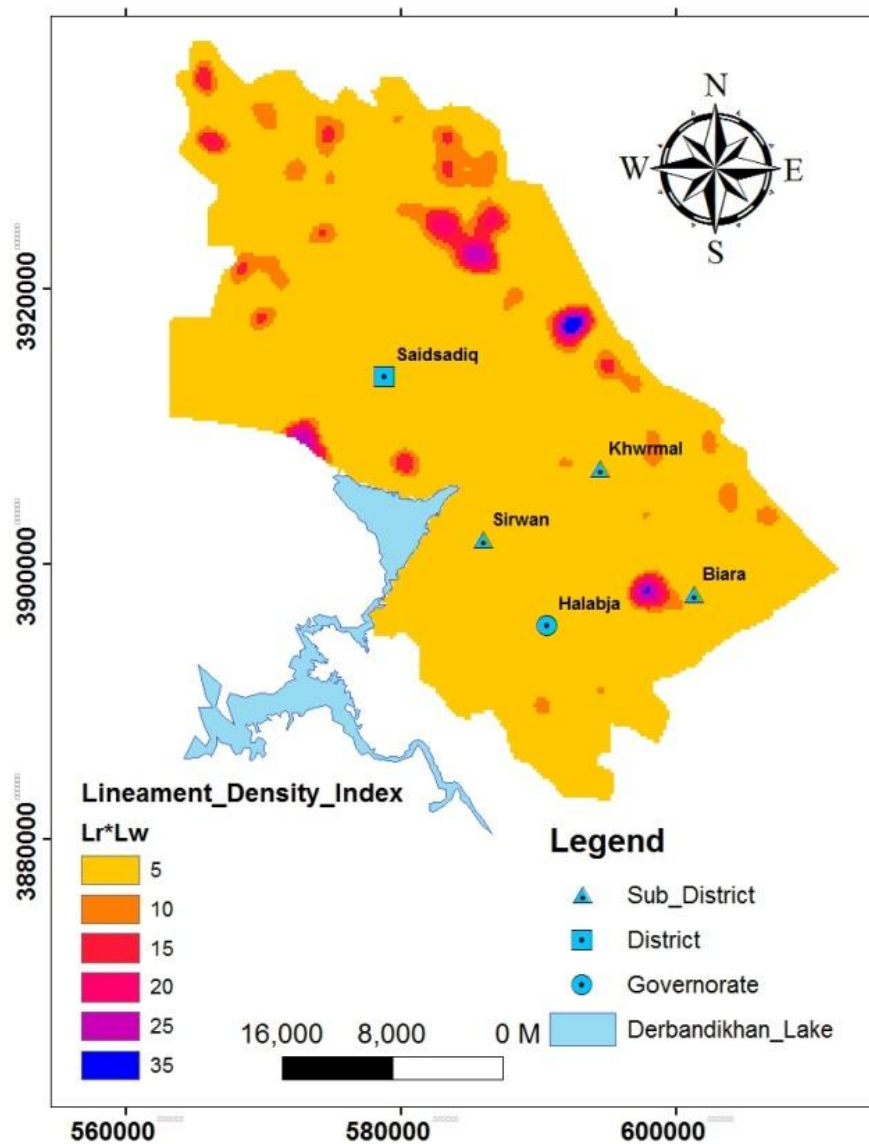
Figure 5.13: **Lineament index map for the studied basin**

Table 5.13: **Standard and modified DRASTIC index value based on lineament feature at the studied basin**

Vulnerability class	Standard DRASTIC		Modified DRASTIC	
	Index value	Area (%)	Index value	Area (%)
Very low	63-100	34	68-100	29
Low	>100-125	13	>100-125	14
Moderate	>125-150	48	>125-150	47
High	>150-191	5	>150-196	10
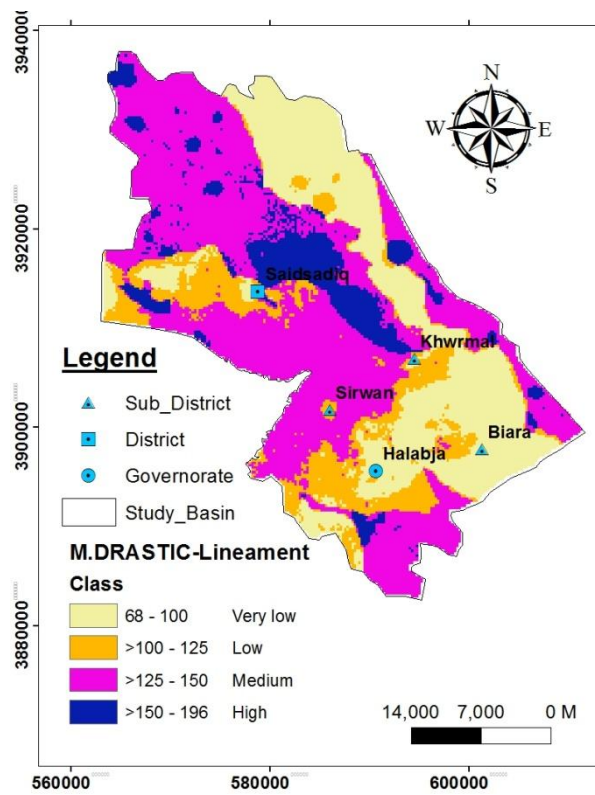
Figure 5.14: **Modified DRASTIC lineament index map for the studied basin**

169

5.6 Analytic Hierarchy Process (AHP) Applied to DRASTIC Model

Analytical Hierarchical Process (AHP) is an approach for decision making that involves structuring multiple choice criteria onto a hierarchy, assessing the relative importance of these criteria, comparing alternatives for each criterion and determining an overall ranking of the alternatives. The foundation of the Analytic Hierarchy Process (AHP) is a set of axioms that carefully delimits the scope of the problem environment (Saaty,1986). It is based on the well-defined mathematical structure of consistent matrices and their associated right eigenvector's ability to generate true or approximate weights (Merkin et al.,1979) and (Satty, 1994) The AHP methodology compares criteria, or parameters with respect to a criterion, in a natural, pair wise mode. To do so, the AHP uses a fundamental scale of absolute numbers that have been proven in practice and validated by physical and decision problem experiments. The fundamental scale has been shown to be a scale that captures individual preferences with respect to quantitative and qualitative attributes just as well or better than other scales (Satty 1980 and Satty 1994).

In the AHP, selection criteria can be identified and weighted, and the collected data can also be analysed, accelerating the process of decision making. The hierarchy is deconstructed into a pair comparison matrix. This pairwise comparison is used to determine the relative importance of each parameter in terms of each criterion. In typical analytic hierarchy studies, the (9) point scale is used, where each point equates to an expression of the relative importance of two factors. These studies use a scale with values ranging from 1 to 9 as shown in the Table (5.14). This will enable the decision maker to assess the contribution of each factor to reach the objective independently through pairwise comparison.

The typical structure to the decision problem is formed and consists of numbers, which were represented by symbol *m*; while alternatives were given

numbers represented by symbol *n*. Each alternative can be evaluated in terms of the decision criteria as well as each criterion being estimated by its weight. The values of a_{ij} (i = 1, 2, 3, …, m) and (j = 1, 2, 3, …, n) are used to signify the performance values in terms of the ith and jth in a matrix (Uyan, 2014). The typical comparison matrix for any problem and the relative importance of the criteria can be represented in a decision matrix as follows:

$$A = \begin{bmatrix} a11 & a12 & a13 & a1n \\ a21 & a22 & a23 & a2n \\ a31 & a32 & a33 & a3n \\ \cdot & \cdot & \cdot & \cdot \\ \cdot & \cdot & \cdot & \cdot \\ \cdot & \cdot & \cdot & \cdot \\ \cdot & \cdot & \cdot & \cdot \\ am1 & am2 & am3 & amm \end{bmatrix} \qquad \text{…………..} \quad (5.9)$$

Table 5.14: Scale of relative importance for pairwise comparison (Saaty, 1980)

Intensity of importance	Definition
1	Equal importance
2	Equal to moderately importance
3	Moderate importance
4	Moderate to strong importance
5	Strong importance
6	Strong to very strong importance
7	Very strong importance
8	Very to extremely strong importance
9	Extreme importance

The priority vector is determined by normalising the eigen value to 1 (divided by their sum) as follows, (Uyan, 2014):

$$Pri = \frac{Egi}{\sum_{i=1}^{n} Egi} \quad ....(5.10)$$

where Egi is the eigenvalue for the row i ($Egi = \sqrt[n]{a11 * a12 * a13 ... ... a1n}$) and n is the number of elements in row i. The lambda max (λmax) was obtained from the following formula, (Uyan, 2014):

$$\lambda max = \sum_{j=1}^{n} [Wj \sum_{i=1}^{m} aij] ....(5.11)$$

where a_{ij} is the sum of criteria in each column in the matrix and W_j is the value of weight for each criterion, which is corresponding to the priority vector in the matrix of decision. So, in this study λmax = 7.03. The consistency index (CI) is determined by the following formula:

$$CI = \frac{\lambda max - n}{n - 1} \quad ……...….…(5.12)$$

Where n is the size of the matrix. In this study, n = 7 and λmax = 7.03; therefore CI = 0.005. The consistency ratio (CR) was obtained according to Saaty (1980) as follows:

$$CR = \frac{CI}{RI} \quad ....(5.13)$$

where RI_7 is random index (RI = 1.32) for n = 7 (Table 5.15), where this table displays the mean random index value for matrixes with different size. If the CR is less than 0.1, the ratio indicates a reasonable consistency level in the pairwise comparison. In this study CR = 0.004 < 0.1, the pairwise comparison matrices were prepared for 7 parameters (Table 5.16).

In the process of weight assesing, the importance and weight of each parameter were compared with each parameter in this study. It was done through the adoption of the opinions of experts who have worked in this field. Each parameter was given a value of weight that it deserves by adopting the

method of simple additive weighting. Then, these weights were used and applied in preparing the comparison matrix of the AHP to get the right weight for each parameter (Tables 5.15 and 5.16). A total of 7 map layers were entered in the Map Algebra tool in the GIS through the summation of the products of multiplying the weight of each criterion (W) (which was calculated by the AHP method) by the rating value of the parameter which was calculated by using rate-weight modification method (Viz section 5.3.1). This helped to create the map of weight modified DRASTIC vulnerability index based on the AHP method (Table 5.16).

Table 5.15: Random inconsistency indices for different values of (n) (Chang et al., 2007; Isalou et al., 2013)

n	1	2	3	4	5	6	7
RI	0	0	0.58	0.9	1.12	1.24	1.32

Table 5.16: Pairwise comparisons matrix for selecting suitable landfill site, eigenvector and significance weights

	D	I	R	A	C	S	T	Eigenvector	Priority Vector (Weight)	DRASTIC Weight	Modified DRASTIC weight
D	1.0	1.0	2.0	3.0	3.0	5.0	7.0	2.5	0.28	5.00	6.42
I	1.0	1.0	2.0	3.0	3.0	5.0	7.0	2.51	0.28	5.0	6.42
R	0.5	0.5	1.0	2.0	2.0	3.0	5.0	1.47	0.16	4.0	3.76
A	0.33	0.33	0.5	1.0	1.0	2.0	3.0	0.85	0.10	3.0	2.19
C	0.33	0.33	0.5	1.0	1.0	2.0	3.0	0.85	0.10	3.0	2.19
S	0.20	0.20	0.33	0.50	0.50	1.0	2.0	0.49	0.05	2.0	1.25
T	0.14	0.14	0.20	0.33	0.33	0.5	1.0	0.30	0.03	1.0	0.77
SUM	3.5	3.5	6.5	10.8	10.8	18.5	28.0	8.99	1.00	23.0	23.0

After setting up the weight for each parameter using the AHP method, the final vulnerability map was obtained by running the model in the (ArcGIS 10.3) environment by using the seven parametric data layers. Accordingly, vulnerability classes of the study area were reclassified into five classes based on the proposed table recommended by Aller et al., (1987) (Table 5.3) that describes the relative probability of contamination of the groundwater resources. The obtained map is shown in the Figure (5.15). These five classes are: V.low, low, medium, high, and V.high. V.low groundwater vulnerability risk zone index <100 which covers an area of 30% ; low vulnerability risk zone index >100-125 covering 7% of the whole area within the studied basin, moderate vulnerability zone index >125-150 covered 25%, high vulnerability zone (index: >150-200) covered   only 35% of the whole area.V.high vulnerability zone with index value of more than 200 covered 3% of the whole studied basin.

5.7 VLDA Vulnerability Model

On the basis of the DRASTIC model for assessing groundwater vulnerability and in accordance with certain principles, VLDA model is proposed by Zhou et al. (2012). VLDA principally reflects the lithology of vadose zone (V), signifying soil media and impact on vadose zone, in DRASTIC model, which controls various physicochemical processes of infiltration waters in the vadose zone. The Pattern of Land Use (L), demonstrating two indicies of DRASTIC model, including net recharge of aquifer and topography, which reflect the amount and process of water consumption or discharge of unit area, as well as types of pollution sources and quantity of pollutants.
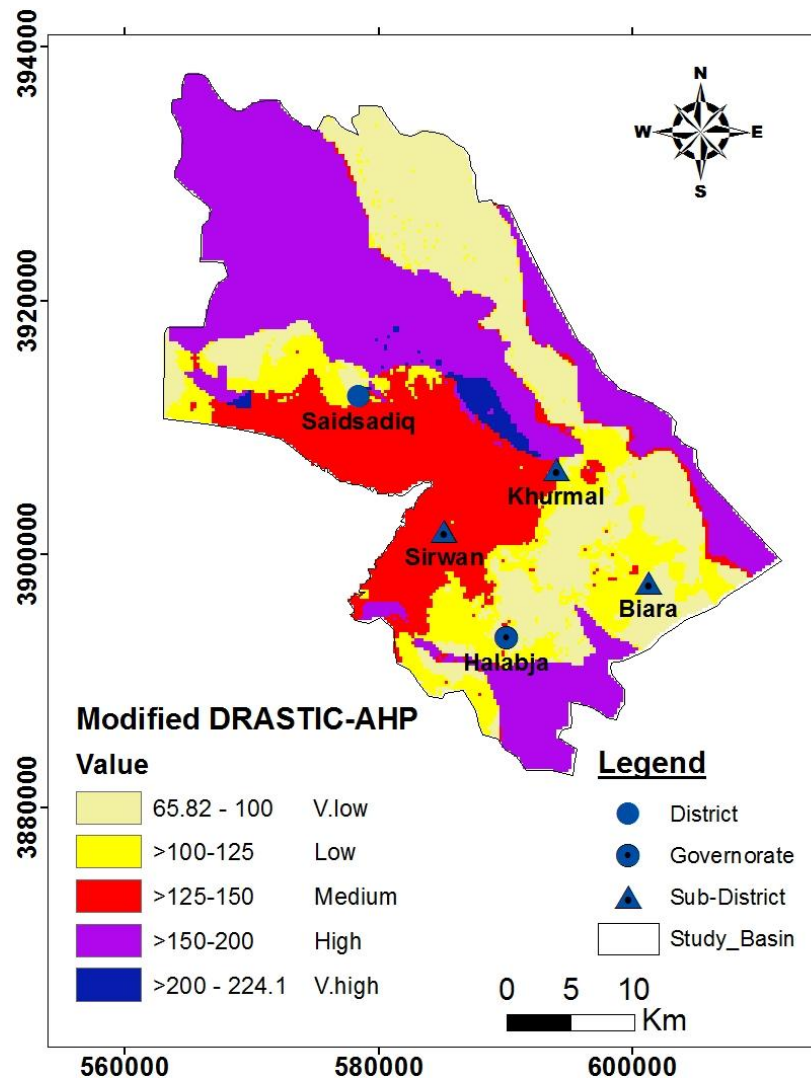
Figure 5.15: **Modified DRASTIC index map using AHP method**

Groundwater depth (D), which determines contact time of pollutants with vadose zone media, and aquifer characteristics (A), representing aquifer media and hydraulic conductivity, which greatly affect the infiltration routes of pollutants after the pollutants enter the aquifer. Therefore, VLDA model is established based on these four indexes for evaluating groundwater vulnerability. In addition, consistent weight can be assigned to each of the four indexes depending on its impact on groundwater vulnerability. Based on the principles of universality, intelligibility and readability (Zhou et al, 2012), the inclusive assessment method is used for this study to assess groundwater vulnerability of the studied basin. The vulnerability comprehensive

assessment index (*DI*) is the weighted sum of the above mentioned four indexes, as computed conferring to the following formula, (Zhou et al., 2012):

$$DI= \sum_{j=1}^{4}(WijRij)\ldots\ldots\ldots\ldots..(5.14)$$

Where *DI* is the comprehensive assessment index of the ith sub-system of the groundwater vulnerability system into the studied basin. Wij is the weight of the jth comprehensive assessment index of the ith sub-system, and $\sum_{j=1}^{4} Wij = 1$. Rij is the value to the jth assessment index of the ith subsystem;4 is the number of indexes.

The smaller the DI value signifier the lower vulnerability of the groundwater system. Quite the reverse, the bigger the DI is the higher the vulnerability of the groundwater system and the poorer the stability will be.

5.7.1 Weight Determination in VLDA Model

For evaluating the groundwater vulnerability, different weights were proposed by different researchers. For instance, in applying DRASTIC model, Aller et al. (1987) assigned the weight 5, 4, 3, 2, 1, 5 and 3 to depth of groundwater, net recharge, aquifer media, soil media, topography, impact on vadose zone and hydraulic conductivity, respectively. Correspondingly, the weights of V, L, D and A in VLDA model as proposed by (Zhou, 2009) are 7, 5, 5 and 6, respectively, and after normalization, the weight is (0.304, 0.217, 0.217 and 0.261) respectively.

When using DRASTIC model, for the same set of indexes mentioned above, Ibe and Nwankwor (2001) provided the following weights: 5, 3, 3, 2, 1, 5, 4 and the corresponding weight of VLDA model is 7, 4, 5, 7, or 0.304,

0.174, 0.217, 0.304, respectively, after normalization. Dixon (2005) contributed the following weights 5, 4, 3, 5, 3, 4 and 2 for DRASTIC model, and the corresponding weight of VLDA model is 9, 7, 5 and 5 or 0.346, 0.269, 0.192 and 0.192 after normalization, respectively. Bukowski et al. (2006) gave weights 3, 4, 4, 4.5, 2, 4.5 and 2.5 therefore, the corresponding weight of V, L, D, A in VLDA model is 8.5, 6, 3 and 6.5 or 0.354, 0.250, 0.125 and 0.271, respectively, after normalization. Panagopoulos et al., (2006) set the weights of groundwater depth, net recharge, aquifer types, topography, vadose zone as 3, 1, 5, 2 and 2.5, respectively, and the corresponding weight of V, L, D, A in VLDA model is 2.5, 3, 3 and 5 or 0.185, 0.222, 0.222 and 0.370, respectively, after normalization.

In addition the weight of groundwater depth, net recharges of aquifer, aquifer medium, soil , LULC, topography and hydraulic conductivity as 5, 4, 3, 3, 3 and 2, respectively, which was proposed by Nobre et al., (2007), and the corresponding weight of V, L, D, A in VLDA model is 3, 7, 5 and 5 or 0.150, 0.350, 0.250 and 0.250 after normalization, respectively.

In applying DRASTIC model, Kourosh et al., (2008) set the normalized mean effective weight for groundwater depth, net recharge of aquifer, aquifer medium, soil medium, topography, vadose zone and hydraulic conductivity as 0.130, 0.203, 0.096, 0.121, 0.099, 0.213, and 0.138, respectively. Correspondingly, the weight of V, L, D, A in VLDA model is 0.334, 0.302, 0.130 and 0.234, respectively. Furthermore, (Zhou, 2009) proposed the normalized weights from the average of all above mentioned value of weights which are 0.312, 0.227, 0.177 and 0.284, respectively for VLDA parameters.

As a result, on the basis of the arithmetic averages from previously applied normalized weights, the weight value for VLDA proposed to be 0.286, 0.251, 0.191 and 0.271, respectively .While, the new corresponding weights of DRASTIC model for the studied basin were proposed using sensitivity analysis method. As illustrated by Babiker et al., (2005), the weights used to

calculate the vulnerability index might change based on the different geological and hydrogeological conditions of the study area. Sensitivity analysis evaluates the effective weights of each parameter.

The effective weight is the function of the value of a single parameter as well as the weight assigned to it by the DRASTIC model (Babiker et al. 2005). The impact on each parameter in the index computation was assessed by achieving a sensitivity analysis. Equation (5.15) was used to calculate the effective weight of each parameter (Javadi et al., 2011).

$$W = \left(\frac{PrPw}{V}\right) * 100 \ldots\ldots\ldots(5.15)$$

Where: W is the effective weight of each parameter, Pr is the rating value. Pw is the weight value of each parameter, and V is the overall vulnerability index.

According to the result of sensitivity analysis, the proposed weights used for DRASTIC indexes in the studied basin were 5.2, 3.8, 3.4, 2.6, 1, 5.6 and 1.4, respectively. Congruently, the weight of VLDA model measured as 8.2, 4.8, 5.2 and 4.8. After normalization the weight are 0.357, 0.209, 0.226 and 0.209, respectively, (Table 5.17).

Table 5.17: Calculated weights of indexes in VLDA model

Calculation of indexes	Lithology of vadose zone (V)	Pattern of land use (L)	Groundwater depth (D)	Aquifer characteristics (A)
Weights-Sensitivity analysis	0.357	0.209	0.226	0.209
Weights-proposed by reasearchers	0.286	0.251	0.191	0.271

Lithology of the vadose zone controls various physicochemical processes of seepage water in the vadose zone. The finest particles of the medium are the smaller quantity of contaminants reaching the aquifer will be, therefore lowering the possibility vulnerability of groundwater. According to the geological map (Figure 1.4) and based upon the stratigraphic profile recorded during drilling processes of the drilled wells in the basin, highly fissured limestone, non-fractured cherty limestone, silt, marl and mixture of gravel, sand and clay are the major ingredients incorporated into the media of vadose zone in the studied basin. According to the scoring principle of VLDA model (Table 5.18), vulnerability scores of lithology of the vadose zone in the area are set between 3 and 10, and the weighted scores are between 1,071 and 3.57, as shown in the Figure (5.16).

Table 5.18: Weighted scores of Lithology of Vadose Zone (V)

Lithology of Vadose Zone (V)	Highly fractured and fissured Limestone	Mixture of gravel ,sand and clay	Compacted cherty limeston, interbede of silt and sand	Marl
Scores	10	6	5	3
Average weighted scores by sensitivity analysis	3.57	2.142	1.785	1.071
Weighted scores by researchers	2.86	1.43	1.716	0.858
Area (Km^2)	518.8	443.2	306.8	9.2
Area (%)	40.6	34.68	24.01	0.72

Pattern of land use (L) defines water utilization or discharge in addition to the types of pollution sources and quantity of pollutants. In the urban area, the possibility for waste (dirty) waters entering groundwater is comparatively high. Thus, the groundwater is relatively vulnerable; in normal farmland, wet land and agricultural area pollutants may enter the groundwater. Thus, the vulnerability of the groundwater is at a moderate level; in barren land and natural vegetation area, no artificial pollutant enters the groundwater. Thus, the groundwater has a relatively low vulnerability. The land uses map of the studied basin constructed previously (Viz section 5.4). Is in compliance with the scoring principle of VLDA model, weight of land use for the area within the studied basin ranged from 3 to 8, and the weighted scores ranged from 0.627 to 1.672 from the weights calculated based on sensitivity analysis (Table 5.19 and Figure 5.17).
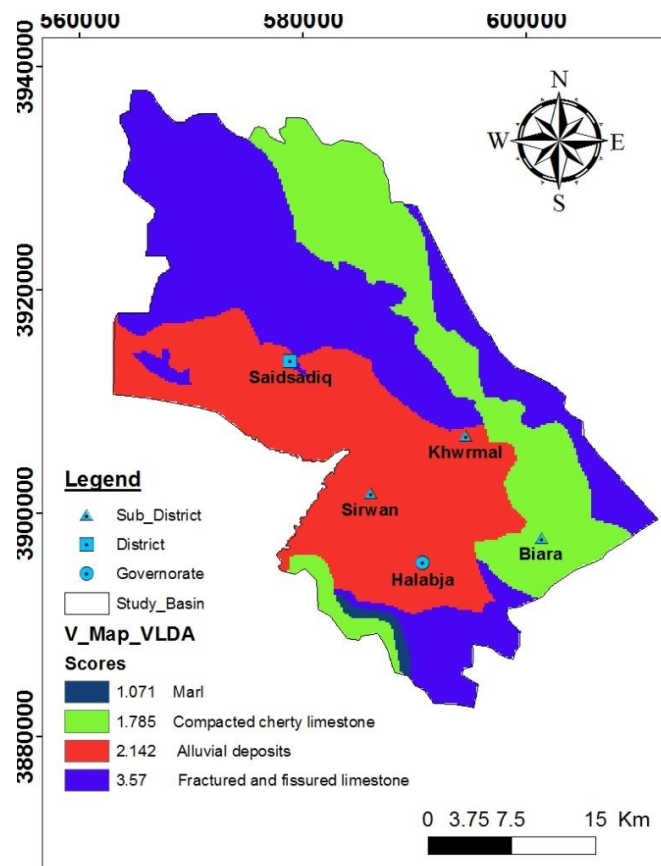
Figure 5.16: Weighted scores of Lithology of Vadose Zone (V)

The depth to groundwater (D) is described as the distance from unsaturated zone that pollutant desires to travel through to reach the water table.Depth to groundwater map was constructed previously (viz section 5.2). Ten classes were achieved for the current studied basin. These are 0-1.5, 1.5-4.5,4.5-7.5,7.5-10,10-12.5,12.5-15,15-23,23-30 and more than 30 m. In complaince with the scoring standard of VLDA model, scores of groundwater depth ranged from 1 to 10, and the weighted scores range between 0.226 and 2.26 (Table 5.20 and Figure 5.18).

Table 5.19: Weighted scores of Pattern of Land Use (L)

Pattern of land use	Urban area	Agricultural and water or wet land	Barren land and vegetation
Scores	8	6	3
Weighted scores by sensitivity analysis	1.672	1.254	0.627
Weighted scores by researchers	2.008	1.506	0.753
Area (Km^2)	17	455	806
Area (%)	1.3	35.6	63.1

The flow system of groundwater regulates the transmission path of the pollutants and length of the route, while aquifer characteristics (i.e. type of aquifer and hydraulic conductivity or water yield property of the aquifer) have reflective influence on the groundwater leakage path. The Hydraulic conductivity (C) describes the ability of the aquifer material to transmit water through it and contaminant migration is controlled by the permeability of the media (cited in Hamamin, 2011). The hydraulic conductivity map was

constructed previously (viz section 5.2). In addition, the average of yield of each aquifer was computed based upon the discharge of about 100 watering wells. According to the hydraulic conductivity and yield of water wells, water yields property of aquifers in the studied basin were classified and divided into five grades in high rich storage zone to limited rich storage zone (Table 5.21). In acquiescence with scoring principle of VLDA model, scores of aquifer characteristics of the studied basin are set between 1 to 9), and the weighted scores are between 0.209 to 1.881, (Figure 5.19).
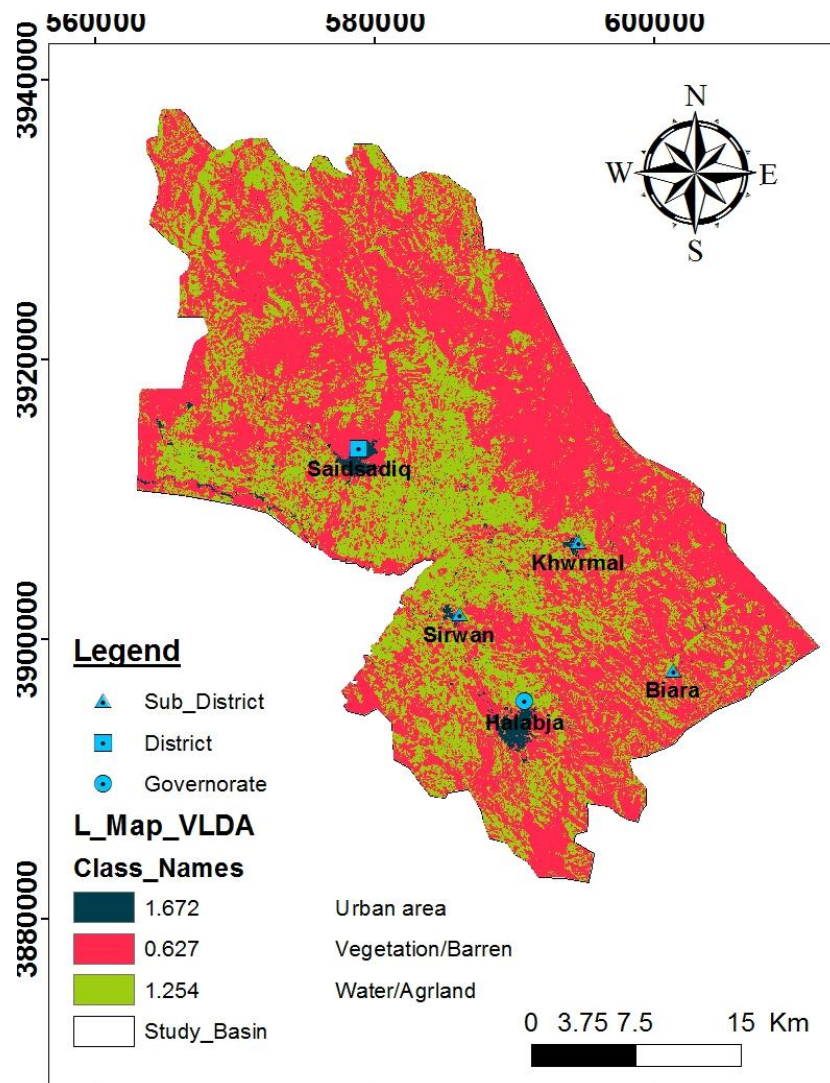
Figure 5.17: Weighted scores of Pattern of Land Use (L)
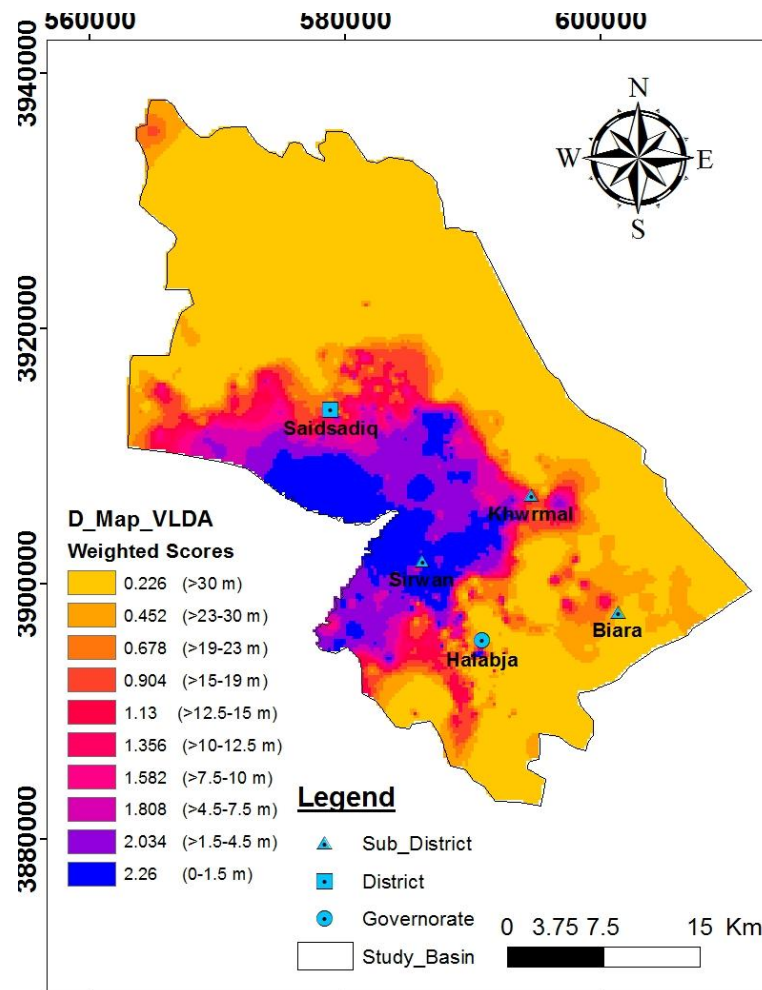
Figure 5.18: Weighted scores of Groundwater Depth (D)

After the weighted scores were attained for the four indexes required for the VLDA model. The weights were used for this study calculated based upon the sensitivity analysis method. The GIS technique was used to combine the four scores and to classify the area in terms of vulnerability zoning, (Figure 5.20). The vulnerability outcome reveals that a total of 4 ranges of vulnerability indexes was noted ranging from low to very high with vulnerability indexes 2.133-4 , >4-6, >6-8 and > 8 . The area of low vulnerability (vulnerability index2.133-4) occupies an area of 26 Km^2 or 2% of whole area and located in the south west of the basin. Very high vulnerability class covered the central part of the basin of index value of >8 and an area of 1% or 13Km^2. This area is characterized by high water

table level and presence of several springs with fractured limestone. This means this region where (V, D and A) have the highest values.The High vulnerability classes occupied most of mountains area that is surrounding the basin and the central part within the area. This vulnerability zone covered an area of 677 Km^2 or 53% of the whole area. Finally, medium vulnerability zones cover an area of 562 Km^2 or 44% of all studied area and positioned South East and North West. The last two vulnerability classes high and moderate occupied most of the studied basins refer to the exhaustive human activities; good water yield property of aquifers and vadose zone composed mainly of fissured limestone and coarse-grain materials.

5.8 COP Vulnerability Model

The COP abbreviated form originates from the three initials of variables in particular, flow concentration(C), overlying layers (O) and precipitation (P), (Vias et al.,2006). The hypothetical premise of this strategy, as indicated by (Daly et al., 2002 ; Goldscheider, and Popescu,2004) is to assess the ordinary protection for groundwater (O variable) controlled by the properties of overlying soils and the unsaturated zone, and also to gauge how this assurance can be adjusted by diffuse, infiltration (C factor) and the climatic conditions (P Factor – precipitation). The COP-Index map can be computed from equation (5.16):

$$COP \ Index \ Map = C*O*P \ \ldots\ldots\ldots\ldots. \ (5.16)$$

Table 5.20: Weighted scores of Groundwater Depth (D)

Groundwater depth (D)	Scores	Weighted scores by sensitivity analysis	Weighted scores by researchers	Area (Km^2) &%
0-1.5	10	2.26	1.91	97.5 (7.6%)
>1.5-4.5	9	2.034	1.719	93.3 (7.3%)
>4.5-7.5	8	1.808	1.528	48.8 (3.8%)
>7.5-10	7	1.582	1.337	22.7 (1.8%)
>10.-12.5	6	1.356	1.146	28.8 (2.3%)
>12.5-15	5	1.13	0.955	35.2 (2.8%)
>15-19	4	0.904	0.764	57.7 (4.5%)
>19-23	3	0.678	0.573	55.8 (4.4%)
>23-30	2	0.452	0.382	118.6 (56.3%)
>30	1	0.226	0.191	719.6 (9.3%)

5.8.1 C- Factor

The C component is reasonable for water to bypass the protection given by the overlying layers (Daly et al., 2002), or it is the concentration of flow maps and represents the sorts of infiltration happening to the catchment. It implies that the extent to which precipitation at or close to the outcrop of the aquifer is gathered into an intergranular media, swallow gap and fissured rocks by passing the vadose zone. This is set up from the EPIK technique (Doerfliger and Zwahlen1998) and the PI strategy (Goldscheider et al.,2000) .

In the COP model, the catchment range is for two primary zones; the first zone (Scenario 1) contains the revive territory of karst elements specifically sinkholes. The second zone (Scenario 2) comprises a range where no surface karst elements were recognized. In the present study, the second scenario connected to the calculation of the C component because of absence of the swallow opening. The C Factor computed in view of equation (5.17), (Vias et al., 2006):

$$C \text{ score} = sf * sv \ldots\ldots\ldots\ldots (5.17)$$

Where, sf is the surface feature and sv is the slope and vegetation.
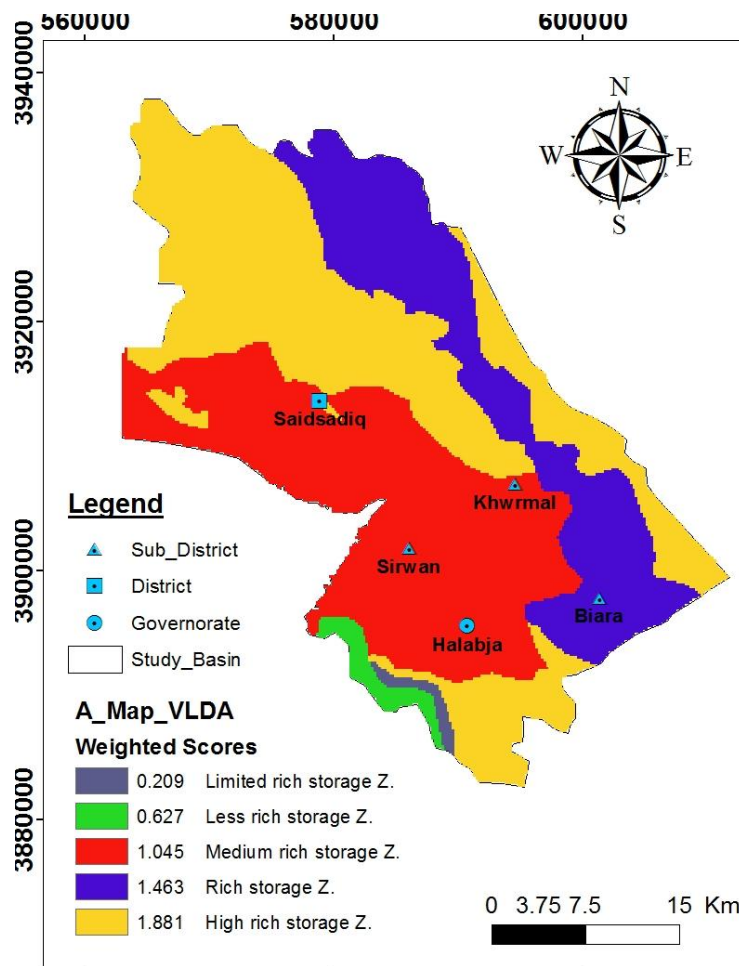
Figure 5.19: Weighted scores of Aquifer Characteristics (A)

The Surface features' parameters incorporate those geomorphological elements particular about carbonate rocks and the vicinity or nonappearance of any overlying layers (porous or impermeable), which decide the significance of runoff and/or infiltration progressions. The assessment of vegetation and slope as conducted by Vias et al., (2006) is entirely unique and the assessment is entirely unique in relation to that in Scenario 1, since slopes are more extreme and vegetation is mislaid; surface runoff or contaminant flows far from the aquifer. This circumstance is regular on the slopes of carbonate aquifers in mountainous regions in the studied basin.
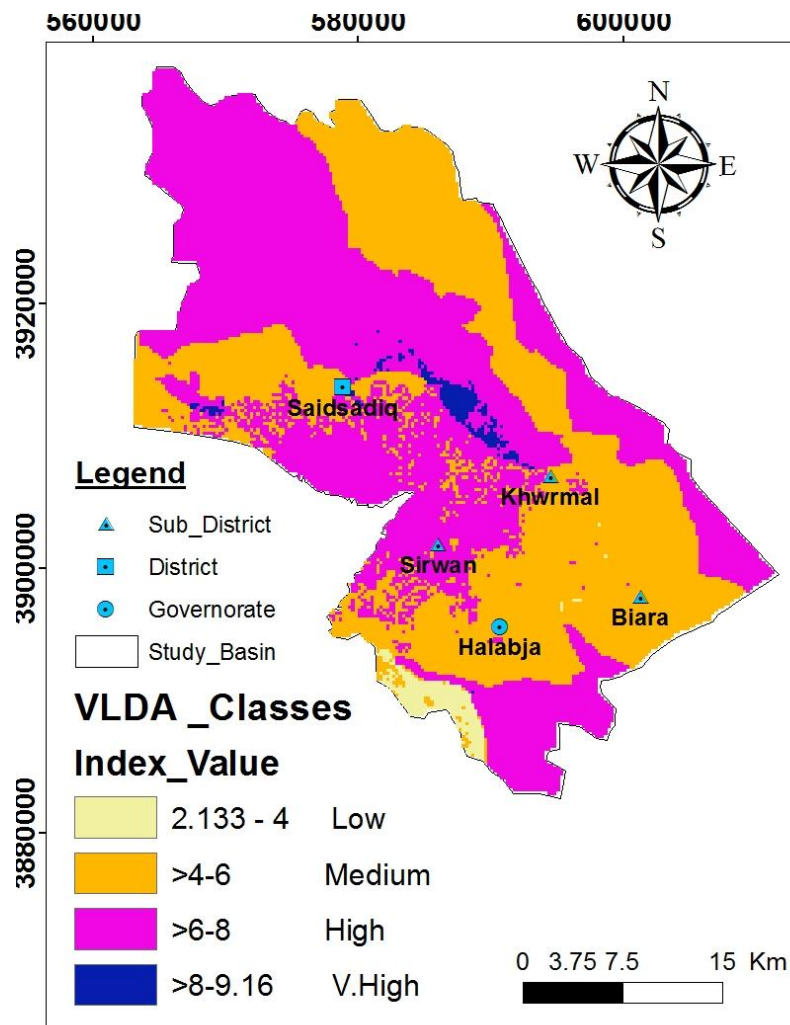
Figure 5.20: VLDA vulnerability index map of the studied basin

To map the C-Factor, it is required to construct (*sf* and *sv*) maps as mentioned previously. The required data onto both *sf* and *sv* maps were extracted from land use-land cover, geological and soil maps. *sf* map was constructed and weighted based on Vias et al., (2006). Slope was extracted from the Digital Elevation Model (DEM) in percent, and reclassified into 4 categories ≤8%, 8<S<31, 31<S<76, and >76, which were assigned weights accordingly for constructing sv map. Surface feature, slopes and type of vegetation were assigned values as per Table (5.22).

Table 5.21: Weighted scores of Aquifer Characteristics (A)

Aquifer type	High rich storage zone	Rich storage zone	Medium rich storage zone	Less rich storage zone	Limited rich storage zone
Unit yield (m3/day)	> 700	> 550-700	> 300-550	> 150-300	0-150
Scores	9	7	5	3	1
Weighted scores by sensitivity analysis	1.881	1.463	1.045	0.627	0.209
Weighted scores by researchers	2.439	1.897	1.355	0.813	0.271
Area (Km^2)	518.7	284.6	443.3	22.1	9.3
Area (%)	40.6	22.3	34.7	1.7	0.7

The final C- map results from the multiplication of surface features and slope and vegetation indices (Figure 5.21). Based on the result of C-score, the

studied basin is classified into three categories in terms of reduction of protection including (moderate, low and very low) of 0.56-0.6, >0.6-0.8 and >0.8-0.95, respectively.

5.8.2 O- Factor

The O factor encapsulates the overlying layers over the saturated zone, and it considers the protection provided for the aquifer by the physical properties and thickness of the layers. This factor is partitioned into four subdivisions by (Daly et al., 2002) specifically topsoil, subsoil, nonkarstic rocks and unsaturated karstic rocks. In terms of hydrogeological roles, to evaluate the O component, the following equation is applied, (Vias et al., 2006):

$$Oscore= [OS] + [OL]………….\ (5.18)$$

Table 5.22: Calculation of *sf* and *sv* sub-factors

sf-Sub-factor		*sv*-Sub-factor		
Geological unit	***sf***	**Slope%**	**Vegetation**	***sv***
Balambo Fn.	0.75	≤ 8	----	0.75
Qulqula Group	0.75	> 8-31	Low	0.85
Recent deposits	1	> 31-76	Low	0.95
Avroman Fn.	0.75	> 76	-----	1
Tanjero Fn.	1			
Shiranish Fn.	1			
Jurassic Formations	0.75			
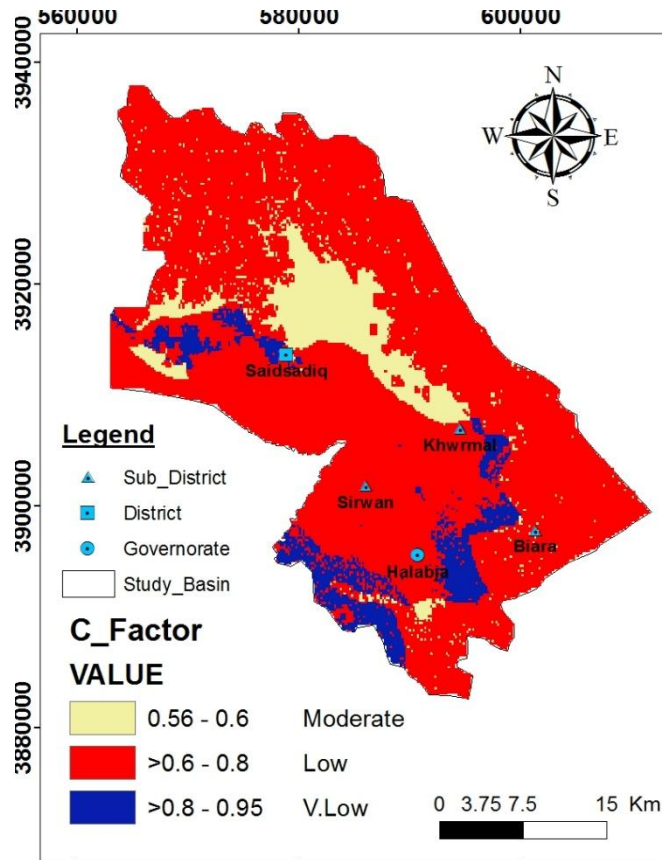
Figure 5.21: C-factor map for the studied basin

(*OS*) signifies the soil character, including texture, grain size and thickness of the soil cover. The thicker the soil cover, the higher the likelihood of contaminant reduction. The OS sub-factor increases from increasing thickness and fining soil texture designating a low vulnerability, (Table 5.23).

(*OL*) is the lithology sub-factor which is reflecting the reduction capability of each layer within the unsaturated zone. The valuation principles of its quantification are the rock nature (mostly effective porosity and hydraulic conductivity) and the scale of fracturing (ly), the thickness of each layer (*m*) and every confining condition (*cn*) (Vias et al.,2006). Consecutive summing of the products of the multiplication of thickness and lithology of each layer, gives up an index which is connected with the protection (Layer index = ∑(*ly*

· m)). The confining condition parameter (cn) is a weighting coefficient for the layer index. The values allocated to the (cn) parameter provide the highest shield to the confined aquifer while an unconfined aquifer is not affected by this parameter (cn=1), (Vias et al., 2006), Table (5.24).

The value of O-Factor decreases when the outcrop materials are composed of carbonate and the soil is absent or poorly developed and it signifies high vulnerability. While with high or moderate protection, the value of O-Factor for the subsurface material increases as a result of high degree of protection and presence of soil or low permeable materials or lithology. Finally, the O-Factor map was constructed by the summation of both OL and Os sub-factors, Figure (5.22).

Table 5.23: Calculation of *OS* sub-factor (Vias et al., 2006)

OS-Sub-factor		
Type of Soil	**Thickness (m)**	O_S **-Value**
Thin or no Soil	< 0.5	1
Silty loam	0.5-1	3
Clay	> 1	5

5.8.3 P- Factor

P-Factor as clarified by (Daly et al., 2002) contains the measure of precipitation and factors that influence the rate of penetration, for example, temporal distribution, duration, frequency and intensity of energizing precipitation occasions. The capacity of precipitation to transport a contamination towards the groundwater can be dictated by this factor; vulnerability increment as the capacity of transportation expanded. The P factor is assessed by two sub-factors, namely Quantity of precipitation (PQ) and temporal distribution of precipitation (PI). The (PQ) sub-factor depicts

the impact on precipitation quantity and the yearly recharge on groundwater vulnerability. Vulnerability increment will be as protection reduced and recharge increased too.

Table 5.24: Calculation of O_L sub-factors

OL -Sub-factor				
Geological unit	*ly*	**thickness-*m***	*ly.m*	O_L
Balambo Fn.	3	50	150	1
Qulqula Group	4	50	200	1
Recent deposits	10	15	150	1
Avroman Fn.	2	60	120	1
Tanjero Fn.	60	20	1,200	3
Shiranish Fn.	500	25	12,500	5
Jurassic Formations	2	50	100	1

The (*PI*) sub-factor is identified with the temporal distribution of precipitation in a specific timeframe and in this way it is uncovering of the intensity of precipitation. For the estimation of this sub-factor, two variables are to be considered for a wet year, the mean yearly precipitation and the quantity of rainy days. Along these lines, that values allocated to the (*PI*) sub-factor is more prominent with a higher total of yearly precipitation and lower number of rainy days. These outcomes of bigger amounts of recharge, empower a rapid infiltration through fissures or karst channels, along these lines, expanding groundwater vulnerability. The more noteworthy the rainy day, the more prominent the measures of runoff towards swallow gaps that support concentrated infiltration. Where infiltration is diffuse and moderate, the (PI) sub-factor is low; ordinarily in such conditions, the volumes of recharge are similarly small. Higher estimations of the P component indicate a lower effect on the level of protection given by the O factor. However, lower

values demonstrate that precipitation, as a function of quantity and intensity decreases the protection managed by the O factor and increases groundwater vulnerability.
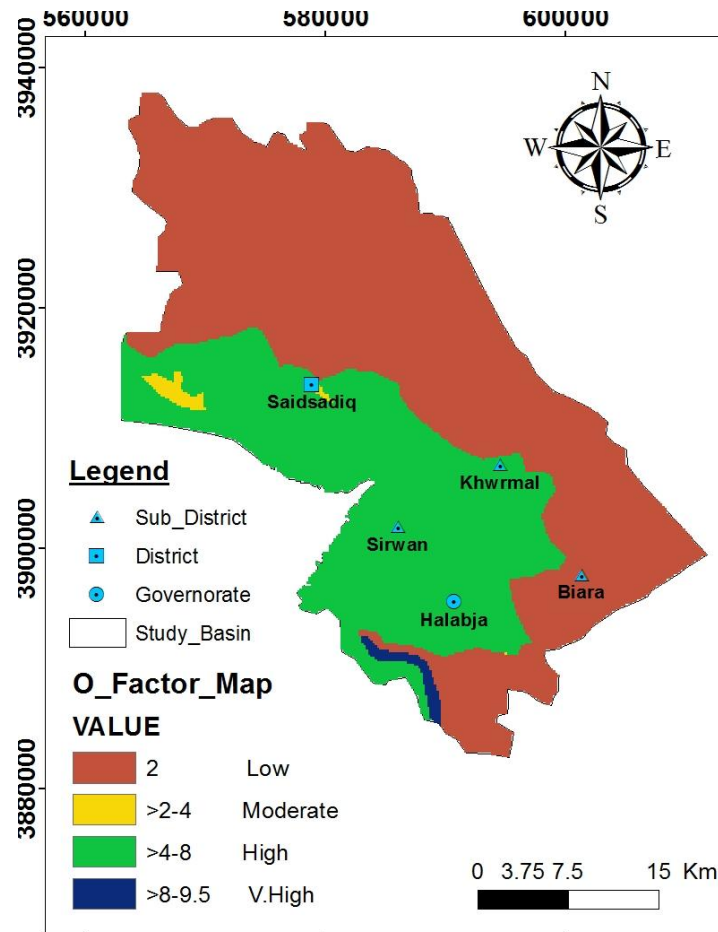
Figure 5.22: O-factor map for the studied basin

The P-Factor signifies the climatic conditions in the studied area. It is also calculated from the summation of two sub-factors (*PQ* and *PI*). Figure (5.23) describes the quantity and intensity of annually precipitation respectively. The average amount of yearly precipitation from 2001-2002 to 2013-2014 was 691.2 mm/year, based upon the analysis of precipitation data for the studied basin achieved from Halabja Meteorological Station. The precipitation intensity is the ratio of the amount of precipitation to the number of rainy days. The number of rainy days from Halabja Meteorological Station in the

studied basin for a mentioned period was about 63 days per year. The results of both *PQ* and *PI* were 0.3 and 0.4, respectively.
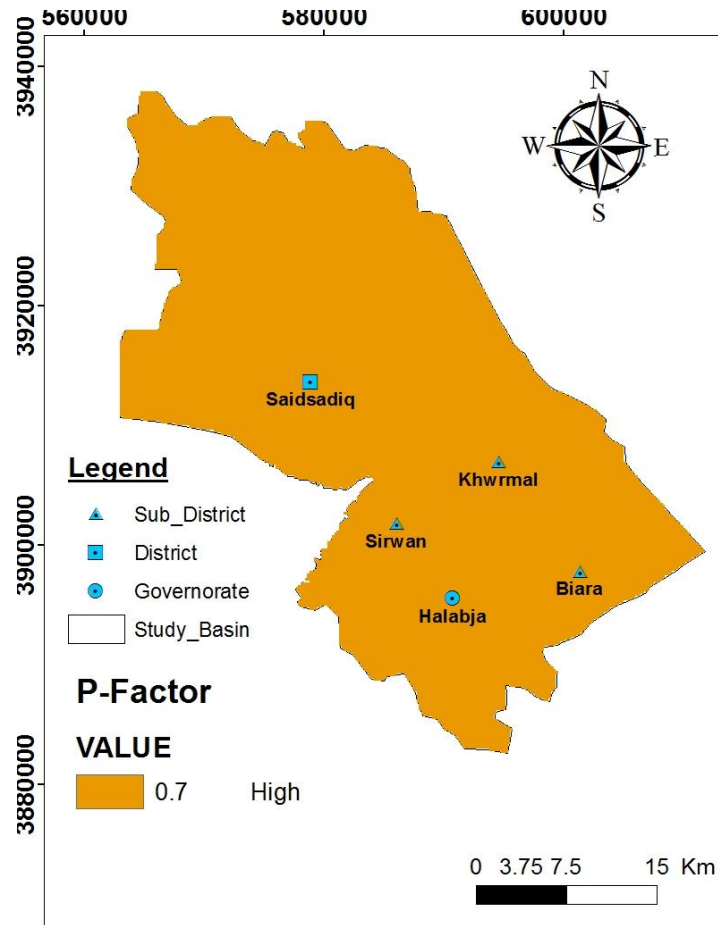
Figure 5.23: P-factor map for the studied basin

The COP Index map for the study basin computed by the multiplication of the three maps for each score, namely C, O, and P using GIS software. The final map was reclassified according to the vulnerability classes as per the COP method, (Vias et al., 2006), Figure (5.24).

From Figure (5.24), based upon the COP model, the area is alienated in to four vulnerability classes ranging from very low to high. The C factor appears to have extremely influenced the final COP map. This is due to the fact that most of the studied areas are characterized by a fissured and trivial karstic carbonate that has a slighter weighting value. High vulnerability zones,

194

covering an area of 767 Km^2 or 60% of the whole area, geologically include the area of the fissured and slight karstic carbonate rocks of different ages. While, low vulnerability class comes in the second order, occupying 37% of the whole area or 473 Km^2, which is mostly characterized by alluvial deposits. The zone with moderate and very low vulnerability classes covere only 25 and 13 km^2 or 2% and 1% of the total area, respectively.
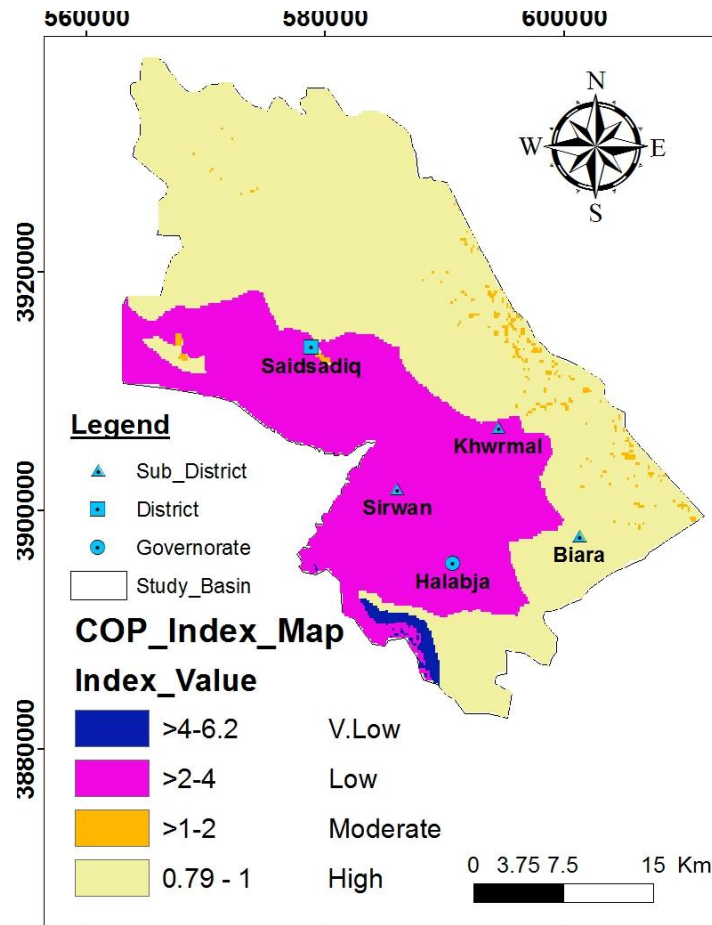
Figure 5.24: COP index map for the studied basin

5.9 Comparison and Validation of the Vulnerability Maps

5.9.1 Comparison of the Vulnerability Maps

The comparison of results from the original DRASTIC model, modified DRASTIC models based upon different modification methods, VLDA and

COP models are given in Table (5.25), and Figures (5.25 and 5.26). The values of standard DRASTIC, DRASTIC-Lineament modification and COP models are distributed in four classes. While the values of DRASTIC-rate weight modification, DRASTIC-LULC modification, DRASTIC-AHP modification and VLDA models are distributed in five classes. Whereas the values of DRASTIC and DRASTIC-Lineament modification attain their peak in medium vulnerability class 5; DRASTIC-rate weight modification, DRASTIC-LULC modification, DRASTIC-AHP modification, COP and VLDA models values attain their peak in the high vulnerability class.
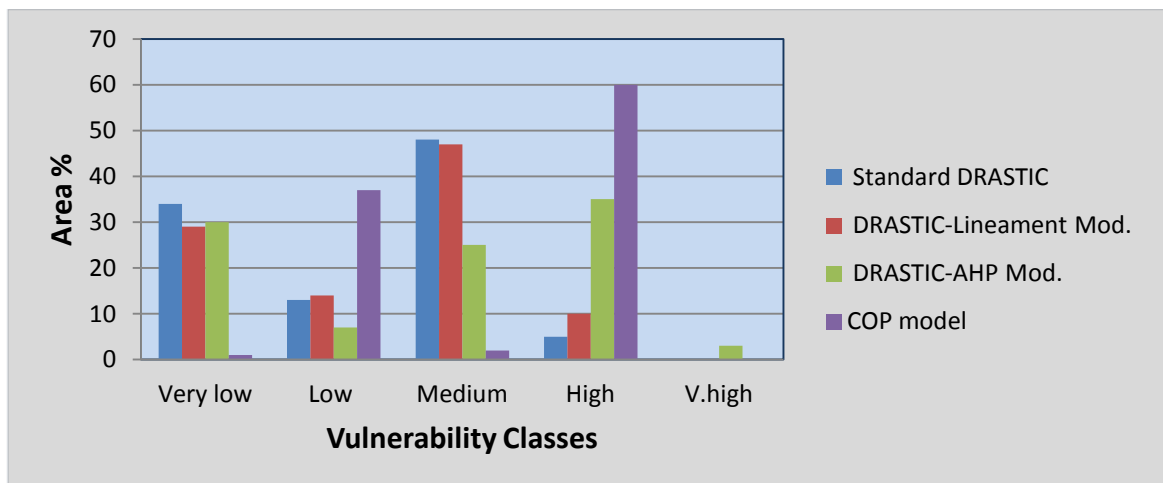
Figure 5.25: Comparison of the percentage areas in the vulnerability classes using standard DRASTIC,DRASTIC lineament mod., DRASTIC AHP-mod. and COP models
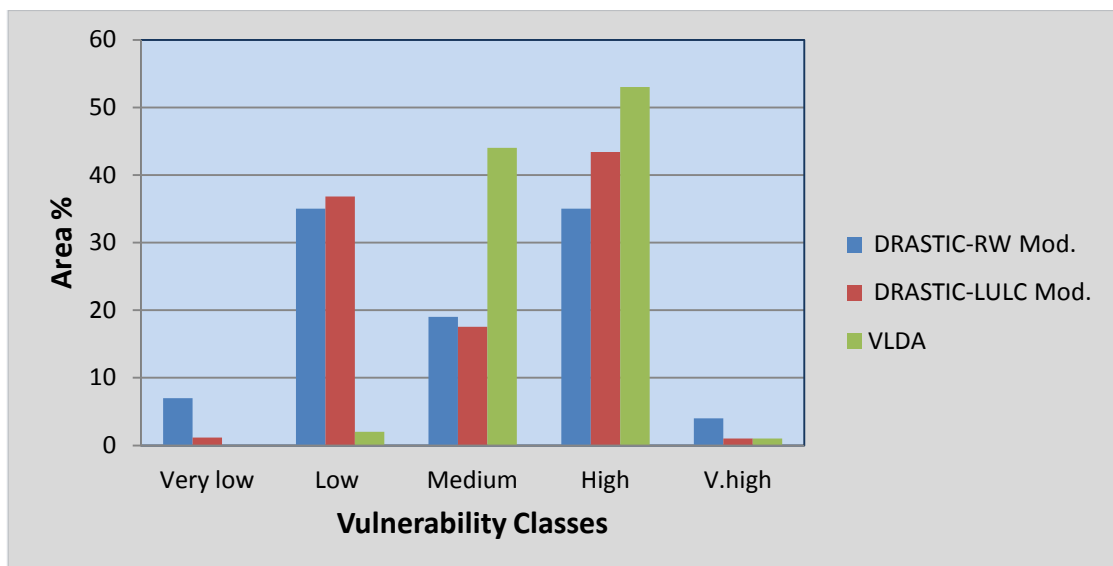
Figure 5.26: Comparison of the percentage areas in the vulnerability classes using DRASTIC RW mod., DRASTIC LUL-mod. and VLDA models

5.9.2 Validation of the Vulnerability Maps

It was envisaged that comparison of the projected risk of groundwater pollution (vulnerability) to the actual groundwater quality status, would help validate the vulnerability approach on the one hand, and indicating the extent of risk for the carrying capacity of the system on the other hand. Therefore, each vulnerability map should be confirmed after construction in order to estimate the validity of the theoretical sympathetic of current hydrogeological conditions (Bruy'ere et al., 2001 and Perrin et al., 2004). Several methods can be applied for the validation of vulnerability assessments; these include hydrographs, chemo-graphs and tracers (natural or artificial), (Zwahlen,2004). For this purpose, correlation between maps of DRASTIC, modified DRASTIC, VLDA and COP models were attempted in two ways as explained in the following sections.

5.9.2.1 Validation against the Nitrate Concentration

In the first approach to validate all applied models in the studied basin, nitrate concentration analysis has been selected. Nitrate as a pollution indicator can be helpful to recognize the evolution and changes of groundwater quality. In this particular studied case, the nitrate differences between two following seasons (dry and wet) were analyzed from 39 watering wells. The samples were collected and analyzed at the end of September 2014 for the dry season and at the end of May 2015 for the wet season. The selected wells for nitrate concentration measurement located nearly in all vulnerability zones in each model. In relation to nitrate values for the dry season (absence of rainfall for a long period), (Table 5.26), low nitrate levels were identified with concentration value ranging between zero to just above 10 mg/l.

While for the wet season, the concentration significantly rose up and concentration values of above 30 mg/l were recorded. So it can be concluded that groundwater in the current studied basin is capable to receive the contaminant due to its suitability in terms of geological and hydrogeological conditions. This condition refers to several main factors such as rising up the water table in the wet season and vice versa for the dry season. Secondly, the impact on land uses activity is significant in the wet season specifically using fertilizers (nitrate) for different agriculture purposes. Finally, rainfall plays an important role to transport nitrate based on specific condition of aquifer characteristics. Therefore, these considerable variations in nitrate concentration from dry to wet seasons, verify the sensibility of the gradation and distribution of vulnerability levels acquired using the modified DRASTIC model based on (rate and weight modification, effect of LULC, using AHP method and VLDA models).

Table 5.25: Comparison of the number of pixel, the area in km^2 and the area in percentage in the models representing the vulnerability classes obtained from all models

Classes	Standard DRASTIC			DRASTIC-RW Modification			DRASTIC-LULC Modification		
	N.Pixel	Area (Km^2)	Area %	N.Pixel	Area (Km^2)	Area %	N.Pixel	Area (Km^2)	Area %
V.low	11889	435	34	2448	89	7	350	13	1
Low	4546	166	13	12238	447	35	12938	473	37
Medium	16784	613	48	6644	243	19	6294	230	18
High	1748	64	5	12238	447	35	15036	550	43
V.high	0	0	0	1399	51	4	350	13	1
Classes	**DRASTIC-Lineament Modification**			**DRASTIC-AHP Modification**			**VLDA**		
	N.Pixel	Area (Km2)	Area %	N.Pixel	Area (Km2)	Area %	N.Pixel	Area (Km2)	Area %
V.low	10140	371	29	10490	383	30	0	0	0
Low	4895	179	14	2448	89	7	699	26	2
Medium	16434	601	47	8742	320	25	15385	562	44
High	3497	128	10	12238	447	35	11539	677	53
V.high	0	0	0	1049	38	3	350	13	1
Classes	**COP**								
	N.Pixel	Area (Km^2)	Area %						
V.low	350	13	1						
Low	12938	473	37						
Medium	699	26	2						
High	20980	767	60						
V.high	0	0	0						

In addition, standard DRASTIC and COP methods need to be modified based on different patterns that affect the vulnerability system in the studied basin, (Figures 5.27 and 5.28).

In terms of effect of lineament features on standard DRASTIC model, based on this verification, it could be argued that the effect of lineament density is weak on the vulnerability process in the studied basin. Because this model provides nearly the same outcome as realized by standard DRASTIC. This refers to the low distribution of lineament density over the studied basin.

5.9.2.2 Validation against Groundwater Age Using Unstable Isotopes

Determination of ground-water ages can be used to assess the vulnerability of groundwater to contamination, higher vulnerability zone should have a younger groundwater age. Areas of recent recharge are susceptible to contamination from surface waters. Numerous methods exist for age dating groundwater. The simplest, most frequently used, and currently most popular method is the tritium (unstable isotopes) method (Blavoux et al., 2013).

Tritium or ^{3}H is a radioactive isotope of hydrogen (having two neutrons and one proton) with a half-life of 12.4 years (Blavoux et al., 2013). Tritium concentrations are measured in tritium units (TU) where 1 TU is defined as the presence of one tritium in 10^{18} atoms of hydrogen (H). Atmospheric nuclear weapons testing in the 1950s and early 1960s released tritium to the atmosphere at levels of several orders of magnitude above the background concentration (which results from cosmic ray interaction with isotopes in the atmosphere). This atmospheric tritium enters groundwater as HTO (High-Temperature Oxidation) with tritium as part of the water molecule during recharge (UN, ILO and WHO, 1983).

Table 5.26: Mean nitrate concentration in both dry and wet seasons at each models

Vulnerability classes	Mean Nitrate Concentration (mg/l)-Dry season						
	Standard DRASTIC	DRASTIC-RW Mod.	DRASTIC-LULC Mod.	DRASTIC-Lineament Mod.	DRASTIC-AHP Mod.	VLDA	COP
V.low	< 2	0-2	N.D	0-2	< 2	N.D.	0-2
Low	2-4	>10	< 7	>10	2-4	2-4	>10
Medium	>10	>10	>10	>10	>10	>10	>10
High	>10	>10	>10	>10	>10	>10	>10
V.high	N.D.	>10	>10	N.D.	N.D.	>10	N.D.
Vulnerability classes	Mean Nitrate Concentration (mg/l)-Wet season						
	Standard DRASTIC	DRASTIC-RW Mod.	DRASTIC-LULC Mod.	DRASTIC-Lineament Mod.	DRASTIC-AHP Mod.	VLDA	COP
V.low	0-20	20-30	N.D	20-30	0-20	N.D.	20-30
Low	20-30	> 30	Mostly <20	> 20	20-30	20-30	> 30
Medium	>30	> 30	>30	> 30	>30	> 30	> 30
High	>30	>30	>30	>30	>30	> 30	>30
V.high	N.D.	>30	>30	N.D.	N.D.	>30	N.D.
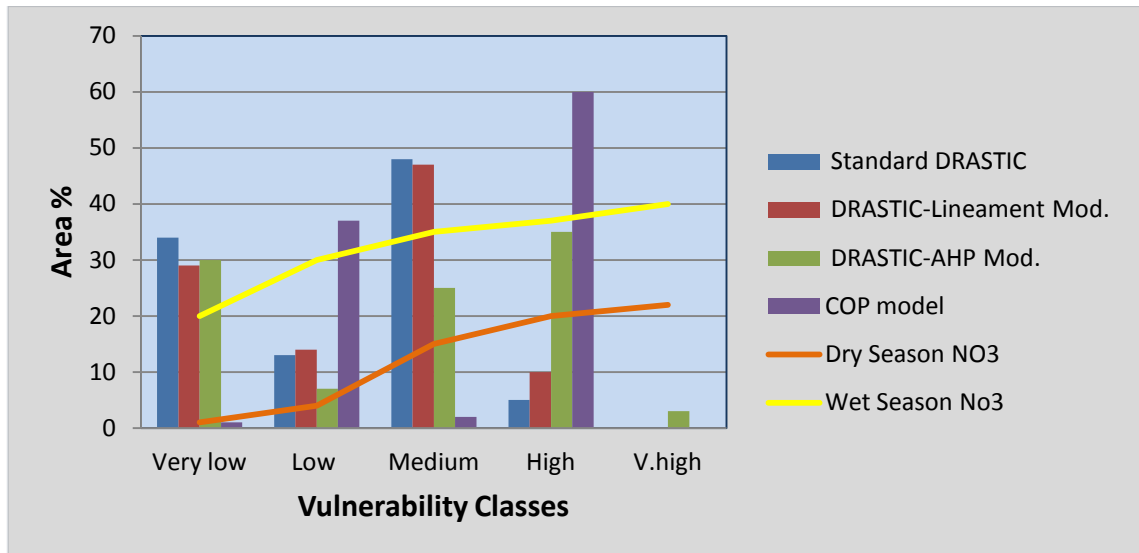
Figure 27: Validation of four applied models with mean nitrate concentration
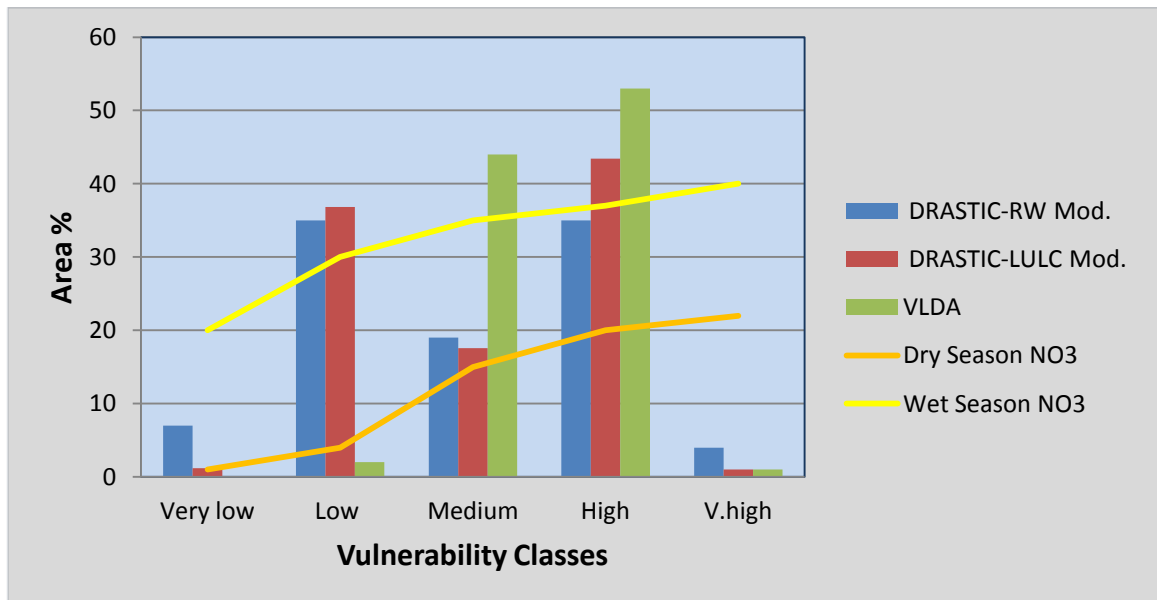
Figure 5.28: Validation of three applied models with mean nitrate concentration

In the earth, small amounts of natural tritium are produced by alpha decay of lithium-7(Kumar and Somashekar, 2011). Natural atmospheric tritium is also generated by secondary neutron cosmic ray bombardment of nitrogen, which then decays to carbon-12 and tritium. Tritium atoms then combine with oxygen, forming water that subsequently falls as precipitation. Before the atmospheric nuclear bomb testing in the 1950s, natural average concentrations

of tritium ranged from approximately 2 to 8 TU, ((Blavoux et al., 2013). Approximately 1.13×10^9 TU was added in the northern hemisphere from atmospheric nuclear bomb testing with the largest tritium concentrations peaking in 1963. Since cessation of atmospheric nuclear tests, tritium concentrations have dropped to between 12 and 15 TU, although small contributions from nuclear power plants occur. As most tritium is disseminated into the environment as water, it enters the hydrologic cycle as precipitation and eventually becomes concentrated in levels detectable in groundwater, (Blavoux et al., 2013).

In the current study, one rain sample and twenty samples of groundwater wells which penetrating different aquifers collected for analyzing unstable isotopes (Tritium) to achieve the groundwater age (viz section 1.7.1). Rain sample had a tritium value of 4.8 TU and a mean value of groundwater samples was 4.28 TU for CKFA, TKA and JKA aquifers and 2.28 and 3.03 TU for CFA and AIA aquifers, respectively, Table 5.27. For the purpose of comparison of changing tritium value with time, there is no previous study concerning tritium value range in the studied basin, while several studies in the world confirmed that tritium levels in meteoric and groundwater waters were decreased with the passage of time, (Davies, 2002). In addition, based on a study on tritium value in spring well samples water by Hamamin and Ali (2013) in Basara basin, they recorded a tritium vale for groundwater samples within the range of 5.5-7 TU and they concluded that the value closely resembles to the present time tritium concentration in precipitation.

Groundwater age estimation using tritium only provides semi-quantitative, "ball park" values. There is no specific classification for age estimation based on tritium results. Mckenzie et al. (2010), classify the age of samples by classifying water as being modern and pre-bomb. Tritium values greater than 0.3 TU is used to represent modern water (i.e. recharge after 1965) and values less than or equal to 0.3 TU to represent pre-bomb spike recharge (i.e.

recharge before 1965). In contrast (William, 2000) classify groundwater age as follows:

- < 0.8 TU indicates submodern water (prior to 1950s)

- 0.8 to 5 TU indicates a mix of submodern and modern water

- >5 to 15 TU indicates modern water (<5 to 10 years)

- >15 to 30 TU indicates some bomb tritium

- >30 recharge occurred in the 1960s to 1970s

Based on both classifications, the tritium value (Table 5.27), indicates that the groundwater is modern or a mix of submodern and modern water. The tritium data provide insight as to the mean residence time of "old" versus "new" groundwater in the study. The basic premise for using groundwater age to establish vulnerability is that groundwater with a relatively rapid vertical transport rate has a younger age. Since most contaminants are present near the earth's surface, younger groundwater is therefore more vulnerable.

Old groundwater is more likely to be isolated from the contaminating activities that are ubiquitous in the urban and suburban environments. Additionally, the results of tritium analysis reveal that groundwater in the CKFA, TKA and JKA aquifers is younger than in both AIA and CFA. Moreover, ground water in the AIA aquifer is younger than CFA as tritium value of AIA is higher than in CFA, (Figure 5.29). In view of this classification, groundwater vulnerability was assessed based on tritium (^{3}H) and groundwater age.

This approach examines the similarity of a spatial pattern of variability of these maps along with a common cross-section line, A-B (Figure 5.30), to see the linear relationship between vulnerability index value and groundwater tritium value. The results show a better match between the patterns of the tritium value of groundwater and vulnerability index value achieved from modified DRASTIC based on (rate and weight, using AHP method, effect of LULC map) and the VLDA model, (Figure 5.31). Therefore based on this

verification, it can be concluded that the vulnerability models achieved from previously mentioned method reflecting the real vulnerability situation in the studied basin.

Table 5.27: Results of Trituim analysis of groundwater samples in the studied basin

Sample code	Site	^{3}H (TU) $\pm$ σ		Average ^{3}H (TU)	Aquifer
ITB	BanisharMosquesWell	4.7	± 0.3		
ITB2	BasakWell	3.8	± 0.3		
ITJ	JalelaVillageWell	4	± 0.3		
ITS1	SarawSwbhanAgha	4.5	± 0.3	4.28	CKFA. TKA and JKA
ITM	Mzgawta	4	± 0.3		
ITSb	SheraBara	4.3	± 0.3		
ITT2	Tawanawal	4.6	± 0.3		
ITD	Darbarulla	4.3	± 0.3		
ITTh	Halabaj-TaymwrHassan	3.3	± 0.3		
ITS	Sirwan	2.3	± 0.3		
ITSs	Shekhan_Shanadactry_ Road_Project	3.1	± 0.3		
ITSm	Soila_Mesh	3	± 0.3	3.03	AIA
ITGs	Gulajoy_Saroo	3.2	± 0.3		
ITMh	MstakaniHajiAhmad	3	± 0.3		
ITT	TazaDe	3	± 0.3		
ITB3	Bezhawa	3.3	± 0.3		
ITX	KharpaneWell	2.4	± 0.3		
ITBk	Balkhay_Khwaroo	2.3	± 0.3	2.28	CFA
ITS2	Sargat	2.1	± 0.3		
ITBb	Bani_Bnok	2.3	± 0.3		
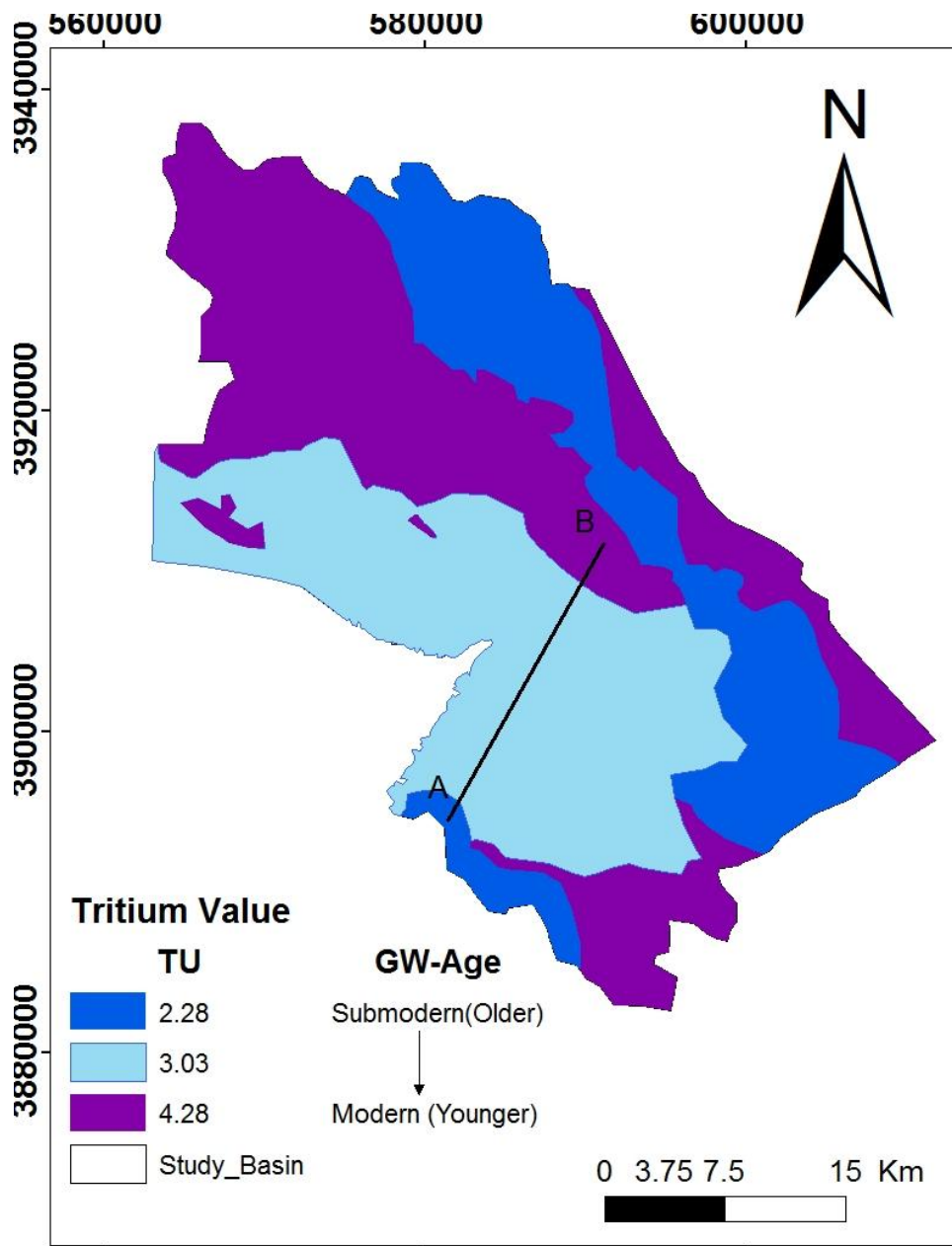
Figure 5.29: Groundwater age and tritium value of aquifers at the studied basin
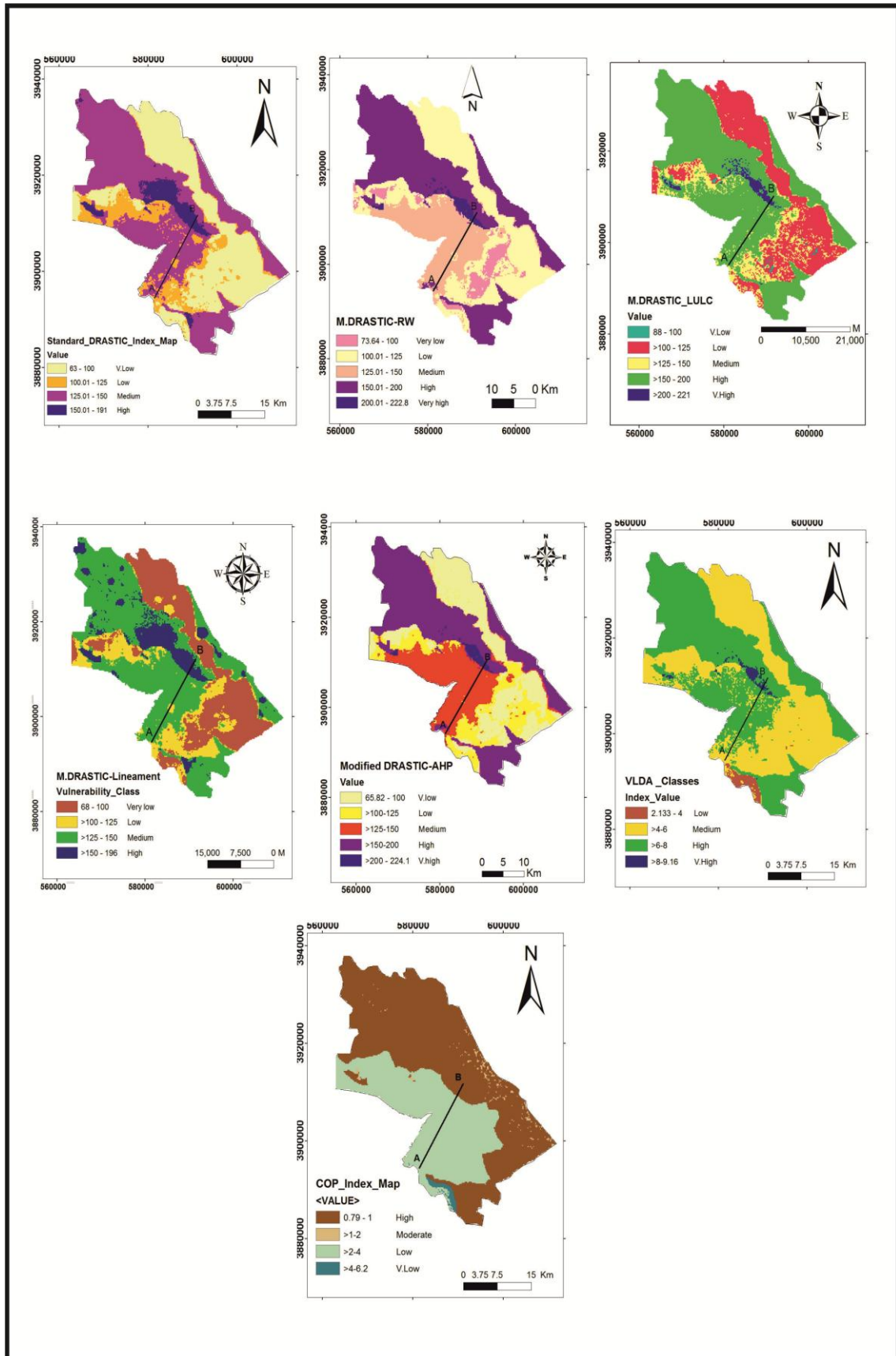
Figure 5.30: Cross section line (A-B) for all applied vulnerability models
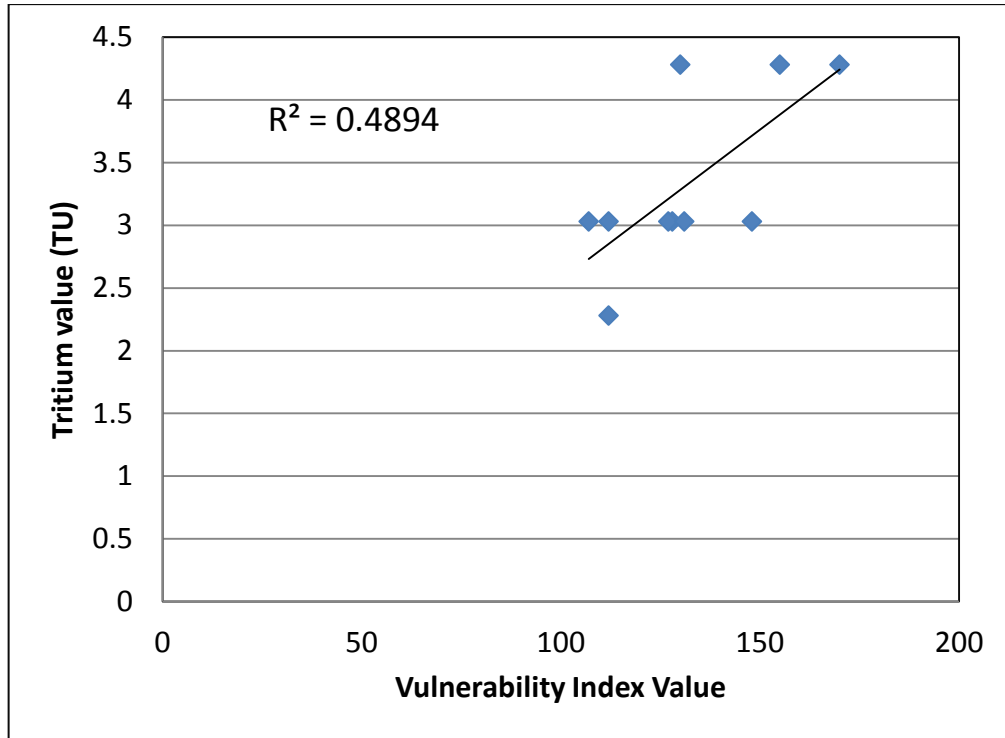
a: Standard DRASTIC index value vs. Tritium value (TU)
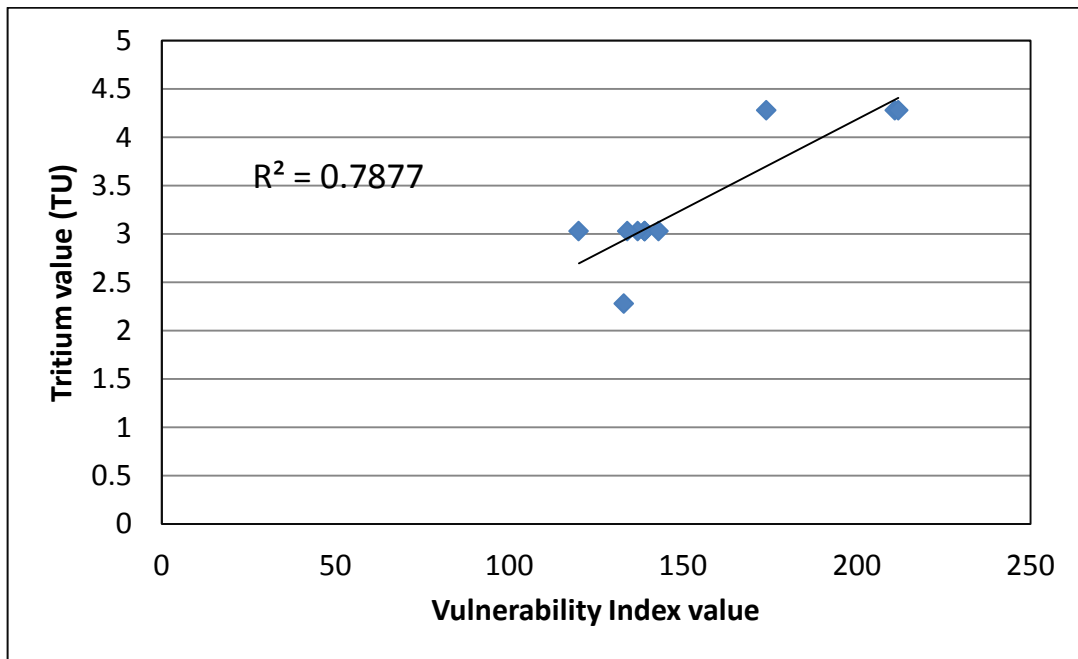
b:Rate-weight modified DRASTIC model vs. Tritium value (TU)
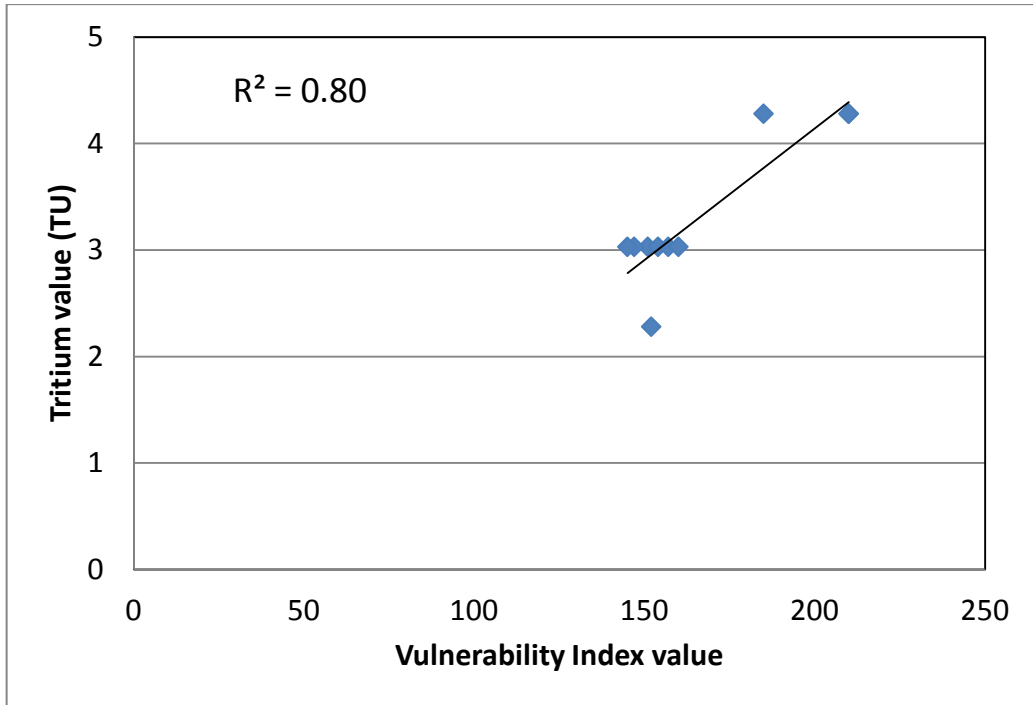
c: Modified DRASTIC model based on LULC map vs. Tritium value (TU)
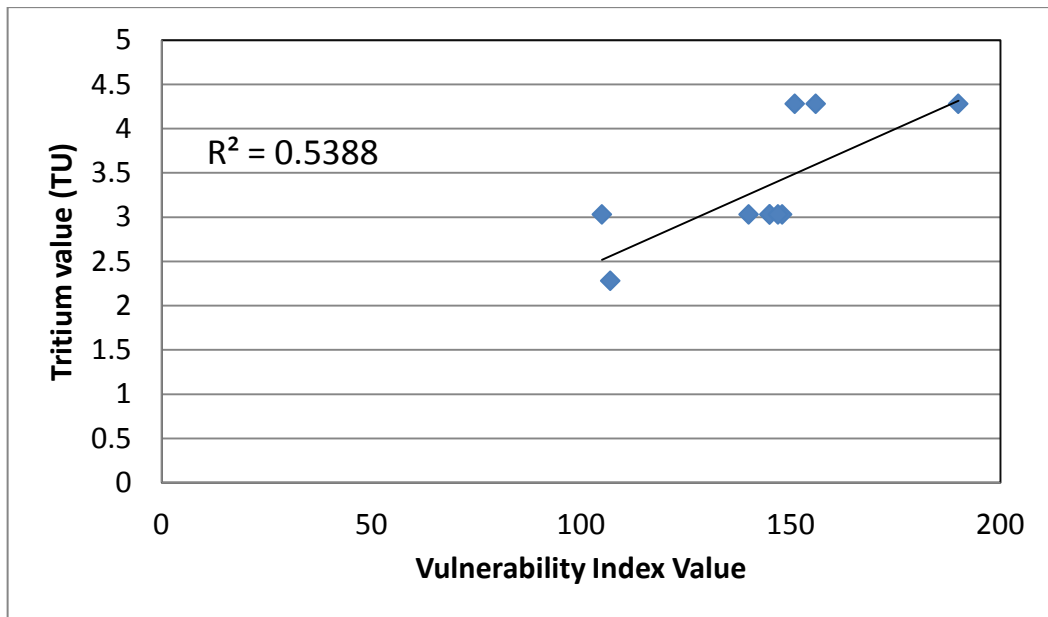
d: Modified DRASTIC model based on lineament density map vs. Tritium value (TU)
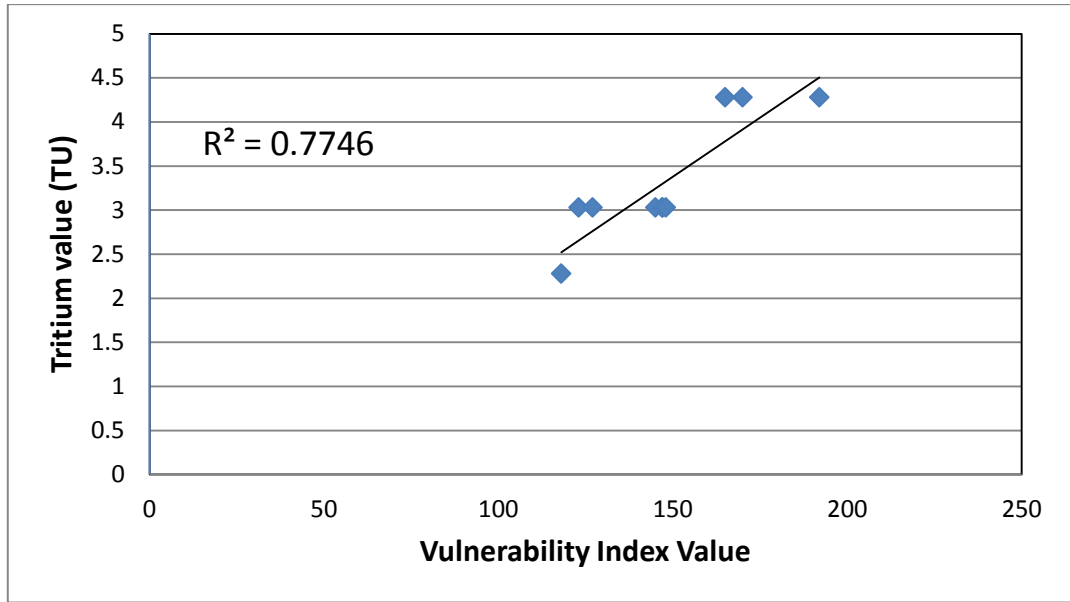
e: Modified DRASTIC model based on AHP Model vs. Tritium value (TU)
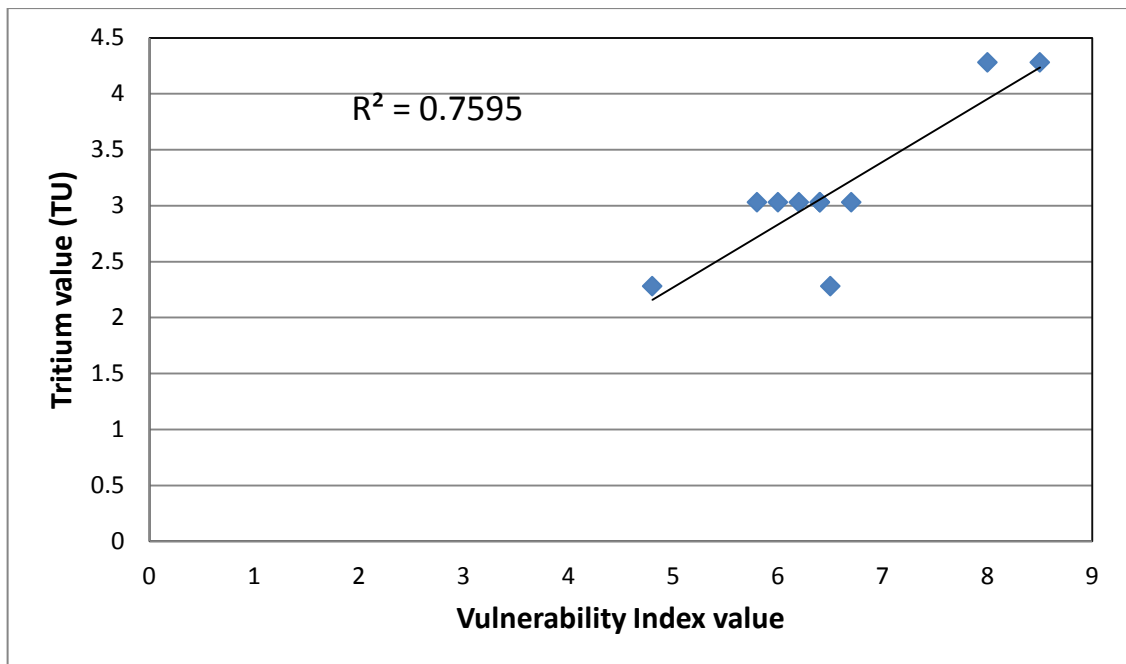
f: VLDA vulnerability model vs. Tritium value (TU)
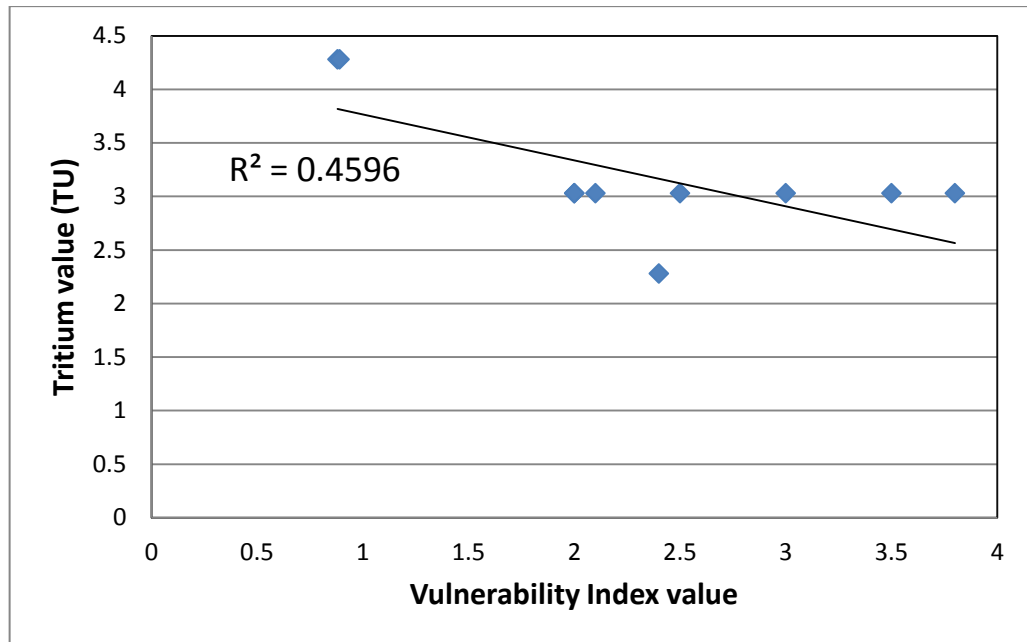
g: COP vulnerability model vs. Tritium value (TU)

Figure 5.31: Regression between all applied vulnerability models for cross-section A-B

Chapter Six

Conclusions
and
Recommendations

Chapter Six
Conclusions and Recommendations

6.1 Conclusions

The detailed systematic study conducted in the present work in terms of climate, geology, hydrogeology, geochemistry and environmental impacts to develop an appropriate method suitable for assessment of the groundwater vulnerability of the studied basin, revealed the following conclusions.

- The total amount of annual water surplus was estimated to be 341.5 mm, based on the meteorological data during the period of 2002 to 2014 for Halabja Meteorological Station. From this amount of surplus, the total rate of 169 mm/year is predicted as surface runoff. While the total expected annual recharge to the aquifers in the study basin is estimated to be around 172.5 mm/year from all fallen precipitation.

- Geochemically, the result of groundwater classification using Piper diagram shows that the majority of the groundwater samples belongs to the field of alkaline water with the presence of bicarbonate . sulfate and chloride. From the Durov diagram, it is clearly revealed that almost quality of all water samples fall into field represents earth alkaline waters with prevailing weak acid anions. This type of water represents temporary hardness and this region revealed to be $Ca-Mg-HCO_3$ water type.

- To evaluate the potential vulnerability of groundwater contamination in the studied basin, the standard DRASTIC index model was applied to a GIS environment. The DRASTIC vulnerability index values ranged between 63 and 199.4. These values were reclassified into four vulnerability classes comprising very low to high.

- In the first attempt on the modified standard DRASTIC model, nitrate concentration was applied to modify the original rate and the sensitivity analysis was applied to establish the effective weight of each parameter in DRASTIC model. The modified DRASTIC vulnerability index values based on rate-weight modifications ranged between (73.64 - 222.8) with five vulnerability classes comprising very low to very high.

- The second attempt to modify standard DRASTIC model is based on the impact of human activity in the vulnerability system in the studied basin. For this reason, LULC map was constructed and was rated and weighted as an additional parameter and then added to the standard DRASTIC model. The modified DRASTIC vulnerability index values ranged between 88 and 221 with five vulnerability classes comprising very low to very high.

- The third trial to modify the standard DRASTIC model was based upon the density of the lineament feature. Lineament as linear features of a landscape may have an effective role in the vulnerability system in the study basin, because of its close relationship with groundwater and act as an assistant factor to transport contaminant toward groundwater easily. The modified DRASTIC vulnerability index values based on the effect of lineament feature ranged between (68 and 196) with four vulnerability classes comprising very low to high.

- The fourth attempt to modify standard DRASTIC model was by the application of Analytical Hierarchical Process (AHP) to assess the weight value of each parameter. The modified DRASTIC vulnerability index values based on AHP method ranged between 65.82 – 224.1 with five vulnerability classes comprising very low to very high.

- Beside DRASTIC model, VLDA model was applied. The vulnerability outcome revealed that a total of 4 ranges of vulnerability indexes was noted ranging from low to very high with vulnerability indexes 2.133-9.16.

- Also COP model was applied to map vulnerability system into the studied basin. Based on this model, the area is alienated into four vulnerability classes ranging from very low to high with index value ranged from 0.79 to 6.2.

- Each vulnerability map should be validated after its construction in order to clarify the validity of the theoretical sympathetic of current hydrogeological conditions and to show the accuracy of the modeled vulnerability system. Two methods were applied for the validation of the result, in the first approach, to validate all applied models in the study basin; nitrate concentration analysis has been selected. Nitrate as a pollution indicator can be helpful to recognize the evolution and changes of groundwater quality. The considerable variation of nitrate level in the groundwater from dry to wet seasons confirms that groundwater in the current studied basin is capable to receive the contaminant. Therefore, these considerable variations in nitrate concentration from dry to wet seasons, verify the sensibility of the gradation and distribution of vulnerability levels acquired using the modified DRASTIC model based on (rate and weight modification, effect of LULC, using AHP method and VLDA models).

- The second approach to validate the achieved vulnerability maps from all applied models, groundwater vulnerability was assessed based on tritium (^{3}H) value and groundwater age. The results demonstrate a better match between the patterns of the tritium value of groundwater and modified DRASTIC based on rate and weight, using AHP, effect of LULC and the VLDA models.

6.2 Recommendations

The study comes up with the following recommendations:

- Groundwater vulnerability and the groundwater risk cannot be completely evaluated without understanding the hydrogeological condition as well as

the groundwater balance, so it would be advisable to extend the above study by increasing the number of monitoring wells both for optimal observation of water level and for lithology. This may help having a better understanding of the interaction of the groundwater regime.

- Assessment of the influence of the horizontal recharge from the drainage system including the canals is highly recommended. It is required to study the effect of these water bodies on the groundwater quality.

- A comprehensive inventory also needs to be prepared about the incident terrestrial contaminant loadings from different types of land use.

- The study recommended that the vulnerability models can be used for prioritization of vulnerable areas in order to prevent the further pollution to groundwater aquifers. There should be a detailed and frequent monitoring in very high, high and moderate vulnerable zones in order to monitor the changing level of pollutants.

- The vulnerability study is also recommended to help for screening the site selection for all types of waste disposal specifically the municipalities waste dumping.

- Iraqi and Kurdistan authorities who deal with planning issues such as the Kurdistan Water Authority, the Environmental Quality Authority , the Ministry of Agriculture and Water Resources and the Ministry of Planning, have to take the issue of groundwater protection into their considerations when deciding about locations and conditions for the establishment of facilities and activities which are possibly hazardous to groundwater. Such as waste disposal sites and sewage treatment plants and different industrial projects, by locating such sites in areas where a contamination of the groundwater resources is likely not to occur (areas of very low and low groundwater vulnerability). Therefore, a deterioration of the groundwater resources can be actively avoided.

References

❖ Abawi S. A., and Hassan M. S., 1990: Environmental engineering water analysis, Dar Al-Hikma press, 296p.

❖ Al-Adamat R.A.N., Foster I.D.L., and Baban S.M.J., (2003). Groundwater Vulnerability and Risk Mapping for The Basaltic Aquifer of The Azraq Basin of Jordan Using GIS, Remote Sensing and DRASTIC. Applied Geography, 23:303–324.

❖ Al-Ansari N, M Abdellatif, M Ezeelden, SS Ali and S.Knutsson,(2014). Climate Change and Future Long Term Trends of Rainfall at North-East Part of Iraq. Published By Journal of Civil Engineering and Architecture, 8 (6), 790-805 p.

❖ Alcamo, J., Florke, M., & Marker, M. (2007). Future Long-Term Changes In Global Water Resources Driven By Socio- Economic and Climatic Changes. Hydrological Sciences Journal, 52(2), 247–275.

❖ Al-Doski J., Mansor S. B. and Shafri H. Z. (2013a). Monitoring Land Cover Changes in Halabja City, Iraq, International Journal of Sensor and Related Networks (IJSRN) Volume 1, Issue1 , P. 01-11.

❖ Al-Doski J., Mansor S. B. and Shafri H. Z. (2013b). NDVI Differencing and Post- Classification to Detect Vegetation Changes in Halabja City, Iraq, IOSR Journal of Applied Geology and Geophysics (IOSR-JAGG).Volume 1, Issue 2, p. 01-10.

❖ Ali S. S., (2007). Geology and Hydrogeology of Sharazoor - Piramagroon Basin In Sulaimani Area, Northeastern Iraq. Unpublished Phd Thesis, Faculty of Mining and Geology, University of Belgrade, Serbia. 317P.

❖ Ali S.S, (2005). Effect Of Slide Masses on Groundwater Occurrence In Some Areas of Sharazoor Plain/NE of Iraq.Published In: Water Resources and Environmental Problems In Karst–Proceeding of Internatuiional Association of Hydrogeologist. Internationasl Confertence, Karst(CVIJIĆ).

❖ Ali, S.S., and Al-Manmi, D.A.M. (2005). Geological and Hydrochemical Study of Zalim Spring, Shahrazoor, Sulamania, Iraq, Iraqi Journal of Earth Science, Vol.5, No.1 P.15-28.

❖ Al-Jaf, A. O. (2008). Error Measurement in Digital Elevation Models In Pinjaween- Halabja Area (3rd Congress of College of Science), Baghdad University, 9 p.

❖ Al-Jaf, A. O. and Al-Azawy, M. A., (2010). Integration of Remote Sensing Images and GIS Techniques on Locate the Mineral Showings in Halabja Area, NE Iraq, Iraqi Bulletin of Geology And Mining, Vol.6, No.1,p 31-46.

❖ Al-Kubaisi, Q. Y., (2004): Annual Aridity Index of Type.1 and Type 2 Mode Options For Climate Classification. Iraqi Journal of Science Vol. 45 C, No.1. Pp. 32-41.

❖ Allen R. G., Pereira L. S., Raes D, And Smith M. M., (1998): Crop Evapotranspiration - Guidelines for Computing Crop Water Requirements - FAO Irrigation and Drainage Paper No. 56, 307p.

❖ Allen R. G., Pereira L. S., Raes D, and Smith M., (2006): Crop Evapotranspiration , Guidelines for Computing Crop Water Requirements - FAO Irrigation And Drainage Paper No. 56, P.23.

❖ Aller L., Bennett T., Lehr JH., Petty RH, And Hackett G. (1987). DRASTIC: A Standardized System for Evaluating Groundwater Pollution Potential Using Hydrogeologic Setting. USEPA Report 600/2-87/035, Robert S. Kerr Environmental Research Laboratory, Ada, Oklahoma74820, 252 P.

❖ Aller, L., Bennett, T., Lehr, J.H. and Petty, R.J. (1985). DRASTIC: A Standardized System or Evaluation Groundwater Pollution Potential Psing Pydrogeologic Pettings. U.S. EPA, Roberts. Kerr Environmental Research Laboratory, Ada, Oklahoma,EPA/600/2-85/0/08.

❖ Al–Manharawi, S. And Hafiz, A., (1997): Fresh Water, Resources and Quality Arabic Press Cairo, 181 p (In Arabic).

❖ Al-Manmi D. A. M., (2002): Chemical And Environmental Study of Groundwater In Sulaimanyia City and its Outskirts unpublished Msc. Thesis, University Of Baghdad (In Arabic), 200 p.

❖ Al-Manmi, D. A. M., (2008). Water Resources Management of Rania Area, Sulaimani, NE of Iraq, Unpublished PhD. Thesis, University of Baghdad, 226 P.

❖ Al-Mashhadani, A.S., Azeez, D.R., Qadir, M.H., (2009). Study of Landcover/Landuse in Sharazur Plain by Using Remote Sensing Techniques, Mesopotamia Journal of Agriculture. Volume 37, No.1. P.1-10.

❖ Al-Rawabdeh A. M., Al-Ansari N. A., Al-Taani A. A., Al-Khateeb F. L., Knutsson S..(2014). Modeling the Risk of Groundwater Contamination Using Modified DRASTIC and GIS in Amman-Zerqa Basin, Jordan. Cent. Eur. J. Eng. 4(3). 2014, 264-280 DOI: 10.2478/ S13531-013-0163-0.

❖ Al-Rawabdeh A. M., Nadhir A. Al-Ansari, Ahmed A. Al-Taani, and Sven Knutsson.(2013). A GIS-Based DRASTIC Model for Assessing Aquifer Vulnerability in Amman-Zerqa Groundwater Basin, Jordan. J. Enginerring. V.5,490-504.

❖ Al-Tamimi, O. S. (2007). Water Resources Evaluation in Diyala River Basin-Middle Part, Unpublished PhD. Thesis, University of Baghdad, College of Science. Baghdad. 190 P. (In Arabic).

❖ Al-Taweel M., Marsh A., Mühl S., Nieuwenhuyse O., Radner K., Rasheed K .And Saber A. S., (2011). New Investigations in the Environment, History, and Archaeology of The Iraqi Hilly Flanks, Shahrizor Survey Project.

❖ Altoviski M. E., (1962): Hand Book of Hydrogeology. Gosgeolitzdat, Moscow, USSR (in Russian), 614p.

❖ Anderson, James R., Et Al. (1976). A Land Use and Land Cover Classification System for use with remote sensor data: geological survey

professional Paper 964. Edited By NJDEP, OIRM, BGIA, 1998, 2000, 2001, 2002, 2005.

❖ APHA, (1998): Standard Methods of the Examination of Water and Wastewater. Washington D.C., American Public Health Association, 759p.

❖ APHA, (2005): Standard Methods of the Examination of Water and Wastewater. Washington D.C., American Public Health Association.

❖ Appelo, C.A.J. And Postma, D., (1999): Geochemistry. Groundwater and Pollution. Rotterdam: A. A. Balkama, 536 p.

❖ Ayres, R.S. and Westcot D.W. (1999). Water Quality for Agriculture, Irrigation and Drainage Paper No. 29, Food and Agriculture Organization of the United Nations. Rome, 1-117.

❖ Babiker, I.S., Mohamed A.A., Tetsuya Hiyama and Kikuo Kato, (2005). A GIS-Based DRASTIC Model for Assessing Aquifer Vulnerability in Kakamigahara Heights, Gifu Prefecture, Central Japan. Science of the Total Environment, 345 (1–3), 127–140.

❖ Barbash, J.E., and Resek, E.A. (1996) Pesticides in Ground Water: Distribution, Trends, and Governing Factors. Chelsea, MI7 Ann Arbor Press, 215 p.

❖ Bartram, J. and Balance, R., (1996): Water Quality Monitoring. A Practical Guide to the Design and Implementation of Fresh Water Quality Studies and Monitoring Programs UNEP/WHO. Chapman and Hall, 383 P.

❖ Barzinji, K. T. (2003). Hydrologic Studies For Goizha - Dabashan and Other Watersheds in Sulaimani Governorate, Unpublished M.Sc. Thesis, College of Agriculture, University of Sulaimani, 224 P.

❖ Baziany M.M.Q. (2006). Stratigraphy and Sedimentology of Former Qulqula Conglomerate Formation, Kurdistan Region, NE- Iraq. Unpublished M.Sc Thesis, Sulaimani University, 98p.

❖ Baziany M.M.Q. and Karim K. H. (2007). A New Concept for the Origin of Accumulated Conglomerates, Previously Known as Qulqula Conglomerate Formation at Avroman- Halabja Area, NE-Iraq., Iraqi Bulletin of Geology and Mining, 3(2), 33-41.

❖ Behmanesh, O., (2003): The Aspects of Water Balance in The Irrigated Area (Southwest Part of Urumieh Lake), M.Sc. Thesis, International Institute for Geo-Information Science and Earth Observation, Netherlands, 75p.

❖ Bellen R.C., Dunnington H.V., Wetzel R., and Morton D. (1959). Lexique Stratigraphique International. Asie, Iraq. Vol. 3C, 10a, 333p.

❖ Berding F. (2003). Agro-Ecological Zoning of the Three Northern Governorates of Iraq, FAO Agricultural Rehabilitation Programme. Plant Production SS, Erbil, Iraq.

❖ Bernardo, S. (1995). Manual De Irrigação, 4th Edition, Vicosa: UFV, 488p.

❖ Bety A.K.S. (2013). Urban Geomorphology of Sulaimani City, Using Remote Sensing and GIS Techniques, Kurdistan Region, Iraq. Unpublished PhD Thesis, Faculty of Science and Science Education, University of Sulaimani, 125 P.

❖ Blavoux, B., Lachassagne, P., Henriot, A., Ladouche, B., Marc, V., Beley, J. and Olive, P. (2013). A Fifty-Year Chronicle of Tritium Data for Characterising the Functioning of the Evian and Thonon (France) Glacial Aquifers. Journal of Hydrology, 494, 116–133. Http://Dx.Doi.Org/10.1016/J.

❖ Bolton, C.M.G. (1958).The Geology of Ranya Area. Site Inv Co. Upubl. Rept., Vol IX B, SOM Library, Baghdad. 117 p.

❖ Boyd, C.E., (2000): Water Quality an Introduction. Kluwer Acad. Publisher, USA, 330p.

❖ Britt, J.K., Dwinell, S.E., and Mcdowell, T.C. (1992) Matrix Decision Procedure to Assess New Pesticides Based on Relative Groundwater

Leaching Potential and Chronic Toxicity. Environmental Toxicology and Chemistry, 11: 721–728.

❖ Bruy`Ere S, Jeannin PY, Dassargues A, Goldscheider N, Popescu C, Sauter M, Vadillo I and Zwahlen F (2001) Evaluation and Validation of Vulnerability Concepts Using a Physically Based Approach. 7th Conference on Limestone Hydrology and Fissured Media,

❖ Buday T.(1980). Regional Geology of Iraq: Vol. 1, Stratigraphy, I.I. Kassab and S.Z. Jassim (Eds) D. G. Geo Survey. Min. Invest. Publication. 445p.

❖ Buday T., and Jassim S.(1987) The Regional Geology of Iraq: Tectonis, Magmatism, and Metamorphism. I.I. Kassab And M.J. Abbas (Eds), Baghdad, 445 P.

❖ Bukowski P., Bromek T. and Augustyniak I. (2006) Using the DRASTIC System to Assess the Vulnerability of Ground Water to Pollution in Mined Areas of tThe Upper Silesian Coal Basin. Mine Water Environ 25:15–22.

❖ Chadha DK, (1999). A Proposed New Diagram for Geochemical Classification of Natural Waters and Interpretation of Chemical Data, Hydrogeology Journal, 1999; 7:431–439.

❖ Chang C, Wu C, Lin C and Et Al. (2007). Evaluating Digital Video Recorder Systems Using Analytic Hierarchy and Analytic Network Processes. Information Sciences 177: 3383–3396.

❖ Chattopadhyay, N. and Hulme, M. (1997). Evaporation and Potential Evapotranspiration in India Under Conditions of Recent and Future Climate Change, Agriculture and Fores Meteorology 87, 55–73.

❖ Chaudhary, B. S., Kumar, M., Roy, A. K., and Ruhal, D. S. (1996). Applications of RS and GIS in Groundwater Investigations in Sohna Block, Gurgaon District, Haryana, India. International Archives of Photogrammetry and Remote Sensing, 31(B-6), 18–23.

❖ Chowdary, V.M., Rao N.H. and Sarma, P.B.S..(2005) Decision Support Framework for Assessment of Non-Point-Source Pollution of Groundwater in Large Irrigation Projects. Agricultural Water Management, 75: 194–225.

❖ Cihlar, J. R. E. Kennedy, P. A. Townsend, J. E. Gross, W. Cohen, P. Bolsrad, and Wang T. (2001). Remote Sensing Change Detection Tools for Natural Resource Managers: Understanding Concepts and Tradeoffs in The Design of Landscape Monitoring Projects, Remote Sensing of Environment, Vol. 113 (7), 2009, p. 1382-1396.

❖ Collins A.G., (1975): Geochemistry of Oil Field Water, Development in Petroleum Science, No.1, Elsevier, Amsterdam, Holland, 496 P.

❖ Corwin, D.L., Vaughan, P.J. and Loague, K. (1997) Modeling Nonpoint Source Pollutants in the Vadose Zone With GIS. Environmental Science and Technology, 31(8):2157–2175.

❖ Crowe, A.S. and Booty, W.G. (1995) Multi-Level Assessment Methodology for Determining The Potential for Groundwater Contamination by Pesticides. Environmental Monitoring and Assessment, 32:239–26.

❖ Daly, D., Dassargues, A., Drew, D., Dunne, S., Goldscheider, N., Neale, S., Popescu, C. and Zwhalen, F. (2002). Main Concepts of The European Approach for (Karst) Groundwater Vulnerability Assessment and Mapping. Hydrogeology Journal , 10, 340-345. Http://Dx.Doi.Org/10.1007/S10040-001-0185-1.

❖ Davies, G. (2002).Results of Ground-Water Tracing Experiments in The Nelson Woosterhumphreytunnel; Cambrian Ground Water Co.: Oak Ridge, TN, USA, P. 14.

❖ Detay, M., (1997). Water Wells–Implementation, Maintenance and Restoration. John Wiley and Sons, London, 379 p.

❖ Dixon B. (2005) Groundwater Vulnerability Mapping: a GIS and Fuzzy Rule Based Integrated Tool. Applied Geography ,25:327–347.

❖ Doerfliger, N. and Zwahlen, F. (1998) Groundwater Vulnerability Mapping in Karstic Re- Gions (EPIK)—Application to Groundwater Protection Zones. Swiss Agency for the Envi- Ronment, Forests and Landscape (SAEFL), Bern.

❖ Domenico, P. A., and Schwartz, F. W. (1990). Physical and Chemical Hydrogeology (Pp. 410–420). New York: Wiley.

❖ Drever, J.I., (1997): The Geochemistry of Natural Water, Surface and Groundwater Environments, 3rd ed., Prentice Hall, USA, 436 P.

❖ Ducci D.,(2010). Aquifer Vulnerability Assessment Methods: The Non-Independence of Parameters Problem. J. Water Resource and Protection, 2010, 2, 298-308 Doi:10.4236/Jwarp.2010.24034 Published Online April 2010 (Http://Www.Scirp.Org/Journal/Jwarp/).

❖ Durov SA., (1948). Natural Waters and Graphic Representation of Their Compositions. Dokl Akad Nauk SSSR, 1948; 59 :87–90.

❖ Dybas, C., (2003). Common Water Measurements. USGS Water Resources,Vol.70 No. 3.P 306–1070
Estimation of Halabja Area, NE of Iraq Un-Published Msc. Thesis, University of Sulaimani (In English).

❖ European Standards (EU), (2004). EU's Drinking-Water Standards. Http://Www.Lenntech.Com.

❖ Fabbri, A.G, and Napolitano, P (1995). The use of Database Management and Geographical Information Systems for Aquifer Vulnerability Analysis. Contribution to the International Scientific Conference on the Occasion of the 50th Anniversary of The Founding of the Vysoka Skola Banska, Ostrava, Czech Republic.

❖ FAO Representation in Iraq (2001).Reconnaissance Soil Map of the Three Northern. Governorates, Iraq. Map Scale =1:1000,000. Erbil Sub-Office.

❖ Faure, G., (1998): Principles and Application of Geochemistry (2nd Edition). Prentice Hall Inc., USA, 600p.

❖ Faust S.D., and Aly O.M., (1981). Chemistry of Natural Waters. ANN ARBOR Sciences.Van Nortrand Reinhold, London. 1312p

❖ Fuest, S., Berlekamp, J., Klein, M., and Matthies, M. (1998) Risk Hazard Mapping of Groundwater Contamination using Long-Term Monitoring Data of Shallow Drinking Water Wells. Journal of Hazardous Materials, 61:197–202.

❖ Garrett, P., Williams, J.S., Rossoll, C.F. and Tolman, A.L. (1989). A Reground Water Vulnerability Classification Systems Viable? in: Proceedings of FOCUS Conference on Eastern Regional Ground Water Issues. National Water Well Association. Pp. 329–343.

❖ Gill, R., (1997). Modern Analytical Geochemistry, an Introduction to Quantitative Chemical Analysis for Earth, Environmental and Materials Scientists. Longman, London, 329 p.

❖ Goldscheider, N. and Popescu, C. (2004). The European Approach. in: Zwahlen, F., Ed., Vulnerability and Risk Mapping for the Protection of Carbonate (Karst) Aquifers , Euro- Pean Commission, Brussels, 17-21.

❖ Goldscheider, N., Klute, M., Sturm, S. and Hotzl, H. (2000). The PI Method A GIS—Based Approach to Mapping Groundwater Vulnerability With Special Consideration of Karst Aquifers. Zeitschrift For. Angewandte Geologie , 46, 157-166.

❖ Goyal, S. K., Chaudhary, B. S., Singh O., Sethi, G. K., and Thakur, P. K. (2010) GIS Based Spatial Distribution Mapping and Suitability Evaluation of Groundwater Quality for Domestic and Agricultural Purpose in Kaithal Distirct, Haryana State, India. Environmental Earth Sci- Ence. in Press, Doi:101007/S12665-010-0472-Z.

❖ Groundwater Directorate in Sulaimaniyah, (2014).Archive Department.

❖ Gupta N., (2014). Groundwater Vulnerability Assessment Using DRASTIC Method in Jabalpur District of Madhya Pradesh. International Journal of Recent Technology and Engineerung, (IJRTE).ISSN:2277—3878, Volume-3, Issue-3, July 2014.

❖ Hamamin D. F. and Ali S. S.(2013). Hydrodynamic study of karstic and intergranular aquifers using isotope geochemistry in Basara basin, Sulaimani, North-Eastern Iraq. Arab J Geosci (2013) 6: 2933 http://sci-hub.cc/10.1007/s12517-012-0572-z.

❖ Hamamin D. F. Qadir R.A , Ali S.S. and Bosch A.P.(2018). Hazard and Risk Intensity Maps for Water-Bearing Units: A Case Study. Published in International Journal of Environmental Science and Technology, Volume 15, Issue 1, Pp 173–184.

❖ Hamamin D. F. (2016). Groundwater Vulnerability Map of Sulaymaniyah Sub-Basin Using SINTACS Model, Sulaymaniyah Governorate, Kurdistan Region, Iraq. Journal of Zankoy Sulaimani, JZS (2016) Special Issue, Geokurdistan II (277-292).

❖ Hamamin D.F. (2011). Hydrogeological Assessment and Groundwater Vulnerability Map of Basara Basin, Sulaimani Governorate, Iraq, Kurdistan Region. Unpublished PhD Thesis, College of Science, University of Sulaimani. 174P.

❖ Hasan M.A., Ahmed K.M., and Sracek O., (2007). Arsenic In Shallow Groundwater of Bangladesh: Investigations from three different Physiographic Setting. Hydrogeology Journal Vol.15;Pp.1507-1522.

❖ Hassan I.O., (1998). Urban Hydrology of Erbil City Region. PhD Thesis, University of Salahaddin. Erbil, Iraq, 120 p.

❖ Hawkins, R. H., (2004). National Engineering Handbook, United States Department of Agriculture Natural Resources Conservation Service, 791 P.

❖ Hem, J.D. (1991). Study and Interpretation of the Chemical Characteristics of Natural Water. USGS Water Supp. Paper No. 2254, 263 p.

❖ Hill RA(1940). Geochemical Patterns in the Coachella Valley, California. Trans And Geophys Union 1940; 21: 46–49.

❖ Holanda, J. S. and Amorim, J. A. (1997). Management and Control Salinity and Irrigated Agriculture Water in: Congresso Brasileiro de Engenharia Setting, 26, Campina Grande, Pp.137-169.

❖ Horton, R. E., (1945): An Approach toward a Physical Interpretation of Infiltration Capacity. J. Soil Sci. Amer., 5, 399–417.

❖ Huang T, Pang Z, Edmunds W. (2012). Soil Profile Evolution Following Land-Use Change: Implications for Groundwater Quantity and Quality. Hydrol. Process 27(8):1238-1252.

❖ Hussain H.M.,Al-Haidarey M.J.S.M., Al-Ansari N. and Knutsson S. (2014). Evaluation and Mapping Groundwater Suitability for Irrigation Using GIS in Najaf Governorate, IRAQ. Journal of Environmental Hydrology .Volume 22(4):1238-1252.

❖ Hussain M.H., (2004). Assessment of Groundwater Vulnerability in Alluvial Interfluves Using GIS. Unpublished Phd Thesis, Department oF Hydrogeology Indian Institute of Technology, Roorkee-247 667 (INDIA) .

❖ Ibe KM and Nwankwor GI (2001) Assessment of Groundwater Vulner-Ability and its Application to the Development of Protection Strategy for the Water-Supply Aquifer in Owerri, Southeastern Nigeria. Environ Monit Assess 67:323–360.

❖ IQS (1996). Iraqi Standards for Drinking Water. Draft of Improving Standards No. 417 /1996. (in Arabic).

❖ Isalou A, Zamani V and Shahmoradi B. (2013). Landfill Site Selection Using Integrated Fuzzy Logic and Analytic Network Process (F-ANP). Environmental Earth Sciences 68: 1745–1755.

❖ Jassim S.Z. and Goff J.C. (2006) Geology of Iraq. Jassim (Eds) D. G. Geo Survey. Min. Invest. Publication. 340p.

❖ Javadi S.,Kavehkar N., Mohammadi K.,Khodadi A. and Kahawita K. (2011).Calibration DRASTIC Using Field Measurement, Sensitivity

Analysis and Statistical Method to Assess Groundwater Vulnerability. Water International , 36(6),p 719-32.

❖ Jwan Al-Doski, Shattri B. Mansor And Helmi Zulhaidi Mohd Shafri. (2013). Monitoring Land Cover Changes In Halabja City, Iraq. International Journal of Sensor and Related Networks (IJSRN) Volume 1,Issue1 , February 2013.

❖ Karim K.H and Ali S.S.(2005) Origin of Dislocated Limestone Blocks on the Slope Side of Baranan (Zirgoez) Homocline: An Attempt to Outlook the Development of Western Part of Sharazoor Plain. Kurdistan Academicians Journal (KAJ), 4(1) Part A.

❖ Karim K.H. (2006). Stratigraphy and Lithology of the Avroman Formation (Triassic), North East Iraq, Iraqi Journal of Earth Sciences, Vol.7, No.1, P.1-12.

❖ Karim K.H., Fatagh A. I., Ibrahim A. O. and Koyi H., (2009). Historical Development of the Present Day Lineaments of The Western Zagros Fold-Thrust Belt: A Case Study from Northeastern Iraq, Kurdistan Region. Iraqi Journal Of Earth Sciences, Vol.9, No.1, P.55-70.

❖ Kim, Y. J. And Hamm, S., (1999). Assessment of the Potential for Groundwater Contamination Using the DRASTIC/EGIS Technique, Cheongju Area, South Korea. Hydrogeology Journal, 7(2), 227-235.

❖ Koterba, M.T., Banks, W.S.L. and Shedlock, R.J. (1993) Pesticides in Shallow Groundwater in the Delmarva Peninsula. Journal of Environmental Quality, 22:500–518.

❖ Kourosh M., Ramin N. and Vahid J.M., (2008). Aquifer Vulnerability Assessment Using GIS and Fuzzy System: A Case Study of Tehran–Karaj Aquifer, Iran. Environ Geol. Doi: 10.1007/S00254- 008-1514-7.

❖ Kumar, P. R. and Somashekar, R. K. (2011). Environmental Tritium and Hydrochemical Investigations to Evaluate Groundwater in Varahi and Markandeya River Basins, Karnataka, India. Journal of Environmental Radioactivity, 102, 153–162.

❖ Langmuir, D., (1997): Aqueous Environmental Geochemistry .Prentice Hall, USA, 600 P.

❖ Lattman H. and Parizek R. (1964). Relationship between Fracture Traces and the Occurrence of Ground Water in Carbonate Rocks. Journal Hydrology, 2, 73-91.

❖ Lee S. (2003). Evaluation of Waste Disposal Site Using the DRASTIC System In Southern Korea. Environmental Geology 44: 654-664.

❖ Lowe, M., and Butler, M. (2003) Ground Water Sensitivity and Vulnerability to Pesticides, Heber and Round Valleys, Wasatch County, Utah. Miscellaneous Publication 03-5, Utah Geological Survey, 23 p.

❖ Maas, R.P., Kucken, D.J., Patch, S.C., Peek, B.T. and Vanengelen, D.L. (1995). Pesticides in Eastern North Carolinarural Supply Wells: Land-Use Factors and Persistence. Journal of Environmental Quality, 24:426–431.

❖ Mas J. F. (1999). Monitoring Land-Cover Changes: A Comparison of Change Detection Techniques, Int. J. Remote Sens., Vol. 20, Pp. 139-152, 1999.

❖ Mathhess, G. (1982). The Properties of Ground Water (1st Ed.). New York: Wiley.

❖ Maxe, L. and Johansson, P.O. (1998). Assessing Groundwater Vulnerability Using Travel Time and Specific Surface Area as Indicators. Hydrogeology Journal, 6:441–449.

❖ Maxe, L. and Johansson, P.O. (1998). Assessing groundwater vulnerability using travel time and specific surface area as indicators. Hydrogeology Journal, 6:441–449.

❖ Maxwell, J.A, (1968): Rock and Mineral Analysis. John Wiley and Sons, Newyork, 584 p.

❖ Mccallister, J. (2015). Pearson Correlation Coefficient: Formula Example and Significance. Available at: Http://Study.Com/Academy/ Lesson/Pearson-Correlation-Coefficient-Formula-Example Significance.

- Mckenzie Jeffrey M., Mark Bryan G., Thompson Lonnie G., Schotterer Ulrich and Lin Ping-Nan. (2010). A hydrogeochemical survey of Kilimanjaro (Tanzania): implications for water sources and ages. Hydrogeology Journal (2010) 18: 985–995.

- Mehta V. K., Walter, M. T. and Degloria, D. S. (2006). A Simple Water Balance Model. Cornell University, Technical Report No.5, 9p.

- Meireles, A., Andrade E. M., Chaves L., Frischkorn, H., and Crisostomo, L. A. (2010). A New Proposal of the Classification of Irrigation Water, Revista Ciência Agronômica, 413: 349-357.

- Merchant G. (1994). GIS-Based Groundwater Pollution Hazard Assessment: A Critical Review of the DRASTC Model, Photogramm Eng. Remote Sensing 60, 1994, 1117-1127.

- Merkin B. G., (1979). Group Choice. John Wiley & Sons, NY.

- Meyer W.B. and Turner B.L., (1992).Global Land Use/Land-Cover Change. Boulder: OIES, p 91-95.

- Montgomery C.W.(1997).Environmental Geology.5th Ed., Mcgraw-Hill, 546 p.

- Moore, J. E. (2002). Field of Hydrogeology. Printed in The United States of America.195 P.

- Mtoni, Y., Mjemah, I.C., Bakundukize, C., Van Camp M., Martens K., and Walraevens K. (2013). Saltwater Intrusion and Nitrate Pollution in the Coastal Aquifer of Dares Salaam, Tanzania. Environ. Earth Sci. 2013, 70, 1091–1111.

- Muhammed, D. A. (2008). Drinking Water Quality Assessment of Halabja/ Sulaimani- Kurdistan Region of Iraq, Unpublished M.Sc. Thesis, College of Agriculture, University of Sulaimani, 158 P.

- National Research Council (NRC) (1993). Ground Water Vulnerability Assessment, Contamination Potential under Conditions of Uncertainty, National Academy Press (Washington, D.C.-USA).

❖ Navulur, K.C.S., and Engel, B.A. (1998). Groundwater vulnerability assessment to non-point source nitrate pollution on a regional scale using GIS. Trans. ASAE 41: 1671–1678.

❖ Neha Gupta, (2014). Groundwater Vulnerability Assessment using DRASTIC Method in Jabalpur District of Madhya Pradesh. International Journal of Recent Technology and Engineering (IJRTE) ISSN: 2277-3878,Volume-3 Issue-3.

❖ Neshat A.,Pradhan B. and Dadras M.(2014).Groundwater Vulnerability Assessment Using an Improved DRASTIC Model in GIS. Resources Conservation and Recycling 86: P74-86.

❖ Neshat A.,Pradhan B., Pirasteh S. and Shafri H.(2013). Estimating Groundwater Vulnerability to Pollution Using a Modified DRASTIC Model in the Kerman Agricultural Area ,Iran. Environmental Earth Science: P1-13.

❖ Nikolov, S. P., (1983). Rainfall Erosion in Northern Iraq. An Aid to Soil Conservation. Ministry of Agriculture and Agrarian Reform. Baghdad, Iraq.

❖ Nobre R.C.M. Rotunno F.O.C. Mansur, W.J Nobre M. and Cosenza, C.A.N (2007). Groundwater Vulnerability and Risk Mapping Using GIS, Modeling and a Fuzzy Logic Tool. Journal of Contaminant Hydrology, 94:277–292.

❖ Palmer, R.C. and Lewis, M.A. (1998). Assessment of Groundwater Vulnerability in England and Wales, in: Robins, N.S. (Ed.), Groundwater Pollution, Aquifer Recharge and Vulnerability Geological Society, London, Special Publications. 130: 191–198.

❖ Panagopoulos G., Antonakos A. and Lambrakis N., (2006). Optimization of the DRASTIC Method for Groundwater Vulnerability Assessment via the Use of Simple Statistical Methods and GIS. Hydrogeology Journal 14:894-911.

❖ Parson, R.M. (1957) .Groundwater Resources of Iraq, Vol. XII: Sulaimania Liwa and Area North Of Khanaquin. R.M. Parson Co., Ministry of Development, Development Board, Iraq, 93 P.

❖ Parson, R.M. (2006). Mini Master Plan for the Public Water Supplies for the Governorate of Sulaimani, Iraq, Public Works- Water Sector. Projects and Contracting Office- United States Missions to Iraq. Iraq- Baghdad, 122 P.

❖ PCI Geomatica, (2001). PCI Geomatica User's Guide Version 9.1. Ontario. Canada: Richmond Hill, 126 p.

❖ Perrin J, Pochon A, Jeannin PY. and Zwahlen F., (2004). Vulnerability Assessment in Karstic Areas: Validation by Field Experiments. Environ Geol 46,237–245.

❖ Pierce J.J, Weiner R.F. and Vesilind P.A. (1998): Environmental Pollution and Control (4th Ed.). Butterworth–Heinermann, USA, 392p.

❖ Polservice (1980). Sharazor Irrigation Project. Feasibility Report, Annex I, Climate and Water Resources, Ministry of Irrigation, Baghdad, P.76.

❖ Rao , N. S. (2006): Seasonal Variation of Groundwater Quality in Apart of Guntur District , Andhra Pradesh India , Environmental Geology Vol. 49 , p .413-429.

❖ Rao, P.S.C., Hornsby, A.C. and Jessup, R.E., (1985). Indices for Ranking the Potential for Pesticde Contamination in Groundwater. Proceedings of Soil Crop Science Society Florida; 1–24.

❖ Rauf L.F., (2014): Groundwater Potential Mapping and Recharge

❖ Rauf M. (2004). Halabjay Shaheed, Sirwan and Said Sadiq Water Supply Project, Feasibility Report Prepared by Water and Environmental Sanitation Planning Team (Group One), P 93.

❖ Raza, S. M., (2009). Sedimentlogy and Geochemistry of the Limestone Successions of the Lower Member of the Qulqula Formation, Kurdistan Region, Ne-Iraq, Unpublished PhD. Thesis, Geology Department, University of Sulaimani. 161 P.

❖ Roy, T.N. (2000). Impact of Sewage Irrigation on Groundwater Regime of Roorkee. M.E. Dissertation, Department of Hydrology, IIT Roorkee, Roorkee, India.

❖ Rupert M.G.(1999). Improvement to the DRASTIC Groundwater Vulnerability Mapping Method, in: USGS. Denver: FS 066-99.

❖ Saaty T. L. (1980). The Analytic Hierarchy Process. Mcgraw Hill, New York.

❖ Saaty T. L. (1986). Axiomatic Foundation of the Analytic Hierarchy Process. Management Science, Vol. 32, Pp. 841-855, 1986.

❖ Saaty T. L. (1994). How to make a Decision: The Analytic Hierarchy Process. Interfaces, Vol. 24, Pp. 19-43, 1994.

❖ Saeed M.A. and Abas K.A (2008). Analysis of Climated and Drought Conditions in the Fedral Region of Kurdistan. International Scientific Journal Environmental Science Http://Environment.Scientific-Journal.Com.

❖ Saether, O.M. and Caritat, P.D., (1997). Geochemical Processes Weathering and Groundwater Recharge in Catchments. A.A. Balkama, Rotterdam, Brookfield, Holland, 400 P.

❖ Saprof Team (Special Assistance for Project Formation), (2008). Water Supply Improvement Project in Kurdistan Region, Republic of Iraq. (Jbic) Nihon Suido Consultants Co., Ltd. 35 P.

❖ Secunda S., Collin M. and Melloul A. J. (1998). Groundwater Vulnerability Assessment Using a Composite Model Combining DRASTIC with Extensive Land Use in Israel's Sharon Region, Journal of Environmental Management 54(1), 1998, 39-57.

❖ Sharbazheri, K. M. I. (2008). Biostratigraphy and Paleoecology of Cretaceous/Tertiary Boundary in the Sulaimani Region, Kurdistan, NE Iraq, Ph.D. Thesis, University of Sulaimani. 219 P.

❖ Shukla, S., Mostaghimi, S., Shanholt, V.O., Collins, M.C. and Ross, B.B. (2000). A County-Level Assessment of Ground Water Contamination by Pesticides. Ground Water Monitoring and Remediation, 20: 104–119.

❖ Shuval H.I., Yekutiel P. and Fattal B. (1985). Epidemiological Evidence for Helminthes and Cholera Transmission by Vegetables Irrigated with Wastewater. Jerusalem - Case Study. Water Science and Technology 17(4/5):433-442.

❖ Statistical Directorate in Sulaimaniyah,(2014).Archive Department.

❖ Stevanovic Z. and Markovic M. (2004). Hydrogeology of Northern Iraq, Climate, Hydrology, Geomorphology and Geology.,Vol.1, 2nd Edition, FAO.

❖ Stevanovic, Z, and Markovic, M., (2003). Hydrogeology of Northern Iraq, Climate, Hydrology, Geomorphology & Geology., Vol.1, 2nd edition, FAO.

❖ Stewart I.T. and Keith L. (2004). Assessing Ground Water Vulnerability with the Type Transfer Function Model in the San Joaquin Valley, California. Journal of Environmental Quality, 33: 1487–1498.

❖ Stoodly, K.D., Lewis, T. and Staintion, C.L., 1980. Applied Statistical Technique. John Wiley and Sons, London. 215 P.

❖ Swennenhuis, J. (2009). CROPWAT Version 8.0. Water Resources Development and Management Service, FAO, Rome.

❖ Tesconi, T. (2000) Water Quality Control, Part III. Human Impact on Water Resources. The Press Democrat. P. 182.

❖ Thornthwaite, C. W, and Mather J. R., (1957). Instructions and Tables for Computing Potential Evapotranspiration and the Water Balance. 3, New Jersey.

❖ Thornthwaite, C. W. and Mather, J. R. (1955). The Water Balance, Publication In Climatology, 8: DTT, Laboratory of Climatology, Publication No. 10, Cenetron, New Jersey, USA. P. 1-86.

❖ Todd, D.K. (2005): Groundwater Hydrology (3rd Edition) .John Wiley and Sons, New York, USA, 650 P.

❖ Todd, D.K., (1980). Groundwater Hydrology (2nd Edition) John Wiley and Sons, New York, USA, 535 P.

❖ UN, ILO and WHO (United Nations, International Labour Organisation and World Health Organization), (1983). Environmental Health Criteria for Selected Radionuclides. Environmental Health Criteria 25. ISBN 92 4 154085 0.

❖ USDA NRCS, (2004): National Engineering Handbook, Part 630 Hydrology, Chapters 9, 20p, and Chapter 10, 79p.

❖ USEPA, (1993). A Review of Methods for Assessing Aquifer Sensitivity and Ground Water Vulnerability to Pesticide Contamination. USEPA, Office of Water, Washington, DC, 147 p.

❖ Uyan M. (2014). MSW Landfill Site Selection by Combining AHP with GIS for Konya, Turkey. Environmental Earth Sciences 71: 1629–1639.

❖ Vias, J.M., Andreo, B., Perles, M.J., Carrasco, I., Vadillo, P. and Jimenez, P., (2006). Proposed Method for Groundwater Vulnerability Mapping in Carbonate (Karstic) Aquifers: The COP Method. Application in Two Pilot Sites in Southern Spain. Hydrogeology Journal , 14, 912-925. Http://Dx.Doi.Org/10.1007/S10040-006-0023-6.

❖ Wang Y., Merkel B. J., Li Y., Ye H., Fu S. and Ihm D., (2007). Vulnerability of Groundwater in Quaternary Aquifers to Orginaic Contamination: A Case Study on Wuhan City, China, Environmental Geology, Vol. 53, No. 3, 2007, Pp. 479-484. Doi:10.1007/S00254-007-0669-Y.

❖ WHO (World Health Organization), (2001). Water Health and Human Rights, World Water Day Http://Www.Worldwaterday.Org/ Wwday / 2001/Thematic/Hmnrights.Html.

❖ WHO (World Health Organization), (2006). Guidelines for Drinking–Water Quality .3rd Ed., Vol.1, Recommendations, Geneva, 515 P.

❖ WHO (World Health Organization), (2008). Guidelines for Drinking-Water Quality. 3rd Edition, Vol.1, Recommendations, Geneva, 668 P.

❖ WHO (World Health Organization), (2011). Guidelines for Drinking-Water Quality - 4th Edition, Recommendations, Geneva, 564 P.

❖ Wiesner, C. J., (1970). Climate, Irrigation and Agriculture, Angus and Robertson, Sydney, 1970.

❖ Wilcoxon F., (1945).Individual Comparison by Ranking Method, Biometrics Bulletin 1, 6, 80-83.

❖ William E. Motzer, (2000). Age Dating Groundwater. Report by Todd Engineers, Bmotzer@Toddengineers.

❖ Worrall, F. and Kolpin D.W., (2004). Aquifer Vulnerability To Pesticide Pollution—Combining Soil, Land-Use and Aquifer Properties with Molecular Descriptors. Journal of Hydrology, 293: 191–204.

❖ Worrall, F. and Tim, B., (2005). The Vulnerability of Groundwater to Pesticide Contamination Estimated Directly from Observations of Presence or Absence in Wells. Journal of Hydrology, 303 : 92–107.

❖ Yakirevich, A., Weisbrod, N., Kuznetsov, M., Rivera Villarreyes, C.A., Benavent, I., Chavez, A.M. and Ferrando, D., (2013). Modeling the Impact of Solute Recycling on Groundwater Salinization Under Irrigated Lands: A Study of the Alto Piura Aquifer, Peru. J. Hydrol. 2013, 482, 25–39.

❖ Zakaria Saleh, , Yaseen T. Mustafa , Diary A. Mohammed , Salahalddin Saeed Ali , Nadhir Al-Ansari and Sven Knutsson,(2013). Estimation of Annual Harvested Runoff at Sulaymaniyah Governorate, Kurdistan Region of Iraq. Vol.5, No.12, 1272-1283 (2013) Published by Natural Science. Http://Dx.Doi.Org/10.4236/Ns.2013.512155.

❖ Zektser, I., Sergey.S., Pozdniakov. P., Michael, S. and Liliya, M.R., (2004). Regional Assessment of Groundwater Vulnerability in the Snake River Plain Aquifer Basin, USA. Geofísica International, 43(4), 697-705.

❖ Zhou J., Li Q. ,Guo Y. , Guo X. , Li X., Zhoa Y. and Jia R., (2012). VLDA Model and its Application in Assessing Phreatic Groundwater Vulnerability: A Case Study of Phreatic Groundwater in the Plain Area of Yanji County, Xinjiang, China. Environmental Earth Science Journal Vol.67, p. 1789-1799.

❖ Zhou JL., (2009).Groundwater Vulnerability Assessment Method of Inland Arid Areas. PhD Thesis, Graduate School of the Chinese Academy of Sciences, Beijing, China, 250p.

❖ Zwahlen F., (2004). Vulnerability and Risk Mapping for the Protection of Carbonate (Karst) Aquifers, Final Report (COST Action 620). European Commission, Brussels, 39 p.

خلاصه

يرافق الزيادة السكانية تغيرات في غطاء الارض وبضمنها توسع المناطق السكانية والتي تحتم زيادة في حجم المياه المستخدمة للاغراض المنزلية والشرب. وبما ان المياه السطحية غير متوفرة في هذه المنطقة فلا بد من استخدام المياه الجوفيه وبصورة متزايدة وبصورة عامة تتواجد المياه الجوفية بصورة جيدة في المناطق التي تتكون من الترسبات النهرية او مكاشف الصخور والتي تقع عليها المناطق السكنية. وتتعرض هذه المناطق لتلوث مياهها الجوفية لعدد من الاسباب استناداً الى هذه الحقائق تمت دراسة قابلية تلوث المياه الجوفية في حوض الدراسة.

تقع منطقة الدراسة (حوض حلبجة – سيد صادق) شمال شرق العراق حيث تعتبر احدى كبرى المدن بخزين مياهها الجوفية. هدف الدراسة هو دراسة التأثيرات البيئية ومراقبة قابلية المياه الجوفية للتلوث وكيفية المحافظة على المياه الجوفية من التلوث.

في هذه الدراسة تم استخدام نموذج DRASTIC والذي يعتبر من النماذج المفيدة جداً في دراسة قابلية واحتمالية تلوث المياه الجوفية وتم تعديل هذا النموذج بطرائق مختلفة باساليب مختلفة اضافة الى استخدام طرائق اخرى خاصة COP وVLDA ضمن منطقة الدراسة. ، تم التحقق من صحة النموذج المطبق من خلال مقارنة النتائج التي توصل اليها مقابل اعمار المياه الجوفية وخصائص نوعية المياه الجوفية الملحوظة لموسمين متتالين.

تم جمع العينات ن الملفات الرسمية والعمل الحقلي لدراسة التأثيرات البيئية اضافة الى استخدامها لاعداد خرائط نموذج DRASTIC لرسم خرائط نموذج الضعف في منطقة الدراسة استناداً الى هذا النموذج، تم تصنيف منطقة لدراسة الى اربع مناطق من مؤشرات الضعف وهي:

مناطق ذات مؤشر ضعيف جداً، مؤشر منخفض، مؤشر معتدل، ومؤشر عالي الضعف وتغطي النسب التالية ٣٤٪، ١٣٪، ٤٨٪، ٥٪ على التوالي.

يستند التعديل الاول الى تعديل معدل الوزن على اساس طريقتين وهي تركيز النترات من 39 عينه من المياه الجوفية لتعديل قيمة التنصيف الموصى بها باستخدام اختبار Wilcoxon rank –sum الاحصائي اللا حدودي واختبار الحساسية لتعديل قيم اوزان الترجيح الموصى بها- تم تطبيق معامل ارتباط Pearson لحساب العلاقة بين قيم DRASTIC وقيم النترات. بالنسبة للنموذج المعدل كان معامل الارتباط ٧٢٪ وهو اعلى بكثير مما تم تحقيقه في النموذج القياسي حيث كان ٤٣٪. صنف الموديل المعدل منطقة الدراسة الى خمس فئات (منخفضة جداً ومنخفضة ومعتدلة وعالية وعالية جداً) مع (٧٪، ٣٥٪، ١٩٪، ٣٥٪، ٤٪) على التوالي.

استند التعديل الثاني لنموذج DRASTIC الى استخدام الاراضي وغطاء الاراضي لمنطقة الدراسة. تم تحضير خرائط استخدام الاراضي والغطاء الارضي (LULC) باستخدام برامج ERDAS IMAGINE من مشهدين مختلفين من (TM) Landsat Thematic Mapper وحيث اوضحت الخريطه ان هناك خمس فئات يمكن تحديدها من استخدام الاراضي وهي: الاراضي القاحلة، الاراضي الزراعية و الاراضي النباتية، المناطق الحضرية والاراضي الرطبة او الماء. ولقد صنفت خريطة DRASTIC المعدلة على اساس LULC المنطقة الى خمسة فئات هي: منخفضة جداً(١,١٧٪)، منخفضة (٣٦. ٨٢٪) متوسطة (١٧,٥٧ ٪)، مرتفعة (٤٣. ٤٢٪) وعالية جداً (١. ٠٢ ٪).

الطريقة الثالثة المستخدمة لتعديل نموذج DRASTIC اعتمدت على سمات الظواهر الخطيه (Lineament feature) لمنطقة الدراسة. وتم تحضير خريطه الظواهر الخطيه باستخدام الخرائط الموضعية المحسنة بالاضافة الى الصور الفضائية (+ETM) باستخدام تقنيات مختلفة في الاستشعار عن بعد ونظم المعلومات الجغرافية حيث اوضحت خريطة الكثافة الخطية انه يمكن التعرف على ست فئات فقط من كثافة السطوح تراوحت بين (0−2.4) كما وصنف النموذج المعدل المنطقة الى اربع فئات: منخفضة جداً (٢٨,٧٥٪)، منخفضة (١٤,٣١٪)، متوسطة (٤٦,٩١٪) وعالية (١٠,٠٤٪).

تمثل الجهد الرابع لتعديل نموذج DRASTIC القياسي هو تطبيق العملية الهرمية التحليلية (AHP) بين (٢٢٤,١−٦٥,٨٢) مع خمسة فئات للضعف تضم (منخفضة جداً الى عالية جداً).

تم تطبيق نماذج VLDA و COP على خريطة نظام الضعف في حوض الدراسة حيث بينت نتائج تطبيق نماذج VLDA وجود ٤ نطاقات لمؤشرات الضعف تميزت من منخفض الى مرتفع جداً مع قيم تراوحت ما بين ٩,١٦ الى ٢,١٣٣، بينما كانت النتائج تطبيق نموذج COP وجود اربعة نطاقات لمؤشرات الضعف تميزت من منخفض جداً الى عالي مع قيم تراوحت ما بين ٠,٧٩ الى ٦,٢.

تمت مقارنة جميع النماذج المطبقة في حوض الدراسة مع بعضها البعض وتم التحقق منها ايضاً لتوضح صحة الارتباط للظروف الهيدروجيولوجية الحالية ولبيان دقة نظام الضعف النموذجي، ولتحقيق ذلك استخدمت طريقتين للتحقق من النتيجة، وفي المنهج الاول تم اختيار تحليل تراكيز النترات وتم تحليل فروقاتها لموسمين متتاليين (جاف ورطب) من خلال تحليل ٣٩ عينه مياه من ابار السقي، في النهج الثاني تم تقييم قابلية تأثر المياه الجوفية استناداً الى قيم التريتيوم (H^3) واعمار المياه الجوفية اكدت النتائج التحقق من حساسية التدرج وتوزيع مستويات الضعف المكتسبة باستخدام نموذج DRASTIC المعدل استناداً الى معدل وتعديل الاوزان واستخدام طريقة AHP وتأثير LULC ونموذج (VLDA).

تقييم حساسية المياه الجوفية للتلوث باستخدام ثلاثة نماذج تقييمية مختلفة في حوض حلبجة ــ سيد صادق الجوفي، شمال شرق العراق

رسالة

مقدمة ال مجلس كلية العلوم ــ جامعة السليمانية كجزء من متطلبات نيل شهادة دكتوراه فلسفة في علوم الأرض (هايدروجيولوجى)

من قبل

توانا عمر عبدالله

ماجستير في جيولوجيا الهندسية ـ٢٠٠٩

جامعة بورتسموث، ئينكلاند

بأشراف

د. نظير الانصاري   د. صلاح الدين سعيد علي

بروفيسور   بروفيسور

كولان ، ٢٧١٨   أيار ، ٢٠١٨

پوخته

زیادکردنی ژمارەی دانیشتوان بە شێوەیەکی ئاسایی دەبێتە هۆی گۆڕانکاری لە تایبەتمەندی یەکانی زەوی دا، بە تایبەتی فراوانبوونی ناوچەی نیشتەجێبوون.ئەمەش کاردەکاتە سەر زیادبوونی بەکارهێنانی ئاو بۆ مەبەستەکانی خواردنەوە و بەکارهێنانەکانی تر.لەم ناوچەی توێژینەوەیەدا، هەروەك ئاشکرایە کە ئاوی سەرزەوی لەرووی چەندێتی یەوە وەك پێویست نی یەبۆ دابین کردنی پێداویستی یەکان، بۆیە پێویستە بە ڕادەیەکی زۆر پەنابرێت بۆ بەکارهێنانی ئاوی ژێرزەوی. هەروەك بەدەرکەوتووە لەم ناوچەیەدا بڕێکی زۆر لە کۆگاکانی ئاوی ژێرزەوی دەکەوێتە ناو کۆگاکانی نیشتووی تازەوچینە بەردینە بەدەرکەوتووەکان کە ناوچەی نیشتەجێ بوون دەکەوێتە سەریان. لەبەرئەوە ئەم ناوچانە ڕووبەڕووی مەترسیەکی زۆری مادده پیسێنەرەکانی ئاوی ژێرزەوی دەبنەوە بەهۆی چەندین سەرچاوەوەهۆکارەوە.لەم ڕوووەوە، هەڵسەنگاندن وتوێژینەوە تایبەت بە هەستیاری ئاوی ژێرزەوی بۆ پیس بوون ئەنجام درا.

ناوچەی توێژینەوەکە (ئاوزێلی هەڵەبجە – سەیدسادق) دەکەوێتە باکووری ڕۆژهەڵاتی عێراق وە دادەنرێت بە یەکێك لە گرنگترین سەرچاوەی کۆگاکانی ئاوی ژێرزەوی لە هەرێمەکەدا لەرووی چەندێتی وجۆرێتی یەوە.مەبەست لەم توێژینەوەیە بریتی یە لە هەڵسەنگاندنی کاریگەرە ژینگەیی یەکان و پیشاندانی هەستیاری کۆگاکانی ئاوی ژێرزەوی ناوچەکە بۆ پیس بوون و هەروەها پاراستنی لە پیسبوون.

لەم توێژینەوەیەدا تاوتوێ ی ئامادەکردنی نەخشەیەکی هەستیاری ئاوی ژێرزەوی بۆ پیس بوون کرا بە بەکارهێنانی ڕێگەی (DRASTIC) ، کە ئەم ڕێگەیە بە یەکێك لە گرنگترین ڕێگاکان دادەنرێت بۆ ئەم مەبەستە.هەروەها چەندین گۆڕانکاری وڕاستکردنەوە بۆ ئەم ڕێگەیە ئەنجام درا بە شێوەیەك کە دەرئەنجامەکان بگونجێت لەگەڵ بارودۆخی هایدرۆجیۆلۆجی ناوچەکەوهەروەها نەخشەی ئامادەکراو ڕووی ڕاستەقینەی هەستیاری ئاوی ژێرزەوی ناوچەکە بۆ پیس بوون نیشان بدات. لەگەڵ ئەم ڕێگەیەدا چەند ڕێگەیەکی تری جیاواز بەکارهێنرا بۆ هەمان مەبەست کە بریتی بوون لە (VLDA , COP) .دەرئەنجامی سەرجەم ئەو ڕێگایانەی بەکارهێنران هەڵسەنگێنران وڕاستێندران بە

بەروارد کردنیان بە تەمەنی ئاوی ژێرزەوی و هەروەها جۆرێتی ئاوی ژێرزەوی لەدوو وەرزی یەك لەدوای یەکدا ،(وەرزی تەڕی و وەرزی ووشك) .

زانیاری کێڵگەیی وهەروەها زانیاری کۆکراوه لە ئەرشیفی لایەن و بەڕێوەبەرایەتیە پەیوەندیدارەکاندا بەکارهێنرا بۆ مەبەستی هەڵسەنگاندنی کاریگەری یە ژینگەیی یەکان و ئامادەکردنی نەخشەی هەستیاری ئاوی ژێرزەوی بۆ پیس بوون بە بەکارهێنانی ڕێگەی پێشنیارکراو (DRASTIC) بە بێ هیچ گۆڕانکاری یەك بۆ ناوچەی ئاوزێڵی تویژینەوەکە.بە پێ ی ئەم نەخشەیە ناوچەی ئاماژەبۆکراو دابەش بووه بەسەر چوار پۆلی هەستیاری کە بریتین لە (زۆر کەم، کەم،مامناوەند،بەرز) کە ڕووبەری هەریەك لەم پۆڵانە بریتین لە (٣٤٪،١٣٪،٤٨٪،٥٪) یەك لەدوای یەك.

یەکەم شێوازی گۆڕانکاری کە ئەنجام درا بۆ ڕێگەی (DRASTIC) بریتی یە لە گۆڕانکاری لە بەهای تێکڕا (Rate value) و بەهای کێش (Weight value) سەرجەم پارامیتەرەکانی ئەم ڕێگەیە، بەکارهێنانی چڕی نایترەیت لە (٣٩) نموونەی وەرگیراوی ئاوی بیرو کانی دا بۆ ئەنجام دانی گۆڕانکاری لە نرخی ڕێژەیی (Rate value) ی پێشنیار کراوی ڕێگەی (DRASTIC) بە بەکارهێنانی ڕێگەی (Wilcoxon rank-sum nonparametric statistical test). لەلایەکی ترەوه ڕێگەی (Sensitivity analysis) بەکارهێنرا بۆ گۆڕانکاری لە پلەی کاریگەری (Weight value) ی پارامیتەرەکان. ڕێگەی (Pearson's Correlation Coefficient) بەکارهێنرا بۆ هەژمارکردنی پەیوەندی نێوان پارامیتەرەکانی (DRASTIC) وچڕی نایترەیت.بۆ نەخشەی گۆڕدراوی (DRASTIC) ئەنجامی ئەم فاکتەرە بریتی بوو لە (٧٢٪) بەڵام بۆ ڕێگەی پێشنیارکراوی (DRASTIC) بریتی بوو لە (٤٣٪). بە پێ ی ئەنجامی نەخشەی گۆڕدراوی (DRASTIC) ناوچەی تویژینەوەکە دابەش بووه بەسەر پێنج پۆلی هەستیاری کە بریتین لە (زۆر کەم، کەم،مامناوەند،بەرز، زۆر بەرز) کە ڕووبەری هەریەك لەم پۆڵانە بریتین لە (٧٪،٣٥٪،١٩٪،٣٥٪،٤٪) یەك لەدوای یەك.

دووەم شێوازی گۆڕانکاری کە ئەنجام درا بۆ ڕێگەی (DRASTIC) بریتی یە لە کاریگەری نەخشەی زەوی بەکارهێنراو و زەوی داپۆشراو (Land Use and Land Cover) لەسەر بارودۆخی هەستیاری ئاوی ژێرزەوی بۆ پیس بوون لە ناوچەکەدا.بۆ ئەم مەبەستە نەخشەی (LULC) ئامادەکرا بە بەکارهێنانی پرۆگرامی کۆمپیوتەری (Erdas Imaging Software) وە بەکارهێنانی دوو

وێنەی هێڵکاری زەوی ناوچەکە(Landsat Thematic Mapper). بە پێ ی نەخشەی (LULC) ناوچەکە دابەش بووە بەسەر پێنج پۆڵی جۆری زەوی دا که بریتی یه (زەوی بەردەڵان ولەوەڕگا ، زەوی کشتوکاڵی ، زەوی گژوگیایی، ناوچەی نیشتەجێ بوون، ناوچەی شێدار یان هەیکەڵی ئاوی). بە پێ ی ئەنجامی نەخشەی گۆڕدراوی (DRASTIC) به هۆی کاریگەری (LULC) ،ناوچەی تویژینەوەکە دابەش بووە بەسەر پێنج پۆڵی هەستیاری که بریتین له (زۆر کەم، کەم،مامناوەند،بەرز، زۆر بەرز) که ڕووبەری هەریەك لەم پۆڵانه بریتین له (١,١٧٪،٣٦,٨٢٪،١٧,٥٧٪،٤٣,٤٢٪،١,٠٢٪) یەك لەدوای یەك.

سێ هەم شێوازی گۆڕانکاری که ئەنجام درا بۆ ڕێگەی (DRASTIC) بریتی یه له کاریگەری (Lineament feature) لەسەر بارودۆخی هەستیاری ئاوی ژێرزەوی بۆ پیس بوون له شوێنی تویژینەوەکە. نەخشەی (Lineament) ئامادەکرا به بەکارهێنانی وێنەی هێڵکاری زەوی (Enhanced Thematic Mapper) بەیارمەتی چەندین تەکنیکی تایبەت به بواری (Remote Sensing) هەروەها به بەکارهێنانی پرۆگرامی زانیاری سیستمی جیۆگرافی (GIS). بە پێ ی نەخشەی (Lineament Density Map) ناوچەکە دابەش بووە بەسەر شەش پۆڵی چڕی (Lineament) که چڕی یەکەی دەکەوێتە نێوان (سفر-٢,٤). بە پێ ی ئەنجامی نەخشەی گۆڕدراوی (DRASTIC) به هۆی کاریگەری (Lineament Feature) ،ناوچەی تویژینەوەکە دابەش بووە بەسەر چوار پۆڵی هەستیاری که بریتین له (زۆر کەم، کەم،مامناوەند،بەرز،) که ڕووبەری هەریەك لەم پۆڵانه بریتین له (٢٨,٧٥٪،١٤,٣١٪،٤٦,٩١٪،١٠,٠٤٪) یەك لەدوای یەك.

چوارەم شێوازی گۆڕانکاری که ئەنجام درا بۆ ڕێگەی (DRASTIC) بریتی یه له بەکارهێنانی ڕێگەی (Analytical Hierarchical Process-AHP) بۆ هەڵسەنگاندنی پلەی کاریگەری هەریەك له پارامیتەرەکان، بە پێ ی ئەم گۆڕانکاری یه ناوچەی تویژینەوەکە دابەش بووە بەسەر پێنج پۆڵی هەستیاری له نێوان (زۆر کەم بۆ زۆر بەرز) وه پلەی هەستیاری له نێوان (٦٥,٨٢ بۆ ٢٢٤,١) دایه.

جگه له ڕێگەی (DRASTIC) دوو ڕێگەی تری جیاواز بەکارهێنرا که بریتین له (, VLDA COP) بۆ ئامادەکردنەی نەخشە هەستیاری ئاوی ژێرزەوی بۆ پیس بوون له ناوچەکەدا.بە پێ ی ئەنجامی (VLDA) ناوچەی تویژینەوەکە دابەش بووە بەسەر چوارپۆڵی هەستیاری له نێوان (کەم بۆ زۆر بەرز) وه پلەی هەستیاری له نێوان (٢,١٣٣ بۆ ٩,١٦) دایه.بەڵام بە پێ ی ڕێگەی (COP) ناوچەکە

به هەمان شێوە دابەش بووە بەسەر چوار پۆلی هەستیاری لە نێوان (زۆر کەم بۆ بەرز) وە پلەی هەستیاری لە نێوان (۰،۷۹ بۆ ٦،۲) دایە.

سەرجەم دەرئەنجامەکانی رێگە جیاوازەکانی بەکارهێنراو بۆ هەڵسەنگاندنی هەستیاری ئاوی ژێرزەوی بۆ پیس بوون بەراووردکران بە یەکتر، هەروەها راستێنران بۆ ئەوەی گرنگی وووردی سەرجەم نەخشە بەدەستهێنراوەکان بچەسپێنرێن. دوو رێگە بەکارهێنرا بۆ ئەم مەبەستە،لە یەکەم رێگەدا چرِی نایترەیت لە (۳۹) نموونەی ئاوی بیروکانی بەکارهێنرا لە دوو وەرزی جیاوازی یەک لە دوای یەکدا کە ئەوانیش (وەرزی تەرِ و وەرزی وشك) بوون.لە دووەم رێگەدا پۆلەکانی هەستیاری ئاوی ژێرزەوی هەڵسەنگێنرا بە پێ ی تەمەنی ئاوی ژێرزەوی بە بەکارهێنانی هاوتای ژینگەیی تریتیۆم (^3H) . ئەنجامی هەردوو رێگەکە پیشانی دا کە دابەش بوونی پۆلەکانی هەستیاری ئاوی ژێرزەوی بۆ پیس بوون بە رێگەکانی گۆرِانکاری (DRASTIC) بە پێ ی (نرخی رِێژەیی (Rate value) وپلەی کاریگەری (Weight value) و کاریگەری (LULC) ورِێگەی (AHP)) هەروەها بەکارهێنانی رێگەی (VLDA) گونجاوترین و رِاستێنترین رێگەن بۆ ئەم مەبەستە، بە شێوازێك کە بگونجێت لەگەڵ بارووودۆخی ناوچەکە لە رِووی هایدرۆجیوۆلۆجی و سروشتی ئاوی ژێرزەوی یەوە.

هەڵسەنگاندنی لاوازی ئاوی ژێرزەوی بۆ پیس بوون بە بەکارهێنانی سێ ڕێگەی جیاوازی هەڵسەنگاندن لە ناوچەی ئاوزێڵی هەڵە بجە – سەیدسادق، ،باکوری ڕۆژهەڵاتی عیڕاق

نامەیەکە

پێشکەش کراوە بە ئە نجومەنی کۆڵجی زانست لە زانکۆی سلێمانی وەك بەشێکی تەواوکەر بۆ بەدەست هێنانی بڕوانامەی دکتۆرای فەلسەفە لە زانستی جیۆلۆجی دا
(هایدرۆجیۆلۆجی)

لەلایەن
توانا عمر عبدالله
ماستەر لە ئەندازیاری جیۆلۆجی دا – ٢٠٠٩
زانکۆی پۆرتسمۆس، ئینگلاند
بە سەرپەرشتی

د. نظير الانصاری   د. صلاح الدین سعید علی

پرۆفیسۆر   پرۆفیسۆر

أيار، ٢٠١٨   گولان ، ٢٧١٨